DEVELOPING A TWO-PRONGED DRUG SCREEN TO IDENTIFY COMPOUNDS THAT PROTECT AGAINST CISPLATIN-INDUCED OTO- AND NEPHROTOXICITY

by

Jaime N. Wertman

Submitted in partial fulfilment of the requirements
for the degree of Doctor of Philosophy

at

Dalhousie University
Halifax, Nova Scotia
November 2019

This thesis is dedicated to my Grandpa, Jim Bowling.

Table of Contents

List of Tables

List of Figures

Abstract

Cisplatin is a chemotherapy used to treat a variety of cancers, including several pediatric malignancies. Cancer survivors are plagued by lifelong cisplatin-induced toxicities, including kidney damage and ototoxicity, or hearing loss. In efforts to find adjuvant compounds that can prevent these toxicities, in this study, I employed a two-pronged oto- and nephrotoxicity drug screen. The zebrafish is an excellent model for studying drug toxicities due to conserved genetics and organ systems. Zebrafish have lateral line neuromasts, analogous to clusters of mammalian cochlear hair cells. Similar to hair cell death in humans, cisplatin exposure causes decreases in neuromast viability, visualized with YO-PRO1, a fluorescent dye. Larvae treated with cisplatin (0.001-0.05 mM) demonstrated a dose-dependent reduction in neuromast fluorescence that I was able to measure rapidly using a biosorter. Zebrafish larvae also possess pronephros structures similar to the mammalian nephron. Glomerular filtration rate (GFR) can be measured in larvae by injecting FITC-tagged inulin into circulation. Inulin is renally-excreted, so decreases in vascular fluorescence approximates GFR. Cisplatin-treated larvae exhibited a reduction in GFR, which was also detectable with the biosorter. I employed an *in vivo* larval neuromast screen to assess the effects of compounds from the Sigma LOPAC®1280 library on cisplatin-induced ototoxicity. I compared these results with an *in vitro* toxicity test of cisplatin +/- the compound library on human proximal tubule cells, and found 22 drugs that were effective in both assays. I validated the protective capacity of two of these adjuvants, dopamine and L-mimosine, with confocal microscopy of the inner ear and the GFR assay. To determine if these protective compounds impact cisplatin's cytotoxic effects, I performed an alamarBlue™ viability assay, an apoptosis-based flow cytometry assay, and a γH2AX-based immunohistochemistry assay designed to detect double strand breaks (DBSs) in DNA. In each of these assays, dopamine and L-mimosine did not reduce the cytotoxicity of cisplatin in SK-N-AS and LAN5 neuroblastoma (NBL) cells, or HSC-3 oral squamous cell carcinoma cells. This project provides technological advances in the field of zebrafish-based drug screening, and identifies dopamine and L-mimosine as candidate oto- and nephroprotective compounds.

List of Abbreviations and Symbols Used

°C: degrees Celsius

%: percent

Å: Ångstrom

µg: microgram

µL: microliter

µM: micromolar

5-FU: 5-fluorouracil

ABR: auditory brainstem response

AC: adenylyl cyclase

AKI: acute kidney injury

ALL: anterior lateral line

ANOVA: analysis of variance

APAF-1: apoptosis protease activating factor 1

ASSR: auditory steady-state response

BAK: BCL-2 antagonist killer 1

BAX: BCL-2 associated X protein

BCL-2: B-cell lymphoma

BIR: break-induced replication

bpm: beats per minute

BUN: blood urea nitrogen

cAMP: cyclic adenosylmethionine

CKD: chronic kidney disease

CNS: central nervous system

CPA: conditioned play audiometry

CRISPR: clustered regulatory interspaced short palindromic repeats

CXCL12: C-X-C chemokine ligand 12

CXCR4: C-X-C chemokine receptor type 4

DAPI: 4′,6-diamidino-2-phenylindole

Da: Daltons

dB: decibels

DDP: diamminedichloroplatinum

DMEM: Dulbecco's Modified Eagle Medium

DMSO: dimethyl sulfoxide

DNA: deoxyribonucleic acid

dpf: days post-fertilization

DPI: diphenyleniodonium chloride

dpt: days post-treatment

dsDNA: double-stranded deoxyribonucleic acid

DSBR: double-stranded break repair

DTT: Dithiothreitol

ENU: ethylnitrosurea

ERK: extracellular regulated kinase

FBS: Fetal bovine serum

FDA: Food and Drug Administration of The United States of America

GEC: glomerular endothelial cells

GPCR: G protein-coupled receptor

HIF-1α: hypoxia-inducible factor 1α

hMATE: Human multidrug and toxin extrusion

HPF: hours post fertilization

hpi: hours post injection

hpt: hours post treatment

hr: hours

HR: Homologous recombination

Hz: Hertz

IMS: (mitochondrial) intermembrane space

JNK/SAPK: Jun N-terminal kinase/stress-activated protein kinase

kHz: kilo Hertz

LOC: lateral olivocochlear (system)

mg/m^2: milligrams per metre squared

min(s): minute(s)

ml: millileter

mM: millimolar

MOC: medial olivocochlear (system)

NAC: N-acetylcysteine

NBL: neuroblastoma

NCI: National Cancer Institute

NEAA: Non-essential amino acids

NER: Nucleotide excision repair

NF-κB: nuclear factor -κB

NSAID: non-steroidal anti-inflammatory drugs

OAE: otoacoustic emissions

OC: olivocochlear (system)

OHCs: outer hair cells

OMM: outer mitochondrial membrane

PEC: parietal epithelial cell

PBS: Phosphate buffered saline

PCD: programmed cell death

PCR: polymerase chain reaction

PFA: Paraformaldehyde

PH: Peak height

PLL: posterior lateral line

POG: Pediatric Oncology Group

PS: Penicillin Streptomycin (Pen Strep)

PTA: pure-tone audiometry

ROS: reactive oxygen species

RT-PCR: reverse transcriptase polymerase chain reaction

RMPI: Roswell Park Memorial Institute Medium

RNA: ribonucleic acid

RT: room temperature

SE: standard error

siRNA: short-interfering ribonucleic acid (RNA)

SD: standard deviation

SDSA: synthesis-dependent strand annealing

SNP: single nucleotide polymorphism

ssDNA: double-stranded deoxyribonucleic acid

STS: sodium thiosulfate

TLS: Translesion DNA synthesis

TNF-α: tumour necrosis factor-α

VRA: visual reinforcement audiometry

WISH: whole-mount *in situ* hybridyzation

WT: wild-type

x *g*: force of gravity

XP: Xeroderma pigmentosum

Acknowledgements

First and foremost, this thesis would not have been possible without my supervisor, Jason Berman. He has allowed me creative liberty with this project, by allowing me to follow my own scientific questions and develop my own methods. He is a constant source of energy, support, and wise words. I am truly grateful to have worked with him over the last several years.

My lab mates throughout the years have been an incredible source of support, friendship, and scientific advice. Special thanks go to Nicole Melong, who was critical to this project from the very beginning. From teaching me how to xenotransplant larvae, to injecting 400 larvae/day with me, to proofreading this entire thesis, her presence is apparent on every page of this document. Olivia Piccolo, thank you for contributing to this work and establishing protocols that were so integral to this study. Benno Orr, thank you for developing a computer program that I couldn't even dream up. Matt Stoyek, thank you for imaging so many fish ears for me. Shelby Steele, Babak Razaghi and Stewart Langley also directly contributed to the critical early stages of this study. Lab members KC, LC, LC, ACS, LM, VKR, SP, and DL, thank you for answering my incessant questions and tolerating my music.

Thank you to my Scientific Advisory Committee (Craig McCormick, Meredith Irwin, Sidney Croul, Graham Dellaire), who have provided input and guidance throughout this project. Special thanks to Craig McCormick for being my co-supervisor for the last portion of this degree, and to his post-doc Eric Pringle for taking me on as an adopted lab member. I would also like to thank Arunika Gunawardena, my Honour's supervisor, for teaching me so much about science *and* life. It means the world to me that we have been able to maintain our professional and personal; relationship.

I am fortunate to have a stellar personal support system that has helped me through this degree. I am lucky to have parents that continue to believe in my scientific endeavours. Mom and Dad, thank you for everything. To my amazing husband Justin, thank you for being my biggest fan. Thank you for being such an amazing partner and for making me laugh, even through some of our worst days. To my fellow PhD Student sister, Debra – thanks for the late-night chats, pick-me up calls, and statistics help. To my newest family members, all of the Stewart clan, thank you for all of the love and kind words through this degree. Special thanks to Melissa Stewart for paving the way before me and being such a wonderful role model and friend. To Grandma and Bubby, thank you for being such fierce female role models. To my brilliant friends – JD, EH, RM, JM, JE, EW, AB, AA (& CE), JL, and JO, whether you are near or far, I know that I can count on you for inspiration or love.

The last thank you goes to the two individuals who have witnessed and sat with me for the lion's share of this thesis work: Olive Danger and Bruce Puddles. Olive – you are the smartest and most loyal dog that I have ever met. Bruce – you are a kind soul, an amazing cuddler, and a constant source of entertainment.

Chapter 1 Introduction

1.1 Cisplatin

Cisplatin (*cis*-diamminedichloroplatinum(II), *cis*-[$PtCl_2(NH_3)_2$]), **Figure 1a**) is one of the oldest chemotherapeutic compounds that is still in use in modern chemotherapy. Although many medicinal chemists have attempted to make alterations to the compound itself in order to either improve its efficacy, or to decrease the toxic side effects of the drug, the original compound is still in use today. This thesis describes a two-pronged *in vitro* and *in vivo* drug screen approach to find compounds that protect against cisplatin-induced oto- and nephrotoxicity.

1.1.1 History and Introduction to Clinical Use

Cis-dichlorodiammine-platinum(II) (cisplatin), was originally known as Peyrone's chloride. This compound was first synthesized by Michele Peyrone in 1844 when he attempted to synthesize Magnus' green salt ([Pt(NH3)4][PtCl4]) (Kauffman, 2010). However, the cytostatic effects of cisplatin were first observed, albeit unintentionally, by Barnett Rosenberg in cultures of *Escherichia coli* (B. Rosenberg, VanCamp, & Krigas, 1965). Rosenberg was a physicist investigating the effects electromagnetic radiation on cell replication, but the electrodes used in the experiments were made of platinum. Upon application of the electromagnetic field, the resultant electrolysis products caused bacterial filament formation, rather than the short rods typically expected. The causative agent of this cytostatic effect was found to be [PtII(NH3)2Cl2], or the rediscovered Peyrone's chloride (B. Rosenberg et al., 1965).

Initial tests done in mice with either sarcoma 180 or leukemia L1210 transplantable murine tumours suggested that intraperitoneal administration of 8mg/kg

cisplatin was effective at inhibiting tumour growth, and extended the lifespan of the animals (Barnett Rosenberg & VanCamp, 1969). Additionally, initial in vitro studies with Chinese hamster cells (CHEF-125) cells demonstrated that the platinum drugs inhibited mitosis and caused changes in chromosomal appearance (Barnett Rosenberg & VanCamp, 1969). Initial studies in humans examined doses and scheduling, with 20 mg/m^2/day for five days selected as the least toxic dose. Further, partial responses were seen in an individual patient each with thyroid carcinoma, bladder cancer and breast cancer. Most strikingly, in 3/11 patients with testicular tumours, complete regression was observed (Higby & Wallace, 1974). These initial reports of tumour response were coupled with evidence of hearing loss, tinnitus, extreme nausea and vomiting, and kidney damage indicated by elevated serum creatinine levels. However, the promising cytotoxic effects of cisplatin on these tumours that were refractory to all other known therapies, warranted further investigation. The United States Food and Drug Administration (FDA) approved cisplatin for use in testicular and bladder cancer in 1978.

1.1.2 Pharmacology and Pharmacokinetics

1.1.2.1 Pharmacology

1.1.2.1.1 Uptake

Cisplatin is a small, platinum-containing compound with square, planar geometry and no net charge (Figure 1.1a). As a result, there is no logical reason why cisplatin could not passively diffuse across the plasma membrane to gain access to the inside of cells. Studies using unilamellar lipid vesicles, with no membrane proteins, demonstrated that cisplatin can enter the cell via passive diffusion, and that cell permeability increases with increased chloride concentration in the media (Eljack et al., 2014). Cisplatin uptake is

also linear with concentration increases, up to the solubility limit, supporting the concept of passive diffusion (Ivy & Kaplan, 2013; S. C. Mann, Andrews, & Howell, 1990). Additionally, if protein-mediated uptake was the main mechanism of drug uptake, one would expect that the addition of cisplatin structural analogs would decrease cisplatin uptake, as they would be competing for protein-binding. However, Andrews et al., measured cisplatin uptake in the absence and presence of carboplatinum, trans-DDP and DACH-Pt, and found that cisplatin uptake was not inhibited (Andrews, Mann, Velury, & Howell, 1987). All of these findings are in contrast with the theory of active, protein-mediated cisplatin uptake, which will be explored below.

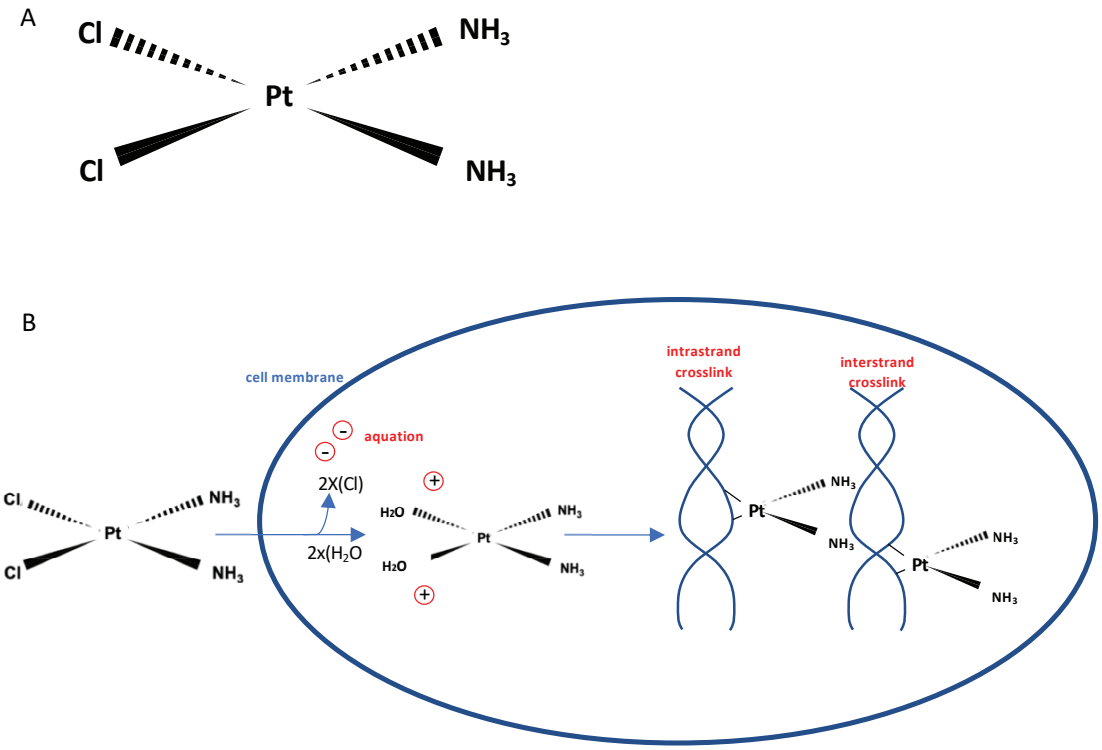

Figure 1.1 Chemical structure of cisplatin and derivatives. A) Cisplatin is a small, planar, square molecule with a central platinum ion, two chloride ions, and two ammonia molecules. This is *cis*- isomer of this molecule. The *trans*- molecular counterpart is much less important in the field of cancer therapeutics. B) Cisplatin enters through the cell membrane, where an aquation reaction occurs, where the chloride groups are replaced with water molecules, creating $[Pt(NH3)2Cl(OH2)]^{+}$ and $[Pt(NH3)2(OH2)2]^{2+}$. This product is able to form covalent bonds with the N^{7} position in purine bases, forming either intrastrand or interstrand crossinks.

Several proteins that may or may not play a significant role in cisplatin uptake are copper transport proteins 1 and 2 (CTR1 and CTR2). Deletion or mutation of CTR1 in both yeast and mouse cells increases resistance to cisplatin (Ishida, Lee, Thiele, & Herskowitz, 2002). Overexpression of CTR1 in ovarian carcinoma cells increased the accumulation of cisplatin in the cells by 81%, but curiously did not drastically increase the overall toxicity of the drug (Holzer et al., 2004). This may be a result of cisplatin uptake and transport to locations in the cell other than the main sites of cisplatin-induced damage (Safaei, 2006). There are also some questions about how effectively cisplatin, at 9.57Å in size (Hilder & Hill, 2007), would be able to fit through the human CTR1 pore, with an estimated diameter of 8 Å (Feo, Aller, & Unger, 2007).

Another important family of cisplatin-transporting proteins is the organic cation transporters (OCTs). Broadly speaking, OCTs move endogenous or exogenous positively charged molecules across the cell membrane in a bidirectional manner. This could include anything from dopamine to cimetidine, or even cisplatin (G Ciarimboli, 2008; Yonezawa & Inui, 2011). There are three subtypes of OCTs in humans: OCT1, OCT2 and OCT3. OCT2 is the main OCT expressed in the kidney, specifically at the basolateral membrane of renal tubular cells (Filipski, Loos, Verweij, & Sparreboom, 2008). Studies overexpressing OCT2 have shown a significant increase in cisplatin uptake, in comparison with control cells (Filipski et al., 2008; Yonezawa et al., 2005). In fact, the OCT2 inhibitor cimetidine has the effect of preventing proximal tubule cell death with cisplatin-exposure (Ludwig, Riethmuller, Geckle, Schwerdt, & Oberleithner, 2004), and reducing nephrotoxicity (Giuliano Ciarimboli et al., 2010; J. A. Sprowl et al., 2013). The implications of OCT2-mediated cisplatin uptake will be highlighted in several sections

below, in the discussion of genetic susceptibility of individuals to cisplatin-induced toxicity.

1.1.2.1.2 Interaction with DNA

Once inside the cell, an aquation reaction occurs, where the chloride groups are replaced with water molecules, creating $[Pt(NH3)2Cl(OH2)]^{+}$ and $[Pt(NH3)2(OH2)2]^{2+}$ (**Figure 1.1b**). This reaction occurs because of the relatively low concentration of chloride within the cell and the high concentration of water (Go & Adjei, 1999). The products of the initial aquation reaction are able to react with both nitrogen donor atoms on both RNA and DNA, and sulfhydryl groups on proteins (Dasari & Bernard Tchounwou, 2014; Fichtinger-Schepman, Van der Veer, Den Hartog, Lohman, & Reedijk, 1985). The main cytotoxic effects occur in the nucleus, where platinum atoms form covalent bonds with the N^7 position in purine bases. This creates 1,2- and 1,3-intrastrand crosslinks and occasionally interstrand crosslinkages (ICLs) (Wang & Lippard, 2005). The most common lesions are the 1,2-intrastrand d(GpG) adducts, and to a lesser extent, and 1,2-intrastrand d(ApG) (Dasari & Bernard Tchounwou, 2014).

ICLs are the most toxic lesions caused by platinum-DNA interaction, as they are usually mostly irreversible covalent bonds that can block both transcription and translation (Deans & West, 2013). While not as toxic as ICLs, intrastrand crosslinks are the most common DNA lesion following cisplatin exposure. Even early nuclear magnetic resonance (NMR) studies demonstrated that the 1,2-intrastrand crosslinks cause a bend in the DNA towards the major groove by approximately 60° and uncoiled the DNA double helix by at least 12° (Herman et al., 1990).

1.1.2.1.3 Cellular Response to Cisplatin-Induced DNA Adducts

ICLs are repaired in cells through homologous recombination (HR), nucleotide excision repair (NER), or translesion DNA synthesis (TLS) (Deans & West, 2013; Enoiu, Jiricny, & Scha, 2012). While mismatch-repair proteins seem to recognize intrastrand crosslinks (O'Brien & Brown, 2006; Wang & Lippard, 2005), the most common mechanism for intrastrand crosslink removal is NER (Furuta et al., 2002; Marteijn, Lans, Vermeulen, & Hoeijmakers, 2014).

The HR pathway is involved in meiosis, the repair of externally-induced DSBs, and collapsed replication forks. There are three main types of HR: the double-strand break repair (DSBR) pathway, the synthesis-dependent strand annealing (SDSA) pathway, and the break-induced replication (BIR) model (Krejci, Altmannova, Spirek, & Zhao, 2012). The control of the HR pathways in cells is critical. This is highlighted by the BRCA1 and BRCA2 mutations, originally identified in families with elevated incidence of breast cancer (Miki, Swensen, Shattuck-Eidens, & Futreal, 1994; Wooster et al., 1995). BRCA1 and BRCA2, the protein products, bind to Rad51-coated filaments, and are required for the HR involved in repairing DSBs and inter-strand crosslinks (Moynahan et al., 1999; Moynahan, Pierce, & Jasin, 2001). This seems to cause a shift in cells to the more error-prone pathways that do not rely on BRCA proteins or Rad51, leading to overall chromosomal instability (Moynahan et al., 2001; Tutt et al., 2001). As a result of these deficiencies in HR, patients with BRCA mutations are more sensitive to platinum-based chemotherapy, and may have improved survival (Chetrit et al., 2008; Sakai et al., 2009)

Nucleotide excision repair (NER) is another pathway of DNA repair that responds to a relatively broad range of DNA lesions, including alkylating-drug induced intra- and

interstrand crosslinks and lesions generated by oxidative damage (Marteijn et al., 2014). NER can be divided into two main modes: global genome NER (GG-NER) and transcription-coupled NER (TC-NER). The former repairs defects across the whole genome, while the latter identifies transcription-blocking lesions (Laat, Jaspers, & Hoeijmakers, 1999). Evidence suggests that transcription-coupled is likely the most important type of NER in the removal of cisplatin-induced lesions (Furuta et al., 2002). Evidence for the importance of NER in the repair of cisplatin-induced lesions comes from studies of patients with Xeroderma pigmentosum (XP). Individuals with XP have a 1000X fold increased risk of developing skin cancer (Cleaver, 1969), due to decreased NER capacity as a result of defects in in seven genes (XPA-XPG) that influence both NER and TLS (Dworaczek & Xiao, 2007). As a result, fibroblasts that are isolated from these patients are more sensitive to cisplatin their wild-type counterparts (Dijt, Fichtinger-schepman, Berends, & Reedijk, 1988). Other important NER-associated proteins include, but are not limited to: ERCC Excision Repair Protein 1 (ERCC1/XPF), XPG, hHR23, and XPC (Wang & Lippard, 2005). The importance of ERCC1 and XPA in the cisplatin-induced NER is emphasized by studies that demonstrate that the low levels of ERCC1, XPA, and XPF protein are one of the reasons why cisplatin is so effective in testicular cancers (Furuta et al., 2002; Welsh et al., 2004).

TLS is involves one of seven mammalian DNA polymerases without proofreading exonuclease activity, which allows base pair addition to occur even in the presence of an error (Lange, Takata, & Wood, 2011). TLS is liable to introduce errors, but is a pathway through which cells may be able to temporarily evade an ICL.

Although the common understanding is that nuclear DNA is the main target for cisplatin, evidence suggests that mitochondrial DNA is also a significant target for cisplatin-

induced damage (Fuertes, Castilla, & Pérez, 2003; Olivero, Semino, Kassim, Lopez-Larraza, & Poirier, 1995; Schumaker, Egorin, Zuhowski, Guo, & Cullen, 2006). In fact, the mitochondrial DNA has been shown to accumulate more platinum adducts than nuclear DNA in several studies (Olivero et al., 1995; Schumaker et al., 2006). Also of note, DNA damage in the mitochondria may be more damaging than the nuclear counterpart as a result of the DNA not being protected by histone proteins and more limited DNA repair pathways (Olivero, Chang, Lopez-Larraza, Cristina Semino-Mora, & Poirier, 1997; Wisnovsky, Jean, & Kelley, 2016).

The DNA damage response (DDR) is a tightly-regulated signal transduction network that regulates many cellular processes, including, but not limited to: DNA repair, cell-cycle control, and apoptosis (programmed cell death; PCD). The types of DNA repair outlined above are just one part of the DDR. When DNA is not repaired, it can provide a signal for the cell to stop progressing through the cell cycle or eventually to undergo apoptosis.

The cell cycle is the series of stages that cells progress through during the overall process of division, including: G1, where the cell grows and organelles are duplicated; S phase, where the chromosomal DNA is duplicated; G2 phase, where the newly synthesized DNA is checked for errors; and mitosis, where the cell divides. This is a highly regulated process that includes proper activity of cyclin proteins, cyclin dependent kinases (CDKs) and checkpoint inhibitor proteins (Mills, Kolb, & Sampson, 2018). To progress through the cell cycle, the cell must pass DNA damage checkpoints that are present at the G1-S transition, before new DNA is synthesized, and at the G2-M transition, before mitosis. If DNA damage is detected at the G1-S checkpoint, the p53 tumour suppressor protein is induced, resulting in transcription of genes like the CDK

inhibitor *p21.* When damage is severe, p53 induction can result in apoptosis through the activation of genes like the proapoptotic protein Bax (Vermeulen, Bockstaele, & Berneman, 2003).

There are two main apoptosis pathways: the extrinsic, or externally induced pathway and the intrinsic pathway (Kischkel et al., 1995; Nunez, Benedict, Hu, & Inohara, 1998). The intrinsic pathway can be activated by DNA damage. The B-cell lymphoma (BCL-2) family of proteins modulate the intrinsic apoptosis pathway; while BCL-2 itself is pro-survival, BCL-2 associated X protein (BAX) and BCL-2 antagonist killer 1 (BAK) are pro-apoptotic binding partners (Edlich, 2018; Oltval, Milliman, & Korsmeyer, 1993). When either of these pro-apoptotic proteins are uninhibited, they will initiate apoptosis by permeabilizing the outer mitochondrial membrane (OMM) and releasing inter-membrane space (IMS) proteins into the cytosol, including cytochrome C (Eskes et al., 1998). Once released from the IMS, cytochrome c forms an "apoptosome" with the already cytosolic apoptosis protease activating factor 1 (APAF-1). This results in the activation of procaspase-9, downstream activation of effector caspases, and apoptosis (Giorgi et al., 2012; Matsui, Gale, & Warchol, 2004). Cisplatin is also known to induce apoptosis via the "externally induced" pathway, through a variety of mechanisms. Cisplatin can activate the extracellular regulated kinase (ERK), p38 and Jun N-terminal kinase/stress-activated protein kinase (JNK/SAPK) enzymes, which can lead to tumour necrosis factor-α (TNF-α) production. This leads to inflammation, and can cause either apoptosis or necrosis (Yao, Panichpisal, Kurtzman, & Nugent, 2007).

Another important signalling component in the cellular response to cisplatin is the induction of reactive oxygen species (ROS) (Dasari & Bernard Tchounwou, 2014). Example of ROS include superoxide (O_2^-), hydrogen peroxide (H_2O_2) and hydroxyl

radicals (OH^-). ROS are generated as a normal byproduct of the electron transport chain in the mitochondria, by cytochrome P450 metabolism, or in peroxisomes. Intracellular ROS levels increase when cisplatin is administered, which can result in damage to many proteins and lipids in the cell. In particular, the mitochondria is a target for cisplatin-induced ROS damage, resulting in dysregulation of calcium homeostasis and reduction of mitochondrial membrane potential (Dasari & Bernard Tchounwou, 2014).

1.1.2.1.4 Efflux

Equally important to the pharmacologic effects of cisplatin uptake into cells is the efflux of cisplatin out of cells. This is an important factor to consider when discussing either the desired pharmacologic anti-cancer effects of cisplatin, or the undesired toxicities of the drug. When efflux is enhanced, resistance can occur.

The copper-transporting P-type ATPases ATP7A and ATP7B seem to play a role in the efflux and intracellular sequestration of cisplatin from cells. The first indication that these transporters may play a role in the handling of cisplatin was when researchers discovered that ATP7B expression decreased the accumulation of cisplatin in cancer cell lines, resulting in resistance (Komatsu et al., 2000). Subsequent studies have suggested that these proteins both play a role in the shuttling of cisplatin either towards the cell membrane for exocytosis, or else towards other cellular compartments, protecting the typical cytotoxicity targets from damage (Kalayda, Wagner, Buß, Reedijk, & Jaehde, 2008; Samimi, Katano, Holzer, Safaei, & Howell, 2004).

Human multidrug and toxin extrusion 1 and 2 (hMATE1 and hMATE2-K, the kidney splice variant) are found on the membrane of proximal tubular cells (Masuda et al., 2006; Otsuka et al., 2005). Studies demonstrate that cisplatin-treated Mate1-/- mice

have increased levels of plasma creatinine and blood urea nitrogen (BUN) in comparison with wild type (WT) mice (Nakamura, Yonezawa, Hashimoto, Katsura, & Inui, 2010); this increased damage is possibly as a result of the lack of efflux transporters, causing overall retention of cisplatin. However, early studies showed that overexpression of hMATE1 and hMATE2-K in Hek239 cells results in the increased accumulation of cisplatin in cells (Yonezawa, Masuda, Yokoo, Katsura, & Inui, 2006). The discrepancy between these findings could be a result of the H^+-mediated bi-directional activity of MATE transporters (Takano, Inui, Okano, Saito, & Hori, 1984).

1.1.2.2 Pharmacokinetic Parameters

While pharmacology is the study of what drugs can do to the body, pharmacokinetics is the equally illuminating assessment of what the body does to drugs. It is broadly defined as absorption, distribution, metabolism, and excretion (ADME). The pharmacokinetics of a compound with life-threatening toxicities, like cisplatin, is particularly important in order to accurately predict the dosage required to produce therapeutic effects without significant toxicities.

Upon venous injection, >90% of cisplatin binds to serum proteins, which is thought to be irreversible and render the compound inactive (Gullo et al., 1980; O'Dwyer, Stevenson, & Johnson, 2000; Urien & Lokiec, 2004). The volume of distribution is 11-12 l/m2 (O'Dwyer et al., 2000). It can be inactivated metabolically inside the cell, or in the bloodstream, by sulfhydryl groups. It is also known to bind covalently with glutathione and thiosulfate (O'Dwyer et al., 2000).

Studies suggest that the plasma elimination of cisplatin is biphasic, with a short and rapid initial clearance phase and a subsequent very slow loss from circulation. In a

one hour infusion, the half life ($t_{1/2}$) was 22 min, and 26.6-50% was excreted in the urine within 48 hr. However, a 20 hr infusion of the drug resulted in less urinary excretion in the first 48 hr, suggesting that the drug was retained in the body more extensively (Gullo et al., 1980). The kidney is the main route for cisplatin excretion (Yao et al., 2007). Cisplatin is filtered both by the glomerulus and the proximal tubules.

1.1.3 Current Clinical Usage

The current on-label indications for cisplatin include advanced bladder, ovarian, and testicular cancer. However, it is used off-label for a wide variety of solid tumours, including triple-negative breast cancer, advanced bladder cancer, metastatic anal carcinoma, cervical cancer, esophageal and gastric cancers, some endometrial carcinomas, head and neck cancer, multiple myeloma, malignant pleural mesothelioma, refractory/relapsed Non-Hodgkin's lymphoma, Hodgkin's lymphoma, non-small cell lung cancer, metastatic penile cancer, osteosarcoma, small-cell lung cancer, advanced pancreatic cancer, and unknown primary cancers in adults. In pediatric populations, it is used to treat germ cell tumours, hepatoblastoma, medulloblastoma, high-risk neuroblastoma (NBL), and osteosarcoma (Kelland, 2007; Prestayko, Crooke, & Carter, 1980).

1.2 Cisplatin-Induced Toxicities

Cisplatin is a highly-effective anticancer agent, despite having several dose-limiting toxicities. In fact, the nephro-, oto-, and gastrointestinal toxicities are so intense that it has been questioned if the drug would even be approved if presented to regulatory authorities in modern times (Kelland, 2007). Nonetheless, the utility of cisplatin cannot

be ignored; thus, the hunt for strategies to reduce toxicities without altering the anticancer effects of cisplatin continues.

1.2.1 Ototoxicity

1.2.1.2 The Structure and Function of the Mammalian Ear

In order to best understand how cisplatin-induced hearing loss occurs, it is first helpful to understand the basic anatomy and physiology of the mammalian ear structures, which can be seen in **Figure 1.2**. The basic mammalian ear is divided into three parts: the outer, middle and inner ear (Ekdale, 2016). The outer, visible ear consists of the aurica, or pinna, which basically functions in the collection of sound waves. The sound waves are then funneled into the external acoustic meatus, or the ear canal, which then reach the tympanic membrane, a 0.1 mm thick membranous structure that separates the outer and middle ear (Alberti, 2001; Ekdale, 2016). The middle ear is a small air-filled chamber between the outer and inner ear. It is also connected to the back of the nose with a tube called Eustachian tubule. The middle ear also contains the malleus, incus, and stapes, the three tiny connected bones that span the region from the tympanic membrane to the oval window, which is the start of the inner ear (Alberti, 2001). The main function of these bones is to transmit sound waves from the outer to the inner ear. The inner ear is housed within a structure called the bony labyrinth, consisting of the vestibule, three semicircular canals, and the spiral shaped cochlea. It contains a collection of soft tissue sacs and tubules called the membranous labyrinth, including: the semicircular canals, and associated ampullae, which are involved in balance and the detection of rotational changes; the utricle and the saccule in the vestibule portion; and the spiral-shaped Organ of Corti, which is involved in hearing and contains the sensory hair cells (Ekdale, 2016). These hair cells are innervated by cranial nerve VIII. These inner ear structures are filled

with fluid: the bony labyrinth is filled with perilymph fluid with roughly the same composition as extracellular fluid, while the cochlear duct and membranous structures are filled with endolymph, which is more similar to intracellular fluid (Ekdale, 2016).

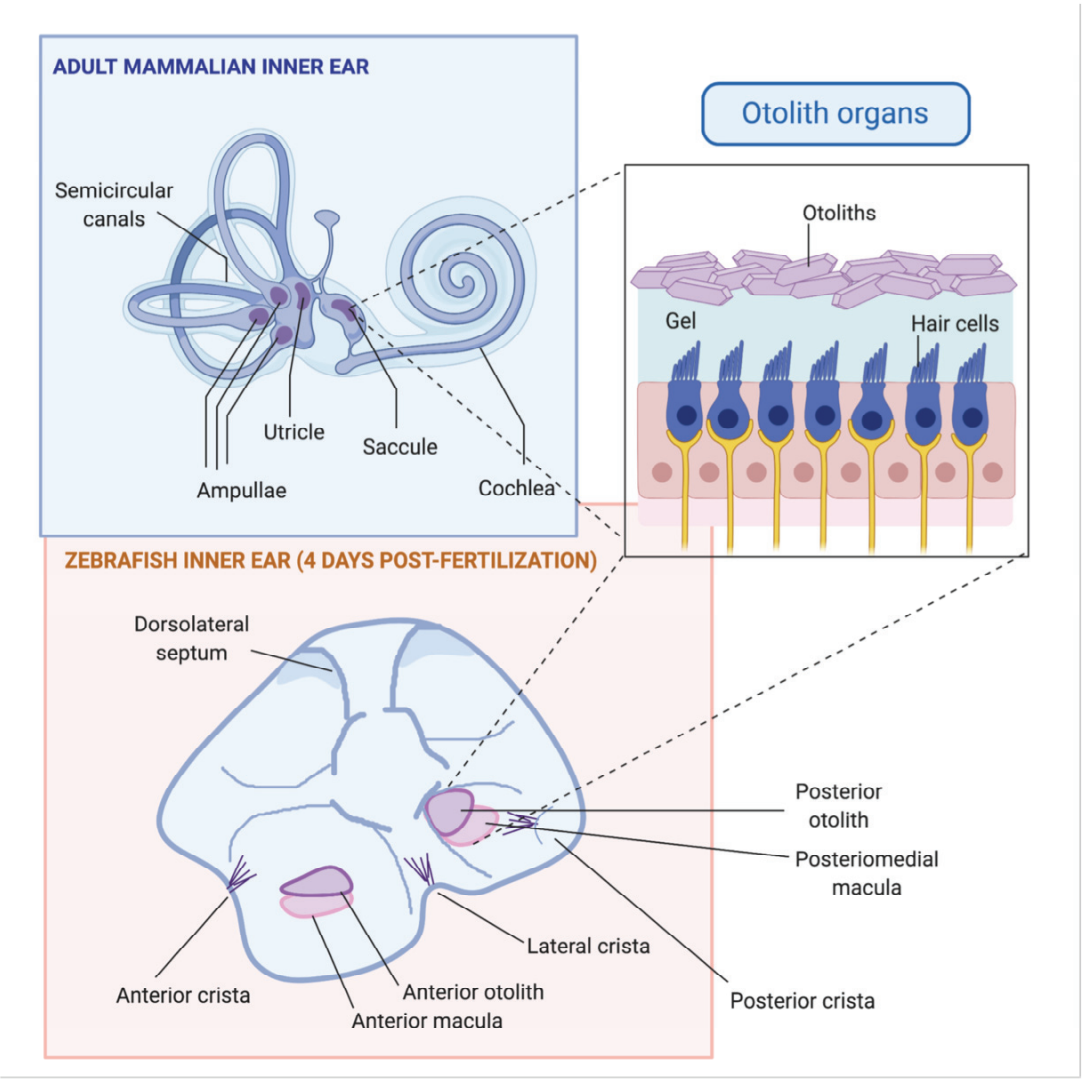

Figure 1.2 Anatomy of the inner ear in adult mammals and zebrafish larvae. The adult mammalian inner ear consists of the semicircular canals and associated ampullae (rotational movement detection), the saccule and utricle (linear movement detection), and the cochlea structure, containing the Organ of Corti (sound detection). The utricle and saccule hair cells are overlayed by otoliths, that are similar to those found in the zebrafish inner ear. The larval zebrafish inner ear contains three cristae patches and two macular patches, the anterior macula and posteriomedial macula, each overlayed by their own otolith structures.

When sound waves reach the ear, they are channeled through the pinna and ear canal to the tympanic membrane. The tympanic membrane then vibrates, causing serial

vibrations through the middle ear bone structures that amplify the vibrations. The stapes then interacts with the oval window, which transmits this signal to the cochlea. The endolymph inside the Organ of Corti ripples and creates waves following displacement via the oval window. These waves cause the movement of the stereocilia that are attached to the hair cells, which in turn transmit the mechanical waves of sound into electrical signals. Ions flow into the hair cell structures, causing the release of neurotransmitters into the afferent or efferent nerve, which will be transmitted to the brain via cranial nerve VIII (Alberti, 2001).

1.2.1.3 Incidence and Impact of Cisplatin-Induced Hearing Loss

Irreversible, bilateral hearing loss is one of the most common toxicities associated with cisplatin therapy. The incidence of cisplatin-induced hearing loss is a difficult statistic to capture as a result of various treatment regimens, population demographics, and methods of ototoxicity measurement and grading. However, it has been estimated that between 23-50% of adults (Ganesan et al., 2018), and approximately 61% of pediatric patients treated with cisplatin will develop some level of ototoxicity (Knight, Kraemer, & Neuwelt, 2005). The burden of this hearing loss is great – it can impact language skills in children, quality of life, and act as a financial strain on the healthcare system, as a result of patients needing speech therapy, hearing aids, or cochlear implants. Studies have shown that of 1,218 children with minimal sensorineural hearing loss, 37% have failed at least one grade, compared with 3% in the hearing population (Bess, Dodd-Murphy, & Parker, 1998). Hearing loss can be treated in a variety of ways, including hearing aids and cochlear implants. While these are useful strategies, they come with their own challenges. Many parents report that hearing aid use in young children can be

difficult, and emotionally challenging for everyone involved (Muñoz et al., 2015), and cochlear implants are only approved by the FDA in patients with dramatic hearing loss, and usually require intensive speech therapy (Papsin & Gordon, 2007).

Cisplatin-induced hearing loss is largely a result of death of the outer hair cells (OHCs), and eventually inner ear hair cells. As a result of the anatomical and "tonotropic" arrangement of the hair cells in the ear, damage occurs first at the base of the cochlea, which results in loss in the ability to sense high-frequency sounds. The damage then progresses towards the top of the cochlea, resulting in the loss of lower frequency detection (Z. F. Mann & Kelley, 2011). These cells do not regenerate, and the loss is permanent (Knight, Kraemer, Winter, & Neuwelt, 2007; Schell et al., 1989). This loss in hearing may or may not be accompanied by vertigo (dizziness) and/or tinnitus (ringing in the ears) (Langer, Zehnhoff-dinnesen, Radtke, Meitert, & Zolk, 2013). High-frequency hearing loss is particularly detrimental in pediatric populations, where language skills are still developing (Knight et al., 2007, 2005; Stelmachowicz, Pittman, Hoover, Lewis, & Moeller, 2004). Some high-frequency sounds (above 2,000 Hz) include "s," "f," "sh," and "t," and account for approximately half of all non-vowel sounds in English (Stelmachowicz et al., 2004). While individuals that are older at the time of their hearing loss are often able to infer meaning based on context and other non-auditory cues, children that have not yet developed their language skills are unlikely to be as adaptable. As a result, survivors with hearing loss can have a reduced quality of life in comparison with their hearing peers (Knight et al., 2005; Wake, Hughes, Hons, Collins, & Poulakis, 2004). Unfortunately, children are also more susceptible to cisplatin-induced hearing loss, which will be discussed further below.

Additionally, late-onset hearing loss (LOHL) is particularly problematic in pediatric populations. LOHL is defined as changes to hearing that are not detectable until after the cessation of cisplatin treatment, meaning the physician is by definition unable to alter the cisplatin dose (Berg, Spitzer, & Garvin, 1999; Kolinsky, Hayashi, Karzon, Mao, & Hayashi, 2010). One study reports a range of 1 month-50 months between cisplatin treatment completion and detection of hearing loss (Berg et al., 1999), while another reports deterioration at up to 136 months following therapy (Bertolini et al., 2004). Incidence of this LOHL is not insignificant, at approximately 51% of pediatric patients (Kolinsky et al., 2010). Importantly, in each of these studies there was no recovery of hearing function, supporting the notion that this ototoxicity is permanent.

1.2.1.4 Proposed Mechanisms of Ototoxicity

Platinum compounds, including cisplatin and carboplatin, are only some of the compounds that can cause ototoxicity. Macrolide and aminoglycoside antibiotics, loop diuretics, and antimalarials are all also ototoxic (Arslan, Orzan, & Santarelli, 1999; L P Rybak & Ramkumar, 2007). Aminoglycoside antibiotics include streptomycin, neomycin, kanamycin and gentamicin that are used clinically to treat diseases caused by gram-negative bacteria. They are known to cause sensorineural hearing loss in 15-33% of patients. Aminoglycosides and cisplatin both cause death in the outer hair cells at the base of the cochlea, largely as a result of increased intracellular levels of ROS (L P Rybak & Ramkumar, 2007). Although the mechanism through which ROS levels are elevated may differ, the end result of cochlear hair cell death is similar between the two drug classes. However, the following will focus primarily on the mechanisms of cisplatin-induced ototoxicity.

There are multiple mechanisms through which cisplatin exposure has been linked to hearing loss. The most obvious pathway is related to the desired molecular action of the drug, that is – inducing cell death as a result of DNA cross linkages, but in the incorrect cells. The sequence of this damage is similar to the therapeutic effects in cancer cells: DNA binding causing crosslinking and cell cycle disruption, the induction of the p53 cell cycle regulating tumour suppressor protein, and eventual apoptosis (Goncalve, Silveira, Teixeira, & Hyppolito, 2013). Cisplatin damage is more detrimental in locations like the cochlear hair cells partially because they do not have regenerative capacity, and cannot be replaced with healthy cells (Brock et al., 2012; Langer et al., 2013). The specific ototoxicity of cisplatin is thought to be supported by the localization of both CTR1 and OCT2 transporters in the cochlea (Giuliano Ciarimboli, 2012; Giuliano Ciarimboli et al., 2010). As these transporters have been shown to facilitate the transmembrane transport of cisplatin, it makes sense that these transporters are found in the cochlea, where cisplatin accumulates and causes toxicity. However, there are several other pathways that are important in the evaluation of cisplatin-induced ototoxicity, some of which will be outlined here.

One of the main mechanisms through which cisplatin is known to cause cell death in mammalian hair cells it through elevated levels of ROS. While the protective effects of antioxidants like N-acetylcysteine (NAC) had hinted at the involvement of ROS in ototoxin-induced hair cell death (Kopke et al., 1997; Pierson & Moller, 1981), direct observation of hydroxyl radicals (OH^-) was first shown in cochlear explants (Clerici, Hensley, Dimartino, & Allan, 1996). Once levels of ROS increase, this can overwhelm the antioxidant system that normally detoxifies and protects the cell from ROS-induced damage. When unchecked, elevated levels of ROS can lead of lipid peroxidation, calcium

influx into the cochlear cells, pro-apoptotic enzyme activation, and apoptosis (Leonard P. Rybak, Whitworth, Mukherjea, & Ramkumar, 2007). Though increased levels of ROS and decreased abundance of antioxidants are clearly important in this process, there are several pathways through which this increased oxidative load can arise.

Increased levels of ROS seem to be accompanied by decreased levels of antioxidant enzymes in the cochlea. Early studies of the rat cochlea following intraperitoneal (IP) injections with cisplatin reported significantly reduced levels of superoxide dismutase (SOD), glutathione reductase, glutathione peroxidase, and catalase (P. Rybak & Whitworth, 1999). There was also associated decreases in cochlear glutathione (GSH) and NADPH, which are involved in the function of multiple antioxidants (Leonard P. Rybak et al., 2007). Although GSH plays an important role in protecting the organ of Corti from damage, application of a GSH synthesis inhibitor buthionine sulfoximine (BSO) to organotropinc cochlear explant cultures did not impact neomycin-induced damage. This is in contrast with other studies that indicate that dietary supplementation with GSH may protect against cisplatin- or noise-induced hearing loss (NIHL) (Lautermann, Song, Mclaren, & Schacht, 1995; Ohinata, Yamasoba, Schacht, & Miller, 2000). This discordance indicates that either overlapping protective systems might compensate for the lack of GSH, or that the relationship between GSH and neomycin-induced ototoxicity is more complex than previously thought (Majumder, Duchen, & Gale, 2015).

The NADPH oxidase (NOX) 3 (NOX3) is a dual oxidase capable of generating superoxide (O_2^-) that is highly expressed in the inner ear (Banfi et al., 2004; Watanabe, Hess, Bloch, & Michel, 2000). NOX3-transfected HEK293 cells produce low levels of O_2^-, but ROS production was elevated upon co-transfection with other NOX subunits, or

in the presence of cisplatin (Banfi et al., 2004). Further, cisplatin treatment is known to increase the expression of NOX3, which would cause more ROS generation, creating a toxic positive feedback system (D Mukherjea, Whitworth, & Nandish, 2006). Knockdown of NOX3 by transtypmanic administration of short-interfering RNA (siRNA) results in protection of the OHCs and cochlea from cisplatin-induced apoptosis and changes to auditory brainstem response (ABR) in rats (Debashree Mukherjea et al., 2010; Leonard P Rybak, Mukherjea, Jajoo, Kaur, & Ramkumar, 2017).

1.2.1.5 Mechanisms of Ototoxicity Detection

Pure-tone audiometry (PTA) is the gold standard method to assess hearing ability. This utilizes a piece of equipment called an audiometer that can create and deliver tones of various frequencies (measured in Hertz, Hz) and intensities (measured in decibels). Tones of various frequencies (approximately 250-8000 Hz) are presented to the test subject at increasing intensities until they are heard (Stach, 1998). The resultant audiogram, or record of the test, displays the required intensity (related to the average among individuals) for a given frequency to be heard approximately 50% of the time in each ear (Landier, 2016; Stach, 1998). As previously mentioned, cisplatin treatment typically results in the loss of sensitivity to higher frequency sounds before the lower frequencies, resulting in a characteristic “sloping” audiogram. An example of an audiogram report of a cisplatin-treated patient with grade 4 hearing loss can be found in **Figure 1.3**. Adding high-frequency audiological testing during ototoxin exposure has been suggested (Arora et al., 2009).

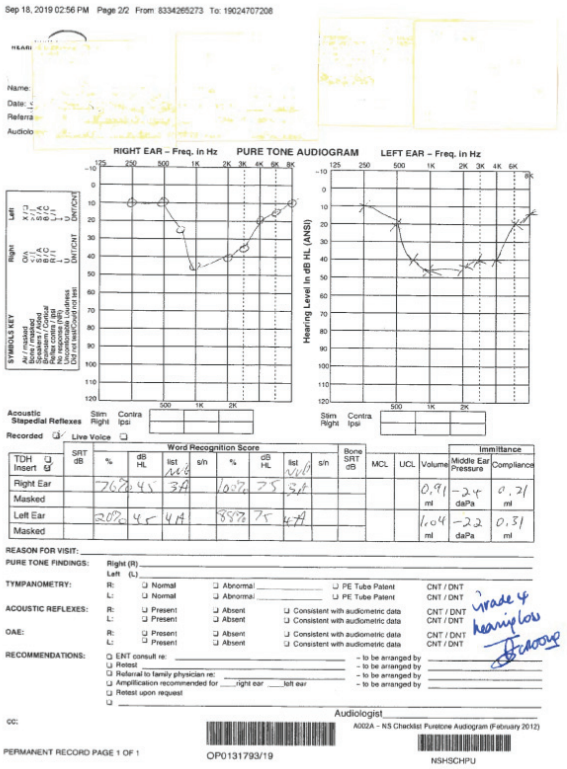

Figure 1.3 Audiogram of cisplatin-treated patient displaying Grade 4 hearing loss. Audiogram reports the frequency of sound presented, in Hertz (Hz) along the x-axis and the hearing level, in decibels (dB). The louder the sound needs to be presented before detection by the patient, the more profound the hearing loss is. This patient exhibits Grade 4 hearing loss.

An important consideration for audiometric testing is the challenges associated with assessing pediatric populations. While children 5 years and older typically can participate in pure-tone audiometric testing, younger patients benefit from conditioned play audiometry (CPA), or visual reinforcement audiometry (VRA) in the case of children 6 months-2 years (Smits et al., 2006). When these tests are not possible, the audiologist can test auditory brainstem response (ABR), or auditory steady-state response (ASSR) (Bass & Bhagat, 2014). Particularly important for the pediatric oncology population is extended high-frequency audiometry (EHF, >8000 Hz) and evoked otoacoustic emission (OAE) testing, which is a method to test the function of the cochlear outer hair cells, as these tests have shown to detect changes in hearing that occur prior to

cisplatin-induced damage that occurs in frequencies important for speech recognition (Knight et al., 2007).

Although the schedule of audiologic testing will vary depending on the patient characteristics, treatment schedule, and cancer type, testing typically follows a standard outline. The American Speech Language and Hearing Association (ASHA) suggests baseline tests should be done prior to treatment, then testing is done before each chemotherapy cycle, then follow-up testing is typically done at 1, 3, and 6-months post-treatment (*Audiologic management of individuals receiving cochleotoxic drug therapy*, 1994; Paken, Govender, Pillay, & Sewram, 2016).

1.2.1.6 Ototoxicity Grading Schema

The grading of hearing loss is extremely important; the description of damage/impact can impact decision making processes for physicians. Typically, scales span from 0 to 4, with 0 being normal hearing, and 4 being significant/profound changes to hearing abilities (Landier, 2016). There are several grading schema in use currently, and their benefits and disadvantages are found in **Appendix A**. The National Cancer Institute "Common Terminology Criteria for Adverse Events" (NCI "CTCAE") defines hearing loss grades in adults as the following: Grades 0-4: 0 = no hearing loss; Grade 1 = 15-25dB average loss at 2 adjacent frequencies in 1 or both ears, or subjective complaints; Grade 2 = >25dB loss averaged at 2 adjacent frequencies in 1 or both ears; Grade 3 = >25dB loss averaged 3 adjacent frequencies in 1 or both ears; Grade 4 = profound bilateral hearing loss, >80dB at 2kHz and up ("Common termniology criteria for adverse events (CTCAE)," 2017). Platinum administration is withheld at Grade 4 or below. There have been recent efforts to unify the grading of ototoxicity, not only to

facilitate patient care, but also to allow for accurate reporting of toxicities across clinical trials (Bass & Bhagat, 2014; Brock et al., 2012; K. W. Chang & Chinosornvatana, 2010).

1.2.1.7 Susceptibility to Ototoxicity

There is significant interpatient variability in the occurrence and severity of hearing loss. The most obvious and well recognized risk factors for ototoxicity is the cumulative dose of cisplatin (Allen et al., 1998; Bokemeyer et al., 1998; Y. Li, Womer, & Silber, 2004; Reddel et al., 1982), and the administration of a large dose at once, also known as a bolus (Kopelman, Budnick, Sessions, Kramer, & Wong, 1988; Y. Li et al., 2004; Reddel et al., 1982). Although reports vary with respect to incidence of ototoxicity at various cumulative doses, studies in adult patient with testicular cancer suggest that observable changes to hearing were not observed at doses $\leq$300mg/m^2, but that at doses $\geq$400mg/m^2, changes were often observed in patients at frequencies important for speech recognition (Biro et al., 2006). Additional clinical risk factors include cranial radiation (Bhandare, Antonelli, Morris, Malayapa, & Mendenhall, 2007; K. W. Chang & Chinosornvatana, 2010) and concomitant administration of aminoglycoside antibiotics (Bokemeyer et al., 1998; Waguespack & Ricci, 2005). A more contentious factor is whether or not the use of vincristine (a vinca alkaloid chemotherapy that inhibits microtubule function) increases cisplatin-induced ototoxicity risk, with case reports supporting this, and larger scale studies refuting it (Aydogdu et al., 2013; Lugassy & Shapira, 1996; Riga, Psarommatis, Korres, Lyra, & Papadeas, 2006).

Even more profound than cumulative dose was the age of patient at the time of treatment. Specifically, children <5 years of age are at up to 20 time increased risk of developing ototoxicity in comparison with patients between 15-20 years old (Allen et al.,

1998; Y. Li et al., 2004). Following review of at least 7 clinical studies, it has been determined that the risk of developing moderate to severe cisplatin-induced ototoxicity in pediatric populations (mean age <14 years old) increases 5-7% with each additional 100mg/m^2 cumulative cisplatin dose (Langer et al., 2013). Interestingly, some studies report sex differences with respect to cisplatin-induced ototoxicity, with males being more likely to develop hearing loss than females (Knight et al., 2005; Ross et al., 2009; Yancey et al., 2012); however, this is not consistent (Bertolini et al., 2004; Lewis et al., 2009).

It should also be noted that while cumulative dose is a significant risk factor for cisplatin-induced ototoxicity, it does not fully explain interpatient variability. For example, in one study some patients did not develop ototoxicity at cumulative doses from 360-480mg/m^2, but others showed signed of ototoxicity at cumulative doses of 120mg/m^2 (Krefeld et al., 2006). Even more disconcerting was that the serum concentration of platinum (either free or bound) was not predictive of whether or not the patient developed hearing loss, suggesting that typical methods of serum-based drug monitoring might not help clinicians predict which patients are at the highest risk (Krefeld et al., 2006; Landier, 2016).

The first attempts to address the potential genetic predisposition to developing cisplatin-induced ototoxicity were rational in design, meaning the researchers had some *a priori* knowledge of the impact of the genetic product on the pharmacology of cisplatin. An example is glutathione S-transferases (GSTs), which are known to play a role in the scavenging of ROS, and is expressed in hair cells of the mammalian ear. One study compared the likelihood of ototoxicity (divided into either highly-sensitive or not-sensitive) with three GST polymorphic alleles. The authors found that there was a

correlation between the GSTM3*B allele (lysine at position 172 instead of asparagine) and individuals that were resistant to cisplatin-induced hearing loss (Peters et al., 2000). Later, another study found associations with protection from cisplatin-induced hearing loss in individuals with a *GSTP1* GG genotype, in contrast to the AG or AA genotype. In this study, only 7% of testicular cancer survivors with the GG genotype had severe hearing loss, while survivors with the other genotypes had more than triple the rate of severe hearing loss (23.4%) (D. Townsend, Deng, Zhang, Lapus, & Hanigan, 2003).

Low-density lipoprotein-related protein 2 (Megalin) is a large endocytic receptor that has multiple diverse functions, including a role in the reabsorption of molecules from the renal proximal tubule (D Mukherjea & Rybak, 2011). It is also highly expressed in cells of the stria vascularis in the inner ear, but not in the sensory hair cells (Mizuta et al., 1999). One study found that, of the two single-nucleotide polymorphisms (SNPs) investigated, only the rs2075252 SNP, with a G to A non-synonymous substitution, was significantly associated with cisplatin-induced hearing loss ≥Grade 2 (Riedemann, Lanvers, Deuster, Peters, & Boos, 2008). This is in contrast with a Canadian study, which showed no significant difference between these SNPs (Ross et al., 2009).

In a Canadian study of pediatric cancer patients treated with cisplatin, researchers assessed 1,949 SNPs thought to be linked to the pharmacokinetics of cisplatin in an initial cohort of 54 patients, then a larger group of 111 patients. The authors identified SNPs in the genes that code for thiopurine *S*-methyltransferase (*TPMT,* rs12201199*)* and catechol *O*-methyltransferase (*COMT,* rs9332377*)* that were associated with hearing loss of ≥Grade 2 (Ross et al., 2009). Further, these authors demonstrated that the presence of more "risk" alleles was associated with an earlier onset of hearing loss (Ross et al., 2009). However, these results were not replicated in a study of 213 medulloblastoma patients, or

in a mouse model with various *TMPT* genotypes (Yang et al., 2013). It has been suggested that discrepancies in the association between these SNPs and the risk of hearing loss could be a result of an insufficient correction for the contribution of ancestry/ethic background to the analysis, and that the initial findings may have been overstated (Hagleitner et al., 2014; Ratain, Cox, & Henderson, 2013).

1.2.2 Nephrotoxicity

1.2.2.1 The Structure and Function of the Mammalian Kidneys

The kidneys are a paired set of bean-shaped organs that lie on either side of the spine, in the upper portion of the abdominal cavity, partially protected by the lowest ribs. The kidneys filter approximately 180 liters of blood/day, removing metabolic waste products, adjusting the pH and osmolarity of bodily fluids. The kidney is divided into two main parts: the surrounding renal cortex and the inner renal medulla. The nephron, or the functional unit of the kidney, spans these two regions (McMahon, 2016). The structure of the mammalian kidney and nephron can be found in **Figure 1.4a.** Each kidney is supplied with blood from the renal arteries, and blood exits through the renal veins, which joins with the inferior vena cava.

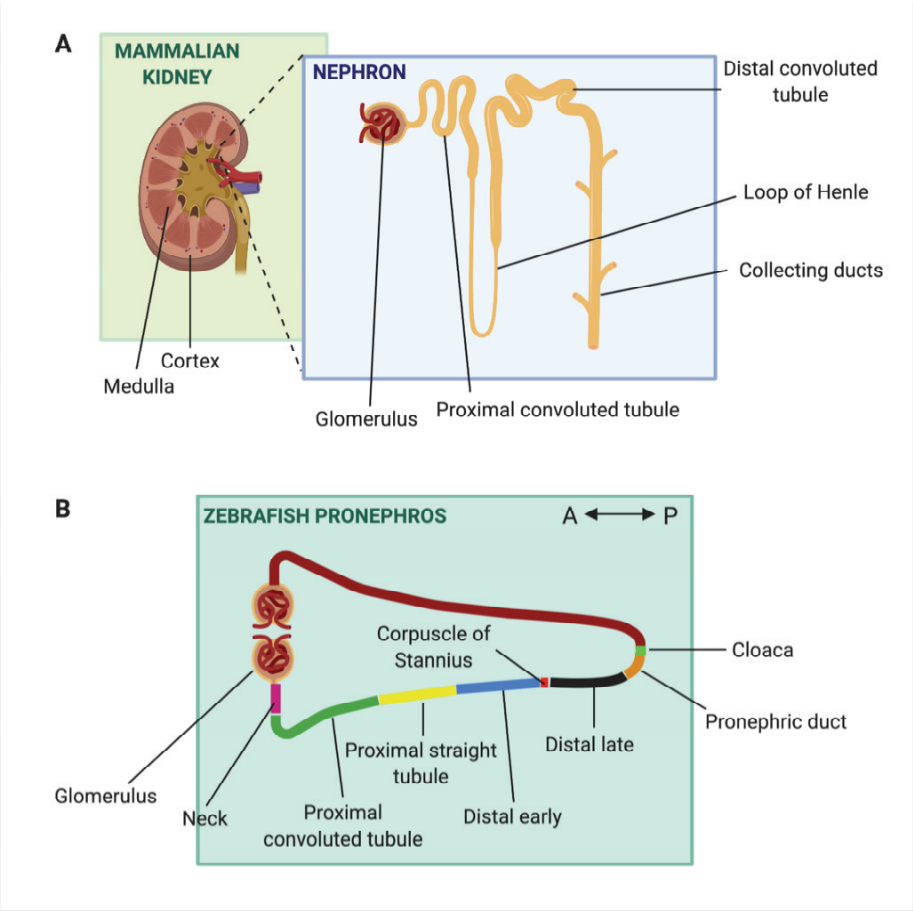

Figure 1.4 Anatomy of the renal systems in humans and zebrafish larvae. A) There are two mammalian kidneys, located on either side of the spine, high up in the abdominal cavity. The kidney consists of the surrounding cortex and interior medulla. The functional unit of the kidney is the nephron. Blood is first filtered at the glomerulus. The filtrate moves through the proximal convoluted tubule, through the loop of Henle, the distal convoluted tubule, then to the collecting ducts. The collecting ducts connect to the ureter and eventually to the bladder. B) The zebrafish pronephros is the functional filtration system in the zebrafish for at least the first two weeks post-fertilization. There are two pronephros structures that run along the sides of the larval spine. The glomeruli meet in the midline, and then the pronephros meet at the cloaca. The glomeruli structures are functionally similar to those found in mammalian kidneys. Recent studies have shown that the pronephros tubule is divided into regions based on gene expression data (Wingert *et al.,* 2007).

The adult kidney is composed of between 1-1.5 million nephrons (Kardasz, 2012). There are two main portions of each nephron: the glomerulus and the tubule. Renal filtration occurs at the renal corpuscle, or the glomerulus. The glomeruli consist of four different cell types: the podocytes that wrap around glomerular capillaries; the glomerular endothelial cells (GECs) that form the glomerular capillaries; the mesangial cells that

form the structure of the glomerulus; and the parietal epithelial cells (PECs), that form a watertight barrier surrounding the glomerulus called the Bowman's capsule (Scott & Quaggin, 2015). The capillaries in the glomerulus are covered in holes, called fenestrae, to facilitate the passage of small molecules. The GECs and the podocytes share surfaces with the glomerular basement membrane, allowing the selective passage of molecules from the blood to Bowman's space, which eventually drains into the proximal tubule (Suh & Miner, 2014). The podocytes interdigitate with each other, forming "podocyte slits" between their small extensions, called finer pedicels. This is another layer of specificity in the filtration process. Typically, all aspects of this multilayered barrier restricts the passage of proteins from the blood to the nephrotic tubule; when compromised, the protein albumin can appear in the urine, which is called proteinurea (Scott & Quaggin, 2015).

The filtrate moves from Bowman's space to the tubular portion, where alterations are made to the filtrate prior to expulsion as urine. Healthy kidneys create approximately 70-85 liters of filtrate/day, yet average humans only excrete several liters of urine/day. The proximal tubule can be divided into three sections: P1 and P2 are located in the cortex, and P3 is in the outer medulla (McMahon, 2016). The cells bordering the proximal tubule are covered in microvilli, are permeable to water, and highly metabolically active. This is the region in which approximately 65% of water, 80% of phosphate, and 80% of calcium is reabsorbed (Kardasz, 2012; McMahon, 2016). From the proximal tubule, filtrate moves through the loop of Henle, which descends into the medulla and then comes back up. This section absorbs about 10-15% of the water in the filtrate. The thin portion of the loop of Henle absorbs water largely as a result of the active uptake of Na^+ from the blood into the interstitium by the distal portions of the loop

(Kardasz, 2012). From the loop of Henle, the relatively hypotonic filtrate enters the distal convoluted tubule, then the collecting tubule. In the distal convoluted tubule, the thiazide-sensitive NaCl cotransporter (NCC) reabsorbs Na^+, and the transient receptor potential cation channel subfamily M member 6 (TRPM6) reabsorbs filtered magnesium (Subramanya & Ellison, 2014). The role of the collecting tubules/ducts is to create the final urine product. This process is regulated by aldosterone levels, altering the relative amounts of Na^+ absorption and K^+ secretion. The collecting tubules also are responsible for the reabsorption of 9% of the water in the original filtrate, a process that is dependent on levels of vasopressin (antidiuretic hormone; ADH) secreted from the posterior pituitary in response to plasma osmolarity (Kardasz, 2012). The daily end product is between 2-3 liters of urine transferred from the collecting tubules, to the ureter, then to the bladder.

1.2.2.2 Incidence and Impact of Cisplatin-Induced Nephrotoxicity

The dose-limiting nephrotoxicity caused by cisplatin treatment has been recognized since the earliest animal and clinical trials with the drug (Gonzales-Vitale, Hayes, Cvitkovic, & Sternberg, 1977; Higby & Wallace, 1974; Kociba & Sleight, 1971). In one early study, single doses of 100mg/m^2 resulted in transient renal toxicity in 9/9 patients, with 5/9 patients exhibiting irreversible renal damage (Higby & Wallace, 1974). With improved treatment regimens and hydration protocols, the incidence of cisplatin-induced acute renal failure has declined significantly, and although it is challenging to approximate, estimates suggest that one third of adult patients that receive cisplatin experience nephrotoxicity (Crona et al., 2017; Latcha et al., 2016). In a recent single-center review of pediatric patients demonstrated that 66% of patients had a detectable

decline in GFR, and 94% had declines in both magnesium and potassium concentrations (Finkel, Goldstein, Steinberg, Granowetter, & Trachtman, 2014). When renal damage is detected, physicians can lower the dose or remove cisplatin completely from the chemotherapy regimen. If the damage is severe or long-lasting, patients may require dialysis or other interventions.

There are two main types of cisplatin-induced kidney damage: acute kidney injury (AKI) and chronic kidney disease (CKD). While cisplatin is typically associated with AKI, these two pathologies are intrinsically linked. Broadly speaking, AKI can be at least partially reversible if treated effectively, and is typically caused by a stressor, with examples like nephrotoxic drug administration, surgery, or hypovolemia (Case, Khan, Khalid, & Khan, 2013). In contrast, CKD is a progressive condition that is fatal without dialysis or kidney transplant. It is typically characterized by inflammation, fibrosis, and hypoxia in the kidney (Ferenbach & Bonventre, 2017). Longitudinal studies suggest that patients that have recovered from AKI have at least a 2 fold increased likelihood of developing subsequent CKD, in comparison with individuals that have never experienced AKI (Bucaloiu, Kirchner, Norfolk, Ii, & Perkins, 2012). Even more concerning, patients without an AKI, but with CKD had a 30.6% mortality rate, while this rate was 42.1% in patients with CKD following recovery from an AKI (Bucaloiu et al., 2012). Additionally, pre-existing CKD is a well-recognized risk factor for AKI (Manohar & Leung, 2018).

AKI typically is detected several days to a week following cisplatin administration, and typically recovers within 2-4 weeks (G. Daugaard & Abildgaard, 1989; Miller, Tadagavadi, Ramesh, & Reeves, 2010). Long-term studies of renal function are somewhat variable. Some studies report no significant changes to GFR over 10 years (Roderick Skinner et al., 2009; Stohr et al., 2007), while others report gradual, but

permanent declines in GFR (Latcha et al., 2016). This discrepancy may be a result of differences in patient populations, as older age at time of cisplatin treatment is known to be correlated with more severe renal impairment (Wen, Zeng, Shu, & Guo, 2015).

1.2.2.3 Proposed Mechanisms of Nephrotoxicity

Similar to cisplatin-induced ototoxicity, there is overlap between the pathogenesis of nephrotoxicity and the desired activity of the drug. However, there are several features of the kidney that heighten the amount of damage that is done to this tissue.

First, cisplatin is mainly excreted renally. This creates a situation where cisplatin is unavoidably in contact with a region that is uniquely susceptible to damage. The concentration of cisplatin in the proximal tubule cells is 5 times greater than that in the serum (Safirstein, Miller, & Guttenplan, 1984), which contributes to the nephrotoxicity of the drug (Kuhlmann, Burkhardt, & Ko, 1997). The concentration of cisplatin is highest in the S3 segment of the proximal tubule, followed by the distal collecting tubule, then the S1 portion of the proximal tubule (Kroning, Lichtenstein, & Nagami, 2000). It is thought that cisplatin is taken up in these regions by passive diffusion, OCT2, and potentially Ctr1-mediated active transport (Giuliano Ciarimboli, 2012; J. A. Sprowl et al., 2013). Once inside the renal tubular cells, evidence suggests that the metabolism of cisplatin mediates nephrotoxicity (D. Townsend et al., 2003). Briefly, cisplatin is conjugated to glutathione, and then is converted to a highly nephrotoxic, reactive thiol. This is accomplished via a γ-glutamyl transpeptidase and cysteine S-conjugate β-lyase-dependent pathways (D. Townsend et al., 2003). Inhibition of either of these pathways blocks the nephrotoxicity of cisplatin (D. M. Townsend & Hanigan, 2002).

While the main site of desired chemotherapeutic action is nuclear DNA, research suggests that other organelles are impacted by cisplatin. Studies suggest that the density of mitochondria and relative integrity of the mitochondrial membrane potential correlate with the sensitivity of cells to cisplatin-induced damage (Hirama, Isonishi, Yasuda, & Ishikawa, 2006; Qian et al., 2005). Further, mitochondrial DNA may be more sensitive to adduct-induced damage as a result of it not being packaged around protective histone proteins, and fewer having repair systems (Manohar & Leung, 2018; Olivero et al., 1997). Mitochondrial stress results in decreased energy production and could lead to caspase-mediated apoptosis.

Inflammation and oxidative stress also play major roles in the nephrotoxicity of cisplatin. The importance of ROS levels is emphasized by the nephroprotective effects of compounds like N-acetylcysteine, which will be discussed below. Inflammation is mediated by TNF-α in the kidneys. One study assessed the role of TNF-α in cisplatin-induced kidney failure by treating mice with cisplatin + TNF-α inhibitors, resulting in decreased renal injury and higher survival rates (Ramesh, Reeves, Ramesh, & Reeves, 2002).

1.2.2.4 Nephrotoxicity Detection

The gold standard for nephrotoxicity detection is measuring the glomerular filtration rate (GFR) of an exogenous filtration marker, like inulin. Normal GFR values for young men and women are 130 ml/min/1.73m^2 and 120ml/min/1.73m^2, respectively. The normal rate declines with age. The definition of CKD is $\leq$60 ml/min/1.73m^2 (Stevens, Coresh, Greene, & Levey, 2006). However, this method is expensive, time consuming, requires an intra-venous (IV), and somewhat variable. Typically, clinical

practice will estimate GFR based on endogenous filtration markers, including serum creatinine levels. Creatinine is a small protein that filters freely across the glomerulus, and unlike inulin, can also be secreted by renal tubules (Jonge & Verweij, 2006). Mean serum creatinine values for men and women are 1.13 and 0.93 mg/dl, although these values vary by race (Jones et al., 1998). Most clinical trials exclude patients from the study of cisplatin-induced nephrotoxicity with serum creatinine >1.5mg/dl or creatinine clearance values <50ml/min (Crona et al., 2017). GFR values can be estimated by a variety of formulas, including the Cockcroft-Gault and the Modification of Diet in Renal Disease (MDRD) equations (Stevens et al., 2006). Both of these equations use age, sex, weight, and serum creatinine levels, but the MDRD equation includes a modifier for black subjects.

There are additional aspects to renal health that can be modified with cisplatin exposure. Blood urea nitrogen (BUN) levels are another measure of renal function. BUN is produced as a normal by-product of protein digestion, and the range for "normal" values is 7-20mg/dl. Proteinuria is another feature of cisplatin-induced tubular damage that can be detected clinically (Deconti, Toftness, Lange, & Creasey, 1973; Jonge & Verweij, 2006; Miller et al., 2010). Levels of protein, usually albumin, are often monitored for signs of damage to the tubules (Barratt, Mclaine, & Soothill, 1970; Crona et al., 2017). Albumin levels are often reported as an albumin:creatinine level. The National Kidney Foundation describes anything <30mg/g normal. Another important measure for cisplatin-induced renal damage is serum levels of magnesium. Low levels of magnesium, or hypomagnesemia, is a well-recognized characteristic of cisplatin therapy (Schilsky & Anderson, 1979), occurring in at least 30% of patients. Novel biomarkers for the early detection of either AKI or CKD during or after cisplatin treatment like the

kidney injury molecule-1 (KIM-1) (Tekce, Uyeturk, Tekce, Uyeturk, & Aktas, 2015) are under investigation, but none are currently used in clinical practice.

1.2.2.5 Nephrotoxicity Grading Schema

Similar to ototoxicity, there is a wide degree of variability in the reporting of cisplatin-induced nephrotoxicity. A recent systematic review of the literature determined that of 24 research studies using both cisplatin and a hydration regimen, nine studies defined nephrotoxicity according to the Common Terminology Criteria for Adverse Events (CTCAE) version 4.0, which have been slightly refined for version 5.0 ("Common termniology criteria for adverse events (CTCAE)," 2017). The current classification of acute kidney injury in this schema is: Grade 2= >1.5-3X baseline creatinine clearance levels or >1.5-3X the upper level of normal (ULN); Grade 3=hospitalization indicated; Grade 4=Life-threatening consequences, dialysis indicated; Grade 5= Death. Five of the studies in the systematic review defined nephrotoxicity as a change in creatinine clearance, with various specifications (Crona et al., 2017). The remaining 10 studies used self-defined parameters for nephrotoxicity. It is important to remember that basal levels of calculated GFR and/or creatinine clearance differ person-person based on a variety of parameters; thus, it is typically more important to measure the change in an individual's parameters over time, rather than the absolute rate.

1.2.2.6 Susceptibility to Cisplatin-Induced Nephrotoxicity

Similar to ototoxicity, there is significant variability in the likelihood of patients developing cisplatin-induced nephrotoxicity. High cumulative doses (Caglar et al., 2002) and higher dose rates are known to increase risk of nephrotoxicity (Erdlenbruch et al.,

2001; R Skinner et al., 1998; Stewart, Mikhael, & Deidre, 1997). Generally speaking, longer infusions are preferable to shorter administrations of the same amount of drug. For example, in pediatric patients receiving cisplatin, a dose rate of <40mg/m^2/day was significantly less likely to produce symptoms of nephrotoxicity than dose rates >40mg/m^2/day (R Skinner et al., 1998).

In contrast with ototoxicity, elderly patients seem to have an increased risk of developing cisplatin-induced nephrotoxicity (Argiris, Li, Murphy, Langer, & Forastiere, 2004; Wen et al., 2015). However, it is important to note that kidney function typically declines with age (Stevens et al., 2006); as such, determining the contribution of cisplatin to the overall decline of kidney function can be more challenging. However, even studies of pediatric populations suggest that long term renal outcomes are worse in patients that were older at the time of treatment (Roderick Skinner et al., 2009).

Other risk factors for cisplatin-induced nephrotoxicity include concomitant administration of nephrotoxic compounds, including gemcitabine and/or non-steroidal anti-inflammatories (NSAIDs) (Stewart et al., 1997). Pre-existing conditions including liver disease and diabetes can also be risk factors for nephrotoxicity. Interestingly, patients with lower blood albumin levels are more likely to develop symptoms of cisplatin-induced nephrotoxicity, likely as a result of more available, unbound cisplatin (Manohar & Leung, 2018; Stewart et al., 1997).

Similar to ototoxicity, evidence suggests that there are some genetic polymorphisms that predispose or protect individuals from cisplatin-induced nephrotoxicity. One example is *SLC22A2*, which encodes OCT2, the protein known to play a role in cisplatin uptake, specifically in renal tubule cells (Filipski, Mathijssen, Mikkelsen, Schinkel, & Sparreboom, 2009). This study assessed correlations between

SNPs in *SLC22A2* and the susceptibility to cisplatin-induced nephrotoxicity, and the authors found that a G to T substitution at rs316019 was associated with significantly less toxicity in comparison to individuals with the wild-type gene (Filipski et al., 2009). However, a recent systematic review examined the 14 polymorphic genes determined to be relevant to cisplatin-induced nephrotoxicity by 28 individual studies, and found that only three variants were consistently reported as significant contributors: *SLC22A2, ERCC1 and ERCC2* (Zazuli et al., 2018). Unsurprisingly, all of these genes produce proteins that play a major role in either cisplatin uptake (*SCL22A2)* or the repair of cisplatin-induced DNA damage (*ERCC1* and *ERCC2).*

1.2.3 Attempts to Mitigate Toxicities

Ever since the initial clinical trials using cisplatin, the dose-limiting toxic side effects have been known. Thus, there has been enormous effort put into the hunt for either less toxic analogs of cisplatin, dose modification strategies to avoid toxicity, and adjuvant drugs that can protect against cisplatin-induced toxicity.

As previously mentioned, high single doses of cisplatin are more likely to cause both oto- and nephrotoxicity (Erdlenbruch et al., 2001; Kopelman et al., 1988; Y. Li et al., 2004; Reddel et al., 1982; R Skinner et al., 1998; Stewart et al., 1997). Thus, early on, clinicians recognized the benefit of longer infusion times, and the avoidance of a bolus administration. Typically, any cisplatin infusion of >50mg/m^2 is done relatively slowly, over several hours, with hydration therapy (Lokich, 2001).

The profound toxicity of cisplatin led chemists to search for analogs with similar efficacy, but better toxicity profile. Carboplatin, a variant of cisplatin, was introduced in the 1980s as a cisplatin alternative. While gastrointestinal toxicity and nephrotoxicity

toxicity profiles are improved, nausea is similar, and myelosuppression is dose-limiting. Carboplatin was approved for use in ovarian cancer by the FDA in 1989. However, studies show that 20-40X higher doses of carboplatin are required to produce the same number of DNA-drug adducts, likely as a result of slower aquation of carboplatin in comparison with cisplatin (Knox, Friedlos, Lydall, & Roberts, 1986). Further, efficacy may be inferior in certain cancers like germ cell tumours (Shaikh, Nathan, Hale, Uleryk, & Fraizer, 2013). Oxaliplatin is a newer platinum compound that has yet a different toxicity and activity profile. Oxaliplatin is effective in colon cancers, especially in combination with 5-fluorouracil (5-FU), which have historically been recognized as insensitive to both cisplatin and carboplatin (Kelland, 2007; Raymond, Faivre, Chaney, Woynarowski, & Cvitkovic, 2002). As a result of several very successful Phase III clinical trials (de Gramont et al., 2000; Giacchetti et al., 2000; Goldberg et al., 2004; Rothenberg et al., 2003), oxaliplatin was approved for use in metastatic colorectal cancer (as a second line therapy) and then previously untreated colorectal cancer in combination with 5-FU and leucovorin in 2002 and 2004, respectively (Kelland, 2007). Dose limiting toxicities of oxaliplatin include myelotoxicity and peripheral nerve damage (Alcindor & Beauger, 2011). Cisplatin is still the mainstay of many treatment regimens, as equivalency in therapeutic effects have not been demonstrated for these compounds in most tumour types (Kelland, 2007; Lokich, 2001; Pasetto, D'Andrea, Brandes, Rossi, & Monfardini, 2006). However, having a variety of platinum compounds may prove useful in instances of drug resistance or individual patients that are high-risk for certain toxicities.

It is also well-established that adequate hydration protocols are beneficial in avoiding cisplatin-induced toxicity (Crona et al., 2017). Even before cisplatin was

approved by the FDA, it was recognized that treatment with cisplatin was improved greatly with aggressive prehydration techniques (Cvitkovic, Spaulding, Bethune, Martin, & Whitmore, 1977). Several studies support the safety and efficacy of short hydration regimens as equivalent in benefit to continuous infusion (Ouchi, Asano, Aono, Watanabe, & Kato, 2014; Tiseo et al., 2007). A recent systematic review of 24 studies investigating the effects of hydration with or without forced diuresis and/or magnesium supplementation suggest the following dose-specific guidelines: $<50mg/m^2$ = short-duration (2-6 hr) outpatient hydration, low volume hydration +/- potassium supplementation; $\geq 50mg/m^2$ = same as previous, +/- magnesium supplementation (8-16 mEq); $>100mg/m^2$ or patients with hypertension = same as previous, consider adding mannitol (Crona et al., 2017).

There are a wide variety of pre-clinically tested oto- and nephroproective agents discovered every year. Several recent discoveries include cyclin-dependent kinase 2 (CDK-2) inhibitors, including kenpaullone (Teitz et al., 2018), and a mechanoelectrical transducer (MET) channel inhibitor ORC-13661 (Kitcher et al., 2019). The following is not meant to be a complete review, but an overview of trends, and some more well-studied examples.

Antioxidants have long been investigated as a potential oto- and nephroprotective treatment strategy, likely as a result of the known role of elevates ROS levels in these regions following cisplatin treatment. Some examples include melatonin (Sener et al., 2000), vitamins C and E (Kadikoylu et al., 2004; Weijl et al., 2004), lipoic acid (Leonard P Rybak, Husain, Whitworth, & Somani, 1999; P. Rybak & Whitworth, 1999), and D-methionine (Campbell et al., 2007; Campbell, Rybak, Meech, & Hughes, 1996; Lorito et al., 2011; Ototoxicity et al., 2004).

Amifostine, originally known as WR-2721, was developed with the intent of protecting healthy tissues from anti-cancer radiotherapy. Early animal trials suggested protection against radiation-induced toxicities, including skin ulceration. However, there was also modest (15%) protection to the transplanted mammary tumours by amifostine (Yuhas, Jackson, & Harbor, 1969). Amifostine is converted to the its active form once dephosphorylated by alkaline phosphatase, where it acts as a thiol, capable of scavenging ROS and protecting cells from damage (Kouvaris, Kouloulias, & Vlahos, 2007). Various clinical trials have assessed the efficacy of amifostine for the prevention of cisplatin-induced hearing loss in pediatric populations, with varying results. An early study included amifostine (740 mg/m^2/dose) for a 15 min IV infusion prior to cisplatin infusion for the treatment of osteosarcoma. The authors did not observe oto- or nephroprotection with amifostine, and 93% of patients in the experimental arm reported grade 3 vomiting toxicity (Gallegos-Castorena et al., 2007). The same dose was tested in patients with hepatoblastoma; this study also demonstrated a lack of protection (Katzenstein et al., 2009). In a subsequent study of average-risk medulloblastoma patients, 600 mg/m^2/dose amifostine was given both immediately prior to and 3 hr into cisplatin treatment. At a one-year follow-up, this dosing regimen resulted in significant (14.5 vs. 37.1%) protection against grade 3 or 4 ototoxicity (Fouladi et al., 2018). Currently, amifostine is approved by the FDA for the use in protecting against both radiation-induced xerostomia (dry mouth) in head and neck cancer patients; however, it has also shown efficacy in protecting patients with ovarian cancer from cisplatin-induced cumulative renal damage (Lorusso et al., 2003).

N-acetylcysteine (NAC) is a precursor to glutathione, a naturally occurring cellular antioxidant. World Health Organization (WHO) List of Essential Medicines

included acetylcysteine as a result of its activity as an antidote for acute liver toxicity associated with acetaminophen overdose (Green, Reynolds, & Albert, 2013; "World Health Organization Model List of Essential Medicines, 21st List," 2019). N-acetylcysteine has also shown protection against radiographic contrast agent-induced renal damage (Tepel et al., 2000). Studies in rats demonstrated that NAC (400 mg/kg) protected against cisplatin-induced elevation in BUN and creatinine (Dickey, Wu, Muldoon, & Neuwelt, 2005), and against cisplatin-induced changes in ABR, especially at high frequencies (Dickey, Muldoon, Kraemer, & Neuwelt, 2004). Interestingly, these researchers noted that NAC seemed to have a general protective effect, as the rats treated with cisplatin + NAC experienced less overall weight loss in comparison with the cisplatin + saline-treated controls (Dickey et al., 2004). Evidence suggests that NAC (+/- sodium thiosulfate) protected the bone marrow from chemotherapy-induced damage in a rat xenograft model, without modification of the anti-cancer effects of the drug. However, this study was using carboplatin, not cisplatin (Neuwelt, Pagel, Kraemer, Peterson, & Muldoon, 2004). Rat studies of both neuroblastoma (NBL) and medulloblastoma xenografts demonstrate that 30 min pretreatment with NAC significantly reduced the anti-cancer efficacy of cisplatin, while treatment with NAC 4 hr following treatment did not. Interestingly, NAC only provided nephroprotection in the NBL treatment group (L. Muldoon, Wu, Pagel, & Neuwelt, 2015). Currently, NAC is being investigated in a Phase I clinical trial with pediatric oncology patients being treated with cisplatin ("NAC to Prevent Cisplatin-Induced Hearing Loss" NCT02094625). Dose escalation trials were performed, and the current dose is 450 mg/kg, given IV over one hour, 4 hr following cisplatin treatment.

Sodium thiosulfate (STS) is the antidote for cyanide poisoning, and is also on the WHO List of Essential Medicines for this purpose ("World Health Organization Model List of Essential Medicines, 21st List," 2019). It has been tested in models of rat models of toxicity, and while a of $8g/m^2$ was otoprotective, it was not consistently nephroprotective in the *in vivo* experiments (Dickey et al., 2005). In an earlier animal study (Doolittle et al., 2001) and a follow up clinical study (Doolittle et al., 2001), STS was effective at reducing ototoxicity, while not impacting the anti-cancer efficacy of the platinum compound, but these studies used carboplatin not cisplatin. Furthermore, these studies emphasize the importance of timing in the administration of protective compounds. Past studies have determined pre-treatment with NAC and post-treatment with STS seems to reduce toxicities, while reducing potential interference with cancer-related cytotoxicity (Dickey et al., 2005; Doolittle et al., 2001; Neuwelt et al., 2004). Phase III clinical trials using STS for otoprotection in cisplatin-treated pediatric patients have been completed recently (Freyer et al., 2017). While patients in the treatment arm had a reduced incidence in hearing loss in comparison with the control group (28.6% vs. 56.4%), there was significantly lower survival in participants with disseminated disease that received STS treatment (Freyer et al., 2017). This result is particularly worrisome for pediatric cancers like NBL, in which 50% of patients already have metastatic disease at the time of diagnosis (Morgenstern, Baruchel, & Irwin, 2013).

1.2.4 Models of Cisplatin-Induced Toxicity

The methods to study cisplatin-induced toxicity range in complexity, from *in vitro* cell culture studies, to organoid, or *ex vivo* animal experiments, to experiments completed

in zebrafish, to those completed in mouse and rat models. The following will discuss some of the main models used in relevant studies.

The use of cell culture to study healthy human tissues is complicated by the fact that healthy human cells are not transformed, and thus will not replicate indefinitely. Several kidney cell lines have been developed for the study of kidney function, including LLC-RK1 (rabbit), OK (opossum), LLC-PK1 (pig), MDCK (dog), HK-2 cells (human), and HK-5 (human) cells (Gstraunthaler, Pfaller, & Kotanko, 1985; Racusen et al., 1996; Ryan et al., 1994; Y. R. Zhang & Yuan, 2010). It is important to recall that the popular HEK-293 cell line was isolated from a fetus and is likely of adrenal origin; as such, this cell line is not an appropriate model for healthy renal cells.

The availability of human hair cell models to study ototoxicity is more challenging. Until very recently, the otic cell lines available were mostly derived from the Immortomouse, which is an animal that expresses a stably incorporated copy of *ts*A58 that is inducible by γ-interferon. Cells isolated from this mouse that are cultured at 33ºC and exposed to γ-interferon will allow for proliferation of the cells without differentiation (Jat et al., 1991). HEI-OC1 (House Ear Institute-Organ of Corti 1) cells are one of the most popular cell lines derived from Immortomouse cochleas (Kalinec, Webster, Lim, & Kalinec, 2003). A variety of cell lines from different developmental stages and anatomical locations of the mouse have been isolated over time (Rivolta & Holley, 2002). However, these cells need to be cultured at a different temperature than the typical 37ºC and are not human cells. More recently, hair-like cells have been differentiated from rat bone marrow mesenchymal stem cells (Qin et al., 2011) and *ex vivo* expanded otospheres have been derived from mouse cochlea (Lou, Nakagawa, Ohnishi, Nishimura, & Ito, 2013). Further, researchers have been able to induce inner ear organoids that contain hair

cells (Jeong et al., 2018; Koehler et al., 2017). However, the efficiency and cost of this type of technology is unlikely to be amenable to high-throughput screening in the near future.

Murine studies, both whole-animal and with the isolated organ of Corti, have been used to study hearing loss. Advantages of using either mice include the fact that they are mammals, amenable to a battery of well-established behavioural tests, and the availability of a wide array of genetic information, including many established mutant lines (Avraham, 2003). However, mice are known to be relatively resistant to drug-induced ototoxicity, resulting in difficulty when interpreting data (Blakley, Hochman, Wellman, Gooi, & Hussain, 2008; H. C. Ou, Santos, Raible, Simon, & Edwin, 2010). This, combined with the relative expense of maintaining mice, makes this species unsuitable for medium-high throughput drug screening.

1.3 Zebrafish

1.3.1 History of Use in Research

The zebrafish, or *Danio rerio*, is a freshwater fish native to the Ganges river in India. It has been a popular aquarium species for years, likely as a result of its hearty and adaptable nature. Zebrafish were initially used as a model organism for developmental biology (Lieschke & Currie, 2007). External fertilization and transparent embryos enable the straightforward visualization of the early stages of organogenesis and development, without the need for expensive equipment. Further, they are relatively inexpensive to maintain, have quick generation times, produce large numbers of offspring, and develop rapidly (Zon & Peterson, 2005).

1.3.2 Use in Cancer Research

It is widely accepted that fish species spontaneously develop cancer, which is also true for zebrafish. The initial work establishing the utility of zebrafish as a cancer model organism to was the observation that low-level carcinogen exposure could lead to tumour formation in zebrafish (Pliss, Zabezhinski, Petrov, & Khudoley, 1982). This led researchers to studies exposing zebrafish to carcinogens like ethylnitrosurea (ENU) and N-methyl-nitroguanadine (MNNG), resulting in a variety of cancer, including skin papillomas and rhabdomyosarcoma (Jan, Reddy, Miller, Hendricks, & Bailey, 2000; Spitsbergen et al., 2000). Discoveries in the field of transgenics spurred the next wave of zebrafish cancer models, including the *Myc-recombination activating gene 2 (rag2)* leukemia model (Langenau et al., 2003) and the *tp53* mutant fish line that develops peripheral nerve sheath tumours (Berghmans et al., 2005). The development of new genome editing technologies, like clustered regularly interspaced palindromic repeats (CRISPR)-Cas9 based knock-out or knock-in approaches have revolutionized disease modelling in the zebrafish, allowing researchers a quicker, easier, and often more precise genome editing (Prykhozhij, Caceres, & Berman, 2017).

Another method to study cancer in the zebrafish is with xenotransplantation (XT), or the transfer of human cancer cells into the zebrafish (Haldi, Ton, Seng, & McGrath, 2006; Lee, Seftor, Bonde, Cornell, & Hendrix, 2005; Wertman, Veinotte, Dellaire, & Berman, 2016; C. Yan et al., 2019). These studies can be done in the larval stages, when the adaptive immune system has not yet developed, obviating the need for immunosuppression, or at the adult stage. The Berman lab has pioneered the use of larval XT studies for the study of cancer cell line proliferation and response to chemotherapeutics (Corkery, Dellaire, & Berman, 2011), cancer cell migration (El-

Naggar et al., 2015), and the assessment of primary cancer cell behaviour and response to drugs *in vivo* (Bentley et al., 2015). Additionally, this XT model has been used to assess the impacts of visnagin, a compound that was found to prevent doxorubicin-induced pericardial edema in a zebrafish drug screen, on the anticancer efficacy of doxorubicin *in vivo* (Liu et al., 2014).

1.3.3 Use of Zebrafish in the Study of Drug-Induced Toxicities

There are many attributes of the zebrafish that make it well-suited to the study of toxicology. The small size of the larvae, the ease with which most compounds can simply be added to the water, the optical clarity, and rich of developmental biology knowledge makes zebrafish amenable to most toxicology experiments (Spitsbergen & Kent, 2003). As a result, the zebrafish has been used extensively for the study of cisplatin-induced toxicity. Typically, researchers have either added cisplatin to the E3 water surrounding the larvae, or injected it directly into the circulation of either larvae or adults (Hentschel et al., 2005; H. Ou, Raible, & Rubel, 2007). Significant for this study, the zebrafish lateral line has been used to study cisplatin-induced ototoxicity and is visibly and functionally damaged following treatment (Buck, Winter, Redfern, & Whit, 2012; H. Ou et al., 2007). The zebrafish larval kidney structure, the pronephros, is also known to be functionally impaired following the injection of cisplatin (Hentschel et al., 2005). For the purposes of the present study, I will focus on the use of zebrafish to study oto- and nephrotoxicity.

1.3.3.1 Ototoxicity

The zebrafish is an attractive model to study ototoxicity as a result of the ease of visualization of the lateral line and inner ear structures, in addition to their similarity to human organs. The zebrafish possesses an accessible/superficial lateral line system that contains neuromast clusters that are functionally related to hair cells within the mammalian ear (Baxendale & Whitfield, 2016; Ghysen & Dambly-Chaudière, 2007). For the purposes of this work, the lateral line was used for drug screening and initial scheduling and dose optimization, while inner ear assessment was used for further validation.

1.3.3.1.1 The Lateral Line

The zebrafish lateral line is a sensory system found in fish and amphibians that is similar to the mammalian auditory system (Baxendale & Whitfield, 2016). It consists of distinct organ structures called neuromasts that are arranged in canonical, species-specific patterns (Dambly-Chaudière et al., 2003). Originally thought to be mucus-secreting structures, neuromasts were eventually established to have some type of sensory capabilities based on the physical similarity between neuromast hair cells and inner ear hair cells. Sven Dijkgraaf eventually devised the term *ferntastinn,* meaning "touch at a distance," describing the mechanosensory abilities of the lateral line (Chitnis, Nogare, & Matsuda, 2012; Dijkgraaf, 1989). The lateral line has since been recognized for its unique role in regulating rheotaxis, or the ability of teleost species to orient themselves into the flow of water (Montgomery, Baker, & Carton, 1997). The lateral line now has established

roles in feeding and prey detection, obstacle avoidance, and schooling behaviours (Baxendale & Whitfield, 2016; Chitnis et al., 2012).

The zebrafish lateral line consists of two main portions: the anterior lateral line (ALL), which consists of the neuromasts surrounding the head and jaw of the fish, which are innervated by the ALL ganglion, anterior to the ear; and the posterior lateral line (PLL), running along the body of the fish, with sensory neurons located caudal to the ear (Dambly-Chaudière et al., 2003; Gompel, Cubedo, Thisse, Thisse, & Dambly-Chaudie, 2001). Development of the PLL is strictly regulated and has thus been subject of intense study. The PLL forms from a group of called the lateral branch of the PLL primordium, which can be found posterior to the otic vesicle (Gompel et al., 2001; Kimmel, Ballard, Kimmel, Ullmann, & Schilling, 1995). This primordium detaches from the basement membrane, and begins to migrate along the side of the embryo, by approximately 20 hours post fertilization (hpf) (Gompel et al., 2001; Kimmel et al., 1995). A small subset (approximately 20 cells) remain in the original location, eventually forming the PLL ganglion (Gompel et al., 2001). The rest of the migratory primordium moves caudally, depositing clusters of 20-30 cells at regularly-spaced intervals along the body of the fish, which are called protoneuromasts (Ghysen & Dambly-Chaudière, 2007; Gompel et al., 2001). This migratory process results in the ALL neuromasts surrounding the head, and 5 PLL neuromasts along the side of the fish, with 5 neuromasts along each side of the tail, with 2-3 terminal PLL neuromasts close to the caudal fin (Ghysen & Dambly-Chaudière, 2007).

Each neuromast is comprised of a group of hair cells (20 ± 2 cells/neuromast in 10-day old fish), which each possess one kinocilia, and multiple stereocilia (Dambly-Chaudière et al., 2003; Williams & Holder, 2000). The kinocilium responds to movement

in two ways. When moved in one direction, it results in cell depolarization, and when moved in the opposite direction, results in hyperpolarization (Dambly-Chaudière et al., 2003). The hair cell bodies are at the base and contain the nuclei. The hair cells are surrounded with two types of non-sensory cells: the supporting cells between the hair cells, that keep their kinocilia from touching each other, and the mantle cells, that secrete the gelatinous substance that makes up the culupa that wraps around the cilia (Dambly-Chaudière et al., 2003; Williams & Holder, 2000). Each neuromast is coupled with at least two sensory afferent neurons, and two efferent inputs: an inhibitory input from the hindbrain, and an excitatory from the forebrain (Dambly-Chaudière et al., 2003; Ghysen & Dambly-Chaudière, 2007). Interestingly, zebrafish neuromasts consistently regenerate and are usually in a state of turnover. This helps to explain the ability of zebrafish to regenerate neuromasts and hair cells following damage with ototoxins like aminoglycoside antibiotics, platinum agents, environmental toxins like copper, and noise (Chitnis et al., 2012; Williams & Holder, 2000). While the regenerative potential of zebrafish hair cells is exciting and like other regenerative features, has been explored in studies of regenerative medicine (J. A. Harris et al., 2003; Williams & Holder, 2000), it is beyond the scope of this particular study.

The lateral line is particularly well-suited to experimental manipulation and examination as a result of its superficial location on the fish. The lateral line primordium and mature lateral line can be detected using typical light microscopy methods. However, for experimental manipulations, researchers typically label one or more aspects of the neuromast cluster with a stable transgenic marker, or a stain (Baxendale & Whitfield, 2016). 2-(4-Dimethylaminostyryl)-*N*-ethylpyridinium iodide (DASPEI), FM1-43, YO-PRO1 and FM 4-64 all label sensory hair cells in living specimens (Baxendale &

Whitfield, 2016; Mcdermott et al., 2010; Tamara M Stawicki, Esterberg, Hailey, Raible, & Rubel, 2015; Whitfield, Granato, Eeden, Schach, & Brand, 1997). Additionally, phalloidin can be used to stain filamentous actin, and thus label the stereocilia of hair cells for either enumeration or morphological comparisons in fixed samples (Baxendale & Whitfield, 2016; Haddon & Lewis, 1996). Phalloidin can be conjugated to a variety of fluorescent dyes, including FITC. Another mechanism to visualize the lateral line is with the use of transgenic fluorescent reporter lines. These will be discussed below in combination with the reporter lines that can be used to assess inner ear structures.

1.3.3.1.2 The Inner Ear

The zebrafish ear is functionally analogous to the mammalian inner ear, although they do not possess an outer or middle ear, or cochlear structure (Fay & Popper, 1999). Although studies of the adult zebrafish ear are useful for many types of experiments, adult ears will only be discussed briefly here, as this study only focused on larval fish. The adult zebrafish ear has three main chambers: the utricle, saccule, and lagena. There are three semicircular canals that merge with the utricle (Haddon & Lewis, 1996). The saccule is thought to be the auditory organ (Zeddies & Fay, 2005), the utricle acts mainly as a vestibular organ (Riley & Moorman, 2000), the lagena is of mixed function (Khorevin, 2008), and the semicircular canals sense rotational motion (Baxendale & Whitfield, 2016). The utricle, saccule and lagena are all overlaid by otoliths, deposits of calcium carbonate and proteins (Baxendale & Whitfield, 2016). The adult zebrafish possesses bony structures called the Weberin ossicles, which transmit noise-induced vibrations from the gas-filled swim bladder to the sensory hair cell patch of the saccule. (Higgs, Rollo, Souza, & Popper, 2003; Zeddies & Fay, 2005).

During larval development, hair cells are visible with phalloidin labelling at 24-30hpf. At 5dpf, there are three smaller visible patches of hair cells, called the anterior, lateral, and posterior cristae, which are the sensory patches within the semicircular canals. At this point there are also two maculae patches: the anterior and the posteriomedial maculae (Haddon & Lewis, 1996). A schematic of the zebrafish larval inner ear can be found in comparison with the human inner ear, in **Figure 1.2.** All main structures of the adult zebrafish inner ear are present by 5dpf, save for the third otolith and two more maculae. Studies suggest that the zebrafish larvae can detect both sound and water movements at 5dpf (Zeddies & Fay, 2005).

Similar to the lateral line structures, the zebrafish inner ear can be visualized with a variety of stains and antibodies. In order to stain the inner ear, the otolith must first be dissolved/permeabilized, typically with Triton-X-100 (Baxendale & Whitfield, 2016). Phalloidin effectively labels both the hair cell stereocilia and the hair cell plate below. This can be combined with anti-acetylated Tubulin antibodies to mark kinocilia (Baxendale & Whitfield, 2016). To observe the overall structure of the developing canal and lumen structures, anesthetized larvae can be injected in the ear with fluorescein dextran, then imaged immediately (Feng & Xu, 2010; Hammond & Whitfield, 2006).

The zebrafish also allows researchers the opportunity to perform genetic modifications, creating reporter lines that facilitates the visual observation of specific cell or tissue types (Wertman et al., 2016). There are many combinations of promoters and different reporter genes, with many new ones being developed all the time. For example, the *myo6b* and *pou4f3* promoters have been used to couple reporter proteins to sensory hair cell stereociliary bundles (Buck et al., 2012; Obholzer et al., 2008; T. M. Stawicki et al., 2014; Xiao, Roeser, Staub, & Baier, 2005). Additionally, these promoters can be used

to drive the expression of proteins capable of elucidating function of different cell types, like calcium reporting proteins for live imaging (Esterberg, Hailey, Coffin, Raible, & Rubel, 2013; Esterberg, Hailey, Rubel, & Raible, 2014).

One of the main benefits of working with zebrafish is that as a vertebrate, it is possible to undertake behavioural analyses that would be challenging or impossible in lower organisms. An excellent example of this is the battery of tests that is available to study the function of the zebrafish lateral line and inner ear. Behavioural tests can be as simple as counting the percentage of larvae that are correctly oriented, dorsal side up, in their culture dish. Larvae lacking a vestibular function may be laying on their side, or swimming in circles (Baxendale & Whitfield, 2016). Rheotaxis tests can also be done relatively simply, using an individual larva in a well of a 24-well plate. Water is pipetted against the side of the well to cause circular water flow. The response can then be observed and scored, based on whether or not the larva orients itself into the flow of the water (Buck et al., 2012). More complex and precise measurements can be made of either larvae or adult fish using a specialized flume, within which the specimen can be videotaped and observed (Suli, Watson, Rubel, & Raible, 2012). Another method to test the vestibular function of adult fish is by using a "drop test," in which adult fish are dropped into a novel environment from a net at 10 cm above the surface of the water. This experiment can be recorded, measuring the amount of time taken to revert to a regular dorsal-up swimming position (Baxendale & Whitfield, 2016). In order to measure the function of the auditory function of both larval and adult zebrafish, the specimens are exposed to a sound of known decibels and frequency, and are video recorded to determine whether or not they exhibit an "escape response." This escape response looks like a distinct and obvious C-shaped flex in larvae in response to a stimulus (Bang,

Yelick, Malicki, & Sewell, 2002; Baxendale & Whitfield, 2016; Buck et al., 2012). However, this auditory-evoked startle response test requires the use of a high-speed camera and software that is capable of analyzing the videos.

1.3.3.2 Nephrotoxicity

1.3.3.2.1 The Pronephros

The zebrafish pronephros structure consists of two nephrotic tubules that run along the body of the fish, which each have a glomerulus that fuse in the centre, just ventral of the dorsal aorta. The tubules fuse at their posterior ends, joining together at the cloaca (Drummond et al., 1998). Similar to mammals, the zebrafish glomerulus consists of podocytes that interdigitate and form a filter-like surface that allows passage of small molecules through into the surrounding capillaries, while larger molecules remain in the blood filtrate (Drummond & Davidson, 2010). Until recently, it was thought that the tubular structure of each nephron was a simple, undivided tube structure (Drummond & Davidson, 2010; Wingert & Davidson, 2008). With gene expression analysis, however, it has since been determined that the zebrafish pronephros can be divided into multiple subsections (Wingert et al., 2007). This study used *in situ* hybridization assays to determine the spatial patterning of the expression of genes known to be related to the zebrafish pronephros and kidney. Based on the spatial expression of this set of genes, including 15 solute transporters, the pronephros appears to be functionally divided into 8 segments. This newly-defined pronephros structure is compared with the mammalian nephron in **Figure 1.4b.** This study was also the first to highlight the importance of retinoic acid (RA) in the process of proximal nephron patterning, and caudal (*cdx*)

transcription factors in the positioning of the pronephros along the anterioposterior axis (Wingert et al., 2007).

Following epiboly, at approximately 10 hpf, the intermediate mesoderm (IM) forms a band of cells that will give rise to the kidney (Kimmel et al., 1995). This specification relies heavily on appropriate expression of the paired domain transcription factor (pax2.1) and intact RA signalling (Drummond & Davidson, 2010). Tubule formation is the result of mesenchymal-epithelial transitioning, resulting in polarized epithelial cells, where basal portions of cells express the ion transport proteins (Drummond et al., 1998). By 24 hpf, cells of the glomerulus already express the *nephrin* and *podocin* genes that are specific to podocytes, which will prevent massive edema in the larvae (A. Kramer-Zucker, Wiessner, Jensen, & Drummond, 2005). By 48 hpf, epithelial cells can be detected within the glomeruli, and filtration is functional at 4 days post fertilization (dpf) (Drummond et al., 1998; A. Kramer-Zucker et al., 2005).

The study of the zebrafish pronephros can be completed in a variety of ways. H&E staining (Noonan et al., 2016), or electron microscopy (Hentschel et al., 2005)-based analysis can detect some cell and tissue-level changes to the pronephros structure. Other well-known techniques like whole-mount *in situ* hybridization (WISH) or immunofluorescence can also be used to identify specific patterns of gene or protein expression. Pronephros tubules can also be isolated from 2-3 day post-fertilization (dpf) larvae using a 1 hr preincubation with dithiothreitol (DTT) to remove the mucous layer, then a 3-6 hr incubation with collagenase. Following this, tubules can be retrieved using a dissecting microscope (Drummond & Davidson, 2010). The function of the pronephros can be assessed with injection of fluorescent rhodamine dextran into the circulation of the larvae. When filtered, these dextrans can be observed either in endosomes of the tubule

cells (Drummond et al., 1998), or as they exit the larvae via the cloaca (A. G. Kramer-Zucker et al., 2005). A similar experimental system uses injection of fluorescently-labelled inulin into the circulatory system. Inulin is a polysaccharide that is exclusively excreted in the urine; thus, decreases in vascular larval fluorescence represent a functional measure of the filtration capacity of the larvae, or the glomerular filtration rate (GFR) (Hentschel et al., 2005; Rider et al., 2012). This latter approach is optimized and exploited in this thesis.

1.3.3.2.2 The Adult Zebrafish Mesonephros

Since this study deals with larval pronephros structures, the adult zebrafish kidney will be outlined only briefly here. The adult kidney structure is called the mesonephros and is a flat structure located dorsally in the fish (Drummond & Davidson, 2010; Gerlach, Schrader, & Wingert, 2011). At approximately 14 dpf, the mesonephros begins to form around the pronephros, adding nephrons to the structure. By 6 months of age, the mesonephros will contain approximately 450 nephrons (W. Zhou, Boucher, Bollig, Englert, & Hildebrandt, 2010). The mesonephros continues to add nephrons while the fish is accumulating biomass, up until at least 18 months of age (McCampbell, Springer, & Wingert, 2015; W. Zhou et al., 2010). Unlike the larval pronephros, the structures in the mesonephros are branching, with multiple nephrons merging into distal late tubule segments that will ultimately drain into shared collecting ducts (McCampbell et al., 2015).

Similar to larval pronephros studies, histological H&E staining or immunohistochemistry on fish sections are popular methods to examine the mesonephros. Dextran and inulin studies measuring kidney function can also be used in

adults. The kidney can also be surgically removed from both fixed and unfixed specimens, allowing for access to the kidney structures and cells for analysis (Gerlach et al., 2011). Transgenic reporter lines are also a useful tool in the examination of both the pronephros and the mesonephros. For example, *cdh17::*GFP/*pod::*mCherry double transgenic fish express GFP in the ducts and tubules of both pronephric and mesonephric kidney, and mCherry in the pronephric and mesonephric podocytes of the glomeruli (W. Zhou et al., 2010).

1.4 Drug Screening

1.4.1 Overview

Broadly speaking, there are two main types of drug discovery: rational, or target based, and phenotypic, or unbiased drug screens (D C Swinney, 2013; David C Swinney & Anthony, 2011). Analysis of small-molecule compounds approved by the FDA between 1999 and 2008 suggests that 56% were discovered through phenotypic studies vs. 34% that were discovered from target-based screening (David C Swinney & Anthony, 2011), indicating a clear role for phenotype-based screens. Further, phenotype-based screens allow for the identification of potentially unrecognized molecular mechanisms of action of known compounds.

1.4.2 Zebrafish Drug Screens

The small size, high-fecundity, optical transparency, and similar body plan and organ systems to mammals render the zebrafish well-suited to drug screening. Further, most compounds are able to absorb into the larvae, a barrier that can be overcome by injecting the compound into the larvae (Milan, Peterson, Ruskin, Peterson, & Macrae,

2003). Studies have shown the conservation of phenotypic effects of drugs between humans and zebrafish larvae on several occasions. Examples range from the conservation of the highly addictive nature of opioids in a zebrafish self-administration model of drug seeking behaviour (Bossé & Peterson, 2017) to conservation of the effects of cardiac drugs that cause QT elongation in humans (Milan et al., 2003).

As a result of this amenability to high-throughput screening, in addition to the accessibility to the lateral line, researchers have used the zebrafish as a tool for the *in vivo* assessment of compounds that influence hearing (H. C. Ou et al., 2010). Neomycin has known to cause the death of zebrafish lateral line hair cells as early as 2000 (J. A. Harris et al., 2003), while cisplatin was first recognized to cause dose-dependent increases in lateral line hair cell death in 2007 (H. Ou et al., 2007). Since this point, multiple studies have used the lateral line-screening method to identify potential compounds that could protect against ototoxin-induced hair cell death (H. C. Ou et al., 2009; Owens et al., 2008; Teitz et al., 2018; Andrew J. Thomas et al., 2015).

Lateral line-based ototoxicity screens typically involve treating the larvae in a 96-well plate with a library of compounds, +/- the ototoxin in question, at a defined dose, and one or more specific viability stain, like YO-PRO1, FM-143, or DASPEI to label components of the lateral line (H. C. Ou et al., 2010). The larvae are then observed using fluorescent microscopy, and can be scored either manually, or with an automated algorithm (H. C. Ou et al., 2009; Philip et al., 2018; Andrew J. Thomas et al., 2015).

These studies have used a variety of drug libraries, including the ActiProbe 10K library of 10,000 drug-like small molecules (Andrew J. Thomas et al., 2015), the Diverset E library of drug-like compounds (Owens et al., 2008), and the NINDS Custom Collection II library of 1,040 drugs and bioactive compounds (H. C. Ou et al., 2009). To

the best of my knowledge, there are no public reports of the Sigma LOPAC®^{1280} library of pharmacologically active compounds being tested in an *in vivo* zebrafish larval model of cisplatin-induced ototoxicity. This library consists of 1,280 compounds that span a variety of drug types, ranging from kinases to drugs that modulate gene regulation. The medium size of this library, in addition to the inclusion of many FDA-approved compounds, led me to use it for this study.

1.5 Hypothesis and Objectives

I hypothesize that the use of a two-pronged *in vivo* zebrafish larvae ototoxicity and *in vitro* proximal tubule cell line nephrotoxicity assay will lead to the identification of 1-2 candidate compounds that protect against these cisplatin-induced toxicities, without modifying the anti-cancer effects of cisplatin.

Specific Objectives

To establish a medium-high throughput platform for the *in vivo* assessment of cisplatin-induced lateral line ototoxicity and cisplatin-induced alterations in glomerular filtration (GFR).

To perform an *in vivo* ototoxicity screen and an *in vitro* nephrotoxicity screen, assessing the Sigma LOPAC®^{1280} library of pharmacologically active compounds for potential oto- and nephroprotective agents.

To establish whether the candidate protective compounds interfere with the anti-cancer effects of cisplatin.

Chapter 2 Materials & Methods

2.1 Zebrafish Husbandry

The use of zebrafish in this study was approved by, and carried out in accordance with, the policies of the Dalhousie University Committee on Laboratory Animals (Protocols #17-131 and #17-055). Adult *Danio rerio* (zebrafish) were housed in a recirculating commercial housing system (Pentair) at 28°C in 14 hr:10 hr light:dark cycles and bred according to standard protocol (Westerfield, 1995). Embryos were maintained in E3 medium (5 nM NaCl, 0.17 mM KCl, 0.33 mM $CaCl_2$, 0.33 mM $MgSO_4$) in a 28°C temperature-controlled incubator in 10 cm plates at approximately 100 embryos/plate. Deceased embryos were removed daily to ensure the health of the surrounding embryos. Additionally, the residual chorions of zebrafish larvae that had naturally hatched were removed from the plates to prevent bacterial buildup. Zebrafish embryos (0-72 hours post-fertilization; hpf) are considered to enter the larval stage after 72 hpf, and all larvae were used experimentally before 7 days post fertilization (dpf). All experiments used *casper* zebrafish mutants, unless otherwise stated (White et al., 2008).

2.2 YO-PRO1 Staining

When examining the neuromast structures, larvae were stained with YO-PRO™1 Iodide 491-509 (Molecular Probes), a carbocyanine nucleic acid stain typically used to label apoptotic cells in tissue culture applications. The stain also specifically labels viable hair cell nuclei of the zebrafish larval neuromast structures (Baxendale & Whitfield, 2016). Larvae were treated with the compounds specified, rinsed 3X in methylene blue-free E3 media, then stained in 2 μM YO-PRO™1 in methylene blue-free E3 media for 1

hr at 28°C. Larvae were then rinsed 3X with methylene blue-free E3 media, then examined with either fluorescent microscopy on an inverted Axio Observer Z1 microscope (Carl Zeiss), or using the Biosorter (Union Biometrica Inc.).

2.3 LP Sampler and Biosorter Use

In order to facilitate high-throughput analysis of zebrafish lateral line staining, I used a biosorting system akin to flow cytometry, but for large particles. For this purpose, I used a biosorter with or without an associated Large Particle Handler (Union Biometrica Inc.). When sampling from a 96-well plate, larvae were arrayed with 4 larvae/well, using the biosorter to accurately array the larvae. The biosorter has a live recovery rate of approximately 95%. I selected 4 larvae/well because ≥5 larvae/well resulted in a higher rate of death due to crowing. With the possibility of one larvae being lost/well, I decided that 3 larvae/well was too few. Immediately prior to biosorting from the 96-well plate, larvae were exposed to 0.2 mg/ml of the anesthetic tricaine, ensuring linear passage of the larvae through the tubing. For these experiments, the unit was fitted with a 500 μM fluidics and optics core assembly (FOCA), 1000 μM fluid handling tubing, and a 488 nm laser. Data was automatically collected on all channels simultaneously, with readouts of total fluorescence, peak height, and peak width of fluorescence. For YO-PRO-1™ studies, peak height green fluorescence correlated most closely with cisplatin dose; thus, this was selected to be the reported parameter (**Figure 2.1**).

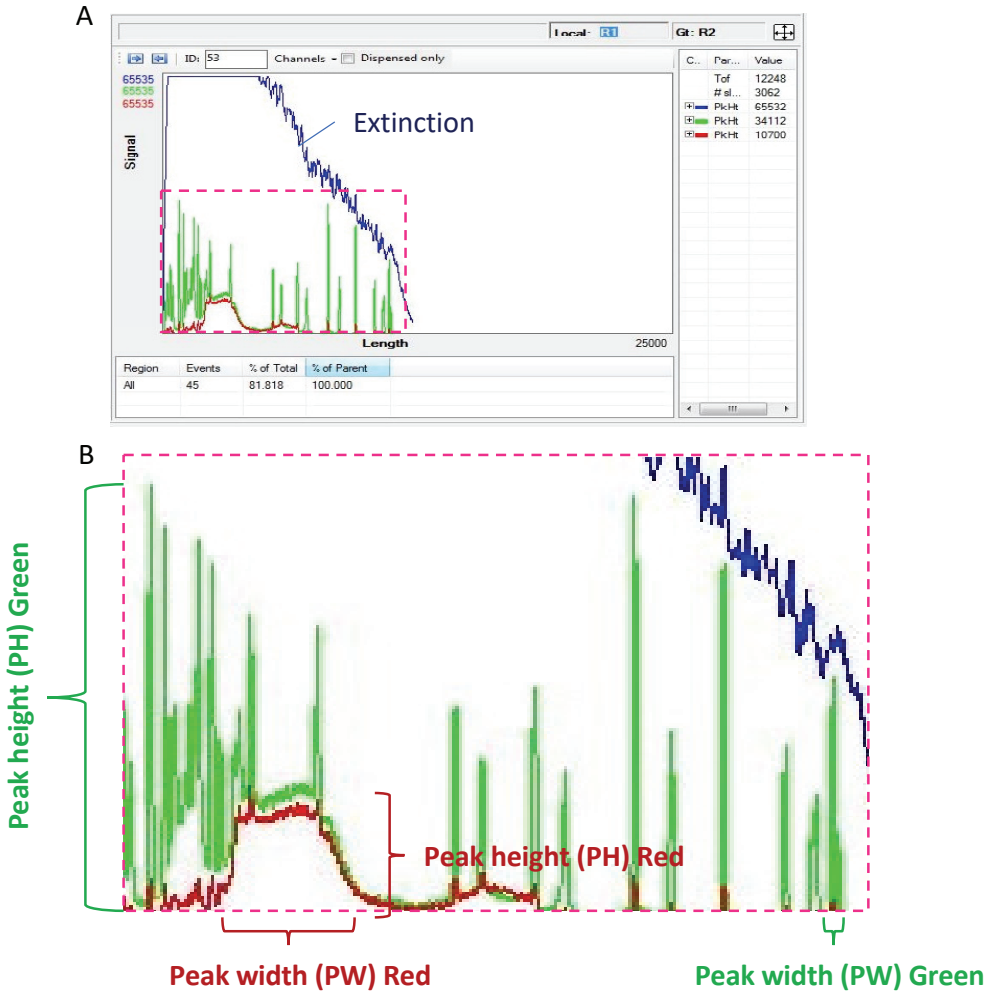

Figure 2.1 Representative biosorter plot of an untreated larvae stained with YO-PRO1, labelling neuromast structures green. A group of 72 hours post fertilization (hpf) *casper* zebrafish larvae were labelled with 2µM YO-PRO1 for 1hr, rinsed, then biosorted using the Union Biometrica Biosorter. This is a representative plot of graphical data output. A) Representative full window from the bossorter software. B) Zoomed in plot, taken from A). The dark blue line corresponds to extinction, which correlated to both the length and opacity of the object that passes through the biosorter. This is how zebrafish larval plots are oriented, as the larval head is more opaque than the tail. Thus, the machine is capable or orienting the fluorescent plots, and resulting data, in a uniform direction, regardless of which end of the larvae enters the flow cell first. Here, the head is on the left, the red hump corresponds to yolk sac autofluorescence, and the green peaks correspond to YO-PRO1 labelling of neuromasts. Overall fluorescence is measured in each channel selected, here, only red and green. Total fluorescence is a measure similar to the "area under the curve" fluorescence. The biosorter also reports peak height (PH) and peak width (PW) in each channel. PH corresponds to the highest peak in each channel. PW corresponds to the widest peak of the plot. For the following experiments, PH green fluorescence was reported for YO-PRO1 neuromast staining, and total green fluorescence was reported for inulin fluorescence.

2.4 Inulin-Based Glomerular Filtration Rate (GFR) Assay

The *in vivo* assessment of GFR was adapted from published studies by Hentschel *et al.,* 2005. This assay utilizes the knowledge that the polysaccharide inulin is not metabolized and is filtered exclusively at the nephron. Thus, when FITC-tagged inulin (Sigma Aldrich) is injected into the circulation of zebrafish larvae, decreases in fluorescence over time are representative of GFR. FITC-inulin was prepared by dissolving it at a concentration of 5% w/v in 0.9% sodium chloride (NaCl). This was then dialysed with 1000 Da dialysis tubing overnight to remove unbound FITC. Pretreated larvae were injected with approximately 2 nl of this inulin solution at 96 hpf via the common cardinal vein, using the PL1 Picoinjector (Harvard Apparatus). Immediately after injection, larvae were screened by fluorescence imaging using a Discovery V20 Stereomicroscope (Carl Zeiss) to remove uninjected larvae, then sorted using a biosorter. Three representative larvae from each group were imaged using the Zeiss SteREO Discovery.V20 dissecting microscope (Carl Zeiss). All larvae were allowed to develop naturally, which at this time point, would include pronephros filtration for 2 hr at 35°C, at which point the larvae were biosorted and imaged again. Data is presented as the fold change in overall green fluorescence, with the 0 hr timepoint set to 1. The experiment was completed three times, with a minimum of 50 larvae measured/group. For glomerular filtration rate (GFR) studies, overall green fluorescence was assessed. A representative fluorescence profile from stained larvae can be seen in **Figure 2.1**, where different parameters are elucidated.

2.5 Heart Rate Assessment

Casper zebrafish larvae were treated at 72 hpf with either vehicle control or 0.125 mM cisplatin. The next day, larvae were rinsed and assessed visually under a dissecting microscope to count heart rate for periods of 15 sec. Larvae were each assessed twice, and the average of the two counts were recorded. At least 5 larvae per drug treatment were assessed. Results are reported as beats per minute (BPM).

2.6 Cell Culture

All human cell lines were cultured at 37°C and 5% CO_2 in standard cell culture conditions. All cell lines were cultured, split, and frozen down according to their specific requirements. SK-N-AS, SK-N-SH, and LAN5 neuroblastoma (NBL) cell lines were a gift from Dr. Meredith Irwin (Sick Kids, Toronto, ON). HK-2 kidney proximal tubule cells and HSC-3 oral squamous carcinoma cells were purchased from ATCC. Cell culture media, supplement requirements, and trypsinization requirements can be found in **Table 2.1**.

Table 2.1 Cell culture requirements

Cell Line	Media	Supplements	Trypsinization/centrifugation
SK-N-AS	DMEM	10% fetal bovine serum (FBS), 1% penicillin/streptomycin (PS), 1% non-essential amino acids(NEAA)	5 min trypsin, 5 min X 300g
LAN5	RPMI	10% FBS, 1% PS	3-5 min trypsin, 5 min X 300g
HK-2	Keratinocyte Serum-Free Media	Recombinant human epidermal growth factor, bovine pituitary extract (provided with media)	2-3 min trypsin, 7 min X 100g
HSC-3	EMEM	10% FBS, 1% PS	5 min trypsin, 5 min X 300g

2.7 alamarBlue™ Assay

Cells were trypsinized, collected, counted, and plated in 96-well plates such that the cells were approximately 85% confluent at the endpoint of the assay in control wells. Cells were treated at the specified time point with each compound at the required concentration. Cells were incubated for either 24 or 48 hr, then 10% alamarBlue™ Cell Viability Reagent (Thermo Fisher Scientific) was added to each required well. Cells with alamarBlue™ were incubated for 2.5 hr, then read on a plate reader for fluorescence (excitation/emission = 560/590 nm). Controls included a negative control, with the regular cell growth media and no alamarBlue™, a negative experimental control, with the regular cell growth media and 10% alamarBlue™; and a positive control, with cells, regular growth media, 10% alamarBlue™ and no drug. For analysis, the average of at least two wells with identical treatment was measured. The negative experimental control value was subtracted from this value, to account for any fluorescence arising from the cell culture media and alamarBlue™ itself. This value was then compared to the positive control for statistical analysis. Experiments were completed a minimum of 3 times.

When used for drug screening, HK-2 cells were treated with either vehicle control, the approximate EC50 of cisplatin alone (0.005 mM), or 0.005 mM cisplatin + each of the compounds from the Sigma LOPAC®^{1280} Compound library at a final concentration of 0.01 mM. Each compound was assessed in at least two separate wells and the values were averaged. An alamarBlue™ Cell Viability assay was performed as described above. Data is represented as fold change from control, or untreated cells. Hits were defined as those compounds that resulted in viability levels between 0.9-1.1 fold of control values.

2.8 Sigma LOPAC®^{1280} Compound Library

The Sigma LOPAC®^{1280} Compound library of pharmacologically active compounds was purchased from Millipore Sigma. The library is provided at 10 mM in dimethyl sulfoxide (DMSO). A 10 µl portion of the library was transferred to sterile 96-well plates, then covered with a sterile close-sealing mat and the plate lid. These plates were maintained at -80°C for further use.

2.9 Phalloidin Staining

To examine the inner ear hair cells of drug-treated larvae, larvae were fixed, permeabilized and then stained with Alexa Fluor^{TM}488 Phalloidin (Molecular Probes), in a protocol similar to that described by Baxendale and Whitfield, 2016. *Casper* larvae were pretreated at 60 hpf with vehicle control or either 0.03 mM dopamine or 0.03 mM L-mimosine. At 72 hpf, these same larvae were treated with either vehicle control, or 0.1 mM cisplatin for 48 hr. The larvae were rinsed 3X in E3 media, then fixed overnight at 4°C in 4% paraformaldehyde (PFA) in PBS. All subsequent incubations were at room temperature (RT) on a shaker. The fixed larvae were then rinsed twice in 0.2% Triton-X in PBS (PBS-Tx), then permeabilized in 2% PBS-Tx for 2 hr. The larvae were then rinsed two more times, then stained with Alexa Fluor^{TM}488 Phalloidin prepared at a concentration of 1:20 in 1% PBS-Tween for 1.5 hr in the dark. The samples were protected from light from this point forward. The larvae were then rinsed 6X 10 min in 0.2% PBS-Tx and examined with confocal microscopy.

2.10 Confocal Microscopy

After exposure to phalloidin, zebrafish larvae were rinsed 4X 15 minutes in PBS, then placed in a solution of 3:1 glycerol:Tris buffer (pH 8.1) containing 2% n-propyl gallate. Whole zebrafish larvae were mounted on standard slides with a 1.5-ounce cover slip (VWR International). Specimens were viewed through a Zeiss LSM510 confocal microscope (Carl Zeiss), using Zeiss Zen2009 software (Carl Zeiss). Specimens were epi-illuminated with a mercury lamp (X-Cite 120Q; Lumen Dynamics Inc.), or with 30 mW argon (488 nm) laser (Carl Zeiss), directed through a 488/543 nm dichroic mirror (HFT 488/543; Carl Zeiss) onto the preparation. Emitted fluorescence was collected with a 25×0.80 NA objective (LCI Plan-Neofluar; Carl Zeiss) through a 505-530 nm filter (BP505-530; Carl Zeiss). Z-stacks were taken at regions of interest surrounding optic placode tissues and ranged from 27-42 μm in depth. Z-stack scans also encompassed a region of 10 μm above and below the regions of interest to ensure that all structures were captured, while limiting issues of light scattering associated with tissue deeper scans.

To ensure that differences in hair cell stereocilia appearance were not due to differences in fluorophore labelling a standard scanning protocol was created within Zen and used for all specimens (2.0 digital zoom; 488 nm laser: 55% power, 500 master gain, 1.0 digital gain, 0.0 digital offset, 1.0 AU pinhole; set relative to control treatment groups).

2.11 Histology

Larvae were pretreated with vehicle control or either dopamine or L-mimosine at 0.03 mM for 12 hr, then were treated with either the vehicle control or 0.125 mM freshly-

prepared cisplatin for the indicated amount of time. Larvae were euthanized, then fixed in freshly prepared 4% paraformaldehyde (PFA) in PBS overnight at 4°C. Fixed larvae were pre-embedded in 1.5% Ultrapure™ low melting point agarose (Sigma Aldrich, Carlsbad, CA, USA) aligned in rows, to allow for easy coronal cross sectioning. Embedded larvae were then fixed in 10% neutral buffered formalin for approximately 3 days, then embedded in Surgipath Paraplast (LEICA) with the Tissue Tek Embedding Station, Model TEC EMA-1 (Sakura Finetek USA Inc.). They were then sectioned to 4 μm with a Nikon Eclipse Ni manual microtome with Nikon Plan Fluor objectives (Nikon), and stained with H&E with a Tissue-Tek Prisma automated slide stainer. Slides were preserved with a Tissue-Tek Glas g2 automated cover-slipper (Sakura Finetek USA Inc.). Slides were then examined and imaged with a Nikon Digital Sight DS-L3 (Nikon).

2.12 Apoptosis Quantification with Flow Cytometry

Annexin V is a calcium-dependent phospholipid-binding protein that preferentially binds phosphatidylserine (PS) after it is translocated to the extracellular membrane leaflet during apoptosis. Annexin V Apoptosis Detection kit (Thermo Fisher Scientific) was used for the detection of cells in late stage apoptosis. During late stage of apoptosis, Annexin V bind to PS on the extracellular membrane. Cells were seeded in 6-well plates and according to previously optimized doses and timelines, cells were pretreated with vehicle control or 0.03 mM dopamine or L-mimosine for 12 hr. Cells were then treated with 0.01 mM freshly-prepared cisplatin. Cells ($1x10^6$ cells) were harvested with trypsin-EDTA (Thermo Fisher Scientific). Cells were washed 1X with PBS, and 1X with Annexin V binding buffer. Cells were resuspended in 1X binding buffer at a concentration of 1-5 x 10^6 cells/mL. PE-conjugated Annexin V (5 μl,

excitation/emission spectrum 488/561) was added to 100µl of the cell suspension and incubated for 15 min at RT in the dark. Samples were centrifuged and resuspended in 1ml of Annexin binding buffer. SYTOXBlue dead cell stain (1 µL, excitation/emission spectrum 444/480 nm) was added to each sample and incubated for 15 min at RT in the dark. Samples were placed on ice and subjected to flow cytometry using the BD FACSCanto flow cytometer. Data was analyzed using BD FACSDiva Software. Gating strategies for doublet discrimination and dead cell exclusion are demonstrated in **Appendix B**.

2.13 Immunohistochemistry (IHC)

γH2AX (Phospho S139) monoclonal antibody was used to identify the presence of DNA double strand breaks. Cells were seeded on sterile 18 x 18 mm coverslips (Globe Scientific Inc.) in 6-well plates. Cells were pretreated with vehicle control or 0.03 mM dopamine or L-mimosine for 12 hr. Cells were then treated with 0.01 mM freshly-prepared cisplatin. The next day, cells were fixed with 4% PFA (in PBS) for 20 min at 37°C. This time point was chosen as a result of a literature search that concluded that 24hr following cisplatin administration is indicative of longer-term cytotoxicity (Olive & Banath, 2009). Following fixation, cells were washed 3X with PBS, and maintained in 1X PBST at 4°C until antibody incubation. Fixed samples were permeabilized by incubating coverslips with 0.3% Triton-X-100 in PBS for 30 min at RT. Following permeabilization, samples were washed 3X with PBST. Samples were incubated with blocking buffer (5% donkey serum in PBST) for 1hr at RT. In a dark humidity chamber, samples were incubated with phospho-histone H2A.X (Ser139) (20E3) rabbit monoclonal antibody (Cell Signalling Technology) at 1:400 in 2.5% donkey serum in PBST overnight

at 4°C. Following primary antibody incubation, samples were washed 4X with PBST. Subsequently, samples were incubated in a dark humidity chamber with donkey polyclonal secondary antibody to rabbit IgG-H&L (Alexa Fluor 647) at 1:400 dilution, and 1:1000 DAPI (4',6-Diamidino-2-Phenylindole, Dihydrochloride) (Invitrogen) in 2.5% donkey serum in PBST for 1 hr at RT. Samples were then washed 4X with PBST. Following washing, coverslips were mounted with Dako Fluorescent mounting medium (Dako) onto Superfrost plus microslides (Thermo Fisher Scientific) and kept in the dark at RT overnight. Coverslips were stored at 4°C until imaging. Imaging of samples was done using the Zeiss LSM 710 Laser scanning confocal microscope. Four images were acquired for each treatment group/replicate. N=3.

2.14 Quantification of Phosphorylated γH2AX Staining

Quantification of γH2AX staining was performed using a custom ImageJ (Fiji) macro, written by Benno Orr (University of Toronto) (Rueden et al., 2017; Schindelin et al., 2012). For each image, ROIs for individual nuclei were generated from a thresholded duplicate of the DAPI channel. Thresholding was performed with the "Triangle" method, background noise was reduced using the default "Despeckle" functionality, and holes within thresholder nuclei below a 500-pixel size cut-off and above a 0.5 circularity cut-off were filled. Non-overlapping nuclei were detected as thresholded particles above size and circularity cut-offs of 1000 pixels and 0.65, respectively. Nuclei with overlap were separated with the default "Watershed" functionality and detected as particles above a size and circularity cut-offs of 1000 pixels and 0.8, respectively. For each nucleus ROI, measurements were collected for area, integrated density of DAPI and γH2AX channels, and γH2AX foci count (accomplished with the default "Find Maxima" functionality using

a prominence parameter of "20"). Data is reported as γH2AX integrated density/DAPI integrated density, with each data point corresponding to an individual nucleus.

2.15 Xenotransplantation (XT) of human cancer cells into zebrafish embryos and drug treatments

To assess the *in vivo* effects of both cisplatin and the candidate oto- and nephroprotective agents, *casper* zebrafish embryos were xenografted with human cancer cell lines. Approximately $5x10^6$ cancer cells were harvested as outlined in **Table 2.1**. Cells were resuspended in 10 ml of PBS and 5 µg/ml of CellTracker Orange CMTMR Dye (ThermoFisher). The cells were incubated for 20min at 37°C, then collected by centrifugation. Cells were washed 2X with cell culture medium and 1X with PBS. Cells were resuspended to a final volume of 100-150µl in culture medium, listed in **Table 2.1** for injection.

Naturally dechorionated 48 hpf *casper* zebrafish embryos were lightly anesthetized with 0.09 mg/mL tricaine solution (Sigma-Aldrich) and arrayed on an agarose plate for cell transplantation as per previously published methods (Corkery, Dellaire, & Berman, 2011). The labeled cells were loaded into a pulled glass capillary needle and allowed to settle through the media to the bottom. The needle was then attached to a PLI-100A Pico-Liter microinjection system (Harvard Apparatus) and larval yolk sacs were manually injected with 50-100 cells. Approximately 6 hr after injection, larvae were screened for the presence of an obvious bolus of cells that were uniform in size using a fluorescent Discovery V20 stereomicroscope. Larvae were maintained at 35°C for the remainder of the experiment, an established midpoint between the optimal

temperature for zebrafish development (28°C) and human cell growth (37°C) (Corkery et al., 2011).

Suitable larvae (those with uniformly sized boli of fluorescent cancer cells in the yolk sac) were separated into experimental groups of approximately 50 larvae. Larvae were examined daily, and dead larvae and debris were removed. Following screening, larvae were pretreated with vehicle control, or either 0.03 mM dopamine or L-mimosine. The following morning, 12 hr after protective agent pretreatment, larvae were rinsed, then treated with 0.25 mM freshly-prepared cisplatin. The next day, dead larvae were removed, and the larvae were treated with fresh E3 media (vehicle control) or cisplatin. The following day, 48 hr after cisplatin treatment, quantification of cancer cell number was enumerated with an *ex vivo* method.

2.16 *Ex Vivo* Quantification of Xenografted Cell Proliferation

For XT cell proliferation data, cells were quantified *ex vivo* 72 hours post injection (hpi) (**Figure 2.2**). Approximately twenty larvae were euthanized by tricaine overdose (1 mg/ml) and dissociated into a single-cell suspension in a collagenase solution (Sigma-Aldrich) for 25-35 min. Once dissociated, 200 µl of FBS was added to help slow the collagenase prior to removal. The sample was centrifuged at 300x*g* for 5 min, the supernatant was discarded, and the sample was washed with a 30% v/v FBS in PBS (30% FBS:PBS) solution and centrifuged. The supernatant was discarded again, leaving a pellet of zebrafish cells, containing the fluorescently labeled XT human cancer cells. The sample was resuspended in 10 µl/larva solution of 30% FBS:PBS for imaging. Ten 10 µl boli of this sample were pipetted onto a specialized "PTFE" Printed glass slide (5 mm well diameter, Electron Microscopy Sciences) and allowed to settle for 9 min. The boli

were individually imaged using an inverted Axio Observer Z1 microscope (Carl Zeiss) and images were analyzed using ImageJ software (NIH), as in previously published methods (Corkery et al., 2011). Results are displayed as fold change in comparison with untreated control larvae.

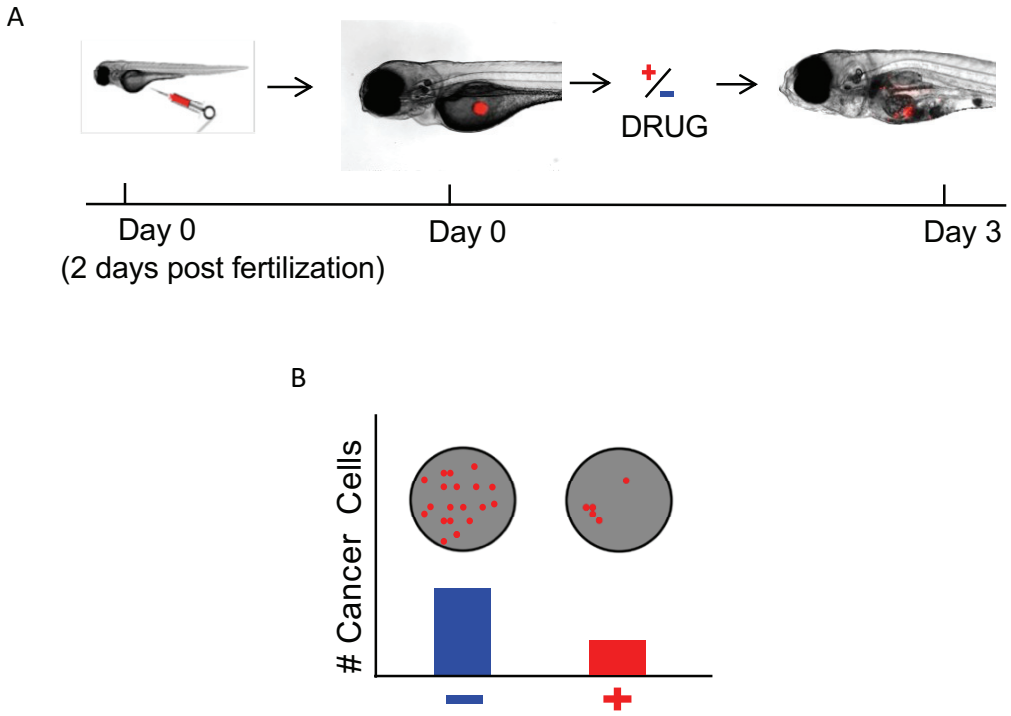

Figure 2.2 Schematic representation of zebrafish larvae xenograft assay. A) 48 hours post fertilization (hpf) zebrafish larvae were injected with 50-100 fluorescently-labelled human cancer cells in the yolk sac. Approximately 6hr following injection, larvae were screened for the presence of a boli of fluorescent cancer cells under a fluorescent microscope. Positive larvae were divided into groups of approximately 50 larvae, and at approximately 60hpf, were treated with vehicle control, 0.03mM dopamine, or 0.03mM L-mimosine. The following day, at 72hpf, larvae were rinsed, then treated with 0.25mM freshly-prepared cisplatin. Larvae were retreated with cisplatin the following day. The next day, at 48 hours post injection (hpi), 20 larvae/treatment group were dissociated into a single cell suspension with a collagenase mixture, and were then imaged with a fluorescent microscope. The number of fluorescent cancer cells was established using ImageJ, then data is represented as fold change in cancer cell number in relation to the untreated control larvae.

2.17 Statistics

All data were collected in Microsoft Excel (Office 365 Version 16.22, Microsoft,). Statistical analysis and graph construction were completed in Prism 8 for MacOS (Version 8.1.2, GraphPad Software Inc.). All experiments were completed at least 3 times, and error bars represent standard deviation, unless otherwise noted.

The ototoxicity and nephrotoxicity dose-response curve was assessed using methods defined by Ritz et al., 2015, using R software with the *drc* extension package. The graphs presenting the data show a scatterplot with the model represented with a blue line. The grey borders represent the 95% confidence intervals of the line. Briefly, this constitutes a four-parameter log-logistic model that takes into account the following parameters: *b,* the steepness of the dose-response curve; *c* and *d,* the lower and upper limits of the response; and *e,* the ED50, or the effective dose at which half of maximal effect is observed (Ritz, Baty, Streibig, & Gerhard, 2015). The equation is as follows:

$$f(x, (b, c, d, e)) = c + \frac{d-c}{(1 + \exp(b(\log(x) - \log(e))))}$$

Chapter 3 Results I: Assay development

3.1 Lateral Line Neuromast Assessment Demonstrates That Cisplatin-Induces Lateral Line Damage

The lateral line of the zebrafish consists of discrete sensory clusters of cells called neuromasts (Ghysen & Dambly-Chaudière, 2007). The hair cells contained within the neuromasts of the lateral line are analogous to those in the mammalian inner ear; thus, the lateral line has served as an excellent model to study ototoxicity in zebrafish (Esterberg et al., 2016; J. A. Harris et al., 2003; H. Ou et al., 2007; Teitz et al., 2018; A. J. Thomas et al., 2013). Assessment of larval zebrafish neuromast structures is typically accomplished by staining the larvae with a specific neuromast stain, like YO-PRO1, then imaging the larvae and performing some type of quantitative or semiquantitative analysis based on cell number (Baxendale & Whitfield, 2016; H. C. Ou et al., 2009; H. Ou et al., 2007; Owens et al., 2008; Andrew J. Thomas et al., 2015). However, these assessments often involve imaging each larva individually, which is too time-consuming for medium-high throughput drug screens. Alternatively, researchers can use a variety of multi-well imaging systems. However, these systems are usually expensive and often do not have established methods for ensuring the correct orientation of the larvae in the wells. Additionally, the scoring systems for neuromast health is often restrictive in the number of neuromasts examined, prone to human error, and does not capture all of the information afforded by the lateral line. The following are my attempts to further optimize lateral line assessment for medium-high throughput drug screens.

3.1.1 Cisplatin Treatment Results in Damage to Zebrafish Neuromast Structures that is Detectable with ZEN Software

In order to assess the integrity of neuromast cell clusters without the use of high-throughput imaging equipment, I quantified neuromast health using built-in analysis software, available on our inverted Axio Observer Z1 microscope. I used the ZEN (ZEN2, Blue Edition) software to record the average green fluorescence value from each larval image, then calculated fold change in comparison to the average of the untreated control larvae (**Figure 3.1**). At both magnifications, there was a significant reduction in the average green fluorescence in comparison with the untreated controls (**Figure 3.1a** and **3.1d**, **=p=0.0011, ****=p<0.0001, respectively). Representative histograms and fluorescent images can be found in **Figure 3.1b-c** and **Figure 3.1e-f**.

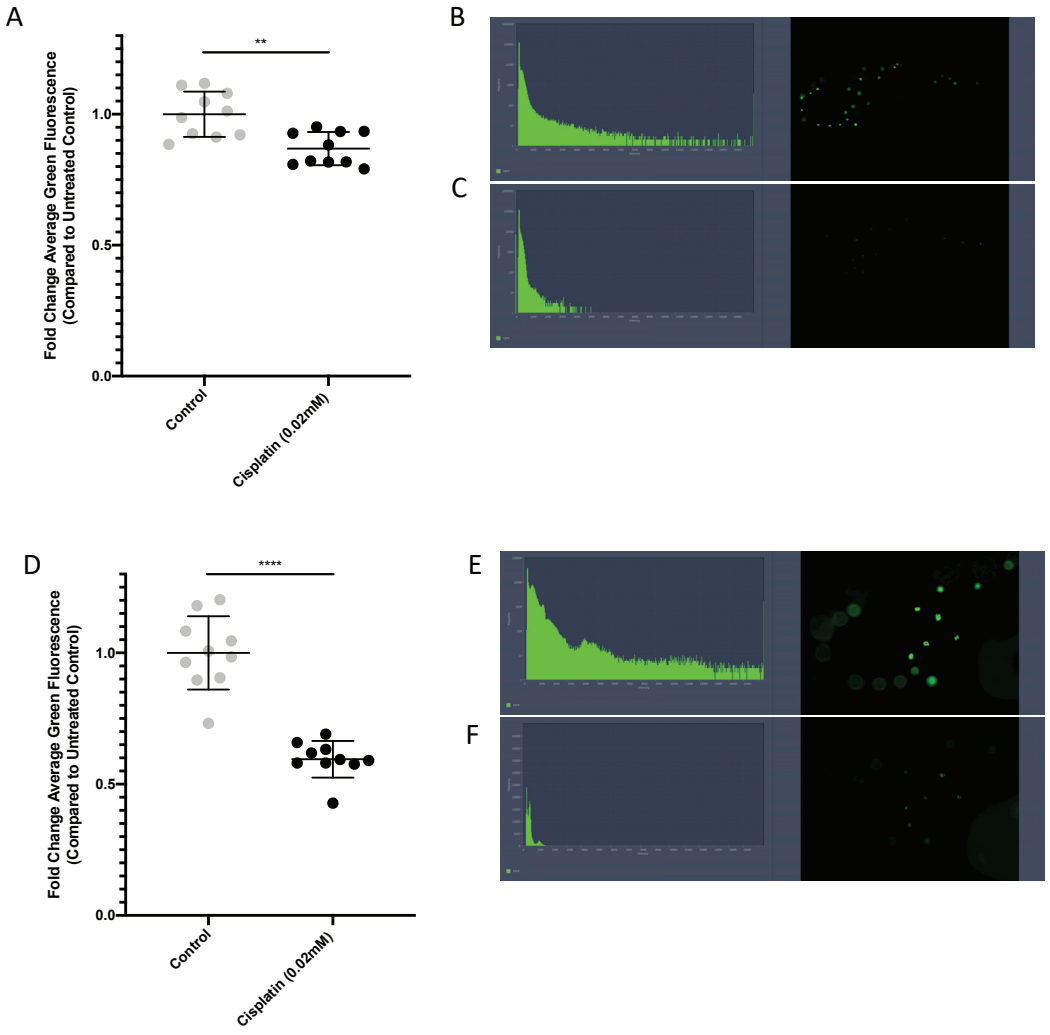

Figure 3.1 Cisplatin treatment results in damage to zebrafish neuromast structures that is detectable with ZEN software. Groups of 5 x 72 hour post fertilization (hpf) *casper* zebrafish larvae were treated with either vehicle control, or 0.02mM freshly-prepared cisplatin for 24hr. At the endpoint, larvae were stained with 2µM YO-PRO1 for 1hr, rinsed, then imaged with fluorescent microscopy. ZEN software was used to analyze the average level of green fluorescence in each image. Data is represented as fold change in comparison to the untreated control. A) Analysis of fluorescence values at 5X magnification. Each data point represents an individual larvae. **=p=0.011, as per two-tailed student's T-test. B-C) Representative larvae and fluorescent histogram for B) untreated control, and C) cisplatin treated larvae. D) Analysis of fluorescence values at 10X magnification. Each data point represents an individual larvae. ****=p<0.0001, as per two-tailed student's T-test. E-F) Representative larvae and fluorescent histogram for E) untreated control, and F) cisplatin treated larvae. N=2 replicates with 5 larvae each. Error bars represent standard deviation (SD).

3.1.2 Cisplatin Treatment Results in Damage to Zebrafish Neuromast Structures that is Detectable with Plate Reader Analysis

In an effort to increase the throughput of this fluorescence-based neuromast integrity assay, I decided to quantify neuromast fluorescence in cisplatin treated and untreated control larvae using a fluorescent plate reader. I treated larvae as above, with vehicle control, 0.05 mM or 0.25 mM cisplatin, then stained the larvae with YO-PRO1, rinsed them 3X, then arrayed 5 larvae/well in a 96-well plate. These results are reported as fold change in comparison to the untreated control larvae (**Figure 3.2**). Results demonstrate a significant difference between untreated and treated larvae (****=p<0.0001), but not between the 0.05 and 0.25 mM treatment groups.

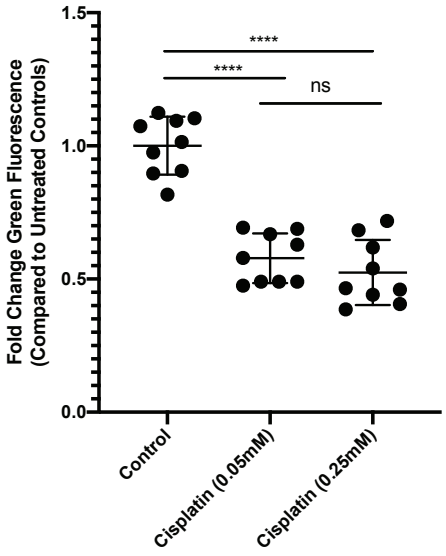

Figure 3.2 Cisplatin treatment results in damage to zebrafish neuromast structures that is detectable using a plate reader. Groups of 72 hour post fertilization (hpf) *casper* zebrafish larvae were treated with either vehicle control, 0.05 or 0.25mM cisplatin for 24hr. At the endpoint, larvae were stained with 2µM YO-PRO1 for 1hr, rinsed, then allotted 5X well in a 96-well plate. Fluorescence values were then acquired using a plate reader. Data is presented as fold change in comparison with untreated controls. Each data point represents the average of 3 reads of an individual well that contained 5 larvae. ****=p<0.0001, as per one-way ANOVA with a Tukey post-test. N=2 replicates with at least 4 wells in each treatment.

3.1.3 Cisplatin Treatment Results in Damage to Zebrafish Neuromast Structures that is Detectable with the Biosorter

It has been established by others that neuromast health decreases with increased cisplatin dose (H. Ou et al., 2007; Philip et al., 2018; Uribe et al., 2013). To determine if the biosorter, a machine akin to a flow cytometer for larger particles, like zebrafish larvae, was a suitable and sensitive instrument to use for the detection of subtle changes in neuromast fluorescence, I treated 72 hpf *casper* zebrafish larvae with increasing doses of freshly-prepared cisplatin (0.001-0.05mM) for 24hr. The following day, the larvae were rinsed and stained with 2 μM YO-PRO1. Larvae were then biosorted, and the peak height (PH) green fluorescence (relative to untreated controls) was plotted against increasing concentrations of cisplatin, which represents a predictable relationship (**Figure 3.3**). This dose-response relationship is represented by the blue line on the scatter plot, with the 95% confidence intervals represented as the grey shaded area, which was calculated using a four-parameter log-logistic model, as described in a recent study (Ritz et al., 2015). Using this model, the EC50, or the effective concentration of cisplatin that resulted in 50% of control levels of neuromast YO-PRO1 PH fluorescence was 0.027 mM. Representative images of larvae from each treatment group can also be found in **Figure 3.4**, along with representative flow plots from the biosorter for each treatment group. The biosorter was used for the remainder of the study to report neuromast fluorescence, as it was the most sensitive and highest throughput method tested. Furthermore, the biosorter enables detection of multiple fluorescent channels and subdivided parameters simultaneously – allowing for more robust post-experiment analysis.

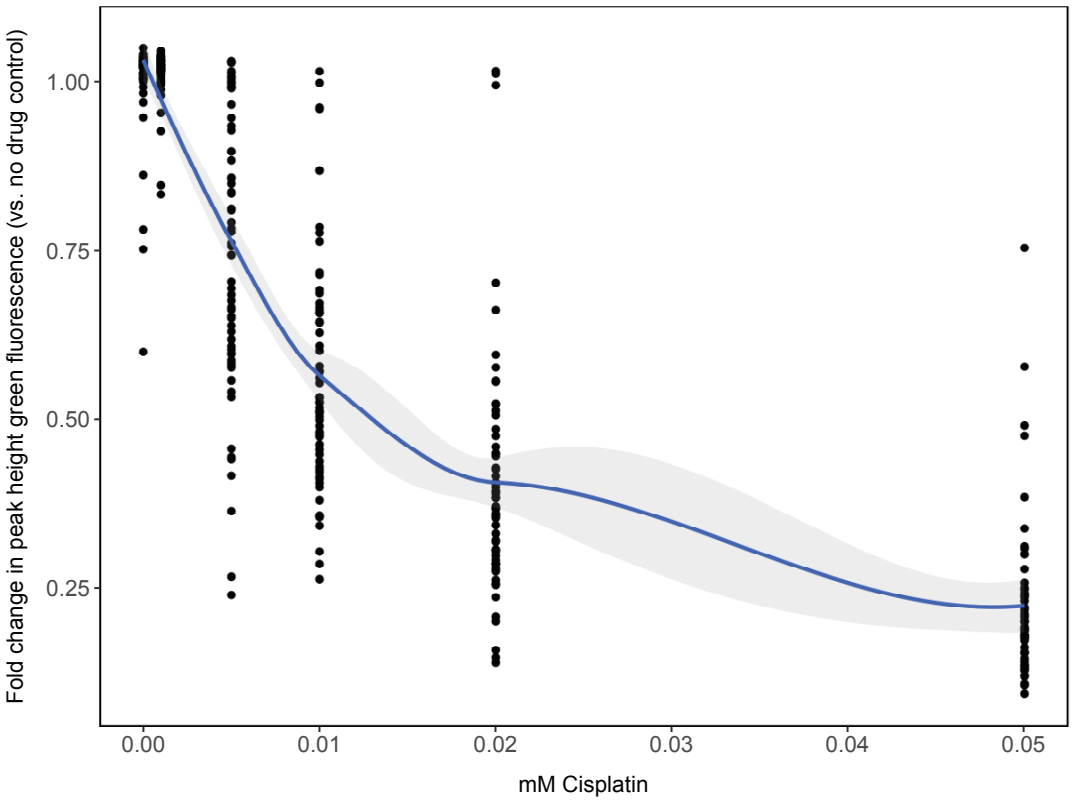

Figure 3.3 Cisplatin treatment results in dose-dependent zebrafish larval neuromast damage that is detectable with a biosorter. Groups of approximately 50 72 hour post fertilization (hpf) *casper* zebrafish larvae were treated with increasing concentrations of freshly-prepared cisplatin for 24hr. At the endpoint, larvae were stained with 2µM YO-PRO1 for 1hr, rinsed, then subjected to biosorter-based fluorescence profiling. Peak height (PH) of green fluorescence is shown (relative to untreated controls). Each data point represents an individual larvae. This dose-response relationship is represented by the blue line on the scatter plot, which was calculated using a four-parameter log-logistic model, as described in a recent study (Ritz et al., 2015). This modelling was done in R with the *drc* extension package. The grey shaded area represents the 95% confidence interval of this particular line.

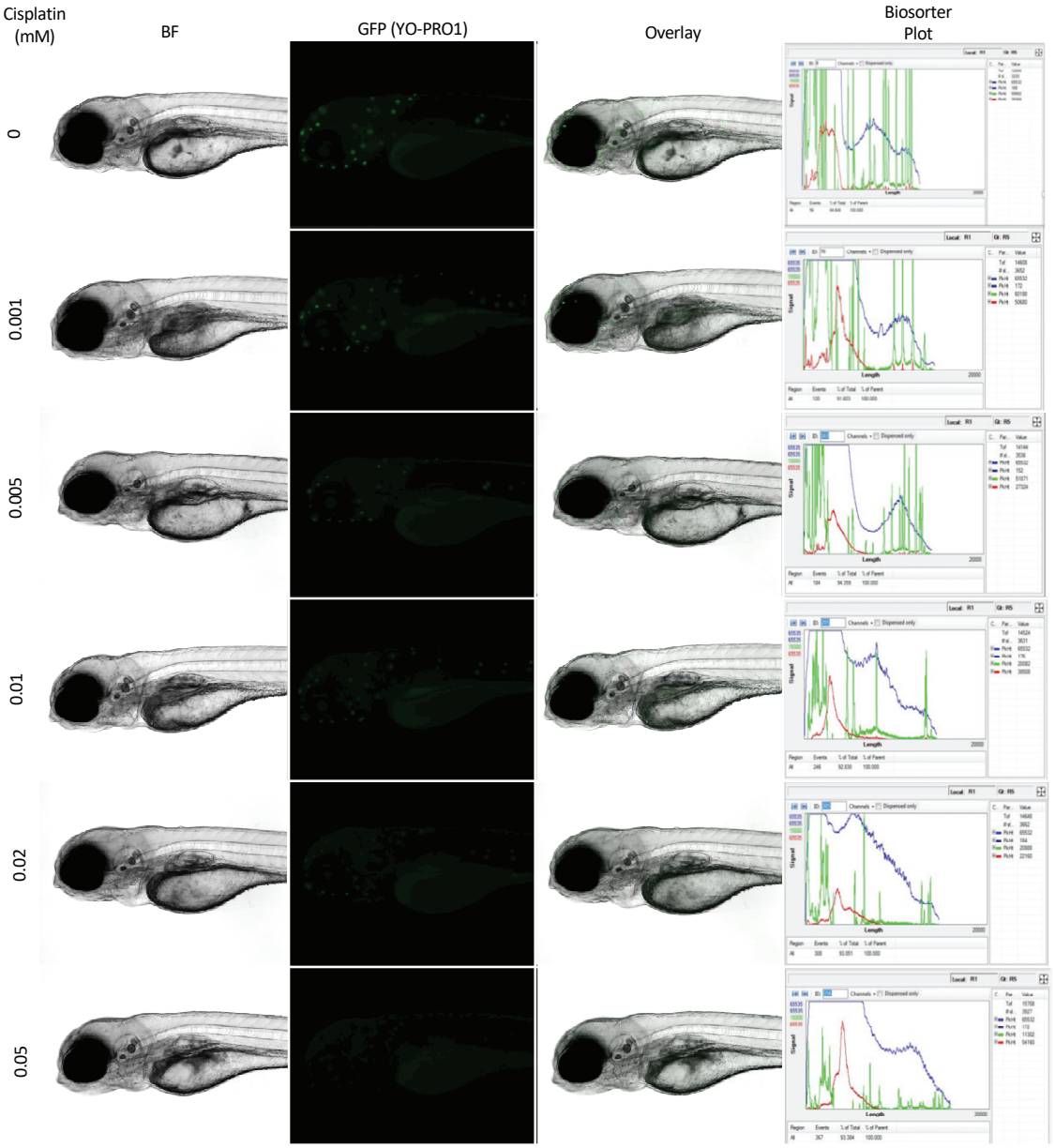

Figure 3.4 Cisplatin treatment results in visible dose-dependent zebrafish larval neuromast damage that is detectable with a biosorter. Groups of approximately 50 72 hour post fertilization (hpf) *casper* zebrafish larvae were treated with increasing concentrations of freshly-prepared cisplatin for 24hr. At the endpoint, larvae were stained with 2µM YO-PRO1 for 1hr, rinsed, then subjected to biosorter-based fluorescence profiling and imaged with a fluorescent microscope. Images depict representative larvae from each treatment group. The left column is a bright field image (BF), the next column is green fluorescence, corresponding to YO-PRO1 labelling of neuromast cell clusters, the next column is the merge of the BF+YO-PRO1, the right hand column is a representative flow plot of each treatment group.

3.2 *In Vivo* Glomerular Filtration (GFR) Assay Demonstrates that Cisplatin Damages Zebrafish Pronephros Function

The zebrafish exhibits glomerular filtration as early as 40 hpf (Drummond et al., 1998). As a result of the transparency of the zebrafish, and the amenability to medium-high throughput assays, the zebrafish is uniquely poised as a whole animal model within which to evaluate physiological processes, like glomerular filtration. I have adapted an inulin-based GFR assay that has been used previously by others for the functional assessment of larval pronephros function (Hentschel et al., 2005; Rider et al., 2012). Inulin filtration is one of the gold standards in the assessment of human renal function, or GFR (Stevens et al., 2006). Briefly, larvae were injected via the common cardinal vein with FITC-inulin, which is only excreted through the glomerulus in the nephron. Larvae were then examined immediately after injection, and after several hours to determine how much inulin had cleared. Previous studies have imaged the larvae and used software to quantify the levels of larval fluorescence at each time point. This is time consuming and prone to human error. This approach also only captures changes in fluorescence in one anatomic region of the fish, which may be misleading as a result of variability in the vascular systems in each larva. This type of analysis also limits the overall number of larvae used per experiment, which obviates the advantage afforded by use of such a small model organism. Thus, the following are my attempts to scale-up the inulin-based assessment of larval GFR.

3.2.1 Cisplatin-Treated Larvae Have Lower Glomerular Filtration Rates (GRFs) in Comparison with Untreated Larvae, and This is Detectable with ImageJ Analysis

It has been established by others that treatment with cisplatin decreases the GFR of zebrafish (Hentschel et al., 2005). Typically, studies will image the larval tail immediately after inulin injection, and then image the same larvae 2-3 hr later and will use a program like ImageJ (NIH) to assess the images for changes in fluorescence. I performed this exact experiment, and determined a significant decrease in the rate of change in green fluorescence in larvae that had been treated with 0.125 mM cisplatin (**Figure 3.5**, *=p=0.0311). This suggests that GFR is lower, or impaired, in the cisplatin-treated larvae.

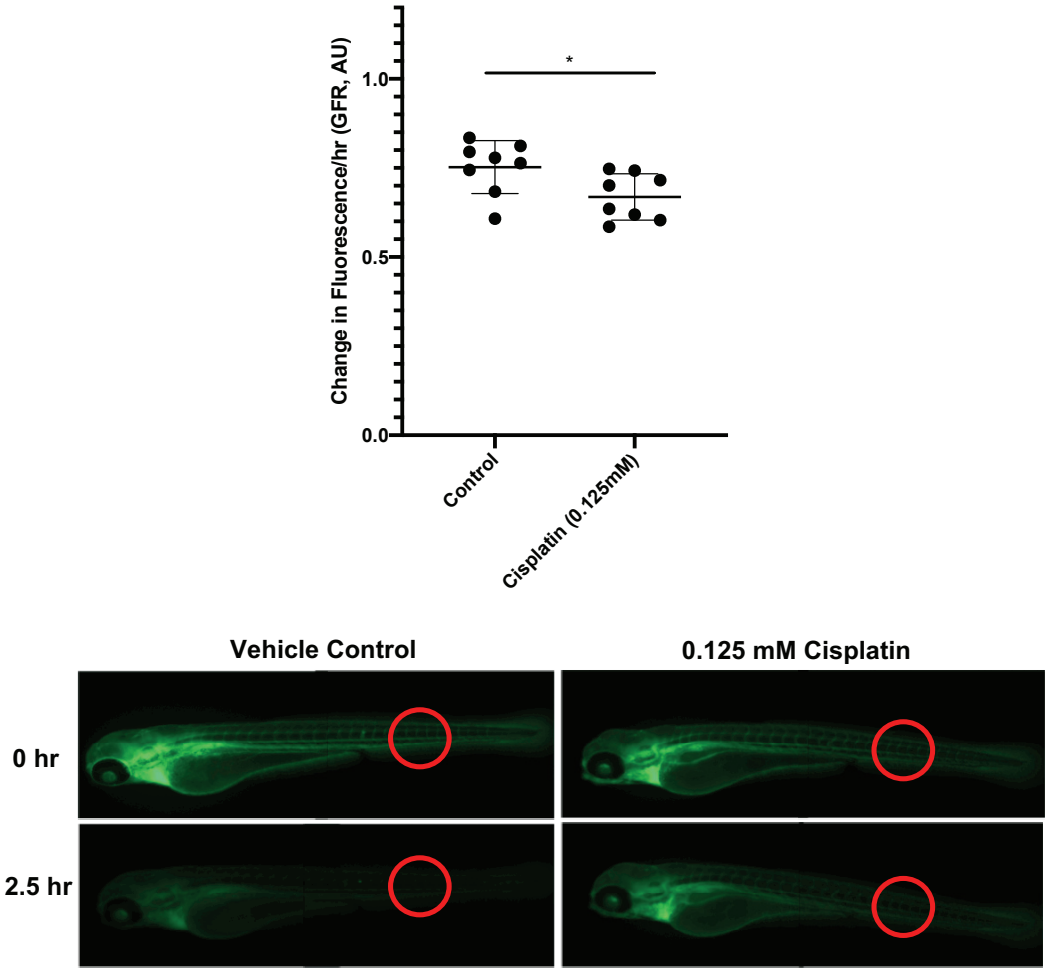

Figure 3.5 Cisplatin-treated larvae have lower glomerular filtration rates (GFRs) in comparison with untreated larvae, and this is detectable with ImageJ analysis. GFR was calculated in a method adapted from Hentschel *et al.,* 2005. 72 hours post fertilization (hpf) *casper* larvae were treated with either vehicle control or 0.125mM cisplatin for 24hr. Larvae were then injected via the common cardinal vein with FITC-inulin. Lavare were then imaged with a fluorescent microscope immediately following injection, then 2.5hr following injection. Images were then assessed using a region of interest (ROI) function superimposed onto the tail of the larvae in ImageJ, like the larvae imaged above. Fold change in fluorescence was calculated for each larvae between time points and results are summarized in the graph above. Each data point represents the fold change in fluorescence of an individual larvae. *=p=0.0311, as per two-tailed student's t-test. N=2, 4 larvae/treatment/experiment.

3.2.2 Cisplatin-Treated Larvae Have Lower Glomerular Filtration Rates (GRFs) in Comparison with Untreated Larvae, and This is Detectable with Plate Reader Analysis

In an effort to increase the throughput and/or sensitivity of this GFR assay, I attempted to utilize a fluorescent plate reader. I did this in two methods, which are outlined schematically in **Figure 3.6a**. First, similar to the experiment assessing lateral line fluorescence, I put 5 FITC-inulin injected larvae/well and read the fluorescence on a plate reader immediately after injection, and then 2 hr later, following the removal of 100 μl of the liquid in the well. I then calculated the fold change in larval fluorescence between the two time points. Second, I measured the fluorescence of the 100 μl of liquid that I had removed from the wells that contained the FITC-inulin injected larvae for two hours. Since the larvae exclusively excrete the FITC-inulin through the nephron, any fluorescence in the surrounding water has been excreted through the zebrafish pronephros. Thus, the greater the water fluorescence, the higher the GFR, indicative of better kidney function. Results for these experiments can be found in **Figure 3.6b** and **c,** respectively. There is a significant difference in the change in larval fluorescence, with a lower level of change in the cisplatin-treated larvae (*=p=0.0445). There was no significant difference between the fluorescence of the water surrounding the larvae, although this is likely a result of there only being two replicates of this experiment (p=0.0843).

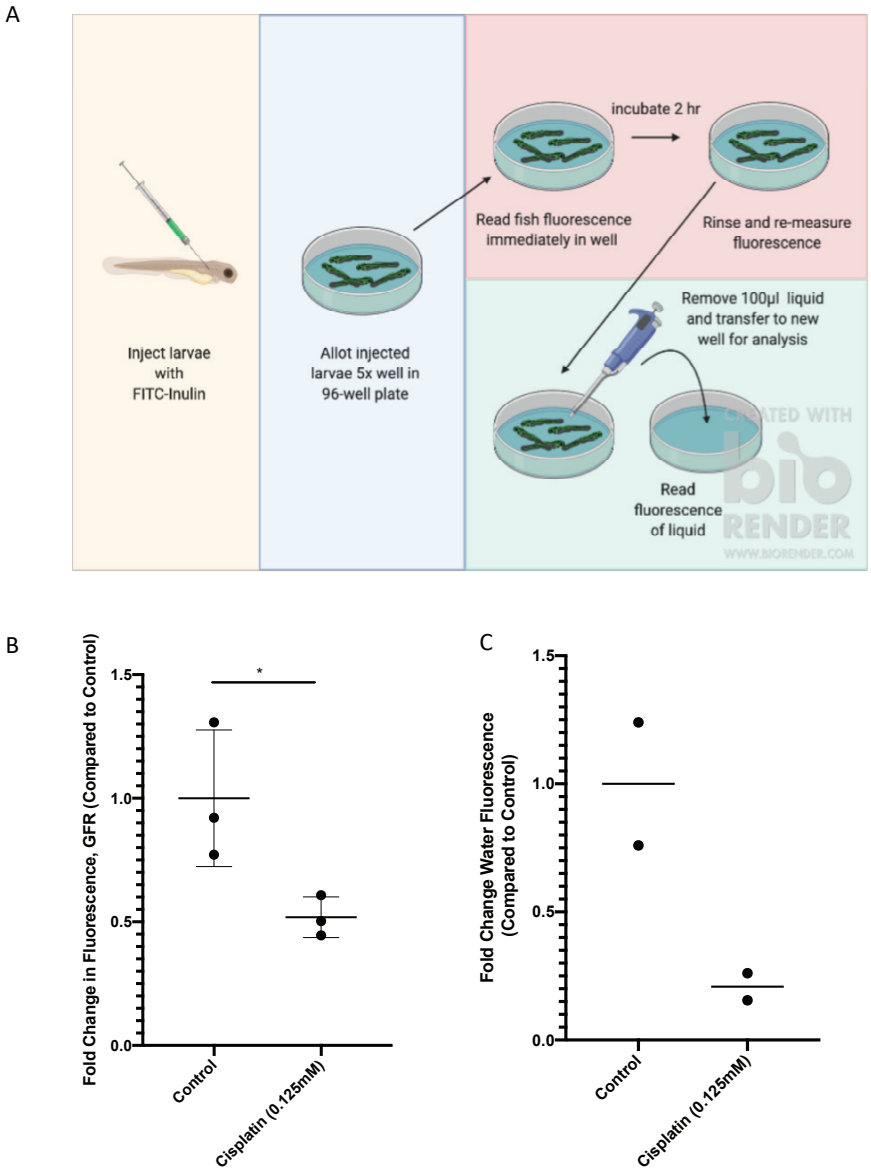

Figure 3.6 Cisplatin-treated larvae have lower glomerular filtration rates (GFRs) in comparison with untreated control larvae, and this is detectable with a plate reader measuring either fish fluorescence or water fluorescence. GFR was quantified in a method adapted from Hentschel *et al.,* 2005. 72 hours post fertilization (hpf) *casper* larvae were treated with either vehicle control or 0.125mM cisplatin for 24hr. Subsequent procedures are outlined above, in image A. Briefly, larvae were injected via the common cardinal vein with FITC-inulin. Larvae were then allotted to wells of a 96-well plate, with 5 larvae/well. Larval fluorescence was measured with a plate reader immediately after injection. Two hours later, 100µl of the liquid surrounding the larvae was removed and put into a new well. Larvae were then rinsed, and the plate reader was used to measure the fluorescence of both the larvae, and the liquid. B) Fold change in larval fluorescence, compared to control untreated larvae. *=p=0.0445, as per two-tailed student's t-test. N=3, 5 larvae/treatment/time point. C) Fluorescence of water removed from wells containing FITC-inulin injected larvae, compared to that from untreated control larvae. N=2, each data point represents water from individual well that contained 5 larvae for 2hr.

3.2.3 Cisplatin-Treated Larvae Have Lower Glomerular Filtration Rates (GFRs) in Comparison with Untreated Larvae, and This is Detectable With a Biosorter

Finally, I decided to determine if the biosorter would be a suitable instrument to measure the change in fluorescence for measuring GFR in the larvae. I treated 72 hpf larvae with either vehicle control or 0.125 mM cisplatin for 24 hr, then injected them via the common cardinal vein with FITC-inulin. Larvae were then assessed using the biosorter for green fluorescence, both immediately after injection, then at two hours post-injection (**Figure 3.7**). Raw fluorescence values were reported, of either total larval fluorescence (**Figure 3.7a,** ****=$p<0.0001$) or for partial profile fluorescence, selecting only the tail portion of the larvae (**Figure 3.7b,** *=$p=0.0345$, **=p-0.0023). The results were similar using either the partial profile, or full fluorescence, so total larval fluorescence was reported in all future experiments. It was also important to measure heart rate (HR) in treated and untreated control larvae, as this experiment is a functional measurement of cardio-renal function (Rider et al., 2012). Briefly, the total amount of inulin that is cleared by the pronephros is intrinsically related to the amount of blood that passes through the glomerulus; thus, changes in HR would be likely to effect the measurement of GFR. Larvae were treated with identical drug conditions as in the GFR assay, then heart rate was counted by visual examination over a period of 15 sec. Each larva was assessed two times, and the rate is an average of these counts. Data is represented as beats per minute (BPM) (**Figure 3.7c**, $p=0.6363$). The biosorter was the highest throughput method that I tested, thus it was used for future GFR experiments.

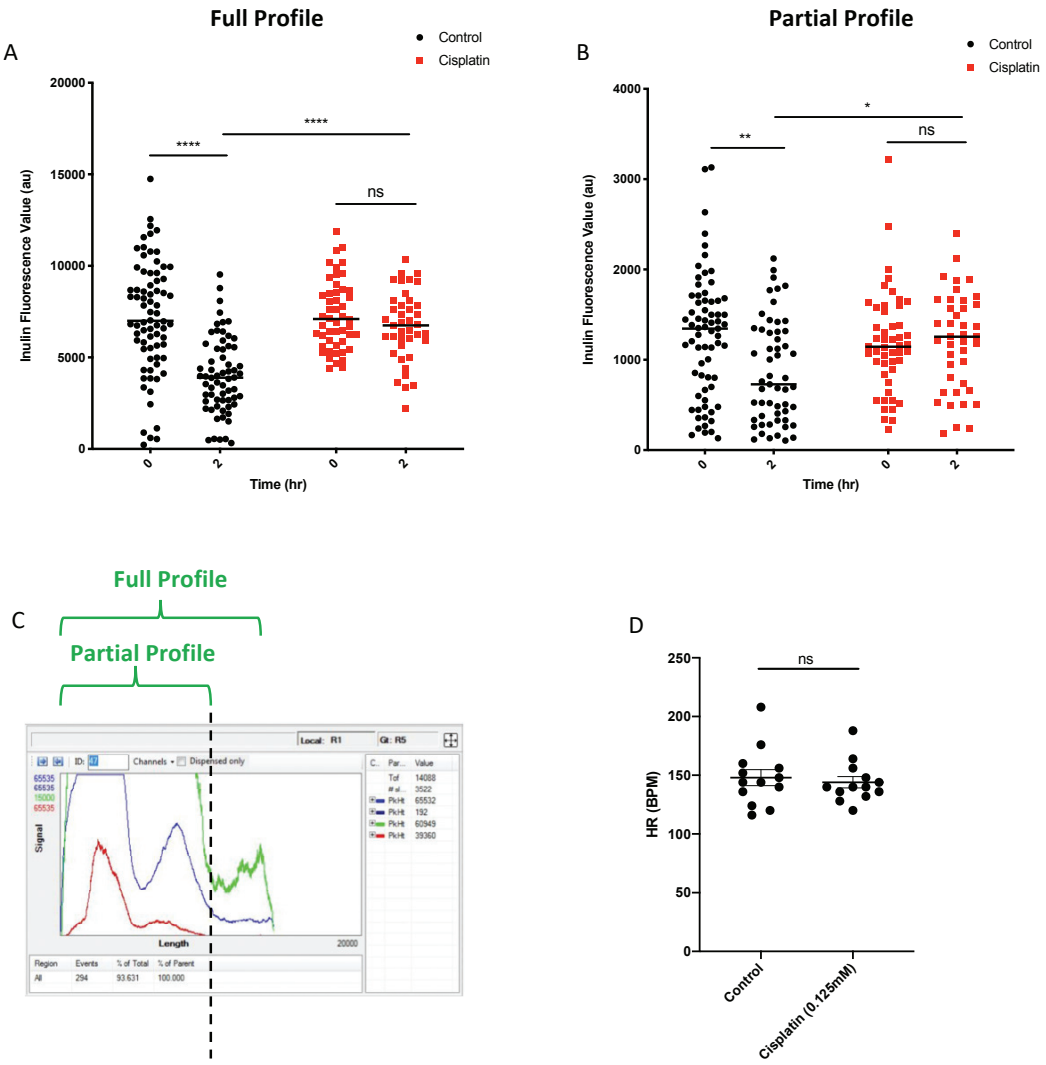

Figure 3.7 Cisplatin-treated larvae have lower glomerular filtration rates (GFRs) in comparison with untreated control larvae, and this is detectable using the biosorter. GFR was quantified in a method adapted from Hentschel *et al.,* 2005. 72 hours post fertilization (hpf) *casper* larvae were treated with either vehicle control or 0.125mM cisplatin for 24hr. Briefly, larvae were then injected via the common cardinal vein with FITC-inulin, then measured with a biosorter immediately following injection and 2hr following injection. Raw fluorescence values at each time point are reported in A) and B). In each graph, each data point represents an individual larvae at each time point. A) Full fluorescence profile, depicted schematically below the graph. ****=p<0.0001, as per two-way ANOVA with a Tukey post-test. N=1. B) Partial fluorescence profile, isolating the tail of each larvae, depicted schematically below the graph. *=p=0.0345, **=p=0.0023, as per two-way ANOVA with a Tukey post-test. N=1. C) Representative plot of biosorter-reported larval fluorescence showing partial and total fluorescence. D) Heart rate (HR) was assessed in treated and control untreated larvae, to determine if HR had an effect on the measured GFR. There was no significant difference between the HRs of treatment groups. Each data point represents an individual larvae. N=2, with 6 larvae/treatment group.

3.3 Summary of Findings

In summary, I have developed high-throughput methods to detect quantitative changes to both cisplatin-induced neuromast viability and cisplatin-induced changes to zebrafish larval GFR. Using the biosorter, it is possible to measure the fluorescence profiles of hundreds of larvae within several minutes. Thus, for the remainder of my thesis, I used the biosorter to perform the *in vivo* ototoxicity drug screen and follow-up *in vivo* GFR experiments.

Chapter 4 Results II: Drug screen and hit verification

4.1 Ototoxicity Screen Reveals 122 Protective Compounds and 35 Toxic Compounds

4.1.2 In Vivo Zebrafish Lateral Line Ototoxicity Screen Reveals 122 Protective Compounds

Once the reproducibility and predictability of the cisplatin-induced ototoxicity was established using the biosorter (**Figure 3.3**), I tested the potential utility of compounds in the Sigma LOPAC®^{1280} library as otoprotectants. Briefly, larvae were either untreated, treated with 0.02 mM of cisplatin alone (near the EC50 calculated in Chapter 3), or treated with 0.02 mM cisplatin + one of the compounds from the Sigma LOPAC®^{1280} library at a final concentration of 0.01 mM. Larvae were then stained with YO-PRO1 and biosorted. The average fold change in PH green neuromast fluorescence, compared to the no drug control value can be seen in **Figure 4.1**. Hits were identified when the PH green fluorescence value was between 0.9 and 1.1X fold of the no drug control value. This screen resulted in a total of 122 potentially otoprotective compounds.

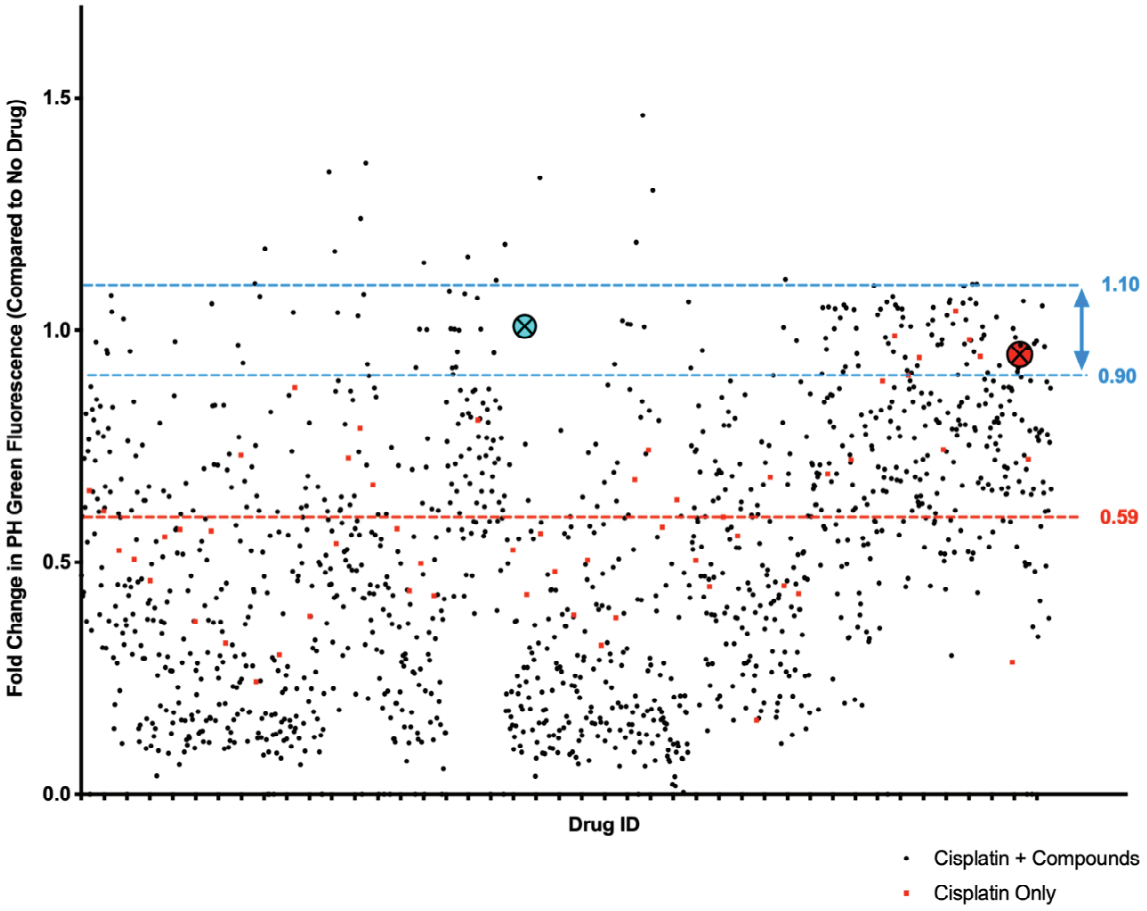

Figure 4.1 ***In vivo*** **ototoxicity drug screen assay results reveal 122 potentially otoprotective compounds.** *Casper* zebrafish larvae were pretreated with either vehicle control, or each of the compounds from the Sigma LOPAC®^{1280} library at a final concentration of 0.01mM. Three hours later, at 72 hours post fertilization (hpf) larvae were treated with either vehicle control or cisplatin at a concentration of 0.02mM, such that larvae were either treated with cisplatin alone or cisplatin+the library compounds. 48hr later, larvae were rinsed, then stained with YO-PRO1 and sorted with a biosoter. Peak height (PH) green fluorescence was compared to untreated larvae. Each compound was tested on four larvae. The aqua point with the X represents dopamine hydrochloride and the red point with the X represents L-mimosine. The blue lines correspond to between 0.9-1.1 fold the control, or untreated values. The red hashed line corresponds to the average of cells treated with cisplatin alone.

4.1.2 In Vivo Lateral Line Ototoxicity Drug Screen Reveals 20 Toxic Compounds

In this assay, toxic compounds were defined as those that resulted in the death of at least 3 of the 4 larvae. It should be noted that since the compounds were not tested without cisplatin, it cannot be stated that the compounds were toxic on their own, but rather that the combination of 0.02 mM cisplatin + 0.01 mM of a compound was toxic to approximately 75% of larvae. An annotated list of these compounds can be found in **Table 4.1**.

Table 4.1 Compounds from the Sigma LOPAC®[1280] compound library that were toxic to ¾ zebrafish larvae at 0.01mM, in combination with 0.02mM cisplatin. Clinical usage information obtained from the ChEMBL database (Gaulton et al., 2017)

Drug ID	Drug Name	Biological Action	Clinical Usage	Hit in *in vitro* nephrotox assay
1, B03	PD 0325901	PD 0325901 is a potent MKK1 (MEK1) and MKK2 (MEK2) inhibitor	Investigated in a Phase II clinical trial in non-small cell lung cancer (NSCLC), did not meet efficacy endpoint (Haura et al., 2010). Investigated for potential utility in neurofibromatosis type 1 (NCT02096471) and colorectal cancer (NCT02510001).	Yes
1, G02	Tryptamine hydrochloride	Serotonin receptor ligand	N/A	Yes
4, A07	Cyproheptadine hydrochloride	5-HT2 serotonin receptor antagonist	First generation antihistamine used clinically for allergies, especially hayfever	
4, A09	Cantharidin	Protein phosphatase 2A inhibitor	In clinical trials to treat molluscum (NCT03377803), listed as an extremely hazardous agent in the USA because it can cause severe chemical burns	
4, B05	Chlorothiazide	Carbonic anhydrase inhibitor, diuretic; antihypertensive	Used clinically as a diuretic and antihypertensive	Yes
4, H08	Calcimycin	Ca^{2+} ionophore used to potentiate responses to NMDA, but not quisqualate glutamate receptors	N/A	
4, H09	Cantharidic Acid	Protein phosphatase 1 (PP1) and 2A (PP2A) inhibitor	N/A	
5, E11	Diacylglycerol Kinase Inhibitor II	Diacylglycerol kinase inhibitor	N/A	
5, H03	(±)-Chloro-APB hydrobromide	D1 dopamine receptor antagonist	N/A	
5, H10	2,3-Dimethoxy-1,4-napthoquinone	Redox cycling agent used to study role of ROS	N/A	
6, A08	4-DAMP methiodide	M3 muscarinic acetylcholine receptor antagonist	N/A	Yes
6, D11	Etazolate hydrochloride	Phosphodiesterase inhibitor	Tested in Phase II clinical trial for adjunct therapy in Alzheimer's disease (NCT00880412), suggested to have anxiolytic effects	Yes

6, F03	DBO-83	Nicotinic acetylcholine receptor agonist	N/A	
6, H06	AC-93253 iodide	Potent, cell permeable, subtype selective retinoic acid receptor (RARalpha) agonist	Studied experimentally *in vitro* and in mice for the treatment of NSCLC (Lai, Lin, Wu, Chen, & Chen, 2017)	Yes
7, F11	NS5806	Increases peak current amplitude of the potassium channel Kv4.3		Yes
7, H09	Fluoxetine hydrochloride	Selective serotonin reuptake inhibitor	Used for the treatment of major depressive disorder, panic disorder, obsessive-compulsive disorder etc. (aka. Prozac)	
10, B06	BBMP	Mitochondrial permeability transition pore (PTP) inhibitor. Potential therapeutics for neurodegenerative diseases	N/A	
15, E05	Tetraethylthiuram disulfide	Alcohol dehydrogenase inhibitor	Approved as second-line therapy in alcohol dependence disorder, also used to treat certain parasitic infections	
16, E09	Wortmannin from Penicillum funiculosum	Potent and specific phosphatidylinositol 3-kinase (PI3-K) inhibitor	N/A	
16, F05	Tyrphostin A9	Selective PDGF tyrosine kinase receptor inhibitor	N/A	

4.2 Nephrotoxicity Screen Reveals 266 Potentially Nephroprotective Compounds

4.2.1 HK-2 Human Kidney Cell Viability Decreases With Increasing Cisplatin Doses

HK-2 cells are human proximal tubule cells that have been transformed with human papilloma 16 virus (Ryan et al., 1994). Like others, I have used these cells as an *in vitro* model of mammalian nephrotoxicity (Gao et al., 2019; Nho et al., 2018; Y. R. Zhang & Yuan, 2010). HK-2 cells were exposed to cisplatin for 48 hr, then were assessed for viability using alamarBlue™. Results demonstrate that HK-2 cells exhibit reduced viability with increasing doses of cisplatin at 48 hours post treatment (hpt, **Figure 4.2**). This dose-response relationship is represented by the blue line on the scatter plot, with the 95% confidence intervals represented as the grey shaded area, which was calculated using a four-parameter log-logistic model, as described in a recent study (Ritz et al., 2015). Using this model, the EC50, or the effective concentration of cisplatin that resulted in 50% of untreated HK-2 cell viability was 0.0084 mM.

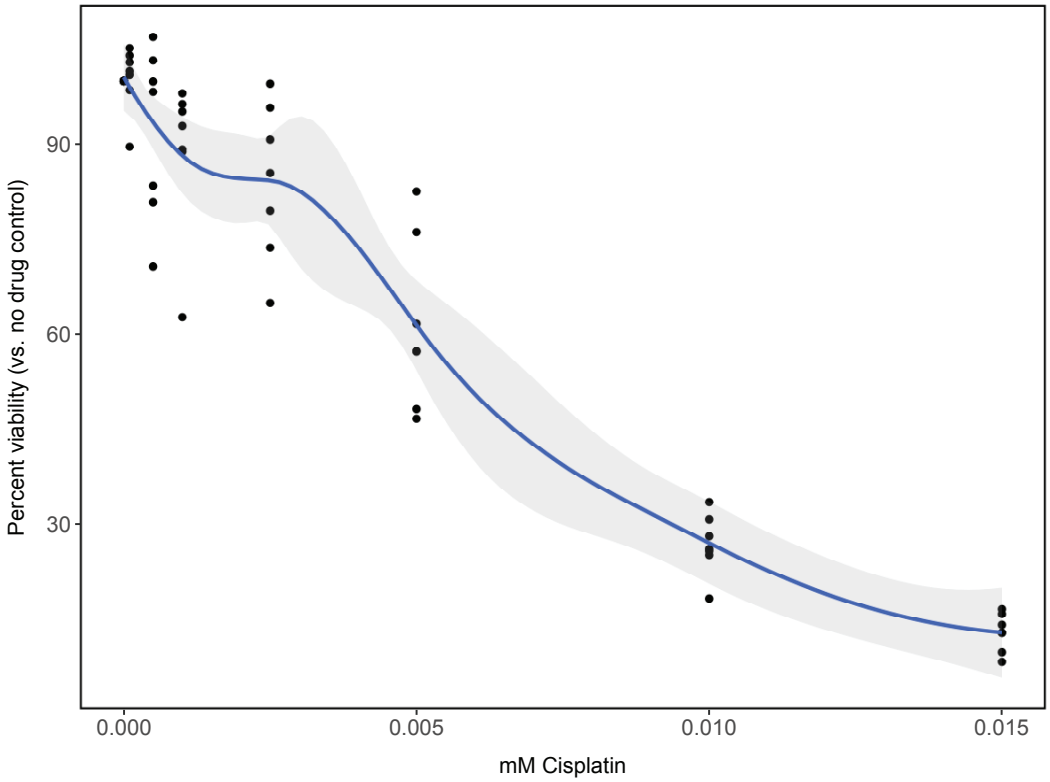

Figure 4.2 Cisplatin treatment results in dose-dependent HK-2 proximal kidney tubule cell death. Human proximal tubule HK-2 cells were treated with increasing doses of freshly-prepared cisplatin (0.0001-0.015mM) for 48hr. Then an alamarBlue™ was used according to manufacturer's instructions to assess relative cell viability (compared to untreated controls). The average of at least 2 wells was used per replicate. N=4. This dose-response relationship is represented by the blue line on the scatter plot, which was calculated using a four-parameter log-logistic model, as described in a recent study (Ritz et al., 2015). This modelling was done in R with the *drc* extension package. The grey shaded area represents the 95% confidence interval of this particular line.

4.2.2 In Vitro HK-2 Nephrotoxicity Drug Screen Reveals 266 Protective Compounds

Following the *in vitro* toxicity curves with cisplatin, HK-2 cells were either untreated, treated with 0.005 mM of cisplatin alone, or treated with 0.005 mM cisplatin (near the value of the calculated EC50) + one of the compounds from the Sigma LOPAC®^{1280} library at a final concentration of 0.01 mM. At the final timepoint, all media was discarded, and the alamarBlue™ viability assay was performed. The viability values were compared to those containing the cisplatin alone (**Figure 4.3**). Hits were defined as those compounds that resulted in average viability readouts of between 0.9-1.1 fold the value of the control wells, or those wells that contained no drug. This resulted in identification of 266 potentially nephroprotective compounds.

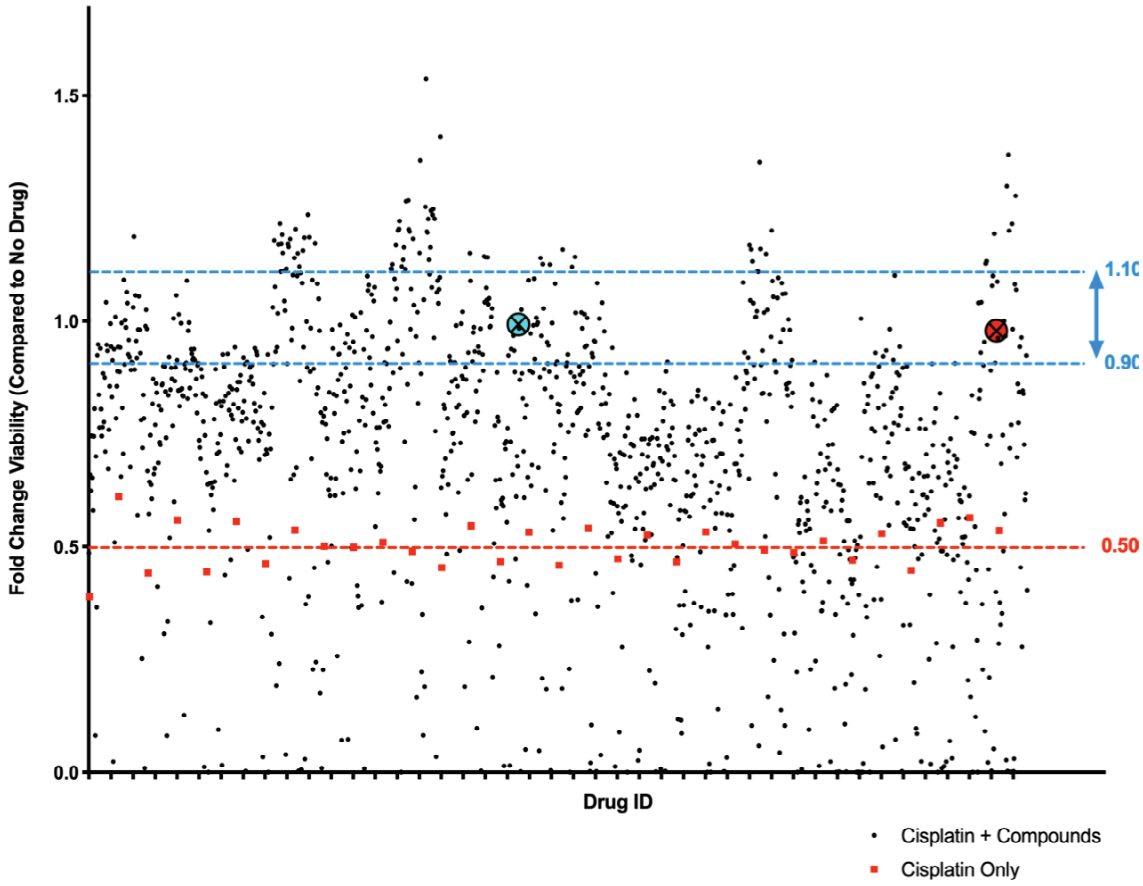

Figure 4.3 ***In vitro*** **nephrotoxicity drug screen assay results in 266 potentially nephroprotective compounds.** HK-2 proximal tubule cells were either treated with vehicle control, 0.005mM cisplatin alone, or cisplatin + each of the compounds from the Sigma LOPAC®^{1280} library at a final concentration of 0.01mM. Two days later, alamarBlue™ was used according to manufacturer's instructions to assess relative cell viability (compared to untreated controls). The average of 2 wells was used per replicate. The aqua point with the X represents dopamine hydrochloride and the red point with the X represents L-mimosine. The blue lines correspond to between 0.9-1.1 fold the control, or untreated values. The red hashed line corresponds to the average of cells treated with cisplatin alone.

4.3 Combining the Findings from the *In Vivo* Ototoxicity screen and the *In Vitro* Nephrotoxicity Screen Reveals 22 Compounds That Were Both Oto- and Nephroprotective

Following completion of both the *in vivo* ototoxicity and *in vitro* nephrotoxicity screens, I cross-referenced the hits to determine if there was overlap between the assays. Assessment revealed that there were 22 compounds that had potential as both oto- and

nephroprotective agents; these compounds, their mechanism of action (as defined by the Sigma LOPAC®[1280] compound library), current clinical usage, and any notes of interest can be found in **Table 4.2**. It should be noted that the compounds that were either oto- or nephroprotective, but not both are not without value. However, for the purposes of this study, emphasis was placed on compounds that had both oto- and nephroprotective potential in efforts to reduce polypharmacy in this already highly-treated population.

Table 4.2 Compounds from the Sigma LOPAC®[1280] compound library that were protective hits in both the *in vitro* nephrotoxicity and *in vivo* ototoxicity screens. Clinical usage information obtained from ChEMBL Database (Gaulton et al., 2017)

Drug ID	Drug Name	Biological Action	Clinical Usage	Notes
1, D06	5-azacytidine	DNA methyltransferase inhibitor	Approved for use in myelodysplatic syndrome (MDS), chronic myelomonocytic leukemia (CML), some advanced solid tumours	
1, E02	(±)-Nipecotic acid	GABA uptake inhibitor	N/A	
1, F07	1-Aminobenzotriazole	Cytochrome P450 and chloroperoxidase inhibitor	N/A	Potent cytochrome P450 inhibitor, used in research (Ortiz de Montellano, 2018)
1, G06	Apigenin	Arrests cell cycle at G2/M phase	N/A	Protects against cisplatin-induced nephrotoxicity in preclinical models (Hassan, Khalaf, Sadek, & Abo-youssef, 2017; Ju et al., 2015) and may have anticancer activities summarized by (X. Yan, Qi, Li, Zhan, & Shao, 2017)
3, F04	Betamethasone	SAID (steroidal anti-inflammatory drug); glucocorticoid	Approved for use in obstructive lung disease, nasal obstruction, eye diseases, eczema and psoriasis	Historically showed some efficacy as an anti-emetic agent in chemotherapy regimens (Sorbe, 1988)
5, F10	Ganaxolone	Positive allosteric modulator of GABA-A receptors	N/A	Reached Phase III clinical trials for use in drug resistant partial onset seizures (NCT01963208)
6, E07	GBR-12909 dihydrochloride (Vanoxerine)	Selective dopamine reuptake inhibitor	N/A	Investigated as a potential treatment for cocaine-abuse disorder (NCT00218049)
7, B03	N-Ethylmaleimide	Sulfhydryl alkylating agent that inactivates NADP-dependent isocitrate dehydrogenase and many endonucleases	N/A	
7, E04	Phenserine	Selective, non-competitive acetylcholinesterase (AChE) inhibitor	N/A	
7, G06	p-Fluoro-L-phenylalanine	Substrate for tyrosine hydroxylase; arrests cells at G2	N/A	
8, C07	**Dopamine hydrochloride**	**Endogenous neurotransmitter**	**Approved for use in shock caused by heart attack, trauma, surgery,**	**Historically investigated as a potential nephroprotective agent for use with cisplatin** (Baldwin, Henderson, & Hickman, 1994; Somlo et al.,

			heart failure, and kidney failure	1995)**, may influence neurotransmission at sensory hair cells (Toro et al., 2015) and is known to be involved in auditory processes (Gittelman, Perkel, & Portfors, 2013)**
9, H05	SB-525334	A potent activin receptor-like kinase (ALK5)/type I TGFß-receptor kinase inhibitor	N/A	
12, G04	Ouabain	Blocks movement of the H5 and H6 transmembrane domains of Na^+-K^+ ATPases	N/A	Historical use for myocardial infarction and angina treatment, used in the treatment of digitalis intoxication (Furstenwerth, 2010), used in poison darts in eastern Africa, defined as an "extremely hazardous substance" in the USA
14, E04	Ritanserin	Potent 5-HT2 serotonin receptor antagonist which passes the blood-brain barrier	N/A	Investigated for use in cocaine dependence (NCT00000187)
14, E08	CP-335963	Aurora 2 kinase inhibitor, PDGF inhibitor, and anti-proliferative	N/A	
15, C11	Tyrphostin 1	EGFR tyrosine kinase inhibitor	N/A	Tyrphostins have been shown to reduce small intestinal damage by cisplatin and 5-Fluorouracil (5-FU) (Zlotnik, Patya, Vanichkin, & Novogrodsky, 2005)
15, G02	'1-(1-Naphthyl)piperazine hydrochloride	5-HT2 serotonin receptor antagonist	N/A	
16, D03	Trifluoperazine dihydrochloride	Xanthogenate derivative with *in vivo* anti-tumor and anti-HIV activity; inhibits phospholipase D and phosphatidylcholine phospholipase C (PIPLC)	Approved for use as an antipsychotic for individuals with schizophrenia, some use as an anxiolytic, D_2 receptor antagonist	Has anti-adrenergic, anti-dopaminergic and anti-cholinergic effects. Thought to minimize hallucinations and delusions through inhibition of the D_2 receptors in the mesocortical and mesolimbic pathways
16, D07	S(-)-UH-301 hydrochloride	Potent and selective 5-HT1A serotonin receptor antagonist	N/A	
16, D09	**L-Mimosine from Koa hoale seeds**	**Potential inhibitor of the cell cycle giving rise to growth arrest in G1-phase. An iron chelator that inhibits DNA replication in mammalian cells. Has been shown to have apoptotic activity in xenotransplanted human pancreatic cancer**	**N/A**	**Inhibits copper containing enzymes tyrosinase and dopamine β-hydroxylase (Hashiguch & Takahashi, 1976), shown to re-activate hypoxia-inducible factor 1α (HIF-1α) and reduce renal fibrosis in a rat model of renal ablation (Yu et al., 2012), blocks proliferation in prostate carcinoma cells (Chung et al., 2011) and breast cancer cells (Kulp & Vulliet, 1996)**

16, D10	AC-55649	Subtype selective retinoic acid receptor beta2 (RARbeta2) agonist	N/A	RARβ may have tumour suppressor activities (Alvarez et al., 2007)
16, F11	Caroverine hydrochloride	Nonselective NMDA and AMPA glutamate receptor antagonist	Used to treat muscle spasms and tinnitus in some countries, not FDA approved	Has antioxidant properties (Udilova, Kozlov, & Bieberschulte, 2003), attenuates noise induced hearing loss in rats (Duan et al., 2006), treats tinnitus in humans (Denk et al., 1997)

4.4 Verification of Protective Compounds Supports the Protective Effects of Two Compounds

4.4.1 Ototoxicity Studies Support the Protective Effects of Dopamine and L-mimosine

In order to verify the validity of these protective compounds, larvae were treated with cisplatin + 0.01 mM of the 24 compounds that were hits in both the oto- and the nephroprotection assays. I avoided other compounds as a result of aspects of either their pharmacology, or their potential mechanism of action. For example, I avoided 1-Aminobenzotriazole because it is a potent cytochrome P450 inhibitor and is thus likely to interact with other drugs in this heavily treated patient population. Along similar lines, I avoided Ouabain as a result of the classification as a "very hazardous substance". Apigenin was another oto- and nephroprotective compound which I did not explore further, as it has already been shown to prevent nephrotoxicity through activity as an antioxidant; thus, it is less likely to be novel (Hassan et al., 2017; Ju et al., 2015). Similarly, caroverine hydrochloride has already been used to treat noise-induced hearing loss in some countries (Denk et al., 1997; Duan et al., 2006). However, the appearance of some of these compounds in the list of protective drugs provided more assurance that the screens produced legitimate hits.

Dopamine and L-mimosine appeared to be some of the most protective compounds. Interestingly, they also shared a similar structure (**Figure 4.4a** and **b).** I was interested in the multiple appearances of the dopaminergic pathway in the list of hits. Dopamine hydrochloride, GBR-12909 dihydrochloride (Vanoxerine, a dopamine reuptake inhibitor), p-Fluoro-L-phenylalanine (substrate for Tyrosine hydroxylase), and L-mimosine (inhibitor of dopamine β-hydroxylase (Hashiguch & Takahashi, 1976))

would all result in the pharmacological result of increased synaptic dopamine levels. An overview of the potential interaction between these compounds can be seen in **Figure 4.5**.

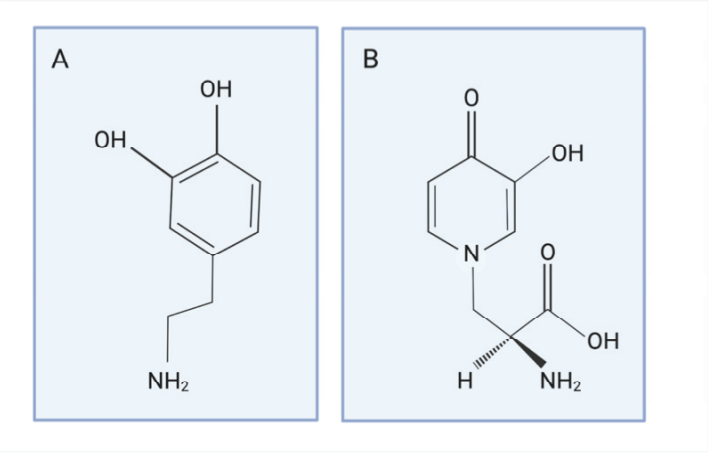

Figure 4.4 Chemical structures of dopamine and L-mimosine. A) Dopamine consists of a catechol structure, containing a benzene ring and two hydroxyl groups in addition to an amine group attached by an ethyl chain. Chemical formula $C_8H_{11}NO_2$. Molecular weight 153.18g/mol. B) L-mimosine is a non-protein amino acid that can be isolated from plants, that is chemically similar to tyrosine. Chemical formula $C_8H_{10}N_2O_4$. Molecular weight 198.18g/mol.

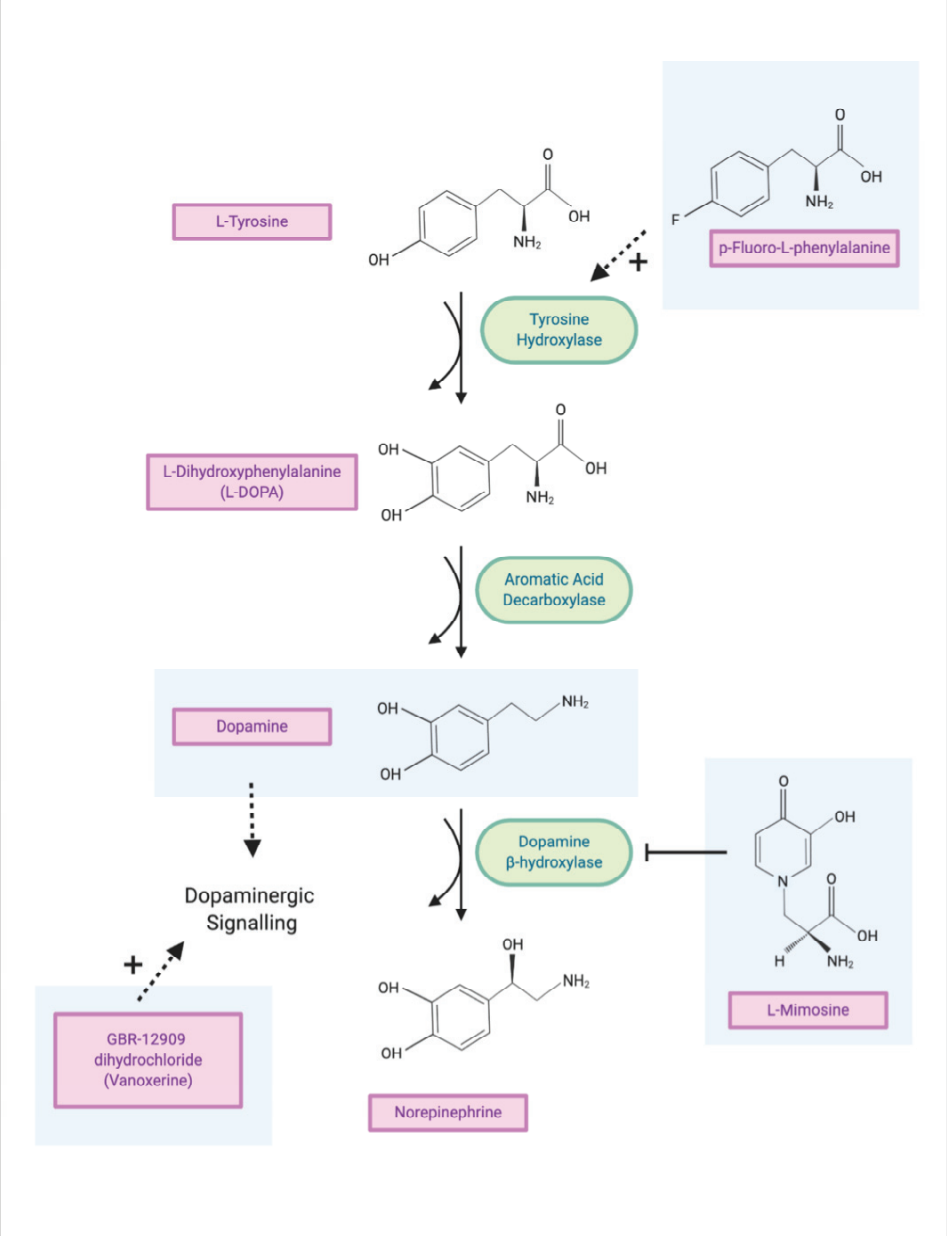

Figure 4.5 Interaction between potentially oto- and nephroprotective compounds with the dopamine biosynthesis pathway. The dopamine biosynthesis pathway consists of intermediates, shown here in their molecular form and in light purple boxes, and enzymes, shown here in green ovals. L-tyrosine is converted to L-hydroxyphenylalanine (L-DOPA) by tyrosine hydroxylase. L-DOPA is converted to dopamine by aromatic acid decarboxylase. Dopamine is a neurotransmitter and can engage in dopaminergic signalling. Dopamine is converted to norepinephrine by dopamine β-hydroxylase. Norepinephrine is also a neurotransmitter, and can also engage in signalling. The compounds that were hits in the oto- and nephrotoxicity screen are shown in front of light blue boxes. Dopamine itself was a hit. L-mimosine is capable of inhibiting dopamine β-hydroxylase. P-fluoro-L-phenylalanine can act as a substrate for tyrosine hydroxylase. GBR-12909 dihydrochloride, also known as Vanoxerine, is a selective dopamine reuptake inhibitor. All of these compounds could have the net pharmacological effect of increasing dopamine levels.

4.4.1.1 Neuromast Studies Confirm Otoprotection by Dopamine and L-mimosine

4.4.1.1.1 Protective Agent Schedule Optimization Suggests that -12 Hour Pretreatment is Optimal for Protection

The timing of protective agent administration is critical. As previously mentioned, the initial *in vivo* drug screen was done with a 3 hr pretreatment with the library compounds prior to cisplatin treatment. The importance of this assessment is exemplified by sodium thiosulphate (STS), an otoprotective agent that is currently in Phase III clinical trials. The administration of this compound must be delayed for at least 4-8 hr following cisplatin dosing in order to decrease the likelihood that STS will interfere with the anticancer effects of cisplatin (Freyer et al., 2017; Harned et al., 2008; L. L. Muldoon et al., 2000). Thus, I performed a time-course assessment of the otoprotective capacity of dopamine, from 12 hr prior to cisplatin treatment until 12 hr following cisplatin treatment. Larvae were treated with 0.01 mM of dopamine (the screening concentration) at the timepoints specified in **Figure 4.6**, then were treated with 0.02 mM cisplatin for 24 hr. Larvae were then stained with YO-PRO1 and biosorted. Results from this experimental replicate can be found in **Figure 4.6**. Based on this initial time-course analysis, 12 hr pretreatment with dopamine was a suitable timepoint to carry forward to the rest of the studies (*=$p<0.05$). In addition, I used this opportunity to test the potential efficacy of STS. I completed the same time course experiment that was completed with dopamine, with STS at a final concentration of 0.005 mM. In this assay, at this concentration, there was no significant protection of the neuromast hair cells from cisplatin-induced damage (**Figure 4.7**).

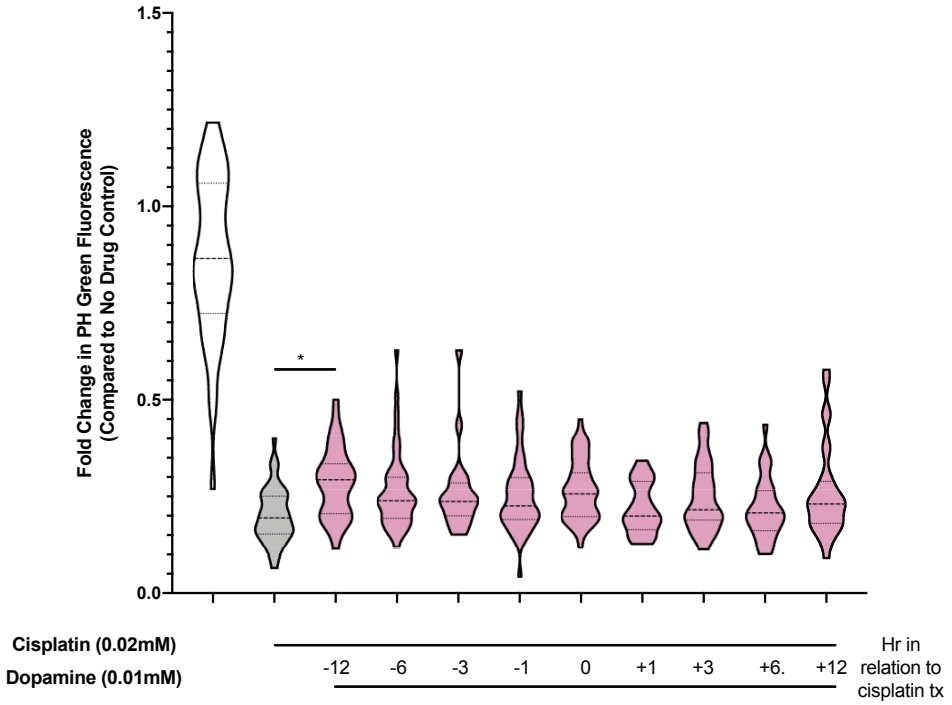

Figure 4.6 Dopamine protects against cisplatin-induced lateral line neuromast damage in a time-dependent manner. *Casper* zebrafish larvae were treated with 0.01mM dopamine either 12, 6, 3, or 1hr prior to, or post treatment with 0.02mM cisplatin. The following day, all larvae were rinsed, then stained with 2μM YO-PRO1 for 1hr, rinsed, then subjected to biosorter-based fluorescence profiling. Fold change in peak height (PH) of green fluorescence is shown (relative to untreated controls). N=1, approximately 50 larvae/treatment group. * = $p<0.05$, as per one-way ANOVA with a Tukey post-test assessing comparisons between the treatment groups indicated.

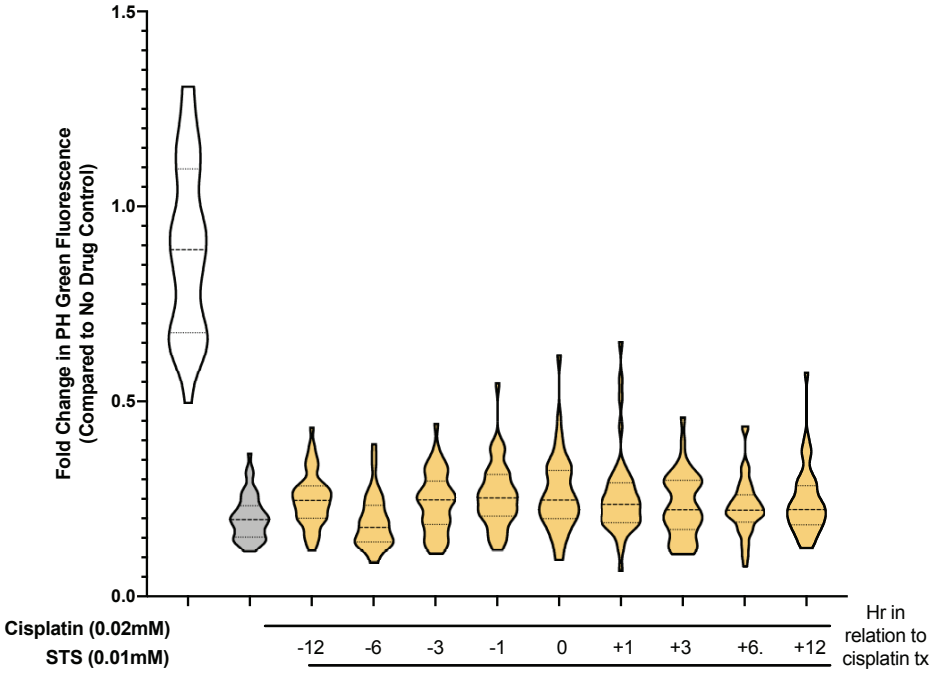

Figure 4.7 Sodium thiosulfate (STS) does not protect lateral line neuromasts from cisplatin-induced damage. *Casper* zebrafish larvae were treated with 0.01mM STS either 12, 6, 3, or 1hr prior to, or post treatment with 0.02mM cisplatin. The following day, all larvae were rinsed, then stained with 2μM YO-PRO1 for 1hr, rinsed, then subjected to biosorter-based fluorescence profiling. Fold change in peak height (PH) of green fluorescence is shown (relative to untreated controls). N=1, approximately 50 larvae/treatment group.

4.4.1.1.2 Protective Agent Dose Optimization Suggests that 0.03mM is an Optimal Dose of both Dopamine and L-mimosine

Following determination of the protective agent administration timing, I aimed to optimize the doses of both dopamine and L-mimosine. The following dose optimization experiments were completed as one large experiment, as displayed in **Figure 4.8**. However, I have divided the graphs into sections to facilitate visualization, in **Figure 4.9a-d**. All of the pretreatments in the following experiments were administered 12 hr prior to cisplatin treatment. First, I assessed the impact of either L-mimosine (0.04 mM)

or dopamine and L-mimosine (0.02 mM/0.02 mM) on neuromast health in the absence of cisplatin (**Figure 4.9a**). There was a slight, albeit significant difference between vehicle-treated larvae and those treated with 0.04 mM L-mimosine (**=p=0.0081), however, there was no difference observed in larvae treated with 0.02mM each of dopamine and L-mimosine. Next, I performed a dopamine pretreatment dose-response curve (0.01-0.04 mM) to determine the optimal protective dose (**Figure 4.9b**). While no dose restored the PH of neuromast fluorescence to control levels, pretreatment of the larvae with 0.01, 0.02 and 0.03 mM of dopamine resulted in significant increase in neuromast health, in comparison with the cisplatin alone group (****=p<0.0001). As there was no significant overall toxicity with 0.03 mM, this is the dose that I used in all subsequent experiments. I performed a similar dose-response curve with L-mimosine (**Figure 4.9c**), and at 0.01, 0.02, 0.03 and 0.04 mM, L-mimosine was significantly protective in comparison with cisplatin alone (****=p<0.0001). During pretreatment with 0.04 mM L-mimosine, some larvae developed some degree of lateral curvature and pericardial edema; thus, all future experiments used 0.03 mM L-mimosine.

It should be noted that none of these optimized treatments resulted in a restoration of neuromast PH fluorescence levels back to the untreated control levels. Thus, I decided to design an experiment aimed at determining whether or not the achieved level of protection was biologically and potentially clinically relevant. I treated larvae with half of the dose of cisplatin (0.01 mM, instead of 0.02 mM), then compared the neuromast PH fluorescence to those larvae that received the full dose of cisplatin (0.02 mM) in addition to being pretreated with the protective agents at their most promising doses (**Figure 4.9d)**. Results demonstrated that larvae pretreated with either 0.04 mM L-mimosine, or 0.02 mM each of dopamine and L-mimosine prior to cisplatin treatment had PH

neuromast fluorescence that is not significantly different from the half dose of cisplatin. Representative images from the most promising treatments, and the full dose of 0.02 mM cisplatin can be found in **Figure 4.10**. Overall, we are able to increase the average fluorescence levels from 0.268 fold of control values, in the 0.02 mM cisplatin treatment group to 0.316 and 0.357 in the groups that were pretreated with 0.03mM dopamine and L-mimosine, respectively. This translates to a 1.179 and 1.332 fold protection, respectively.

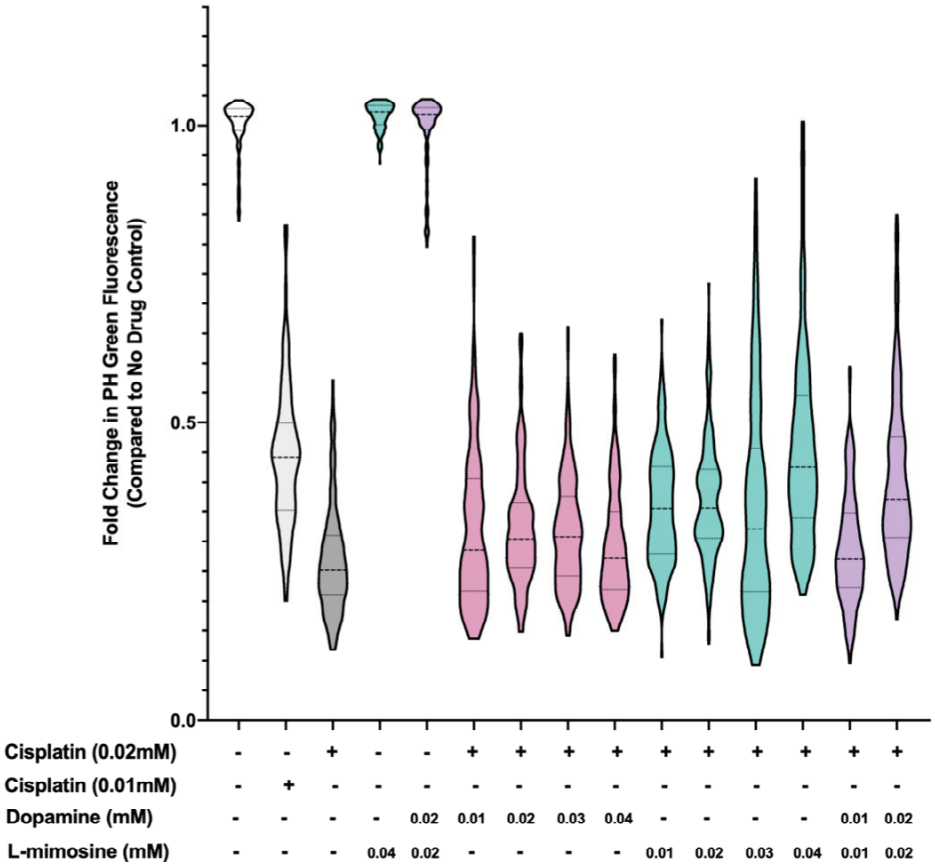

Figure 4.8 Dopamine and L-mimosine partially protect lateral line neuromasts from cisplatin-induced damage. *Casper* zebrafish larvae were pretreated at 60 hours post fertilization (hpf) with either vehicle control, or dopamine and/or L-mimosine at the concentrations specified above. At 72hpf the larvae were then treated with either a vehicle control or freshly-prepared cisplatin at the concentrations specified above. The following day, all larvae were rinsed, then stained with 2μM YO-PRO1 for 1hr, rinsed, then subjected to biosorter-based fluorescence profiling. Fold change in peak height of green fluorescence is shown (relative to untreated controls). These violin plots display the distribution of data and are marked in the centre at the median, and then at the quartiles. For ease of comprehension and visualization, this data will be subdivided into smaller graphs, where statistics will be displayed. N=3, average of 75 larvae/treatment group.

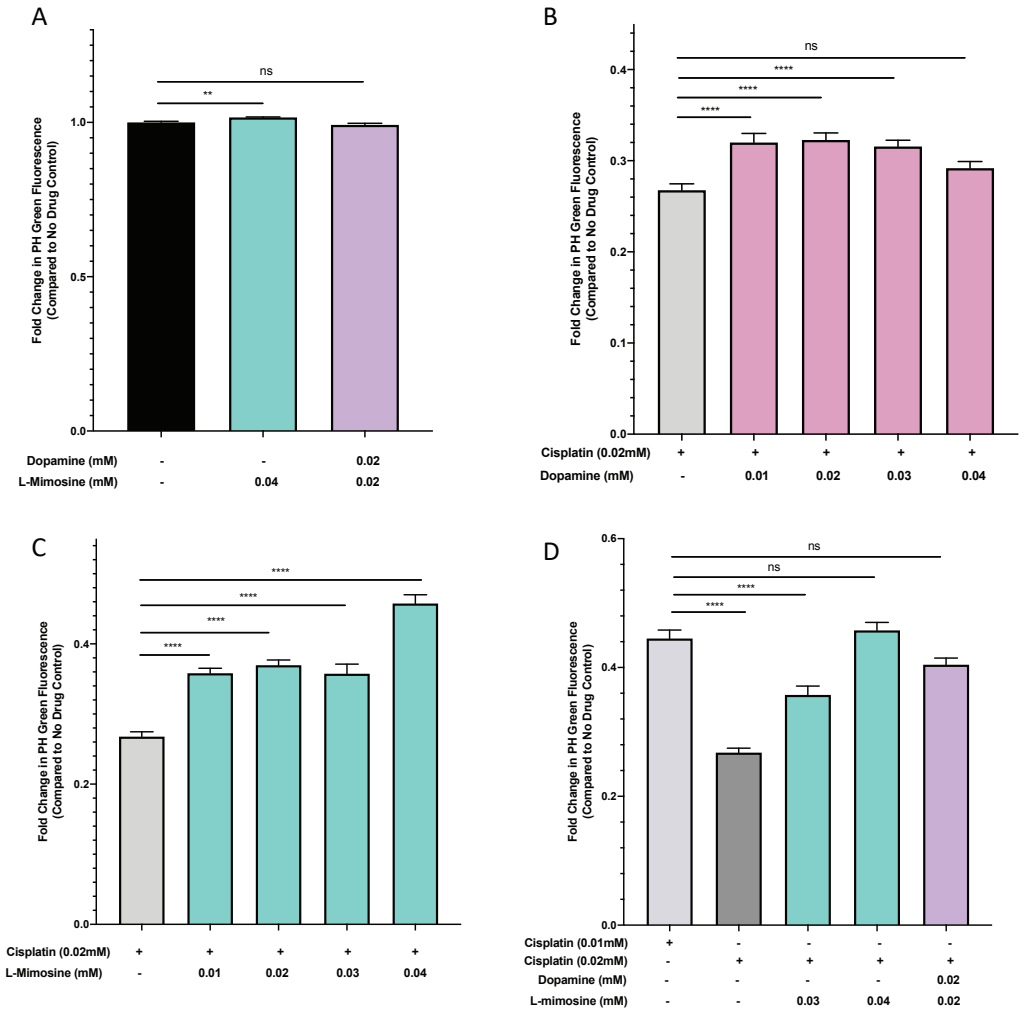

Figure 4.9 Dopamine and L-mimosine protect lateral line neuromasts from cisplatin-induced damage. *Casper* zebrafish larvae were pretreated at 60 hours post fertilization (hpf) with either vehicle control, or dopamine and/or L-mimosine at the concentrations specified above. At 72hpf the larvae were then treated with either a vehicle control or freshly-prepared cisplatin at the concentrations specified above. The following day, all larvae were rinsed, then stained with 2µM YO-PRO1 for 1hr, rinsed, then subjected to biosorter-based fluorescence profiling. Fold change in peak height (PH) of green fluorescence is shown (all relative to untreated controls, even if the control bar does not appear in the graph). A) Analysis of protective agents in the absence of cisplatin shows slight, but statistically significant increase in PH green fluorescence with 0.04mM L-mimosine pretreatment, but not with 0.02mM pretreatment with both dopamine and L-mimosine. **=$p<0.01$, as per one-way ANOVA with a tukey post-test, between indicated groups. B) Dose optimization shows protection with 0.01, 0.02 and 0.03mM dopamine pretreatment. ****=$p<0.0001$, as per one-way ANOVA with a tukey post-test, between indicated groups. C) Dose optimization shows protection with 0.01, 0.02, 0.03, and 0.04mM L-mimosine pretreatment. ****=$p<0.0001$, as per one-way ANOVA with a tukey post-test, between indicated groups. D) Pretreatment with either 0.04mM L-mimosine or co-treatment with 0.02mM dopamine and L-mimosine results in PH neuromast fluorescence that is not significantly different from larvae treated with half the dose of cisplatin, or 0.01mM. ****=$p<0.0001$, as per one-way ANOVA with a tukey post-test, between indicated groups. N=3, average of 75 larvae/treatment group. Error bars represent SEM.

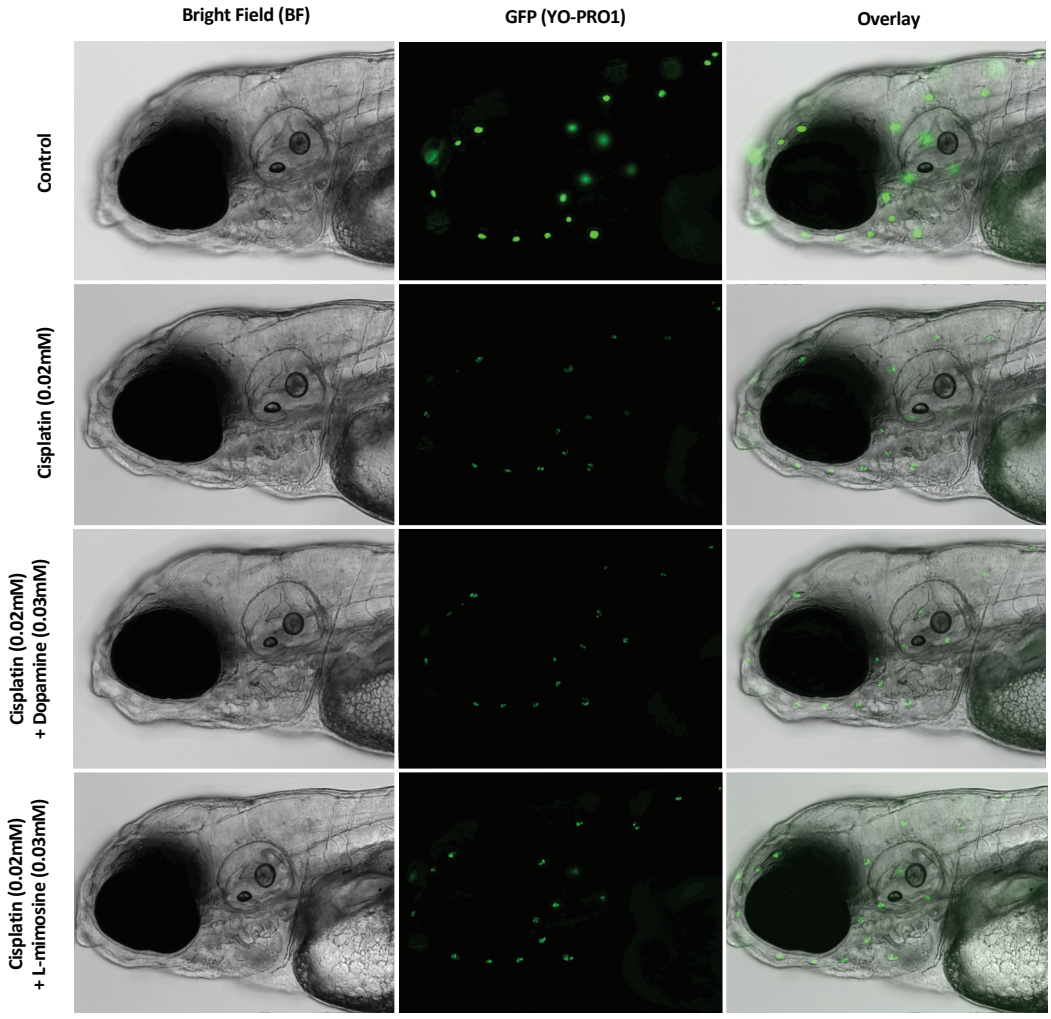

Figure 4.10 Dopamine and L-mimosine visibly protect lateral line neuromasts from cisplatin-induced damage. *Casper* zebrafish larvae were pretreated at 60 hours post fertilization (hpf) with either vehicle control, or dopamine or L-mimosine at the concentrations specified above. At 72hpf the larvae were then treated with either a vehicle control or freshly-prepared cisplatin at the concentrations specified above. The following day, all larvae were rinsed, then stained with 2µM YO-PRO1 for 1hr, rinsed and imaged at 20X on a an inverted Axio Observer Z1 microscope .

4.4.1.2 Dopamine and L-mimosine Protect Zebrafish Inner Ear Hair Cells from Cisplatin-Induced Damage

To determine whether the protective effects of dopamine and L-mimosine were preserved when examining other aspects of ototoxicity, I stained larvae with Alexa Fluor 488 phalloidin, which is known to label the filamentous actin in the stereocilia of zebrafish inner ear hair cells (Baxendale & Whitfield, 2016). I treated groups of larvae with either vehicle control, or 0.03 mM of either dopamine or L-mimosine, then treated them 12 hr later with 0.1 mM cisplatin for 48 hr (**Figure 4.11, a-c**= control, **d-f**= cisplatin alone, **g-i**= cisplatin + dopamine and **j-l**= cisplatin + L-mimosine). Larvae were fixed, permeabilized, then stained with Alexa Fluor 488 phalloidin. Images were taken with the same exposure, intensity, and brightness settings. Confocal imaging was performed by Dr. Matt Stoyek (Dalhousie University). At 48 hr post cisplatin treatment, the hair cell stereocilia appear shorter, more frayed, and fewer in number in larvae that were treated with cisplatin. Treatment with dopamine partially protects the hair cell structures, but L-mimosine seems to provide a greater level of protection from visible cisplatin-induced hair cell damage.

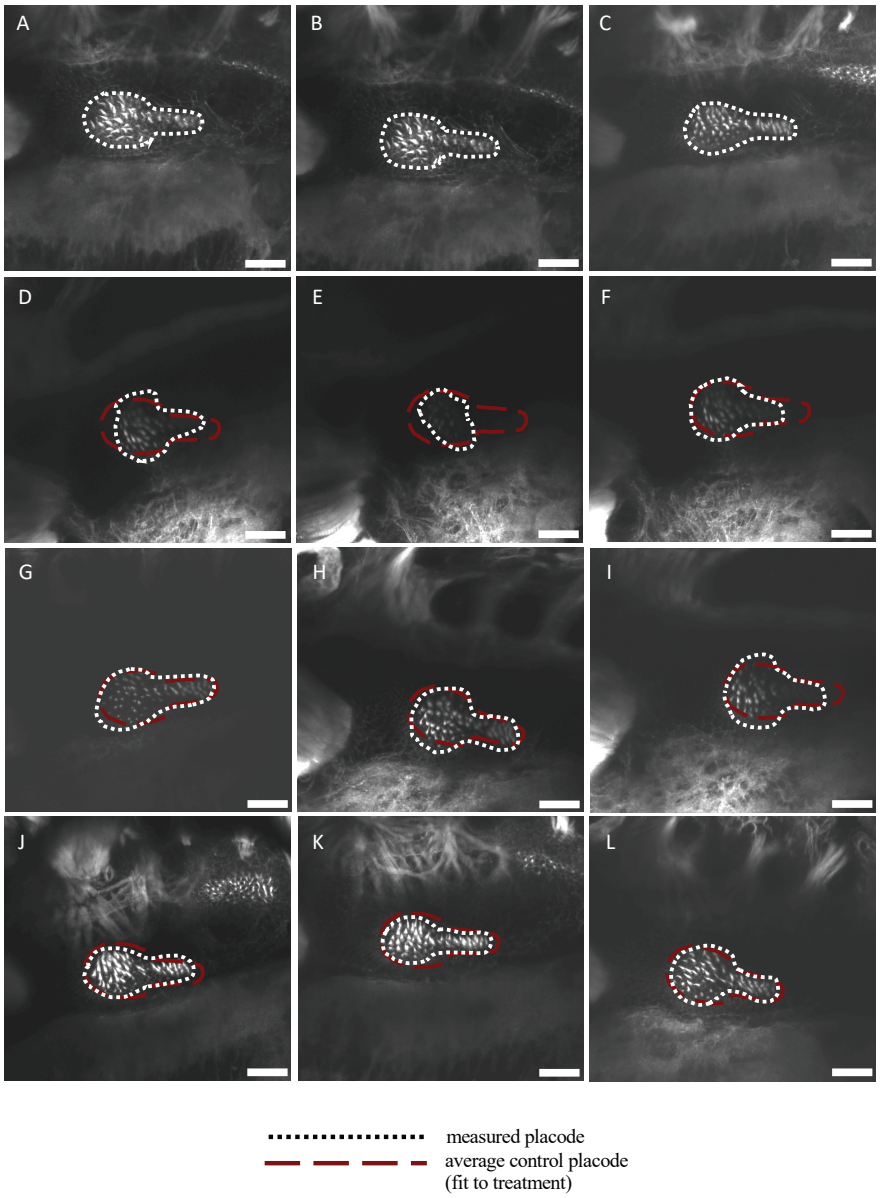

Figure 4.11 Confocal imaging of phalloidin stained inner ear demonstrates that dopamine and L-mimosine protect the inner ear hair cells from cisplatin-induced damage. *Casper* zebrafish larvae were pretreated at 60 hours post fertilization (hpf) with vehicle control, or either 0.03mM dopamine or 0.03mM L-mimosine. At 72hpf, these larvae were either treated with vehicle control or 0.1mM freshly-prepared cisplatin. Two days later (48hr post cisplatin treatment), the larvae were rinsed, then fixed with 4% paraformaldehyde (PFA) in phosphate buffered saline (PBS) overnight at 4ºC. Larvae were then permeabilized in 2% Triton-X in PBS (PBS-Tx) for 2hr, then stained with AlexaFluor488-Phalloidin at a concentration of 1:20, for 1.5hr. Larvae were then rinsed thoroughly with 0.2% PBS-Tx, and imaged with a Zeiss LSM510 confocal microscope. A-C) No drug control, D-F) Cisplatin alone, G-I) Cisplatin + dopamine, J-L) Cisplatin + L-mimosine. All larvae were mounted laterally with the ventral side at the top. Scale bar = 20µm. N=6/treatment. White dashed line represents the average placode area of 3 control larvae, red dashed line represents this average superimposed onto other treatments.

4.4.2 Nephrotoxicity Assays Suggest that Dopamine and L-mimosine Provide Physiological, but Not Histological Protection from Cisplatin-Induced Damage

4.4.2.1 Dopamine and L-mimosine Protect Zebrafish Larval Glomerular Filtration Rate (GFR) from Cisplatin-Induced Damage

In order to perform *in vivo* assessment of glomerular filtration rate (GFR), I employed an inulin-based assay that has been used by others in zebrafish larvae (Hentschel et al., 2005; Rider et al., 2012). Briefly, FITC-labelled inulin was injected into circulation of larvae that had been treated with either vehicle control, cisplatin alone (0.125 mM), or pretreated with either dopamine or L-mimosine (0.03 mM) prior to cisplatin treatment. Inulin injection was performed by Nicole Melong (IWK Health Centre). Inulin is a polysaccharide that is exclusively excreted through the nephron, so decreases in larval fluorescence are a measure of pronephron function. Injected larvae were biosorted immediately following injection, then at 2hr following injection, and results ae displayed as fold change in overall larval fluorescence in relation to the 0hr timepoint (**Figure 4.12**, top panel). Images were taken of representative larvae at both time points (**Figure 4.12**, bottom panel). In the untreated control group, there is a significant difference between the larval fluorescence at 2 hr in comparison with 0 hr (****=$p<0.0001$). In the cisplatin treated group, there is no significant difference between fluorescence at the two timepoints, indicating that the GFR is lower. However, when the larvae were pretreated with either dopamine or L-mimosine, there is a statistical difference between the 0 and 2 hr timepoints (****=$p<0.0001$ in each group). This suggests that the pretreatment has provided a degree of protection against cisplatin-induced changes to larval GFR.

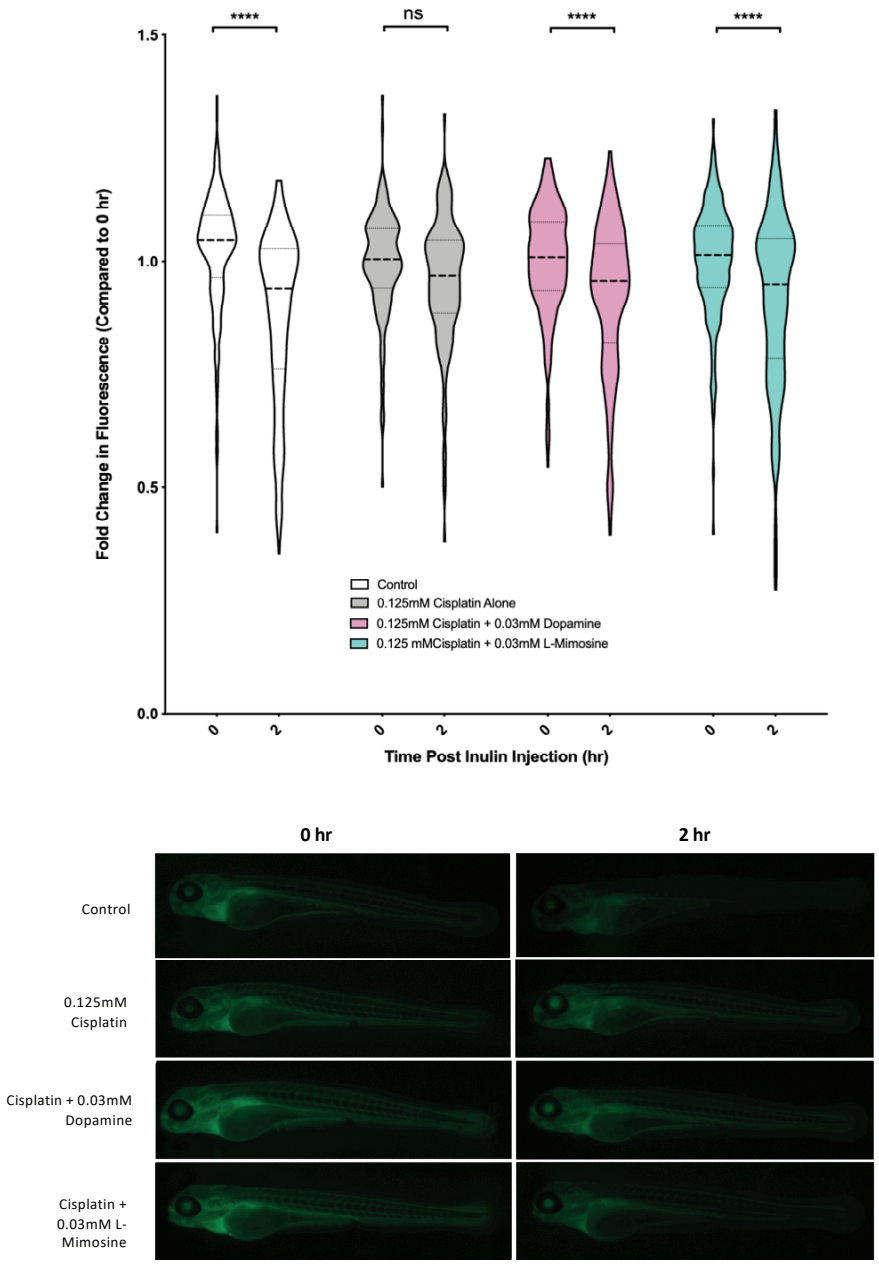

Figure 4.12 ***In vivo*** **glomerular filtration assay demonstrates that dopamine and L-mimosine protect the kidney function in cisplatin-treated larvae.** *Casper* zebrafish larvae were treated with vehicle control or either 0.03mM dopamine or 0.03mM L-mimosine at 60 hours post fertilization (hpf). At 72hpf, larvae were treated with either vehicle control, or 0.125mM freshly-prepared cisplatin. The following day, larvae were rinsed, then injected individually in the common cardinal vein with FITC-Inulin. Immediately following injection, larvae were measured for overall green fluorescence on the biosorter. These larvae were rinsed, then measured again 2hr later. Graph represents the fold change in green fluorescence in comparison to the 0hr time point. **** = $p<0.001$, as per two-way ANOVA with a Tukey post-test. Experiment repeated 3X, with at least 50 larvae/treatment group each time. Representative images of injected larvae at each time point can be found below.

4.4.2.2 Histology Studies Suggest that there is No Visible Cisplatin-Induced Damage in the Zebrafish Pronephros

As a result of the changes to GFR, I decided to assess if there were any visible histological changes at the level of the pronephros structure in treated zebrafish larvae. Briefly, I treated zebrafish larvae in the exact manner as the inulin-based GFR assay, then fixed the larvae at either 1 day post treatment (dpt; **Figure 4.13**), or at 4 dpt (**Figure 4.14**). The larvae were then sectioned and stained with H&E. The embedding, sectioning and staining was completed by the histology lab at the IWK Health Centre (Halifax, NS, Canada), and slides were examined by Dr. Craig Midgen, a pathologist at the IWK Health Centre. At both 1 and 4 dpt, there were no overt differences between treatment groups.

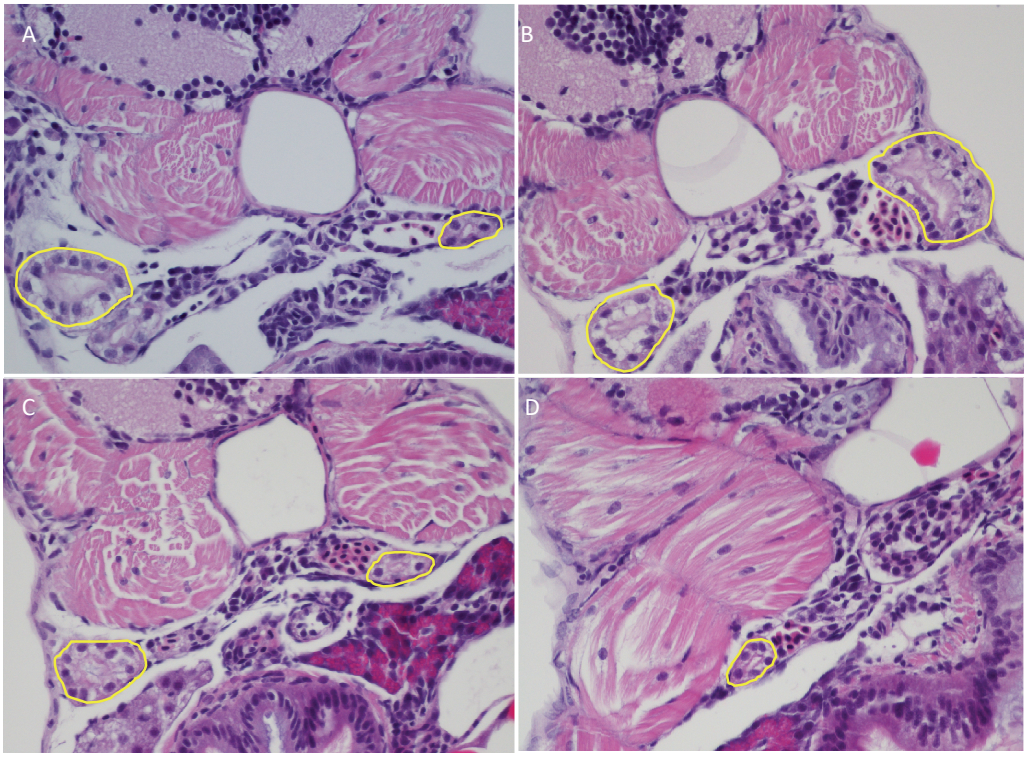

Figure 4.13 Zebrafish pronephros histology does not look significantly different following treatment with cisplatin or either protective agent at 1 day post treatment (dpt). *Casper* zebrafish larvae were treated at 60 hours post fertilization (hpf) with either vehicle control or either 0.03mM dopamine or 0.03mM L-mimosine, then at 72hpf with 0.125mM freshly-prepared cisplatin, or vehicle control. The next day, larvae were sacrificed, then fixed with 4% paraformaldehyde (PFA) in phosphate buffered saline (PBS) overnight at 4ºC. The fixed larvae were then pre-mounted in 1.5% low-melting point agarose, arranged in parallel for paraffin embedding. Paraffin embedded larvae were sectioned, then stained with H&E and examined with light microscopy. A) Untreated control, B) Cisplatin alone, C) Cisplatin + dopamine, D) Cisplatin + L-mimosine. Yellow outlines highlight proximal tubular pronephros structures.

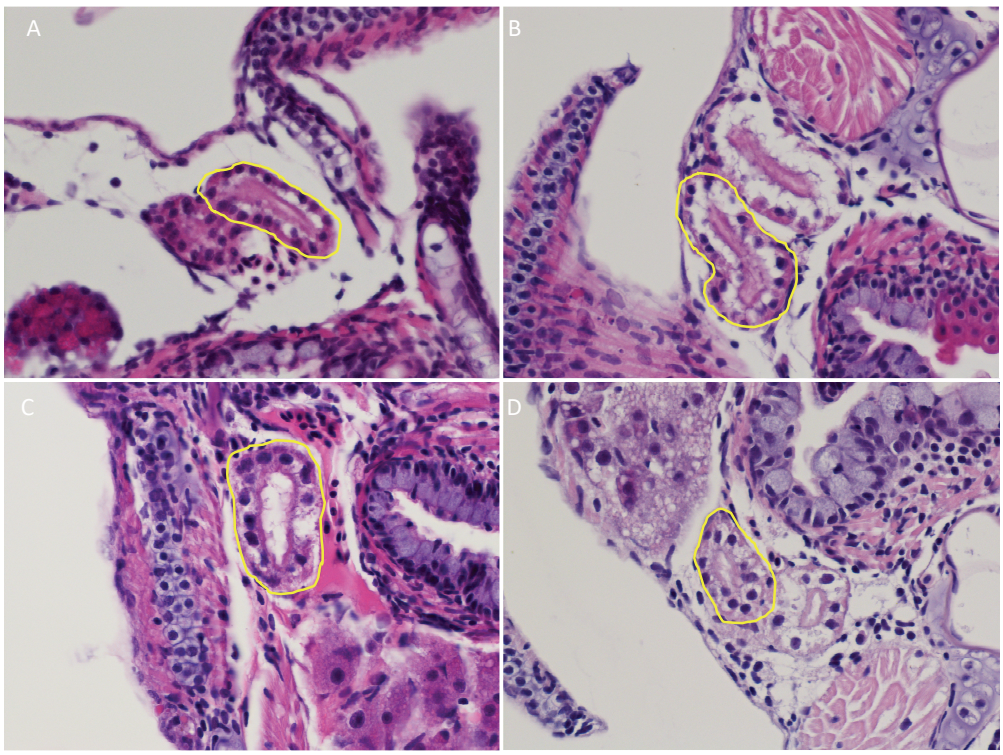

Figure 4.14 Zebrafish pronephros histology does not look significantly different following treatment with cisplatin or either protective agent at 4 day post treatment (dpt). *Casper* zebrafish larvae were treated at 60 hours post fertilization (hpf) with either vehicle control or either 0.03mM dopamine or 0.03mM L-mimosine, then at 72hpf with 0.125mM freshly-prepared cisplatin, or vehicle control. Four days later, larvae were sacrificed, then fixed with 4% paraformaldehyde (PFA) in phosphate buffered saline (PBS) overnight at 4ºC. The fixed larvae were then pre-mounted in 1.5% low-melting point agarose, arranged in parallel for paraffin embedding. Paraffin embedded larvae were sectioned, then stained with H&E and examined with light microscopy. A) Untreated control, B) Cisplatin alone, C) Cisplatin + dopamine, D) Cisplatin + L-mimosine. Yellow outlines highlight proximal tubular pronephros structures.

4. 5 Summary of Findings

In summary, I conducted both an *in vivo* ototoxicity and an *in vitro* nephrotoxicity drug screen with the Sigma LOPAC®[1280] compound library, with the overall goal of identifying compounds that could protect against these cisplatin-induced toxicities. I identified 122 potentially otoprotective compounds, 266 potentially nephroprotective compounds, with 22 compounds that were protective in both assays. Of these, two compounds, dopamine and L-mimosine, were investigated further. Follow-up ototoxicity analysis supports that these compounds protect the lateral line neuromasts and the inner ear hair cells from cisplatin-induced damage. Further, a larval GFR assay supports the nephroprotective effects of these compounds.

Chapter 5 Results III: Characterizing the Potential Chemoprotective Effects of Dopamine and L-mimosine

5.1 Cancer Cell Line Viability Assays Confirm the Cytotoxic Effects of Cisplatin are Not Reduced with Dopamine or L-mimosine

To determine whether the protective agents had any protective effects on cancer cells, I first conducted an alamarBlue™ cell viability assay with three cancer cell lines. I used SK-N-AS (non-MYCN-amplified) and LAN5 (MYCN-amplified) neuroblastoma (NBL) cell lines in addition to HSC-3 oral squamous cell carcinoma cell lines for this purpose. These cell lines are all derived from cancers that are treated clinically with cisplatin. I pretreated the cells in 96-well plates with vehicle control, or either dopamine or L-mimosine at the drug screening concentration (0.01 mM), or the *in vivo* optimized concentration (0.03 mM). I performed alamarBlue™ cell viability assays at both 24 hr and 48 hr following cisplatin treatment (**Figure 5.1** and **5.2**). Results demonstrate the percentage of cell viability, in comparison with the untreated control. At each timepoint, in each cell line, with either dopamine or L-mimosine, there was either no significant difference between cisplatin alone and cisplatin + the protective agents, or there was a significant decrease in cell viability. This indicates a potential additive effect to the toxicity of cisplatin in these cancer cell lines. In no instance did either of the protective agents significantly increase the viability of any of these cancer cell lines in comparison with cisplatin alone (*=$p<0.05$, **=$p<0.01$, ***=$p<0.005$, ****=$p<0.001$).

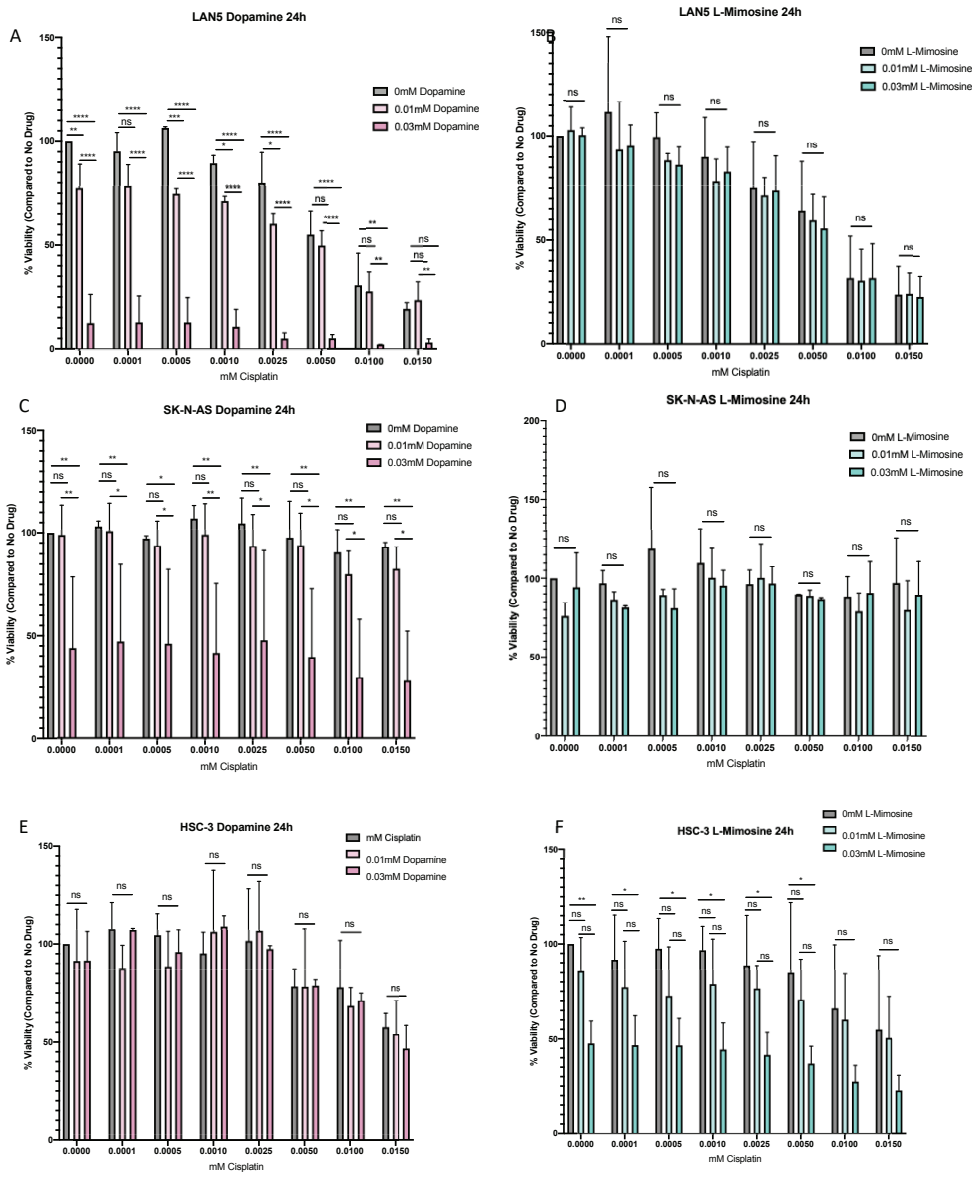

Figure 5.1 Dopamine and L-mimosine do not protect cancer cell lines from cisplatin-induced death 24 hr following cisplatin treatment. SK-N-AS and LAN5 neuroblastoma (NBL) and HSC-3 oral squamous cell carcinoma cell lines were pretreated for 12h with vehicle control, or either dopamine or L-mimosine at concentrations of either 0.01mM or 0.03mM. Cells were then treated with increasing concentrations of freshly-prepared cisplatin (0-0.015mM). At 24hr following cisplatin treatment, an alamarBlue™ cell viability assay was performed according to manufacturer's instructions. Viability results are displayed as % of no drug control. Each treatment was plated in at least two wells, then averaged. A,B) LAN5, C,D) SK-N-AS, E,F) HSC-3. A, C, E) Dopamine, B, D, F) L-mimosine. *=p<0.05, **=p<0.01, ***=p<0.005, ****=p<0.001, as per two-way ANOVA with a Tukey post-test. N=3.

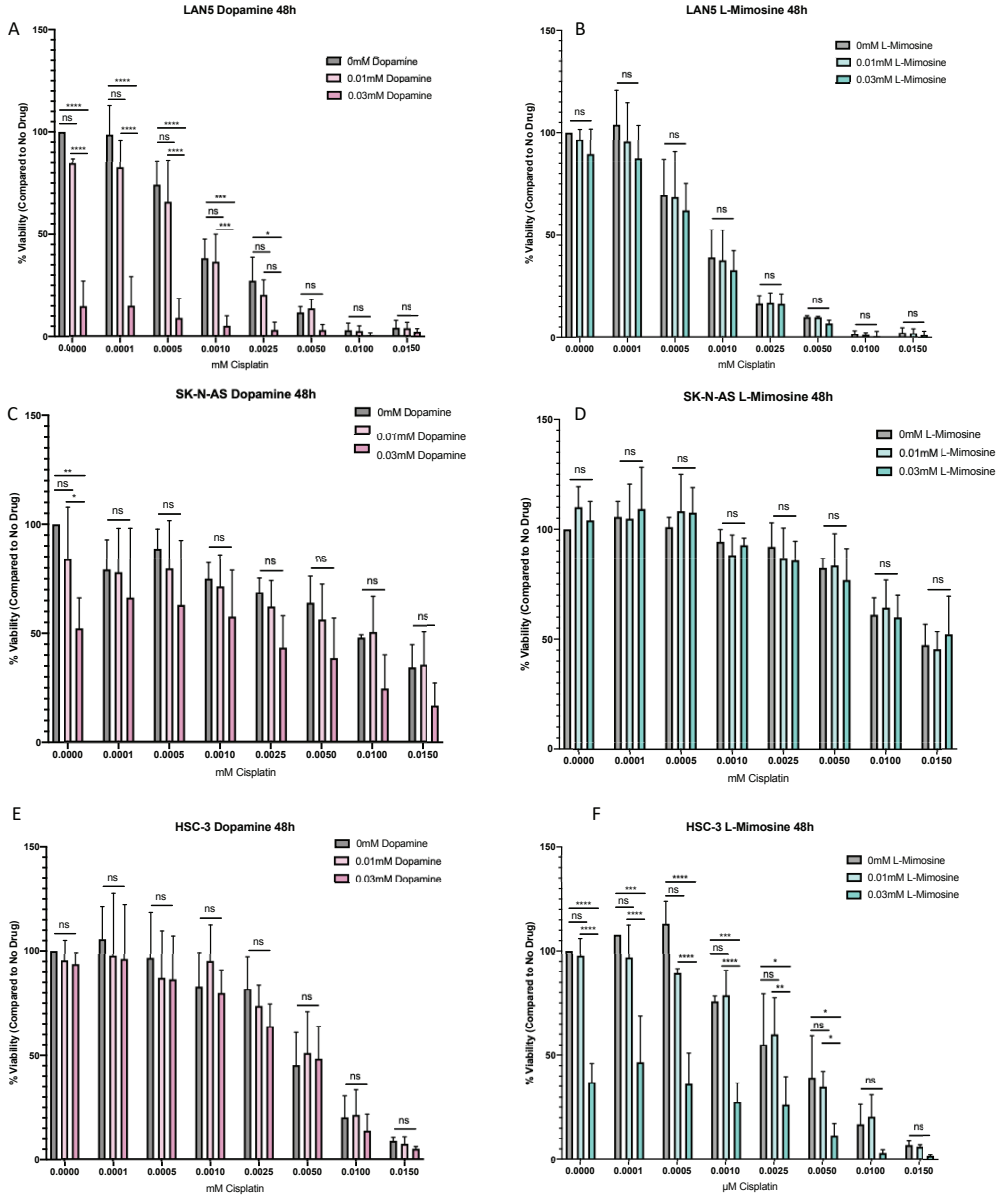

Figure 5.2 Dopamine and L-mimosine do not protect cancer cell lines from cisplatin-induced death 48 hr following cisplatin treatment. SK-N-AS and LAN5 neuroblastoma (NBL) and HSC-3 oral squamous cell carcinoma cell lines were pretreated for 12h with vehicle control, or either dopamine or L-mimosine at concentrations of either 0.01mM or 0.03mM. Cells were then treated with increasing concentrations of freshly-prepared cisplatin (0-0.015mM). At 48hr following cisplatin treatment, an alamarBlue™ cell viability assay was performed according to manufacturer's instructions. Viability results are displayed as % of no drug control. Each treatment was plated in at least two wells, then averaged. A,B) LAN5, C,D) SK-N-AS, E,F) HSC-3. A, C, E) Dopamine, B, D, F) L-mimosine. *=p<0.05, **=p<0.01, ***=p<0.005, ****=p<0.001, as per two-way ANOVA with a Tukey post-test. N=3.

5.2 Cisplatin-Induced Apoptosis Levels in SK-N-AS Neuroblastoma (NBL) Cells are Not Reduced by Dopamine or L-mimosine

Next, I set out to assess whether or not the candidate oto- and nephroprotective compounds inhibited cisplatin-induced apoptosis in SK-N-AS NBL cells. Briefly, cells were pretreated with vehicle control or protective agents at 0.03 mM for 12 hr, then were treated with 0.01 mM cisplatin for 48 hr. These cells were then subjected to Annexin V and SYTOX-based flow cytometry to determine the relative percentage of cells that were in late stages of apoptosis (**Figure 5.3**). Results demonstrate that cisplatin treatment results in an increase in Annexin+/SYTOX- cells in comparison with untreated control cells (*=p=0.0258). Further, pretreatment with either dopamine or L-mimosine does not inhibit cisplatin-induced apoptosis, as levels of Annexin+/SYTOX- cells are still significantly increased in these treatments in comparison with untreated control cells (*=p=0.0133 and ****=p<0.0001). Representative flow plots can be found in the bottom panel of **Figure 5.3**, where the lower left quadrant is Annexin-/SYTOX-, lower right is Annexin+/SYTOX-, upper left is Annexin-/SYTOX+, and upper right is Annexin+/SYTOX+.

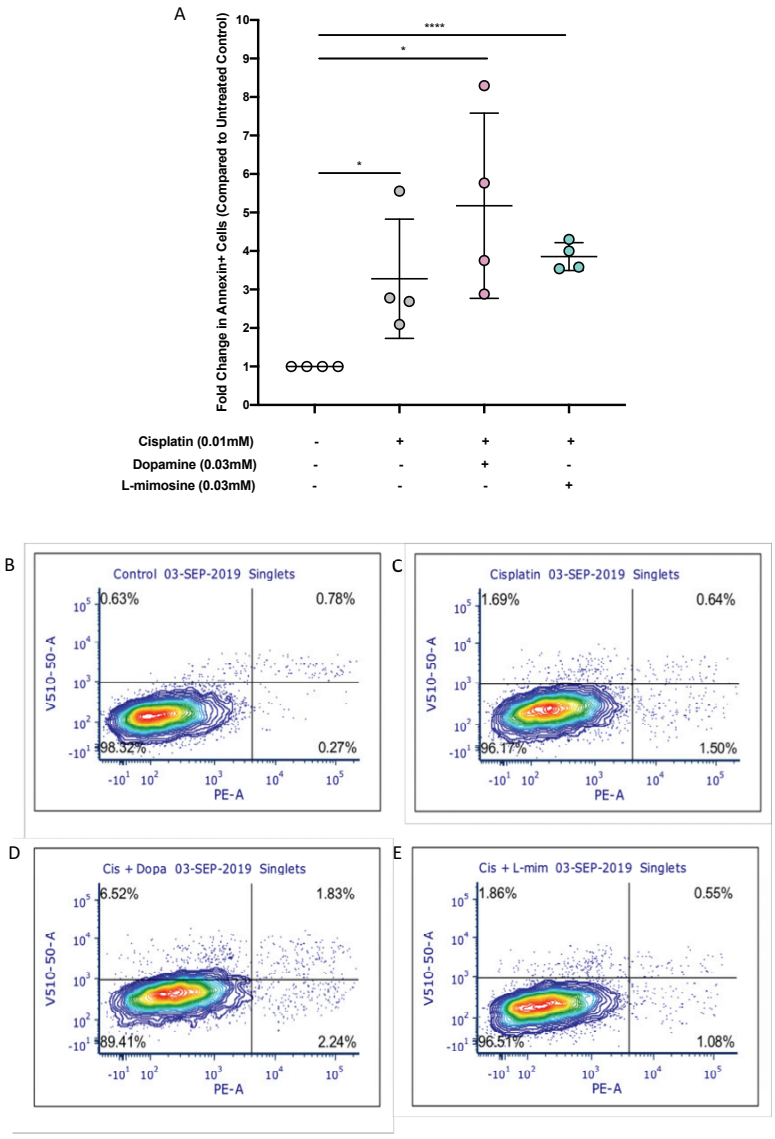

Figure 5.3 Dopamine and L-mimosine do not protect SK-N-AS cells from cisplatin-induced apoptosis. SK-N-AS neuroblastoma (NBL) cells were pretreated for 12h with vehicle control, or either dopamine or L-mimosine at 0.03mM. Cells were then either treated with vehicle control, or 0.01mM of freshly-prepared cisplatin. At 48hr following cisplatin treatment, cells ($1x10^6$) were harvested with trypsin-EDTA, washed, then resuspended in 1X binding buffer at a concentration of $1\text{-}5X10^6$ cells/ml. PE-conjugated Annexin V (excitation/emission 488/561) was added to the cells and incubated for 15min at room temperature (RT) in the dark. Cells were centrifuged, resuspended in 1X binding buffer prior to the addition of SYTOXBlue dead cell stain. Samples were maintained on ice, and assessed using the BD FACSCanto flow cytometer. Data were analyzed using BD FACSDiva Software. A) Graph of fold change Annexin+ cells, gated according to the biological control. *=$p<0.05$, ****=$p<0.0001$, as per two-tailed student's t-tests comparing treatment groups to control. N=4. B-E) Representative flow plots, demonstrating the four quadrants. LL=Annexin-/Sytox-, LR=Annexin+/Sytox-, UL=Annexin-/Sytox+, UR=Annexin+/Sytox+. B) control, C) 0.01mM cisplatin, D) 0.01mM cisplatin + 0.03mM dopamine, E) 0.01mM cisplatin + 0.03mM L-mimosine.

5.3 Cisplatin-Induced Double-Strand Break (DSB) Formation, Indicated by γH2AX Labelling, is Not Reduced with Dopamine or L-mimosine in Cancer Cell Lines

Cisplatin is a DNA-binding agent that causes inter- and intra-strand crosslinks in cellular DNA. The repair of inter-strand crosslinks (ICLs) typically involves the formation of at least a temporary double-stranded break (DSB), which result in the phosphorylation of histone protein H2AX, called γH2AX (Rogakou, Boon, Redon, & Bonner, 1999; Rogakou, Pilch, Orr, Ivanova, & Bonner, 1998). Levels of γH2AX antibody staining 24hr following cisplatin exposure has been reported to correlate with the long-term viability of the cells following treatment (Olive & Banath, 2009). DSB detection can lead to apoptosis. Thus, to investigate the potential contribution of DSB formation to the apoptosis seen in **Figure 5.3,** I pretreated SK-N-AS NBL and HSC-3 oral squamous cell carcinoma cell lines with cisplatin +/- the protective agents, each at 0.03 mM, then were stained with a γH2AX antibody, and visualized with confocal microscopy. I completed cell culture, drug treatments, cell permeabilization and staining protocols, while Olivia Piccolo (Dalhousie University) completed most of the confocal imaging. Quantification of γH2AX staining was performed using a custom ImageJ (Fiji) macro, written by Benno Orr (University of Toronto) (Rueden et al., 2017; Schindelin et al., 2012). Data is reported as γH2AX integrated density/DAPI integrated intensity, and each data entry corresponds to an individual nucleus.

SK-N-AS cells exhibited significantly higher levels of γH2AX staining when treated with 0.01 mM cisplatin (**Figure 5.4,** summary graph in the left panel and representative confocal images on the right, ****=$p<0.0001$). Pretreatment with dopamine or L-mimosine did not alter the ability of cisplatin to induce H2AX phosphorylation in SK-N-AS cells, as these levels were also both significantly higher

than control (****=p<0.0001 in both treatments). Interestingly, it appears as though cells pretreated with L-mimosine showed significantly higher levels of γH2AX staining, in comparison with cells that were treated with cisplatin alone (****=p<0.0001). Similarly, in HSC-3 cells, cisplatin treatment resulted in elevated levels of γH2AX staining, in comparison with untreated control cells (**Figure 5.5**, summary graph in the left panel and representative confocal images on the right, ****=p<0.0001). In HSC-3 cells, it appears as though L-mimosine pretreatment resulted in a decrease in γH2AX staining in comparison with treatment with cisplatin alone (****=p<0.0001), although this treatment did not protect the cells completely, as there was still a significant elevation in staining in comparison with the untreated controls (****=p<0.0001). In contrast, dopamine pretreatment resulted in a significant increase in DSB formation in HSC-3 cells, which was significantly higher than the levels of γH2AX in cells treated with cisplatin alone (****=p<0.0001).

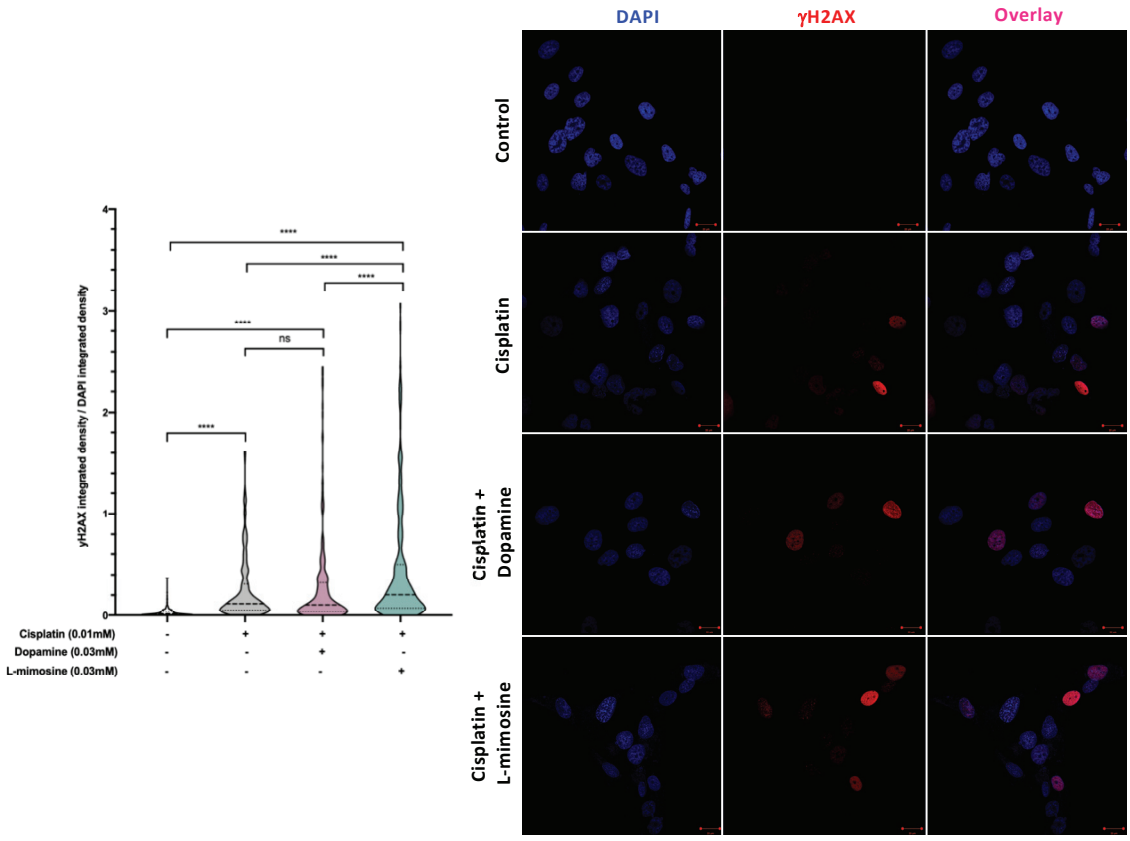

Figure 5.4 Dopamine and L-mimosine do not protect SK-N-AS cells from cisplatin-induced double strand break (DSB) formation. SK-N-AS neuroblastoma (NBL) were grown on coverslips in 6-well plates, and were pretreated for 12h with vehicle control, or either dopamine or L-mimosine at 0.03mM. Cells were then either treated with vehicle control, or 0.01mM of freshly-prepared cisplatin. At 24hr following cisplatin treatment, cells were rinsed and fixed with 4% PFA (in PBS) for 20min at 37°C. Fixed cells were permeabilized with 0.3% Triton-X 100 in PBS for 30min at RT, then rinsed again in PBST. Samples were incubated with 5% donkey serum in PBST for 1hr at RT. In a dark humidity chamber, samples were incubated with phospho-histone H2A.X (Ser139) (20E3) rabbit monoclonal antibody at 1:400 in 2.5% donkey serum in PBST overnight at 4°C. The following day, samples were rinsed, then incubated in a dark humidity chamber with donkey polyclonal secondary antibody to rabbit IgG-H&L (Alexa Fluor 647) at 1:400 dilution, and 1:1000 DAPI (4',6-Diamidino-2-Phenylindole, Dihydrochloride) in 2.5% donkey serum in PBST for 1 hour at RT. Samples were then rinsed with PBST, then the coverslips were mounted upside down on slides with Dako Fluorescent mounting medium. Samples were maintained in the dark at RT overnight, and samples were stored at 4°C until imaging. Imaging of samples was done using the Zeiss LSM 710 Laser scanning Confocal microscope. Quantification of γH2AX staining was performed using a custom ImageJ macro (Fiji), for which more information can be found in **Materials and Methods**. Data is reported as γH2AX integrated density/DAPI integrated density, with each data point corresponding to an individual nucleus. ****=p<0.0001, as per one-way ANOVA with a Tukey post-test. N=3.

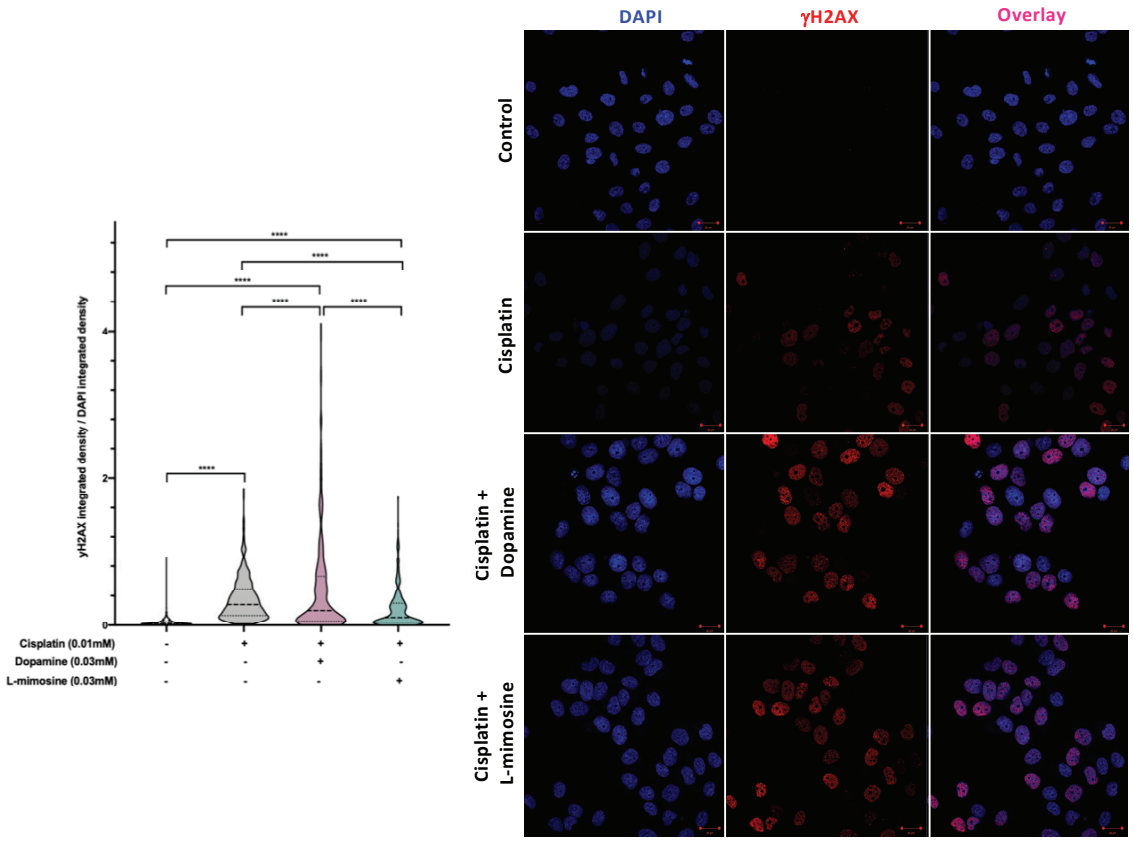

Figure 5.5 Dopamine and L-mimosine do not protect LAN5 cells from cisplatin-induced double strand break (DSB) formation. HSC-3 oral squamous cell carcinoma cells were grown on coverslips in 6-well plates, and were pretreated for 12h with vehicle control, or either dopamine or L-mimosine at 0.03mM. Cells were then either treated with vehicle control, or 0.01mM of freshly-prepared cisplatin. At 24hr following cisplatin treatment, cells were rinsed and fixed with 4% PFA (in PBS) for 20min at 37°C. Fixed cells were permeabilized with 0.3% Triton-X 100 in PBS for 30min at RT, then rinsed again in PBST. Samples were incubated with 5% donkey serum in PBST for 1hr at RT. In a dark humidity chamber, samples were incubated with phospho-histone H2A.X (Ser139) (20E3) rabbit monoclonal antibody at 1:400 in 2.5% donkey serum in PBST overnight at 4°C. The following day, samples were rinsed, then incubated in a dark humidity chamber with donkey polyclonal secondary antibody to rabbit IgG-H&L (Alexa Fluor 647) at 1:400 dilution, and 1:1000 DAPI (4',6-Diamidino-2-Phenylindole, Dihydrochloride) in 2.5% donkey serum in PBST for 1 hour at RT. Samples were then rinsed with PBST, then the coverslips were mounted upside down on slides with Dako Fluorescent mounting medium. Samples were maintained in the dark at RT overnight, and samples were stored at 4°C until imaging. Imaging of samples was done using the Zeiss LSM 710 Laser scanning Confocal microscope. A) Quantification of γH2AX staining was performed using a custom ImageJ macro (Fiji), for which more information can be found in **Materials and Methods**. Data is reported as γH2AX integrated density/DAPI integrated density, with each data point corresponding to an individual nucleus. ****=p<0.0001, as per one-way ANOVA with a Tukey post-test. B) Representative images of treatments. From left to right: DAPI, γH2AX, and overlay. Scale bars = 20µm. N=3.

As a counterpoint, I performed the exact same γH2AX analysis assay using the non-cancerous human kidney proximal tubule cell line (HK-2) that was used in the initial nephrotoxicity screen. Similar to the cancer cell lines, in HK-2 cells, treatment with cisplatin caused an increase in γH2AX staining, in comparison with the untreated controls (**Figure 5.6**, summary graph in the left panel and representative confocal images on the right, ****=$p<0.0001$). L-mimosine pretreatment resulted in a partial protection of HK-2 cells from H2AX phosphorylation, as there was still a significant increase in staining in comparison with control cells (****=$p<0.0001$), but γH2AX levels were still lower than those in the cells that were treated with cisplatin alone (****=$p<0.0001$). In contrast with the cancer cell lines, dopamine pretreatment resulted in significant protection of HK-2 cells from cisplatin induced DSB formation, resulting in levels of γH2AX staining that were not significantly different from control levels.

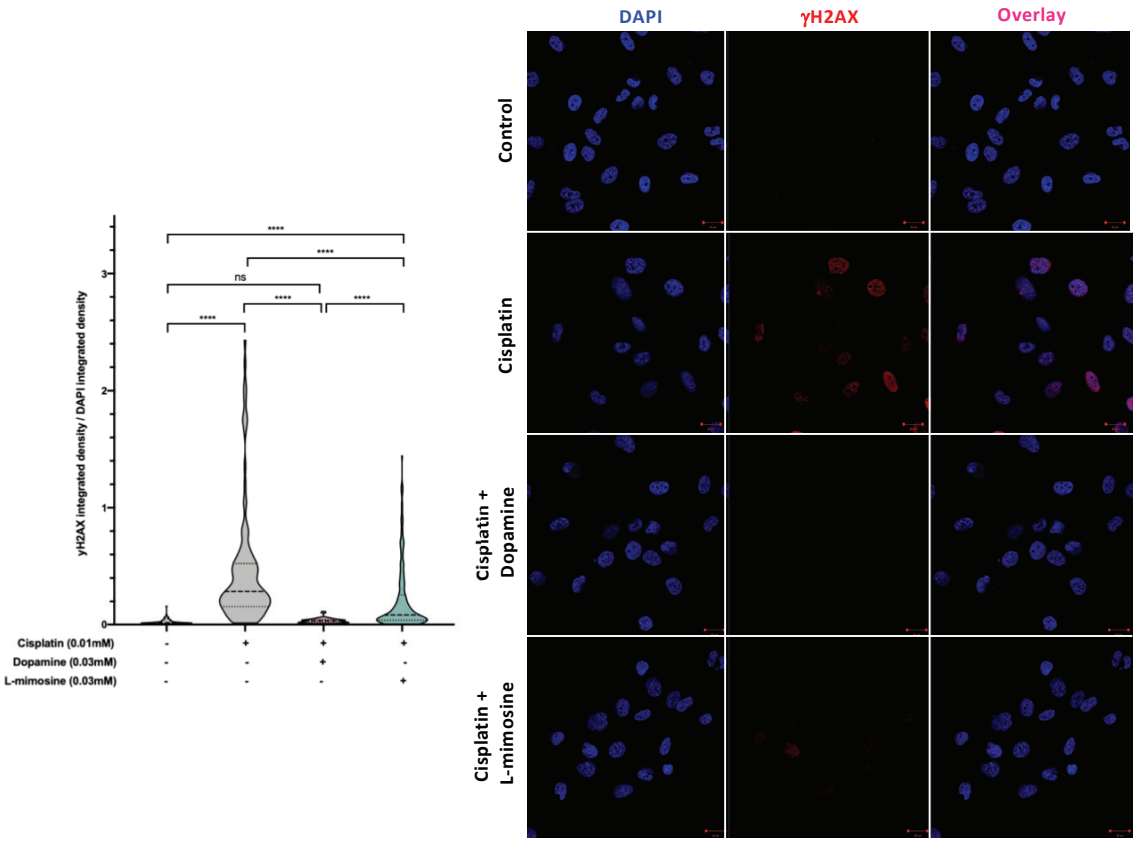

Figure 5.6 Dopamine and L-mimosine at least partially protect HK-2 cells from cisplatin-induced double strand break (DSB) formation. HK-2 human proximal tubule cells were grown on coverslips in 6-well plates, and were pretreated for 12h with vehicle control, or either dopamine or L-mimosine at 0.03mM. Cells were then either treated with vehicle control, or 0.01mM of freshly-prepared cisplatin. At 24hr following cisplatin treatment, cells were rinsed and fixed with 4% PFA (in PBS) for 20min at 37°C. Fixed cells were permeabilized with 0.3% Triton-X 100 in PBS for 30min at RT, then rinsed again in PBST. Samples were incubated with 5% donkey serum in PBST for 1hr at RT. In a dark humidity chamber, samples were incubated with phospho-histone H2A.X (Ser139) (20E3) rabbit monoclonal antibody at 1:400 in 2.5% donkey serum in PBST overnight at 4°C. The following day, samples were rinsed, then incubated in a dark humidity chamber with donkey polyclonal secondary antibody to rabbit IgG-H&L (Alexa Fluor 647) at 1:400 dilution, and 1:1000 DAPI (4',6-Diamidino-2-Phenylindole, Dihydrochloride) in 2.5% donkey serum in PBST for 1 hour at RT. Samples were then rinsed with PBST, then the coverslips were mounted upside down on slides with Dako Fluorescent mounting medium. Samples were maintained in the dark at RT overnight, and samples were stored at 4°C until imaging. Imaging of samples was done using the Zeiss LSM 710 Laser scanning Confocal microscope. A) Quantification of γH2AX staining was performed using a custom ImageJ macro (Fiji), for which more information can be found in **Materials and Methods**. Data is reported as γH2AX integrated density/DAPI integrated density, with each data point corresponding to an individual nucleus. ****=p<0.0001, as per one-way ANOVA with a Tukey post-test. B) Representative images of treatments. From left to right: DAPI, γH2AX, and overlay. Scale bars = 20µm. N=3.

5.4 Xenograft Studies are Inconclusive

In efforts to perform *in vivo* studies of the potential chemoprotective effects of dopamine and L-mimosine, we used our establish zebrafish larval xenograft assay, using SK-N-AS and LAN5 NBL cells and HSC-3 oral squamous cell carcinoma cells. The methods are described in detail in the **Materials and Methods**, and are outlined schematically in **Figure 2.2**. Briefly, *casper* zebrafish embryos were injected at 48 hpf with fluorescently-labeled cancer cells, treated with 0.25 mM cisplatin +/- 12 hr pretreatment with either 0.03 mM dopamine or L-mimosine. Two days following cisplatin treatment, fluorescent cancer cell numbers were assessed (**Figure 5.7**). SK-N-AS cell number was significantly decreased with cisplatin treatment (**Figure 5.7a,** **=p=0.0002). However, it was unclear if the protective agent pretreatment had any effect on cancer cell number, as there was some degree of variability and no statistical significance. In both LAN5 (**Figure 5.7b**) and HSC-3 cells (**Figure 5.7c**), none of the drug treatments had any effect on overall cancer cell number in comparison with the untreated control larvae. Thus, the results are largely inconclusive. However, it is reassuring to note that the pretreatment with dopamine or L-mimosine did not seem to significantly increase the cancer cell number in comparison with control larvae.

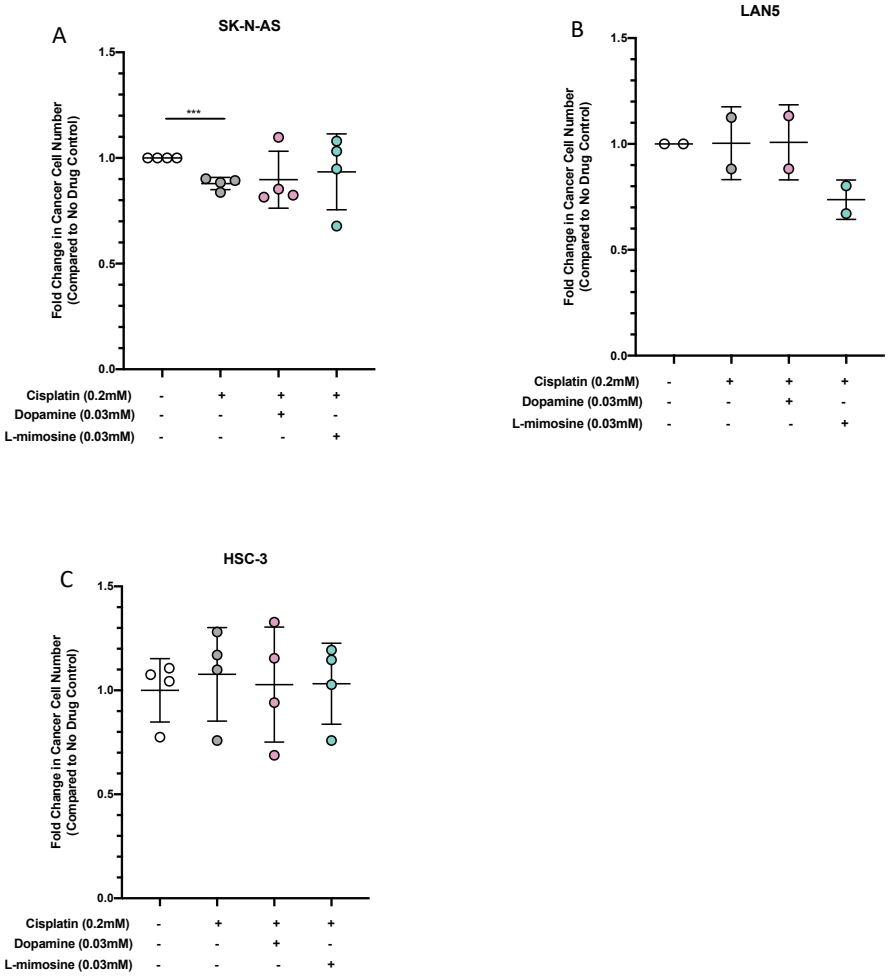

Figure 5.7 Xenotransplant (XT) studies of the potential chemoprotective effects of dopamine and L-mimosine are inconclusive. *Casper* zebrafish larvae were injected at 48 hours post fertilization (hpf) with between 50-100 fluorescently-labeled human cancer cells/larvae in the yolk sac. Approximately 6hr later, larvae were screened with a fluorescent microscope to identify positive larvae, which were then divided into groups, and at 60hpf were treated with vehicle control, or either 0.03mM dopamine or L-mimosine. 12hr later, larvae were rinsed, then treated with 0.25mM cisplatin for 48hr. At the experimental endpoint, larvae were euthanized, and dissociated into a single cell suspension. This cell suspension was imaged with a fluorescent microscope, and the number of cancer cells was enumerated with ImageJ software. Results are displayed as fold change in cell number in comparison with the untreated control larvae. A) SK-N-AS neuroblastoma (NBL) XT results. ***=p=0.0002, as per two-tailed student's t-test, comparing cisplatin treated larvae with the untreated controls. N=4. B) LAN5 NBL cell XT results. N=2. C) HSC-3 oral squamous cell carcinoma results. N=4.

5.5 Summary of Findings

In summary, I have demonstrated that the cytotoxic effects of cisplatin on SK-N-AS and LAN5 NBL cells and HSC-3 cells were preserved, or even amplified, in combination with either dopamine or L-mimosine. Further, the levels of cisplatin-induced apoptosis are not decreased with dopamine or L-mimosine pretreatment. I have also used a γH2AX labelling assay to show that the level of DSB formation is generally not decreased with dopamine or L-mimosine pretreatment. In non-cancerous HK-2 proximal tubule cells, pretreatment with dopamine or L-mimosine protected the cells from cisplatin-induced DSB formation. The *in vivo* xenograft studies are somewhat inconclusive, but demonstrate significant reduction in SK-N-AS cell number with cisplatin treatment; further, pretreatment with either dopamine or L-mimosine did not increase the number of cancer cells in the xenografted larvae.

Chapter 6 Discussion

6.1 Overview of Significant Findings

Cisplatin is one of the oldest chemotherapeutics that is still in clinical use. Cisplatin is highly effective in certain cancers, including testicular cancer, bladder cancer, and ovarian cancer (Kelland, 2007). Despite optimization of dosing schedules, adequate hydration techniques, modification of the original cisplatin compound, and search for protective agents, approximately 30% of patients will develop some form of kidney damage and between 20-60% of patients will exhibit sensorineural hearing loss. As a result, clinicians are faced with challenging decisions, as cisplatin is a potentially life-saving medication for many individuals. There are currently no FDA-approved compounds for the protection from cisplatin-induced ototoxicity. Further, the treatment for cisplatin-induced kidney damage is supportive in nature. Thus, until alternative, equally effective therapies replace cisplatin, its regular use will continue. As a result, the need to identify adjuvant oto- and nephroprotective compounds will continue to be a critical endeavour.

At the outset of this project, the goal was to screen the Sigma LOPAC®^{1280} library of compounds to find adjuvant compounds that could prevent cisplatin-induced oto- and nephrotoxicity. I envisioned a two-pronged drug screen that would allow me to assess the same compound library for potential oto- and nephroprotective effects. I employed a reliable *in vitro* nephrotoxicity assay using a human proximal tubule cell line and an alamarBlue™ viability assay to assess nephroprotection (**Figure 4.2-4.3**). In order to assess ototoxicity, I used the zebrafish lateral line screening system as a surrogate for damage to human hair cells, as others have done previously (H. C. Ou et al., 2009; Owens et al., 2008; Andrew J. Thomas et al., 2015). When paired together, these screens resulted

in the identification of 22 compounds that showed potential as both oto- and nephroprotective (**Table 4.2**).

When I examined the list of compounds that were hits in both assays, it was difficult to ignore the multiple appearances of drugs that impact dopaminergic signalling (**Figure 4.5**). Upon screening these compounds again in an *in vivo* lateral-line based protection assay, it appeared as though dopamine and L-mimosine were two of the most protective compounds. Additionally, dopamine and L-mimosine share similar chemical structures. Thus, I set out to examine the oto- and nephroprotective effects of these two compounds. I found that both dopamine and L-mimosine had relatively modest, but consistent and significant protective effects in a high-throughput *in vivo* lateral line-based ototoxicity assay (**Figure 4.8-4.10**). Dopamine and L-mimosine also protected the zebrafish inner ear hair cells from cisplatin-induced damage (**Figure 4.11**). Further, dopamine and L-mimosine preserved zebrafish larval GFR in the face of potential cisplatin-induced damage (**Figure 4.12**). When assessing the effects of dopamine and L-mimosine on cisplatin-induced cancer cell cytotoxicity, it was apparent that the protective compounds did not protect cancer cell lines from cisplatin-induced decreases in viability (**Figure 5.1-5.2**), cisplatin-induced apoptosis (**Figure 5.3**), or cisplatin-induced increases in DSBs (**Figure 5.4-5.5**). Unsurprisingly, these compounds did provide some degree of protection of non-cancerous human proximal tubule cells from cisplatin-induced DSB formation (**Figure 5.6**). *In vivo* xenotransplant studies were unfortunately inconclusive, but also provided no indication that either dopamine or L-mimosine increased cancer cell number (**Figure 5.7**).

6.2 Drug Screening Platforms

6.2.1 Ototoxicity

It is well-established that the zebrafish lateral line hair cells serve as a good model for human hair cells (Baxendale & Whitfield, 2016); thus, I decided to perform an *in vivo* screen of compounds for their potential protective effects against cisplatin-induced ototoxicity.

The first step in performing this drug screen was to establish a reproducible and medium-high throughput method to assess lateral line health in zebrafish larvae. Neuromast health is typically assessed using a fluorescent vital stains, like YO-PRO1, followed by fluorescence microscopy (Baxendale & Whitfield, 2016). I first validated this approach using the built in ZEN2 software (Blue Edition; **Figure 3.1**). While I was able to differentiate between treated vs. untreated control larvae, this method required imaging each larva, and was therefore not high-throughput. Next, I assessed the possibility of measuring larval neuromast fluorescence using a plate reader (**Figure 3.2).** This method was more high-throughput, yet not sensitive enough to detect significant differences in larval fluorescence between 0.05mM and 0.25mM. Lastly, I assessed the utility of a biosorter, a highly-specialized piece of equipment that is functionally similar to a flow cytometer, but for larger particles. This method was high-throughput, as it could measure the fluorescence profiles of a 96-well plate, with 4 larvae/well, in approximately 30 mins. Additionally, the biosorter was sensitive enough to detect the differences in neuromast fluorescence following treatment with various doses of cisplatin (**Figure 3.3**).

6.2.1.1 Strengths and Shortcomings of Selected Screening Method

In order to assess the potential effects of the compounds from the Sigma LOPAC®[1280] Compound library on cisplatin-induced ototoxicity, I chose to utilize an *in vivo* lateral line-based assessment of neuromast integrity following treatment. This assay relied on the specific labelling of viable hair cell nuclei with the fluorescent stain YO-PRO1 and subsequent fluorescent profiling with the biosorter. One of the major strengths of this assay is that it is an *in vivo* study, using whole animals. This is in contrast to other studies that have used HEI-OC1 immortalized mouse cells (Teitz et al., 2018). Whole organism studies are much more complex as they involve multiple cell and tissue types, but are more likely to identify issues of systemic toxicity, and provide a preliminary screen for absorption and/or bioavailability.

Additionally, the use of the biosorter allowed for the measurement and storage of multiple aspects of larval fluorescent profiles in up to 3 channels simultaneously (**Figure 2.1**). This is in contrast to other zebrafish lateral line screens, that focus on and evaluate one larva/drug in one fluorescent channel, without capturing images for later analysis (H. C. Ou et al., 2009; Owens et al., 2008; Andrew J. Thomas et al., 2015). The biosorter allowed me to assess 4 larvae/compound in an automated and unbiased manner, and analyze the data at a later point. It is worth noting that I performed a medium-throughput screen of 1,280 compounds, while others have done as many as 10,000 compounds (Andrew J. Thomas et al., 2015), indicating that ours is not as high throughput as some other techniques. However, it did not allow me to capture images of each larvae during the screening process, which is a disadvantage. Another positive attribute of the biosorter, like other studies that use visual observation, was that it allowed for the collection of living larvae following screening, which facilitates subsequent imaging or other

experimental manipulation. However, one main limitation of using the biosorter is the cost associated with such a highly specialized piece of equipment.

Another challenge associated with screening for compounds that modify the lateral line is the issue of compound fluorescence. While this is likely not as much of a concern for studies using direct microscopic observation, there were false positives in my screen. When I went to test the potentially protective compounds, between 10-20 of them were false positives as a result of drug autofluorescence. While some of them were obvious, based on the fluorescence profile, others were the result of fluorescent drug uptake and sequestration in various parts of the larva. Several fluorescent compounds localized in a periocular distribution, while others resulted in fluorescent foci in the digestive tract of the larva. The ability to image each larva at the time at which the fluorescence profile was measured would provide more insight into the problem of drug fluorescence.

6.2.2 Nephrotoxicity

During the assay development portion of this project, I was able to modify an *in vivo* inulin-mediated GFR assay, established by others (Hentschel et al., 2005; Rider et al., 2012), to quantify the effects of cisplatin treatment on zebrafish larval GFR (**Figure 3.5, 3.6, 3.7**). When using the biosorter to measure larval fluorescence, this assay is relatively high throughput, but it still requires each larva to be individually, manually injected with FITC-inulin. Even with the help of a highly-skilled Research Associate (Nicole Melong, IWK Health Centre), this crucial and time-sensitive step is limiting. Thus, this *in vivo* assay is not amenable for high-throughput drug screening.

In order to perform a medium-high throughput drug screen, assessing candidate compounds for potential nephroprotective effects, cell lines were the best choice. *In vivo* models are too costly, technically challenging, and laborious. In order to complement the zebrafish-based ototoxicity screen, I wanted to employ a human renal cell model. Cisplatin damages several regions in the kidney, but it is well-recognized that the proximal tubule region is the most susceptible to cisplatin-induced damage (Kroning et al., 2000). My decision to use a human cell line precluded the use of transformed murine cell lines, including LLC-RK1 (rabbit), OK (opossum), LLC-PK1 (pig), and MDCK (dog) kidney cells (Gstraunthaler et al., 1985; Racusen et al., 1996), and I did not want to attempt to use primary cell cultures for a drug screen. Thus, I decided to use the HK-2 transformed human proximal tubule cell line (Ryan et al., 1994).

6.2.2.1 Strengths and Shortcomings of the Selected Screening Method

The HK-2-based viability screening model had the benefit of being relatively rapid, inexpensive, and reliable. The HK-2 cells exhibited predictable dose-response toxicity curves when exposed to freshly-prepared cisplatin (**Figure 4.2**). Further, the HK-2 cells represent a human proximal tubule cell line that is known to recapitulate findings from primary isolated renal tubule cells (Ryan et al., 1994). However, studies report that HK-2 cells do not express normal levels of proximal tubule markers, including APN (Ronco et al., 1990), and may be functionally uncoupled from D_1-mediated adenylyl cyclase (AC) activation, which will be discussed further below (Gildea et al., 2010). Relatively recently, renal proximal tubule epithelial cells have been isolated from a healthy donor, then immortalized with human telomerase reverse transcriptase, creating a cell line called RPTEC/hTERT cells (Simon, Wilson, & Wickliffe, 2014). This is an

additional cell line that could have been used; however, since less is known about this line, I opted for the better-studied HK-2 cells. Studies suggest that a more physiologically relevant, albeit much more technically challenging and costly, method to study human kidney cells is using an *ex vivo* three-dimensional system that includes a degree of continuous fluid sheer stress (FSS) (Adler et al., 2016; Wilmer et al., 2016).

In terms of technical assay selection, I opted to use a viability assay as it would encompass some information about both relative cell number and cell viability. alamarBlue™ is reduced from resazurin to the highly fluorescent resofurin in metabolically active, living cells. The benefits of this assay include the ease of use and relatively inexpensive nature. One problem that I encountered was the interference of fluorescent compounds in the drug library. In an attempt to circumvent this technical issue, when performing the initial drug screen, I removed the cisplatin + the compounds from the wells, added new media, then added the alamarBlue™.

6.2.3 Benefits and Disadvantages of a Two-Pronged Screening Approach

This project utilized a two-pronged drug screen, where I was able to assess both potential nephroprotective effects in an *in vitro* screen and otoprotective effects with an *in vivo* screen in zebrafish larvae. This allowed me to use results from two separate large-scale experiments to prioritize the compounds. As previously mentioned, I decided to focus my efforts on compounds that were hits in both assays. This does not mean that compounds that were only oto- or nephroprotective, are not of value. In fact, many of these compounds likely deserve more investigation. For example, N-acetylcysteine (NAC), an antioxidant compound currently in clinical trials for the protection against cisplatin-induced ototoxicity was a hit in the ototoxicity assay, but not the nephrotoxicity

assay. It is also worth mentioning that there is significant overlap between the mechanisms of oto- and nephrotoxicity, like the importance of elevated ROS levels, but also important differences, including specific drug transporter expression in the kidney vs. cochlea among other things (Giuliano Ciarimboli, 2012; J. Sprowl, Ness, & Sparreboom, 2013). Thus, it is not necessarily the case that oto- and nephroprotective compounds share the same mechanism of protection. However, as a result of intrinsic limitations in both time and personnel, I decided to prioritize compounds that were both oto- and nephroprotective. This strategy was both to avoid polypharmacy in a heavily treated population, and also in the effort to find compounds that would provide at least some degree of protection against both toxicities that occur simultaneously.

Another benefit of using an *in vivo* assay in parallel with a cell-culture based *in vitro* assay is the ability to identify compounds that resulted in systemic toxicity. This was highlighted with my two-pronged *in vitro* and *in vivo* study. In this case, there were 20 compounds that were toxic at a dose of 0.01 mM to at least 75% of larvae when administered with 0.02 mM cisplatin (**Table 4.1**). Importantly, 7 of these compounds were hits in the *in vitro* nephrotoxicity assay. The two-pronged screening approach allowed me to deprioritize the toxic compounds before investing time into further exploration.

6.3 Dopamine as an Oto- and Nephroprotective Agent

6.3.1 Overview

Dopamine is an endogenous catecholaminergic neurotransmitter. There are four main dopaminergic pathways in the brain: the nigrostriatal, mesolimbic, mesocortical and tuberoinfundibular, that each control different aspects of the central nervous system

(CNS) (Beaulieu & Gainetdinov, 2011). However, dopamine signalling also occurs outside the CNS, where it plays important roles in hormonal regulation, cardiovascular function, the immune system, and in the proper function of the renal system (Beaulieu & Gainetdinov, 2011; Jose, Carey, Raymond, Bates, & Felder, 1992; Missale et al., 1998).

6.3.2 Pharmacology

Dopamine binds as a ligand to a family of dopamine receptors. The dopamine receptors are a group of G protein-coupled receptors (GPCRs) that belong to two basic groups: the D1-class (containing D_1 and D_5 receptors), and the D2-class (containing D_2, D_3 and D_4 receptors) (Beaulieu & Gainetdinov, 2011; Missale et al., 1998). Generally speaking, the D1-like class of receptors activate $G\alpha_{s/olf}$ family of G proteins, stimulating production of cyclic AMP (cAMP) by adenylyl cyclase (AC). The D2-like class couple with the $G\alpha_{i/o}$ family of G proteins, resulting in the inhibition of AC, decreasing cAMP production. Another difference is that the D1-like class of dopamine receptor genes do not have any introns, but the members of the D2-like class of receptor genes each have a different number of introns, resulting in the potential for splice variants (Gingrich & Caron, 1993). Dopamine itself activates all five of the dopamine receptors, with variable affinity (Beaulieu & Gainetdinov, 2011). To further complicate the signalling pathways, D_1 and D_5 receptors are only found postsynaptically, while D_2, D_3 and D_4 receptors are found both pre- and postsynaptically (Beaulieu & Gainetdinov, 2011). An overview figure of dopamine signalling can be found in **Figure 6.1**.

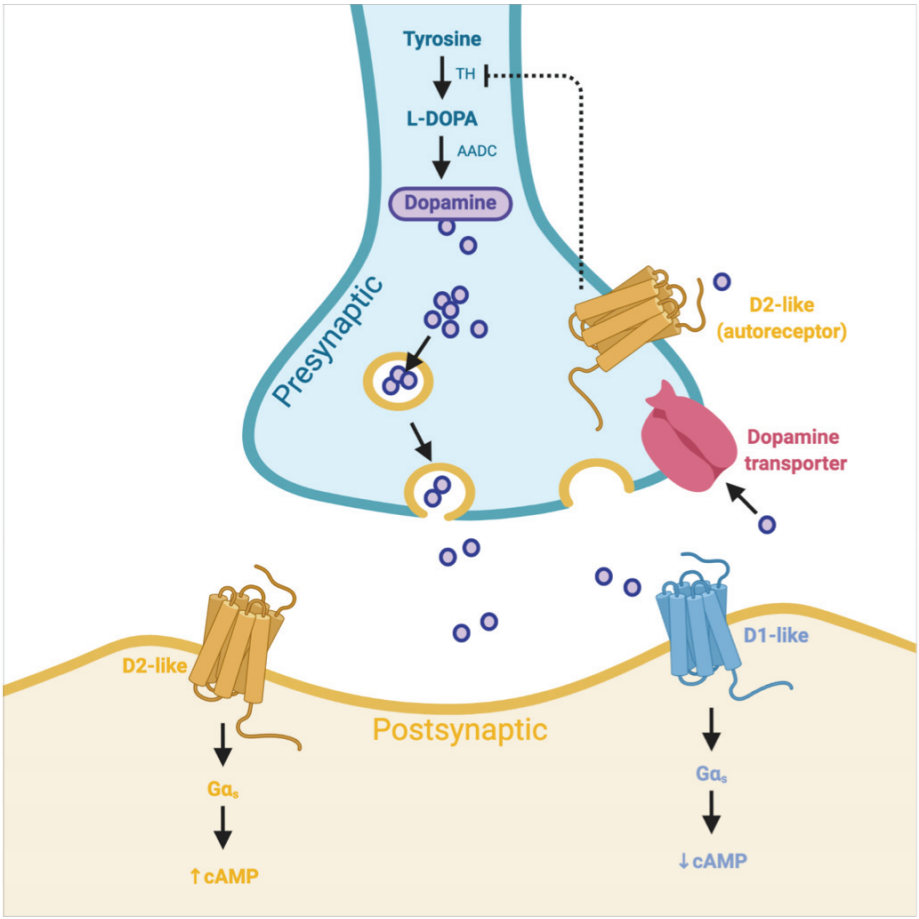

Figure 6.1 Typical dopaminergic synaptic neurotransmission. Dopamine is usually synthesized in the neuron. Tyrosine hydroxylase (TH) creates L-hydroxyphenylalanine (L-DOPA) from tyrosine. Aromatic acid decarboxylase (AADC) converts L-DOPA to dopamine. Dopamine is a neurotransmitter and can engage in dopaminergic signalling. Dopamine can be packaged into synaptic vesicles and released into the synaptic cleft. Once in the cleft, dopamine can bind to D1-like receptors on the postsynaptic membrane, which causes $G\alpha_s$-mediated adenylyl cyclase (AC) stimulation, resulting in increased production of cyclic-AMP (cAMP). Synaptic dopamine can also bind to D2-like receptors either pre- or postsynaptically. These receptors couple with $G\alpha_{i/o}$ G-proteins, which inhibit AC, causing a reduction in the production of cAMP. Presynaptic D2-like receptor stimulation can inhibit the production of dopamine. Dopamine can also be transported across membranes by the dopamine transporter, DAT.

In addition to acting as a ligand at all five dopamine receptors, dopamine can also interact with a variety of enzymes and transporters that are known to play roles in cisplatin-induced pharmacology. One recognized example is OCT2, the transporter that seems to play a role in cisplatin uptake into both renal tubule and cochlear cells, can also transport dopamine (Giuliano Ciarimboli et al., 2010; Filipski et al., 2008, 2009). Nonsynonymous genetic polymorphisms in *SLC22A2,* the gene encoding OCT2 decrease nephrotoxicity in patients (Filipski et al., 2009), a finding that was replicated in four of seven studies that examined this SNP in a recent systematic review (Zazuli et al., 2018). Also of interest, dopamine is metabolized into 3-methoxytyramine by COMT (Beaulieu & Gainetdinov, 2011). This enzyme was found to be polymorphic, and the individuals carrying the SNP were at a significantly elevated risk of developing cisplatin-induced ototoxicity (Ross et al., 2009). This enzyme is also known to be expressed in the sensory hair cells of the inner ear, even though its specific role in hearing is not known (Hagleitner et al., 2014; Sörös, 2012). In addition, the impact of this SNP in the function of the enzyme is unknown (Hagleitner et al., 2014). Studies of COMT-/- mice demonstrated increased intrarenal dopamine levels (M. Zhang et al., 2009). Whether or not these interactions are a serendipitous occurrence is unknown at this time, but warrant further investigation.

The multiple appearances of dopaminergic and serotonergic pathway modulators is also supported by similar findings in a study of both aminoglycoside and cisplatin-induced zebrafish lateral line toxicity (Vlasits, Simon, Raible, Rubel, & Owens, 2012). In this study, researchers screened the ENZO Life Sciences FDA-approved drug library of 640 compounds, and found 10 compounds that protected neuromast hair cells from at least two ototoxins examined. Among the hits was paroxetine, a selective serotonin-

reuptake inhibitor (SSRI) and fluspirilene, an antipsychotic compound that acts as an antagonist at the D_2 dopamine receptor (Vlasits et al., 2012). While these specific compounds did not appear in the present screen, similar compounds did. Additionally, trifluoperazine dihydrochloride, a different D_2-receptor antagonist was a hit in both assays presented here, adding more validity to this study. Lastly, when assessing the results of a drug screen, it is important to examine the overall composition of the drug library to determine whether or not certain pathways could be enriched by higher levels of representation in the library. In this case, the Sigma LOPAC®1280 library contains a total of 15% of compounds that would interact with either the dopaminergic or serotonergic pathway (9% and 6%, respectively). This is a relatively high proportion of compounds, and could translate to misguided importance being placed on these hits.

6.3.3 Effect of Dopamine in Renal and Cochlear Systems

D1 and D2-like receptors are both present in the inner ear (Beaulieu & Gainetdinov, 2011). In mice, D_1, D_2 and D_5 receptors were present in both the embryonic outer hair cells (OHCs) and spiral ganglion cells. In contrast, there was evidence for the presence of D_1, D_2, D_4 and D_5 receptors in the adult cochlea (Maison et al., 2012). Cochlear function was normal in D_3, D_4 and D_5 knock-out (KO) mice, but not in D_1 or D_2 receptor KO animals.

While there are afferent nerve fibers that send information from sensory hair cells to the CNS, there are also efferent nerve fibers that are involved in the feedback from the olivocochlear (OC) system to the cochlear sensory hair cells (Darrow, Maison, & Liberman, 2007). This OC system consists of the medial OC (MOC) portion, that includes fibers that form cholinergic synapses directly on the OHCs, and the lateral

olivocochlear (LOC) efferent fibers that end at the cochlear nerves of the inner hair cells (IHCs) (Maison et al., 2012). Lesions in the LOC cause an increase in the damage to the cochlear nerve dendrites during acute acoustic overexposure (Darrow et al., 2007). There is abundant evidence that dopamine is capable of protecting the auditory nerves from glutamate-mediated excitotoxicity (Lendvai et al., 2011; Nouvian, Gervais, Pujol, Eybalin, & Puel, 2001). It appears as though the dopamine that is released by the LOC can protect the IHC-afferent synapse from noise-induced damage by attenuating glutamate overstimulation (Darrow et al., 2007; Lendvai et al., 2011; Oestreicher, Arnold, Ehrenberger, & Felix, 1997).

The mammalian kidney expresses both D1-like and D2-like receptors (Felder & Jose, 2006; R. C. Harris & Zhang, 2012). Generally speaking, dopamine is synthesized from circulating L-DOPA by aromatic acid decarboxylase, where it decreases sodium reabsorption in the proximal tubule and the collecting duct (R. C. Harris & Zhang, 2012). If dopamine is infused at low doses (0.5-3 μg/kg/min), the net effect is dilation of the renal arteries, resulting in an increase in renal blood flow (Steinhausen, Weis, Fleming, & Dussel, 1986). This finding led researchers and physicians to attempt to decrease cisplatin-induced nephrotoxicity by administration of dopamine, thinking that the increased blood flow would result in quicker excretion (Kellum, 1997). Although there were early reports of the protective effects of dopamine on either the development of, or recovery from kidney damage (Hans et al., 1990; Palmieri et al., 1993), a later clinical study of the potential protective effect of dopamine (2 μg/kg/min) on cisplatin-induced renal impairment demonstrated not only a lack of renal protection, but also increased serum creatinine levels in the dopamine group (Somlo et al., 1995). Subsequent systematic reviews suggest that there is insufficient evidence to support the prophylactic

use of dopamine to prevent renal damage (Crona et al., 2017; Kellum, 1997). This inconsistency in findings may be related to the presence of both D1-like and D2-like receptors in the kidney. Supporting theory of D1-like receptor-mediated renal protection, the D_1 receptor agonist YM-435 was protective in a canine model of ischemic acute renal failure (Yatsu et al., 1998). Additionally, fenoldopam is a dopamine D_1 receptor agonist that is used as an antihypertensive agent that has been investigated as a potential renal protective agent. While systematic reviews suggest that fenoldopam did not reduce death or the need for dialysis in intensive care unit (ICU) patients that already exhibited acute tubular necrosis (Tumlin et al., 2005), it did have some protective effects in the context of reducing post-operative acute kidney injury (AKI), or sudden damage to the kidney (Gillies, Kakar, Parker, Honoré, & Ostermann, 2015). Most of the aforementioned studies that have been done only examine one dose, or one dosing regimen; I believe that this could have led to premature dismissal of the potential of dopamine, or dopamine related compounds for the use for nephroprotection. Thus, I believe that further study is required to determine the relative contribution of D1-like and D2-like dopamine receptor activation in the context of the kidney to assess a potential role for D_1 agonists as a nephroprotective agent.

Given the importance of dopaminergic signalling, it is unsurprising that there are several human pathologies that relate to the mishandling or inappropriate synthesis/breakdown of this neurotransmitter. Parkinson's disease is a progressive nervous system disorder that is characterized by loss of dopaminergic neurons in the midbrain, mostly in specific regions of the substantia nigra (Damier, Hirsch, Agid, & Graybiel, 1999). There is significant correlation between the severity of motor symptoms, including rigidity and bradykinesia (slowness of movement) and tremors and dopamine

loss; thus, much of the symptomatic treatment revolves around the replacement of dopamine. Levodopa (LD), or L-DOPA, is a precursor to dopamine, and was approved for the use in Parkinson's disease by the FDA in 1970. Since then, it has remained the gold-standard for the treatment of symptomatic Parkinson's disease (Salat & Tolosa, 2013; Sethi, 2010). Dopamine itself is not administered, as it does not effectively cross the blood-brain barrier (BBB) (Haddad, Sawalha, Khawaja, Najjar, & Karaman, 2018). However, the administration of L-DOPA as a prodrug allows it to cross the BBB, where it is quickly converted to dopamine (**Figure 4.5**). As a result, between 1-10% of the L-DOPA reaches the brain, meaning high doses are required for desired therapeutic effects. Peripherally, L-DOPA is also converted dopamine, and high peripheral levels of dopamine can cause hypotension and nausea (Salat & Tolosa, 2013). L-DOPA is often administered with a catechol-*O*-methyl transferase (COMT) inhibitor like entacapone or tolcapone, or an aromatic acid decarboxylase inhibitor like carbidopa, in attempts to inhibit the breakdown to L-DOPA to dopamine (Haddad et al., 2018). Interestingly, a literature search also showed that individuals with Parkinson's had a significantly higher incidence of high-frequency, age-dependent sensorineural hearing loss in comparison with age-matched controls (Vitale et al., 2012) and dopaminergic treatment seemed to improve at least some measures of auditory function (Pisani et al., 2015). This adds further support to the notion of the potential positive effects of dopamine on auditory function.

6.3.4 Dopamine Receptor Expression in HK-2 Cells and the Zebrafish

To determine if increased receptor-mediated dopamine signaling could indeed be providing some degree of oto- and nephroprotection, the dopamine receptors would likely

need to be present in the human HK-2 proximal tubule cells and in the zebrafish regions of interest.

There are reports of D_1 receptor expression in HK-2 cells at both the mRNA and protein level (Pokkunuri, Chugh, & Asghar, 2013; Y. R. Zhang & Yuan, 2010); however, another study suggests that the D_1 receptor in HK-2 cells is "functionally uncoupled" from adenylyl cyclase (AC) (Gildea et al., 2010). Researchers suggested that compensation by the D_5 receptor, also shown to be expressed in HK-2 cells, may have masked these effects (Gildea et al., 2010; Pokkunuri et al., 2013). Later studies demonstrated that although the D_1 receptor in HK-2 cells may be uncoupled from the well-known $G\alpha_s$-mediated activation of AC, the receptor could still signal though a $G\alpha_{q/11}$-mediated pathway, resulting in the inhibition of Na-K-ATPase seen by Zhang & Yuan (Pokkunuri et al., 2013; Y. R. Zhang & Yuan, 2010). While I could not find explicit published data about the expression of the D2-type dopamine receptors in HK-2 cells, a search of the GEO profiles database (Edgar, Domrachev, & Lash, 2002) revealed evidence for the expression of both *DRD3* and *DRD4* in this cell line ((Perco et al., 2019; Pirklbauer et al., 2019), GEO accession numbers GSE106156 and GSE118337, respectively). However, I could not find evidence of D_2 receptor expression in this cell line.

As a result of a whole-genome duplication event, there are two homologs of many human genes in the zebrafish. There are currently 14 dopamine receptor genes, or dopamine receptor-like genes according to ZFIN (Ruzicka et al., 2018). These genes, along with the temporal and spatial locations of expression (if available), can be found in **Table 6.1**. Of note, many of the reports of receptor expression whole organism reverse transcriptase polymerase chain reaction (RT-PCR) analysis, which would not allow for

anatomical localization within the larva. However, there is a report of *drd1a* (encoding for zebrafish dopamine receptor d1a)*, drd1b, drd2a, drd2b, drd3, drd4a* and *drd4b* expression in the dissected adult inner ear, but only *drd1b* in the neuromasts (Toro et al., 2015). Additionally, there is a high degree of amino acid similarity between the zebrafish and human proteins, suggesting that ligands may be cross-reactive (**Table 6.1**). I could not find any public information about the expression of zebrafish dopamine receptors in either the pronephros or in the adult mesonephros.

Table 6.1 Zebrafish dopamine receptor gene temporal and spatial expression. All information compiled from ZFIN (Ruzicka et al., 2018). Percentage similarity to human protein product as per positive amino acid overlap. RT-PCR=reverse transcriptase polymerase chain reaction; hpf=hours post fertilization; dpf=days post fertilization, WISH=whole-mouth *in situ* hybridization, NI=no information.

Human gene	Zebrafish gene and % overlap with human protein product	Zebrafish age at time of analysis	Anatomical location of expression	Assay	Reference
DRD1	*drd1a*, 78%	Adult	Inner ear	RT-PCR	(Toro et al., 2015)
DRD1	*drd1b,* 77%	Adult	Inner ear, neuromast, whole organism	RT-PCR	(Toro et al., 2015)
		30 hpf – 5 dpf	Brain regions	WISH	(P. Li et al., 2007)
DRD2	*drd2a,* 68%	Adult	Inner ear, whole organism	RT-PCR	(Toro et al., 2015)
	drd2b, 67%	Adult	Inner ear, whole organism	RT-PCR	(Toro et al., 2015)
DRD2	*drd2l* (like), (61%)	Adult	Ventral hypothalamus	WISH	(Fontaine et al., 2013)
DRD3	*drd3,* 72%	Adult	Inner ear, whole organism	RT-PCR	(Toro et al., 2015)
		16 hpf – 5 dpf	Brain regions	WISH	(Boehmier et al., 2004)
DRD4	*drd4a,* 75%	Adult	Inner ear, whole organism	RT-PCR	(Toro et al., 2015)
		24 hpf – 5 dpf	Brain regions	WISH	(Boehmler, Carr, Thisse, & Thisse, 2007)
DRD4	*drd4b*, 75%	Adult	Inner ear, whole organism	RT-PCR	(Toro et al., 2015)
		16 hpf – 5 dpf	Brain regions	WISH	(Boehmler et al., 2007)
DRD4	*drd4-rs* (related sequence), 72%	24-72 hpf	Whole organism	RT-PCR	(Souders & Schmidt, 2018)
DRD5	*drd5a,* 88%	NI	NI	NI	NI
Unknown	*drd5b*	NI	NI	NI	NI
Unknown	*drd6a*	NI	NI	NI	NI
DRD5	*drd6b*, 70%	NI	NI	NI	NI
	drd7	0.5-72 hpf	Whole organism	RT-PCR	(Souders & Schmidt, 2018)

6.3.5 Potential Mechanisms of Protection

The most straightforward explanation for the oto- and nephroprotective effects of dopamine is that this endogenous ligand binds to the D_1 or D_5 receptors present in the inner ear and/or pronephros structure and causes increases in intracellular cAMP, which seems to provide nephroprotection in some studies (Gillies et al., 2015; Hans et al., 1990;

Palmieri et al., 1993) and cochlear nerve protection from noise-induced hearing damage (Darrow et al., 2007; Lendvai et al., 2011; Nouvian et al., 2001; Oestreicher et al., 1997). This is supported by the appearance of dopamine, p-fluoro-L-phenylalanine (substrate for tyrosine hydroxylase), L-mimosine (inhibitor of dopamine β-hydroxylase) (Hashiguch & Takahashi, 1976) and GBR-12909 (dopamine reuptake inhibitor) in the list of compounds that were hits in the oto- and nephroprotection assay (**Figure 4.5**). Also of note, trifluoperazine dihydrochloride, a D_2 receptor-inhibitor, was a hit in both assays (**Table 4.2**). As previously mentioned, D2-like receptors typically couple with $G\alpha_{i/o}$ proteins, involved in the inhibition of AC, resulting in a decrease in cAMP levels. Thus, a D_2 receptor-inhibitor would have a similar effect net effect of a D_1 receptor agonist. However, the D1-like dopamine receptor agonist, fenoldopam, mentioned previously was one of the 1,280 compounds in the Sigma LOPAC®^{1280}, and was not a hit in either the oto- or nephroprotection assays, providing only marginal levels of protection (0.585 and 0.595, in comparison with the cisplatin-only values of 0.5, respectively). Another curious finding was that although dopamine itself was a hit, levodopa (L-DOPA) was only a hit in the otoprotection study, not the nephroprotection study (0.941 and 0.559, respectively). However, this inconsistency could be a result of incorrect dose or timing of administration, as only the most promising compounds were optimized for these factors. Alternatively, in the case of L-DOPA, the amount of available aromatic acid decarboxylase (AADC) could have limited the production of dopamine from the L-DOPA, masking the effects.

6.3.6 Considerations for Future Validation Studies

In order to determine the specific mechanism of dopamine-mediated oto- and nephroprotection, there are several experiments that would need to be done. One tactic would be a pharmacological approach, obtaining agonists that are specific to each of the dopamine receptors, and assessing their potential protective effects. I would first begin in the *in vitro* nephroprotection assay, as it is easier, then would move to the *in vivo* ototoxicity assay. Examples include SKF-81297 hydrobromide and SKF-82958, both specific to the D_1 receptor. I would avoid compounds like fenoldopam, as they are known to bind to D1-like receptors and to α_2-adrenergic receptors, which could complicate findings. This may even result in the identification of a more protective compound, or a compound that is effective at a lower dose. While this should help to narrow down the potential receptor of interest, it does not necessarily indicate a specific receptor-mediated effect. Thus, it would be beneficial to knock-down each of the dopamine receptors individually in the HK-2 cell line and assess the cells in the alamarBlue™-based nephroprotection assay. I would undertake this type of experiment using siRNA-mediated knock-down, as I do not want to maintain the cells for a long period of time without a receptor that likely plays an important role in their function. If one specific receptor is responsible for the nephroprotection, the cells would no longer be protected from cisplatin-induced toxicity.

6.4 L-mimosine as an Oto- and Nephroprotective Agent

6.4.1 Overview

L-mimosine is a plant amino acid that can be isolated from seeds of the *Leucaena* and *Mimosa* plant genera (Tsai & Ling, 1971). The *Leucaena* genus is native to Central American and areas of Mexico but is now found in most tropical areas globally. These plants have also been used in traditional folk medicine as an emmenagogue, to increase menstruation (Lim, 2012). The *Mimosa* plants genus is native to South and Central America but is considered to be a tropical weed. Various preparations have been used in traditional medicine across cultures, including use as a treatment for insomnia, anxiety, epilepsy, and urinary disorders (Lim, 2014). *L. leucocephala* is an important feed source, as it is inexpensive and fast-growing. However, the presence of mimosine in the leaves makes it toxic when eaten in large quantities. Toxic effects consist of emaciation, alopecia and enlarged thyroid glands were observed when cattle were fed diets consisting of 67-100% *L. leucocephala*; however, smaller percentages of the plant do not seem to negatively influence animal health (Ghosh & Brandyopadhyay, 2007).

6.4.2 Pharmacology and Previous Studies

L-mimosine is a molecule with a wide variety of cellular targets and reported activities. While very early reports suggested that mitosis inhibition was the cause of hair loss in sheep following L-mimosine ingestion (Warda & Harrij, 1976), the earliest detailed study reporting the pharmacological effects of L-mimosine was in 1976. Armed with the recent crystal structural determination of the molecule (Mostad, Romming, & Rosenqvist, 1973), and the knowledge that L-mimosine can chelate copper, these

researchers discovered that this compound can inhibit two copper-containing enzymes, tyrosinase and dopamine β-hydroxylase (Hashiguch & Takahashi, 1976).

Since this point, numerous pharmacological effects have been associated with L-mimosine exposure. This includes the inhibition of prolyl hydroxylases (PHDs) (prolyl 4-hydroxylase and deoxhypusine hydroxylase) (Mccaffrey et al., 1995), which has shown to stabilize hypoxia -inducible factor 1α (HIF-1α) (Warnecke et al., 2003). HIF is a dimeric protein consisting of an α and a β subunit. In normoxic conditions, when oxygen is plentiful, HIF-1α is regularly degraded by the cellular proteasome. In contrast, in hypoxic conditions, HIF-1α dimerizes with the β subunit and acts as a transcriptional regulator, binding to hypoxia-responsive elements to modulate gene expression (Warnecke et al., 2003). This HIF-1α stabilization has been investigated in a variety of experimental contexts. L-mimosine has been shown to induce expression of vascular endothelial growth factor (VEGF) which is a pro-angiogenic factor that is important for tumour progression (Warnecke et al., 2003). Interestingly, L-mimosine-induced HIF-1α activation also seems to be responsible for reduced fibrosis in a rat nephrectomy model of kidney disease (Yu et al., 2012) and reduced damage in mouse kidneys following induced ischemia (Hill et al., 2008). Although not specifically related to HIF-1α, L-mimosine injection also decreases levels of tumour necrosis α (TNF-α), a proinflammatory molecule, and the size of potassium permanganate-induced granulomas (Frydas et al., 2003). L-mimosine has also been investigated as an agent to aid in the healing in the context of dental surgery as a result of its proangiogenic capacity; however, the utility of L-mimosine in this context may be limited as it decreases matrix mineralization (Muller et al., 2015).

L-mimosine is also known to bind iron and copper ions. Studies provide evidence that this iron chelation results in the inhibition of enzymes that are required for cells to progress through the cell cycle (Kulp & Vulliet, 1996). L-mimosine has also been shown to inhibit cyclin D1 expression, a protein that is known to regulate progression through the cell cycle, in a non-small cell lung cancer cell line and PC-3 prostate cancer cells (H. Chang, Lee, Chuang, & Yen, 1999; Chung et al., 2011).

An additional potential pharmacologic effect of L-mimosine treatment has been suggested by a study in a xenotransplant mouse model of pancreatic cancer. Briefly, treatment of tumour-bearing animals with L-mimosine caused an increase in apoptotic cancer cells, and suggest an increase in expression of the multidrug resistance gene (MDR1), which codes for P-glycoprotein (Zalatnai, 2005). P-glycoprotein is an important membrane transporter that is found on the apical membrane of cells in the kidney, liver, intestine, adrenal gland, and BBB, where it is an important transporter involved in the secretion of may substrates, including drugs (Thiebaut, Tsuruot, Hamadat, Gottesman, & Pastan, 1987; S. Zhou, 2008). While cisplatin itself does not seem to be a substrate, cisplatin treatment can increase P-glycoprotein expression (Demeule, Brossard, Be, & Brossard, 1999). Further, studies suggest that P-glycoprotein-positive cells had lower sensitivity to cisplatin-induced apoptosis, in comparison with P-glycoprotein negative-cells. The effect was not a result of decreased cisplatin accumulation in the cancer cells and was likely as a result of less cisplatin-induced caspase-3 activation (Gibalová et al., 2012).

6.4.3 Potential Mechanisms of Protection

One of the potential mechanisms of protection by L-mimosine is closely related to the hypothesis that I have proposed for dopamine. As previously mentioned, L-mimosine, and other compounds that were hits in both the oto- and nephrototoxicity assays (**Figure 4.5**), could have the net effect of increasing dopamine levels. Through the effects of L-mimosine as a dopamine β-hydroxylase inhibitor (Hashiguch & Takahashi, 1976), dopamine levels could be increased and oto- and nephroprotection could occur as a result of D1-like dopamine receptor-mediated signalling. Another possibility is that L-mimosine may interact with one or more of the dopamine receptors themselves, as a result of their similarity in chemical structure. In fact, a preliminary search using ChEMBL suggests D_1, D_2, D_3, and D_4 as potential binding targets for L-mimosine (Gaulton et al., 2017).

However, there is also a significant possibility that the oto- and nephroprotective effects of L-mimosine are unrelated to dopamine. The protection could be a result of the lower rates of caspase activation following treatment with L-mimosine, as seen in other P-glycoprotein-expressing cell lines (Gibalová et al., 2012). However, this would not explain the differential effects of L-mimosine in normal vs. cancerous cells. Another possibility is that the protection is related to L-mimosine-induced PHD inhibition, resulting in stabilized HIF-1α. HIF-1α stabilization is related to lower levels of ROS (Zhao et al., 2014). Similar to the mechanisms of otoprotection by NAC, decreased levels of ROS could result in decreased damage to both sensory hair cells and renal tubular cells.

The multiple reported activities of L-mimosine render it exceedingly challenging to predict a mechanism of action. It is also highly likely that the mechanisms of

protection are not related to one specific effect and are a result of a combination of cellular changes. Regardless, further investigation is needed in order to provide an accurate prediction as to the mechanism of action in this context.

6.4.4 Considerations for Future Validation Studies

As a result of the many potential pharmacological activities by L-mimosine, the overall goal for the next steps in this portion of the project would involve efforts to identify the cellular target(s) for L-mimosine in this study of oto- and nephrotoxicity. The first step that I would undertake is performing the L-mimosine nephroprotection experiment in the HK-2 cells that had each of the dopamine receptors knocked down, as mentioned above. This would provide some indication if L-mimosine is acting as some type of an agonist at these receptors, as was predicted by the ChEMBL database.

I would perform RNA-sequencing (RNA-Seq) of both HK-2 cells and zebrafish larvae treated with cisplatin +/- L-mimosine. While this would not identify the exact target of interest, it would identify changes in gene expression, which could provide information about the mechanism(s) of action. Additionally, it would be interesting to compare the findings from the cell culture model with those from the zebrafish. Pathways that are activated in both model systems would be more likely to be relevant.

I believe that the optimal experiments to determine the mechanism of action of L-mimosine would be to perform target identification using an affinity-based proteomic "pulldown" technique. Very broadly speaking, this involves creating a suitable probe that can be immobilized, exposed to cell lysate, washed carefully to remove non-binding proteins, probe retrieval, tryptic digestion and subsequent mass spectrometric analysis (Strategies, Sato, Murata, Shirakawa, & Uesugi, 2010; Ziegler, Pries, Hedberg, &

Waldmann, 2013). This could be accomplished using something relatively simple, like an alkyl group linker with a retrieval tag, or something more sophisticated, like photo-affinity labelling with an alkyne for conjugation with biotin, as has been done previously (Ban, Shimizu, Minegishi, & Nakamura, 2010; Cote et al., 2011; Ziegler et al., 2013). This technique may be made more difficult by the very small nature of L-mimosine, as modifications to a small structure are generally more likely to modify the pharmacological properties of the compound. Thus, one would need to ensure that the modified L-mimosine compound had similar oto- and nephroprotective effects in comparison with the parent molecule prior to target capture. This would hopefully result in the identification of the target in question, which should allow for further analysis and/or structural optimization through medicinal chemistry.

6.5 Importance of Protective Agents Not Interfering With Cisplatin's Anticancer Effects

6.5.1 Cautionary Tales from History

One of the major concerns with the prevention of chemotherapy-associated toxicity is the problem of inadvertently providing the cancer cells with some degree of protection. This is a particularly pressing concern when dealing with toxicities that are unlikely to be life-threatening (in the exception of very extreme acute kidney injury; AKI). There are several circumstances from recent history that provide examples of protective agents that may not function as well as theorized.

Although this thesis was not investigating anthracycline-induced cardiotoxicity, Dexrazoxane is an example of an FDA approved protective compound against chemotherapy-induced toxicity (Cvetkovic & Scott, 2005). Dexrazoxane is approved in the USA and some European countries for cardioprotection in women receiving

doxorubicin, an anthracycline based therapy, for advanced or metastatic breast cancer. According to a meta-analysis, dexrazoxane reduces the risk of anthracycline-induced risk in cancer patients from 9.81% to 1.66% (van Dalen, Caron, Dickinson, & Kremer, 2008). One study from the Pediatric Oncology Group (POG) evaluated the use of dexrazoxane as a cardioprotectant during doxorubicin treatment of Hodgkin's disease, and found that there was a higher incidence of secondary malignant neoplasms and acute myeloid leukemia (AML)/myelodysplastic syndrome (MDS) correlated with dexrazoxane use (Tebbi et al., 2007). However, these results have not been repeated in other such studies (Vrooman et al., 2011). Nonetheless, clinicians are advised to evaluate each patient individually to determine whether or not dexrazoxane should be used (van Dalen et al., 2008).

The importance of assessing the potential effects of a protective agent on chemotherapeutic efficacy is exemplified by STS, an otoprotective agent that is in Phase III clinical trials. When administered 2 or 6 hr following cisplatin administration, it is known to decrease the anticancer effects of cisplatin in a murine model. However, delaying this administration to 8 hr following cisplatin reduces this effect (L. L. Muldoon et al., 2000). In a clinical trial of 104 pediatric and adolescent cancer patients, 28.6% of patients that received STS exhibited hearing loss versus 56.4% of patients in the control arm (Freyer et al., 2017). Interestingly, overall nephrotoxicity, indicated by hypophosphatemia and hypokalemia, was more common in the STS group in comparison with the control group (25% vs. 13%, respectively). When examining the entire cohort of patients, there was no significant difference between event-free or overall survival between groups at the secondary endpoint (3.5 years was the median follow up). However, when the patients were stratified by extent of disease at time of diagnosis, the

patients that presented with disseminated disease had significantly lower overall and event-free survival in the STS group. Within the patients with disseminated disease, the control group that did not receive STS had four deaths, and the STS group had 11 deaths (Freyer et al., 2017). The potential chemoprotective effects were mentioned in this study, but the authors noted that the difference in survival could have been a result of the wide degree of variability in disease extent and type. However, one of the mechanisms through which STS is known to protect against cisplatin toxicities is through direct binding (likely resulting in inactivation) of cisplatin (Sooriyaarachchi, Narendran, & Gailer, 2012).

6.5.2 Considerations for an Ideal Protective Agent

Ideal drug candidates need to meet a series of qualifications, including a tolerable toxicity profile and acceptable bioavailability. One measure that has been established to describe many of these principles is Lipinski's Rule of Five. This is a concept that emphasizes four physical parameters of a given compound to estimate its solubility and permeability in efforts to determine the "druglikeness." This rule posits that the ideal compound should have no more than one violation of the following criteria: no more than 5 hydrogen bond donors; no more than 10 hydrogen bond acceptors; a molecular mass <500 Daltons (Da); an octanol-water partition coefficient, or LogP that does not exceed 5 (C A Lipinski, 1995; Christopher A Lipinski, Lombardo, Dominy, & Feeney, 2012). Dopamine and L-mimosine each violate zero of these conditions, suggesting that their pharmacokinetic parameters are unlikely to prevent their further development as therapeutics.

Another potential good quality for a novel protective agent would be a compound that does not directly bind to cisplatin. This is emphasized by STS, the otoprotective

compound that resulted in decreased overall survival in patients with disseminated disease. Even though administration of STS was delayed to 8 hrs following cisplatin, it is possible that remaining cisplatin was bound and inactivated by STS. An additional positive attribute of a protective agent would be a mechanism of action that is distinct from the mechanism of cisplatin. While not required, this would provide additional assurance that the protective agent is unlikely to interfere with the chemotherapeutic effects of cisplatin. For example, one of the mechanisms through which cisplatin induces cancer cell death is through elevating the levels of ROS. While NAC, an antioxidant, demonstrates efficacy as an otoprotectant, the fact that it scavenges ROS suggests that it may interfere with the desired mechanism of action of cisplatin.

6.5.3 Future Experiments to Support Lack of Interference with Chemotherapeutic Effects

As previously mentioned, it is of the utmost importance that a protective compound not interfere with the desired chemotherapeutic effects of the drug. In this study, I was able to demonstrate that dopamine and L-mimosine did not interfere with the anticancer effects of cisplatin as measured with an alamarBlue™ assay; in fact, dopamine and L-mimosine sometimes added to the cytotoxicity of cisplatin in several cancer cell lines (**Figure 5.1, 5.2**). Further, dopamine and L-mimosine did not prevent cisplatin-induced apoptosis in SK-N-AS NBL cancer cells (**Figure 5.3**). Lastly, I showed that cisplatin-induced DSB formation was generally unaffected by dopamine or L-mimosine (**Figure 5.4, 5.5**).

However, the results from our xenotransplant-based *in vivo* assays were not as straightforward (**Figure 5.7**). While cisplatin treatment was able to decrease the numbers of SK-N-AS cells, in a significant fashion, it was not a dramatic difference. Cisplatin

treatment also did not have a reproducible effect in the LAN5 NBL or HSC-3 oral squamous cell carcinoma cell lines. I hypothesize that cisplatin did not effectively permeate the barrier into the yolk sac, where the cancer cells were xenotransplanted. While very little is known about the yolk sac of zebrafish larvae, it is known that the bulk of the material consists of lipids. Thus, the relatively polar cisplatin molecule may not be suited to penetrating this area of the zebrafish. Additionally, the yolk sac is a relatively hypoxic region (Pringle et al., 2019). It has been suggested that hypoxia is one mechanism through which cells become resistant to cisplatin treatment (Guo et al., 2018). Nonetheless, it was not possible to assess the potential effects of dopamine on L-mimosine on cisplatin-induced toxicity in a model where cisplatin was not consistently cytotoxic.

There are several potential *in vivo* experiments that could be completed to assess the question of whether or not dopamine and L-mimosine confer chemoprotection to cancer cells. The first is the use of an adult zebrafish xenotransplant model (C. Yan et al., 2019), in which cisplatin could be reproducibly injected into the vasculature of tumour-bearing adult fish. Other options include transgenic zebrafish models of cancer, like the anaplastic lymphoma kinase (*ALK)/MYCN* transgenic fish created by Zhu *et al.,* that develops NBL (Zhu et al., 2012). I would assess the utility of cisplatin in tumour-bearing fish +/- the protective agents in order to assess potential chemoprotective effects of the compounds. Lastly, dopamine and L-mimosine should be tested in murine models of both cisplatin-induced toxicities and cisplatin-induced tumour protection. This could involve either xenotransplant or transgenic models of cisplatin-susceptible cancer.

6.6 Application of Findings to Future Studies

There are two main aspects to the applicability of this study. Firstly, the assay development portion of this project could be taken advantage of by a wide variety of studies. The *in vivo* ototoxicity screen could be used for various libraries of compounds, measuring for potential protective effects, as I have done in this project. However, this could also be used for the identification of potentially ototoxic effects of novel compounds in a high-throughput manner, as has been done in the past using a different method (Chiu, Cunningham, Raible, Rubel, & Ou, 2008). This type of drug screen could also use a different fluorescent marker of interest. This could range from CM-H2-DCFDA to measure levels of ROS in whole zebrafish larvae, as has been done previously (M. Daugaard et al., 2013), to using the zebrafish *mpeg1* fluorescent reporter line, to assess the effects of a library of compounds on macrophage cell number (Ellett, Pase, Hayman, Andrianopoulos, & Lieschke, 2011). Similarly, the FITC-inulin based GFR assay, previously performed with 15 larvae/treatment in two groups (Hentschel et al., 2005), has been greatly expanded for use by employing the biosorter. In this particular assay, I used at least 50 larvae/treatment, with four treatment groups.

The second major avenue for further discovery is the results gleaned from this two-pronged drug screen. The list of 22 compounds that were hits in both the oto- and nephrotoxicity assay all represent viable targets for further investigation. Further, L-mimosine and dopamine are compounds that exhibit obvious oto- and nephroprotective potential; thus, these compounds should be the topic of further experimentation, including the experiments described in this thesis.

6.7 Conclusions and Significance

To conclude, this study has developed and utilized medium-high throughput methods to screen compound libraries for *in vivo* ototoxicity using the zebrafish lateral line, and *in vitro* nephrotoxicity using the HK-2 proximal tubule cell line. Upon compilation of both screens, there were 22 compounds that provided both oto- and nephroprotection. Two of these compounds, dopamine and L-mimosine, provide protection from cisplatin-induced damage to zebrafish lateral line neuromasts, inner ear hair cells, and GFR. Further, these compounds do not confer protection to SK-N-AS, LAN5, and HSC3 cancer cell lines, suggesting that cisplatin efficacy is not compromised. While either of these compounds deserves further investigation, the multiple potential mechanisms of protection by L-mimosine are highly intriguing, and would be my highest priority for further investigation.

This study highlights the utility of zebrafish for both *in vivo* drug screening and preclinical testing. The use of a living organism allowed for the assessment of systemic toxicity in the drug screen, helping to avoid further investigation into toxic compounds. Zebrafish studies also afforded the opportunity for analysis of complex physiological functions, like glomerular filtration, in a relatively high-throughput and low-cost fashion.

It is my hope that both the techniques and preliminary protective agents outlined in this thesis are able to be used by the scientific community moving forward. I hope that dopamine and L-mimosine can move forward into murine models of oto- and nephrotoxicity. Should further investigation go well, I would hope that these compounds could be assessed in a clinical trial, with the ultimate goal of improving the quality of life for patients receiving cisplatin treatment.

References

Adler, M., Ramm, S., Hafner, M., Muhlich, J. L., Gottwald, E. M., Weber, E., … Vaidya, V. S. (2016). A Quantitative Approach to Screen for Nephrotoxic Compounds In Vitro. *J Am Soc Nephrol*, *27*, 1015–1028. https://doi.org/10.1681/ASN.2015010060

Alberti, P. W. (2001). The anatomy and physiology of the ear and hearing. In *Occupational exposure to noise: Evaluation, prevention, and control* (pp. 53–62).

Alcindor, T., & Beauger, N. (2011). Oxaliplatin: a review in the era of molecularly targeted therapy. *Current Oncology*, *18*(1), 18–25.

Allen, G., Tiu, C., Koike, K., Ritchey, A. K., Kurs-Lasky, M., & Wax, M. K. (1998). Transient-evoked otoacoustic emissions in children after cisplatin chemotherapy. *Otolaryngology - Head and Neck Surgery*, *118*(5), 584–588.

Alvarez, S., Germain, P., Alvarez, R., Rodríguez-Barrios, F., Gronemeyer, H., & de Lera, A. R. (2007). Structure, function and modulation of retinoic acid receptor beta, a tumor suppressor. *The International Journal of Biochemistry & Cell Biology*, *39*(7), 1406–1415. https://doi.org/https://doi.org/10.1016/j.biocel.2007.02.010

Andrews, P. A., Mann, S. C., Velury, S., & Howell, S. B. (1987). Cisplatin uptake mediated cisplatin-resistance in human ovarian carcinoma cells. In M. Nicolini (Ed.), *Platinum and other metal coordination compounds in cancer chemotherapy* (pp. 248–254). Padua, Italy: Martinus Nijhoff Publishing.

Argiris, A., Li, Y., Murphy, B. A., Langer, C. J., & Forastiere, A. A. (2004). Outcome of Elderly Patients With Recurrent or Metastatic Head and Neck Cancer Treated With Cisplatin-Based Chemotherapy. *Journal of Clinical Oncology*, *22*(2), 262–268. https://doi.org/10.1200/JCO.2004.08.039

Arora, R., Thakur, J., Azad, R., Mohindroo, N., Sharma, D., & Seam, R. (2009). Cisplatin-based chemotherapy: Add high- frequency audiometry in the regimen. *Indian Journal of Cancer*, *46*(4), 311–317.

Arslan, E., Orzan, E. V. A., & Santarelli, R. (1999). Global Problem of Drug-Induced Hearing Loss. *Ann N Y Acad Sci*, *884*, 1–14.

Audiologic management of individuals receiving cochleotoxic drug therapy. (1994).

Avraham, K. B. (2003). Mouse Models for Deafness: Lessons for the Human Inner Ear and Hearing Loss. *Ear & Hearing*, (24), 332–341. https://doi.org/10.1097/01.AUD.0000079840.96472.DB

Aydogdu, I., Ozturan, O., Kuku, I., Kaya, E., Sevinc, A., & Yildiz, R. (2013). Bilateral Transient Hearing Loss Associated with Vincristine Therapy. *Journal of Chemotherapy*, *12*(6), 530–532. https://doi.org/10.1179/joc.2000.12.6.530

Baldwin, L., Henderson, A., & Hickman, P. (1994). Effect of Postoperative Low-Dose Dopamine on Renal Function after Elective Major Vascular Surgery. *Ann Intern Med*, *120*, 744–747.

Ban, H. S., Shimizu, K., Minegishi, H., & Nakamura, H. (2010). Identification of HSP60 as a Primary Target of o-Carboranylphenoxyacetanilide, an HIF-1 r Inhibitor. *J Am Chem Soc*, *132*, 11870–11871.

Banfi, B., Malgrange, B., Knisz, J., Steger, K., Dubois-dauphin, M., & Krause, K. (2004). NOX3, a Superoxide-generating NADPH Oxidase of the Inner Ear. *The Journal of Biological Chemistry*, *279*(44), 46065–46072. https://doi.org/10.1074/jbc.M403046200

Bang, P. I., Yelick, P. C., Malicki, J. J., & Sewell, W. F. (2002). High-throughput behavioral screening method for detecting auditory response defects in zebrafish. *Journal of Neuroscience Methods*, *118*, 177–187.

Barratt, T. M., Mclaine, P. N., & Soothill, J. F. (1970). Albumin Excretion as a Measure of Glomerular Dysfunction in Children, 496–501.

Bass, J. K., & Bhagat, S. P. (2014). Challenges in Ototoxicity Monitoring in the Pediatric Oncology Population. *J Am Acad Audiol*, *25*, 760–774. https://doi.org/10.3766/jaaa.25.8.6

Baxendale, S., & Whitfield, T. T. (2016). Methods to study the development, anatomy, and function of the zebrafish inner ear across the life course. *Methods in Cell Biology*, *134*, 165–209.

Beaulieu, J., & Gainetdinov, R. R. (2011). The Physiology, Signaling, and Pharmacology of Dopamine Receptors. *Pharmacological Reviews*, *63*(1), 182–217. https://doi.org/10.1124/pr.110.002642.182

Bentley, V., Veinotte, C., Corkery, D., Pinder, J., LeBlanc, M., Bedard, K., … Dellaire, G. (2015). Focused chemical genomics using zebrafish xenotransplantation as a pre-clinical therapeutic platform for T-cell acute lymphoblastic leukemia. *Haematologica*, *100*(1), 70–76. https://doi.org/10.3324/haematol.2014.110742

Berg, A. L., Spitzer, J. B., & Garvin, J. H. (1999). Ototoxic Impact of Cisplatin in Pediatric Oncology Patients. *The Laryngoscope*, *109*, 1806–1814.

Berghmans, S., Murphey, R. D., Wienholds, E., Neuberg, D., Kutok, J. L., Fletcher, C. D. M., … Look, a T. (2005). Tp53 Mutant Zebrafish Develop Malignant Peripheral Nerve Sheath Tumors. *Proceedings of the National Academy of Sciences of the United States of America*, *102*(2), 407–412. https://doi.org/10.1073/pnas.0406252102

Bertolini, P., Lassalle, M., Mercier, G., Raquin, M. A., Izzi, G., Corradini, N., & Hartmann, O. (2004). Platinum compound-related ototoxicity in children: Long-term follow-up reveals continuous worsening of hearing loss. *Journal of Pediatric Hematology/Oncology*, *26*(10), 649–655. https://doi.org/10.1097/01.mph.0000141348.62532.73

Bess, F. H., Dodd-Murphy, J., & Parker, R. A. (1998). Children with Minimal Sensorineural Hearing Loss: Prevalence, Educational Performance, and Functional Status. *Ear and Hearing*, *19*(5). Retrieved from https://journals.lww.com/ear-hearing/Fulltext/1998/10000/Children_with_Minimal_Sensorineural_Hearing_Loss_.1.aspx

Bhandare, N., Antonelli, P., Morris, C., Malayapa, R., & Mendenhall, W. (2007). Ototoxicity after radiotherapy for head and neck tumors. *Int J Radiation Oncology Biol Phys*, *67*(2), 469–479. https://doi.org/10.1016/j.ijrobp.2006.09.017

Biro, K., Noszek, L., Prekopp, P., Nagyivanyi, Geczi, L., Gaudi, I., & Bodrogi, I. (2006). Characteristics and Risk Factors of Cisplatin-Induced Ototoxicity in Testicular Cancer Patients Detected by Distorsion Product Otoacoustic Emission. *Oncology*, *70*, 177–184. https://doi.org/10.1159/000093776

Blakley, B. W., Hochman, J., Wellman, M., Gooi, A., & Hussain, A. E. (2008). Differences in Ototoxicity across Species. *Journal of Otolaryngology - Head & Neck Surgery = Le Journal d'oto-Rhino-Laryngologie et de Chirurgie Cervico-Faciale*, *37*(5), 700—703. Retrieved from http://europepmc.org/abstract/MED/19128679

Boehmier, W., Obrecht-Pflumio, S., Canfield, V., Thisse, C., Thisse, B., & Levenson, R. (2004). Evolution and expression of D2 and D3 dopamine receptor genes in zebrafish. *Developmental Dynamics*, *230*(3), 481–493. https://doi.org/10.1002/dvdy.20075

Boehmler, W., Carr, T., Thisse, C., & Thisse, B. (2007). D4 Dopamine receptor genes of zebrafish and effects of the antipsychotic clozapine on larval swimming behaviour. *Genes, Brain and Behavior*, *6*, 155–166. https://doi.org/10.1111/j.1601-183X.2006.00243.x

Bokemeyer, C., Berger, C. C., Hartmann, J. T., Kollmannsberger, C., Schmoll, H., Kuczyk, M. A., & Kanzl, L. (1998). Analysis of risk factors for cisplatin-induced ototoxicity in patients with testicular cancer. *British Journal of Cancer*, *77*(October 1997), 1355–1362.

Bossé, G. D., & Peterson, R. T. (2017). Development of an opioid self-administration assay to study drug seeking in zebrafish. *Behavioural Brain Research*, *335*(May), 158–166. https://doi.org/10.1016/j.bbr.2017.08.001

Brock, Knight, K. R., Freyer, D. R., Campbell, K. C. M., Steyger, P. S., Blakley, B. W., … Neuwelt, E. A. (2012). Platinum-induced ototoxicity in children: A consensus review on mechanisms, predisposition, and protection, including a new International Society of Pediatric Oncology Boston ototoxicity scale. *Journal of Clinical Oncology*, *30*(19), 2408–2417. https://doi.org/10.1200/JCO.2011.39.1110

Brock, P., Bellman, S., Yeomans, E., Pinkerton, C., & Pritchard, J. (1991). Cisplatin ototoxicity in children: a practical grading system. *Medical and Pediatric Oncology*, *19*(4), 295–300.

Bucaloiu, I. D., Kirchner, H. L., Norfolk, E. R., Ii, J. E. H., & Perkins, R. M. (2012). Increased risk of death and de novo chronic kidney disease following reversible acute kidney injury. *Kidney International*, *81*(5), 477–485. https://doi.org/10.1038/ki.2011.405

Buck, L. M. J., Winter, M. J., Redfern, W. S., & Whit, T. T. (2012). Ototoxin-induced cellular damage in neuromasts disrupts lateral line function in larval zebrafish. *Hearing Research*, *284*, 67–81. https://doi.org/10.1016/j.heares.2011.12.001

Caglar, K., Kinalp, C., Arpaci, F., Turan, M., Saglam, K., Ozturk, B., … Vural, A. (2002). Cumulative prior dose of cisplatin as a cause of the nephrotoxicity of high-dose chemotherapy followed by autologous stem-cell transplantation. *Nephrology Dialysis Transplantation*, *17*, 1931–1935.

Campbell, K. C. M., Meech, R. P., Klemens, J. J., Gerberi, M. T., Dyrstad, S. S. W., Larsen, D. L., … Hughes, L. F. (2007). Prevention of noise-and drug-induced hearing loss with D-methionine. *Hearing Research*, *226*, 92–103. https://doi.org/10.1016/j.heares.2006.11.012

Campbell, K. C. M., Rybak, L. P., Meech, R. P., & Hughes, L. (1996). d-Methionine provides excellent protection from cisplatin ototoxicity in the rat. *Hearing Research*, *102*(1), 90–98. https://doi.org/https://doi.org/10.1016/S0378-5955(96)00152-9

Case, J., Khan, S., Khalid, R., & Khan, A. (2013). Epidemiology of Acute Kidney Injury in the Intensive Care Unit. *Critical Care Research and Practice*, 479730.

Chang, H., Lee, T., Chuang, L., & Yen, M. (1999). Inhibitory effect of mimosine on proliferation of human lung cancer cells is mediated by multiple mechanisms. *Cancer Letters*, *145*, 1–8.

Chang, K. W., & Chinosornvatana, N. (2010). Practical Grading System for Evaluating Cisplatin Ototoxicity in Children. *Journal of Clinical Oncology*, *28*(10), 1788–1795. https://doi.org/10.1200/JCO.2009.24.4228

Chetrit, A., Hirsh-yechezkel, G., Ben-david, Y., Lubin, F., Friedman, E., & Sadetzki, S. (2008). Effect of BRCA1/2 Mutations on Long-Term Survival of Patients With Invasive Ovarian Cancer: The National Israeli Study of Ovarian Cancer. *Journal of Clinical Oncology*, *26*(1), 15–21. https://doi.org/10.1200/JCO.2007.11.6905

Chitnis, A. B., Nogare, D. D., & Matsuda, M. (2012). Building the posterior lateral line system in zebrafish. *Developmental Neurobiology*, *72*(3), 234–255. https://doi.org/10.1002/dneu.20962.Building

Chiu, L., Cunningham, L., Raible, D., Rubel, E., & Ou, H. (2008). Using the Zebrafish Lateral Line to Screen for Ototoxicity. *JARO - Journal of the Association for Research in Otolaryngology*, *9*, 178–190. https://doi.org/10.1007/s10162-008-0118-y

Chung, L., Tsui, K., Feng, T., Lee, S., Chang, P., Juang, H., … Hh, J. (2011). L-mimosine blocks cell proliferation via upregulation of B-cell translocation gene 2 and N-myc downstream regulated gene 1 in prostate carcinoma cells. *Am J Physiol Cell Physiol*, *302*, 676–685. https://doi.org/10.1152/ajpcell.00180.2011

Ciarimboli, G. (2008). Organic cation transporters. *Xenobiotica*, *38*(7–8), 936–971. https://doi.org/10.1080/00498250701882482

Ciarimboli, Giuliano. (2012). Membrane transporters as mediators of cisplatin effects and side effects. *Scientifica*, *2012*, 473829. https://doi.org/10.6064/2012/473829

Ciarimboli, Giuliano, Deuster, D., Knief, A., Sperling, M., Holtkamp, M., Edemir, B., … Koepsell, H. (2010). Organic Cation Transporter 2 Mediates Cisplatin-Induced Oto- and Nephrotoxicity and Is a Target for Protective Interventions. *The American Journal of Pathology*, *176*(3), 1169–1180. https://doi.org/10.2353/ajpath.2010.090610

Cleaver, J. (1969). Xeroderma Pigmentosum: A Human Disease in which an Initial Stage of DNA Repair is Defective. *PNAS*, *63*(2), 428–435.

Clerici, W. J., Hensley, K., Dimartino, D. L., & Allan, D. (1996). Direct detection of ototoxicant-induced reactive oxygen species generation in cochlear explants. *Hearing Research*, *98*, 116–124.

Common termniology criteria for adverse events (CTCAE). (2017). Retrieved from https://ctep.cancer.gov/protocolDevelopment/electronic_applications/ctc.htm#ctc_50

Corkery, Dellaire, G., & Berman, J. N. (2011). Leukaemia xenotransplantation in zebrafish – chemotherapy response assay in vivo. *British Journal of Haematology*, *153*, 786–789.

Cote, M., Misasi, J., Ren, T., Bruchez, A., Lee, K., Filone, M., … Louis, S. (2011). Small molecule inhibitors reveal Niemann-Pick C1 is essential for ebolavirus infection. *Nature*, *477*(7364), 344–348. https://doi.org/10.1038/nature10380.Small

Crona, D., Faso, A., Nishijima, T., McGraw, K., Galsky, M., & Milowshy, M. (2017). A Systematic Review of Strategies to Prevent Cisplatin-Induced Nephrotoxicity. *The Oncologist*, *22*, 609–619.

Cvetkovic, R. S., & Scott, L. J. (2005). Dexrazoxane: A Review of its Use for Cardioprotection During Anthracycline Chemotherapy. *Drugs*, *65*(7), 1005–1024.

Cvitkovic, E., Spaulding, J., Bethune, V., Martin, J., & Whitmore, W. F. (1977). Improvement of Cis-dichlorodiammineplatinum (NSC 119875): Therapeutic index in an animal model. *Cancer*, *39*(4), 1357–1361. https://doi.org/10.1002/1097-0142(197704)39:4<1357::AID-CNCR2820390402>3.0.CO;2-C

Dambly-Chaudière, C., Sapède, D., Soubiran, F., Decorde, K., Gompel, N., & Ghysen, A. (2003). The lateral line of zebrafish: a model system for the analysis of morphogenesis and neural development in vertebrates. *Biology of the Cell*, *95*, 579–587. https://doi.org/10.1016/j.biolcel.2003.10.005

Damier, P., Hirsch, E. C., Agid, Y., & Graybiel, A. M. (1999). The substantia nigra of the human brain II. Patterns of loss of dopamine-containing neurons in Parkinson's disease. *Brain*, *122*, 1437–1448.

Darrow, K., Maison, S., & Liberman, M. (2007). Selective removal of lateral olivocochlear efferents increases vulnerability to acute acoustic injury. *J Neurophysiol*, *97*(2), 1775–1785.

Dasari, S., & Bernard Tchounwou, P. (2014). Cisplatin in cancer therapy: Molecular mechanisms of action. *European Journal of Pharmacology*, *740*, 364–378. https://doi.org/10.1016/j.ejphar.2014.07.025

Daugaard, G., & Abildgaard, U. (1989). Cisplatin nephrotoxicity: a review. *Cancer Chemther Pharmacol*, *25*(1–9).

Daugaard, M., Nitsch, R., Razaghi, B., McDonald, L., Jarrar, A., Torrino, S., … Sorensen, P. H. (2013). Hace1 controls ROS generation of vertebrate Rac1-dependent NADPH oxidase complexes. *Nature Communications*, *4*, 2180. https://doi.org/10.1038/ncomms3180

de Gramont, A., Figer, A., Seymour, M., Homerin, M., Hmissi, A., Cassidy, J., … Bonetti, A. (2000). Leucovorin and Fluorouracil With or Without Oxaliplatin as First-Line Treatment in Advanced Colorectal Cancer. *Journal of Clinical Oncology*, *18*(16), 2938–2947. https://doi.org/10.1200/JCO.2000.18.16.2938

Deans, A. J., & West, S. C. (2013). DNA interstrand crosslink repair and cancer. *Nature Reviews Cancer*, *11*(7), 467–480. https://doi.org/10.1038/nrc3088.DNA

Deconti, R. C., Toftness, B. R., Lange, R. C., & Creasey, W. A. (1973). Clinical and Pharmacological Studies with cis-Diamminedichloroplatinum (II). *Cancer Research*, *33*, 1310–1315.

Demeule, M., Brossard, M., Be, R., & Brossard, M. (1999). Cisplatin induces renal expression of P-glycoprotein and canalicular multispecific organic anion transporter. *American Journal of Physiology - Renal Physiology*, *277*(6), F832-840.

Denk, D., Heinzl, H., Franz, P., Ehrenberger, K., Heinzl, H., Franz, P., … Ehrenberger, K. (1997). Caroverine in Tinnitus Treatment. *Acta Oto-Laryngologica*, *117*, 825–830. https://doi.org/10.3109/00016489709114208

Dickey, D. T., Muldoon, L. L., Kraemer, D. F., & Neuwelt, E. A. (2004). Protection against cisplatin-induced ototoxicity by N-acetylcysteine in a rat model. *Hearing Research*, *193*(1–2), 25–30. https://doi.org/10.1016/j.heares.2004.02.007

Dickey, D. T., Wu, Y. J., Muldoon, L. L., & Neuwelt, E. a. (2005). Protection against cisplatin-induced toxicities by N-acetylcysteine and sodium thiosulfate as assessed at the molecular, cellular, and in vivo levels. *The Journal of Pharmacology and Experimental Therapeutics*, *314*(3), 1052–1058. https://doi.org/10.1124/jpet.105.087601.the

Dijkgraaf, S. (1989). A short personal review of the history of lateral line research. In S. Coombs, P. Gorner, & H. Munz (Eds.), *The Mechanosensory Lateral Line* (pp. 7–14). New York: Springer.

Dijt, F. J., Fichtinger-schepman, A. M. J., Berends, F., & Reedijk, J. (1988). Formation and Repair of Cisplatin-induced Adducts to DNA in Cultured Normal and Repair-deficient Human Fibroblasts. *Cancer Research*, *48*, 6058–6063.

Doolittle, N. D., Muldoon, L. L., Brummett, R. E., Tyson, R. M., Lacy, C., Bubalo, J. S., … Neuwelt, E. A. (2001). Delayed sodium thiosulfate as an otoprotectant against carboplatin-induced hearing loss in patients with malignant brain tumors. *Clinical Cancer Research*, *7*(3), 493–500.

Drummond, I. A., & Davidson, A. J. (2010). *Zebrafish kidney development*. *Methods in Cell Biology* (Third Edit, Vol. 100). Elsevier Inc. https://doi.org/10.1016/B978-0-12-384892-5.00009-8

Drummond, I. A., Majumdar, A., Hentschel, H., Elger, M., Solnica-krezel, L., Rangini, Z., … Fishman, M. C. (1998). Early development of the zebrafish pronephros and analysis of mutations affecting pronephric function. *Development*, *4667*, 4655–4667.

Duan, M., Chen, Z., Qiu, J., Ulfendahl, M., Laurell, G., & Ruan, R. (2006). Low-dose, long-term caroverine administration attenuates impulse noise-induced hearing loss in the rat. *Acta Oto-Laryngologica*, *126*, 1140–1147. https://doi.org/10.1080/00016480500540519

Dworaczek, H., & Xiao, W. (2007). Xeroderma Pigmentosum: A Glimpse Into Nucleotide Excision Repair, Genetic Instability, and Cancer. *Critical Reviews in Oncogenesis*, *13*(2), 159–177.

Edgar, R., Domrachev, M., & Lash, A. (2002). Gene Expression Omnibus: NCBI gene expression and hybridization array data repository. *Nucleic Acids Research*, *30*(1), 207–210.

Edlich, F. (2018). BCL-2 proteins and apoptosis: Recent insights and unknowns. *Biochemical and Biophysical Research Communications*, *500*(1), 26–34. https://doi.org/10.1016/j.bbrc.2017.06.190

Ekdale, E. G. (2016). Form and function of the mammalian inner ear. *Journal of Anatomy*, *228*, 324–337. https://doi.org/10.1111/joa.12308

El-Naggar, A., Veinotte, C., Tognon, C., Corkery, D., Cheng, H., Tirode, F., … Sorensen, P. (2015). Translational activation of HIF1a by YB-1 promotes sarcoma metastasis. *Cancer Cell*, *27*(5), 682–697.

Eljack, N. D., Ma, H. M., Drucker, J., Shen, C., Hambley, T. W., New, E. J., & Clarke, R. J. (2014). Mechanisms of cell uptake and toxicity of the anticancer drug cisplatin. *Metallomics*, *6*, 2126–2133. https://doi.org/10.1039/c4mt00238e

Ellett, F., Pase, L., Hayman, J. W., Andrianopoulos, A., & Lieschke, G. J. (2011). Mpeg1 Promoter Transgenes Direct Macrophage-Lineage Expression in Zebrafish. *Blood*, *117*(4), e49–e56. https://doi.org/10.1182/blood-2010-10-314120

Enoiu, M., Jiricny, J., & Scha, O. D. (2012). Repair of cisplatin-induced DNA interstrand crosslinks by a replication-independent pathway involving transcription-coupled repair and translesion synthesis. *Nucleic Acids Research*, *40*(18), 8953–8964. https://doi.org/10.1093/nar/gks670

Erdlenbruch, B., Pekrun, A., Roth, C., Grunewald, R. W., Kern, W., & Lakomek, M. (2001). Cisplatin nephrotoxicity in children after continuous 72-h and 3X1-h infusions. *Pediatric Nephrology*, *16*(7), 586–593. https://doi.org/10.1007/s004670100610

Eskes, R., Antonsson, B., Osen-sand, A., Montessuit, S., Richter, C., Sadoul, R., … Martinou, J. (1998). Bax-induced Cytochrome C Release from Mitochondria Is Independent of the Permeability Transition Pore but Highly Dependent on Mg 2. *The Journal of Cell Biology*, *143*(1), 217–224.

Esterberg, R., Hailey, D. W., Coffin, A. B., Raible, D. W., & Rubel, E. W. (2013). Disruption of Intracellular Calcium Regulation Is Integral to Aminoglycoside-Induced Hair Cell Death. *The Journal of Neuroscience*, *33*(17), 7513–7525. https://doi.org/10.1523/JNEUROSCI.4559-12.2013

Esterberg, R., Hailey, D. W., Rubel, E. W., & Raible, D. W. (2014). ER–Mitochondrial Calcium Flow Underlies Vulnerability of Mechanosensory Hair Cells to Damage. *The Journal of Neuroscience*, *34*(29), 9703–9719. https://doi.org/10.1523/JNEUROSCI.0281-14.2014

Esterberg, R., Linbo, T., Pickett, S. B., Wu, P., Ou, H. C., Rubel, E. W., & Raible, D. W. (2016). Mitochondrial calcium uptake underlies ROS generation during aminoglycoside-induced hair cell death. *The Journal of Clinical Investigation*, *126*(9). https://doi.org/10.1172/JCI84939DS1

Fay, R. R., & Popper, A. N. (1999). Comparative hearing: Fish and amphibians. In R. R. Fay & A. N. Popper (Eds.), *Springer Handbook of Auditory Research*. New York: Springer.

Felder, R. A., & Jose, P. A. (2006). Mechanisms of Disease: the role of GRK4 in the etiology of essential hypertension and salt sensitivity. *Nature Clinical Practice Nephrology*, *2*(11), 637–650. https://doi.org/10.1038/ncpneph0301

Feng, Y., & Xu, Q. (2010). Pivotal role of hmx2 and hmx3 in zebrafish inner ear and lateral line development. *Developmental Biology*, *339*(2), 507–518. https://doi.org/10.1016/j.ydbio.2009.12.028

Feo, C. J. De, Aller, Æ. S. G., & Unger, V. M. (2007). A structural perspective on copper uptake in eukaryotes, 705–716. https://doi.org/10.1007/s10534-006-9054-7

Ferenbach, D. A., & Bonventre, J. V. (2017). Actue kidney injury and chronic kidney disease: from the laboratory to the clinic. *Nephrol Ther*, *12*, S41–S48. https://doi.org/10.1016/j.nephro.2016.02.005.Acute

Fichtinger-Schepman, A. M. J., Van der Veer, J. L., Den Hartog, J. H. J., Lohman, P. H. M., & Reedijk, J. (1985). Adducts of the antitumor drug cis-diamminedichloroplatinum(II) with DNA: formation, identification, and quantitation. *Biochemistry*, *24*(3), 707–713. https://doi.org/10.1021/bi00324a025

Filipski, K. K., Loos, W. J., Verweij, J., & Sparreboom, A. (2008). Interaction of Cisplatin with the Human Organic Cation Transporter 2. *Clinical Cancer Research*, *14*(12), 3875–3881. https://doi.org/10.1158/1078-0432.CCR-07-4793

Filipski, K. K., Mathijssen, R. H., Mikkelsen, T. S., Schinkel, A. H., & Sparreboom, A. (2009). Contribution of organic cation transporter 2 (OCT2) to cisplatin-induced nephrotoxicity. *Clin Pharmacol Ther*, *86*(4), 396–402. https://doi.org/10.1038/clpt.2009.139.Contribution

Finkel, M., Goldstein, A., Steinberg, Y., Granowetter, L., & Trachtman, H. (2014). Cisplatinum nephrotoxicity in oncology therapeutics: retrospective review of patients treated between 2005 and 2012. *Pediatric Nephrology*, *29*, 2421–2424. https://doi.org/10.1007/s00467-014-2935-z

Fontaine, R., Affaticati, P., Yamamoto, K., Jolly, C., Bureau, C., Baloche, S., … Pasqualini, C. (2013). Dopamine Inhibits Reproduction in Female Zebrafish (Danio rerio) via Three Pituitary D2 Receptor Subtypes. *Neuroendocrinology*, *154*(2), 807–818. https://doi.org/10.1210/en.2012-1759

Fouladi, M., Chintagumpala, M., Ashley, D., Kellie, S., Gururangan, S., Hassall, T., … Gajjar, A. (2018). Amifostine Protects Against Cisplatin-Induced Ototoxicity in Children With Average-Risk Medulloblastoma. *Journal of Clinical Oncology*, *26*(22), 3749–3755. https://doi.org/10.1200/JCO.2007.14.3974

Freyer, D. R., Chen, L., Krailo, M. D., Knight, K., Villaluna, D., Bliss, B., … Sung, L. (2017). Effects of sodium thiosulfate versus observation on development of cisplatin-induced hearing loss in children with cancer (ACCL0431): a multicentre, randomised, controlled, open-label, phase 3 trial. *The Lancet Oncology*, *18*(1), 63–74. https://doi.org/10.1016/S1470-2045(16)30625-8

Frydas, S., Papazahariadou, M., Papaioannou, N., Hatzistilianou, M., Trakatellis, M., Merlittp, D., … Grilli, A. (2003). Effect of the compound L-mimosine in an in vivp model of chronic granuloma formation induced by potassium permanganate (KMNO4). *International Journal of Immunopathology and Pharmacology*, *16*(2), 99–104. https://doi.org/10.1177/039463200301600202

Fuertes, M. A., Castilla, J., & Pérez, C. A. and J. M. (2003). Cisplatin Biochemical Mechanism of Action: From Cytotoxicity to Induction of Cell Death Through Interconnections Between Apoptotic and Necrotic Pathways. *Current Medicinal Chemistry*. https://doi.org/http://dx.doi.org/10.2174/0929867033368484

Furstenwerth, H. (2010). Ouabain – the insulin of the heart. *The International Journal of Clinical Practice*, *64*(November), 1591–1594. https://doi.org/10.1111/j.1742-1241.2010.02395.x

Furuta, T., Ueda, T., Aune, G., Sarasin, A., Kraemer, K. H., & Pommier, Y. (2002). Transcription-coupled Nucleotide Excision Repair as a Determinant of Cisplatin Sensitivity of Human Cells 1. *Cancer Research*, *62*, 4899–4902.

Gallegos-Castorena, S., Martínez-Avalos, A., Mohar-Betancourt, A., Guerrero-Avendaño, G., Zapata-Tarres, M., & Medina-Sanson, A. (2007). Toxicity prevention with amifostine in pediatric osteosarcoma patients treated with cisplatin and doxorubicin. *Pediatric Hematology and Oncology*, *24*, 403–408. https://doi.org/10.1080/08880010701451244

Ganesan, P., Schmiedge, J., Manchaiah, V., Swapna, S., Dhandayutham, S., & Kothandaraman, P. P. (2018). Ototoxicity: A Challenge in Diagnosis and Treatment. *J Audiol Otol*, *22*(2), 59–68.

Gao, H., Zhang, S., Hu, T., Qu, X., Zhai, J., Zhang, Y., … Song, Y. (2019). Chemico-Biological Interactions Omeprazole protects against cisplatin-induced nephrotoxicity by alleviating oxidative stress , inflammation, and transporter-mediated cisplatin accumulation in rats and HK-2 cells. *Chemico-Biological Interactions*, *297*(November 2018), 130–140. https://doi.org/10.1016/j.cbi.2018.11.008

Gaulton, A., Hersey, A., Nowotka, M., Bento, P., Chambers, J., Mendez, D., … Smit, I. (2017). The ChEMBL database in 2017. *Nucl*, *45*, 945–954. https://doi.org/10.1093/nar/gkw1074

Gerlach, G. F., Schrader, L. N., & Wingert, R. A. (2011). Dissection of the Adult Zebrafish Kidney. *Journal of Visualized Experiments*, *54*, e2839. https://doi.org/10.3791/2839

Ghosh, M., & Brandyopadhyay, S. (2007). Mimosine toxicity - A problem of Leucaena feeding in ruminants. *Asian Journal of Animal and Vertinary Advances*, *2*, 63–73.

Ghysen, A., & Dambly-Chaudière, C. (2007). The lateral line microcosmos. *Genes & Development*, *21*, 2118–2130. https://doi.org/10.1101/gad.1568407

Giacchetti, S., Perpoint, B., Zidani, R., Le Bail, N., Faggiuolo, R., Focan, C., … Lévi, F. (2000). Phase III Multicenter Randomized Trial of Oxaliplatin Added to Chronomodulated Fluorouracil–Leucovorin as First-Line Treatment of Metastatic Colorectal Cancer. *Journal of Clinical Oncology*, *18*(1), 136. https://doi.org/10.1200/JCO.2000.18.1.136

Gibalová, L., Šereš, M., Rusnák, A., Ditte, P., Labudová, M., Uhrík, B., … Sulová, Z. (2012). Toxicology in Vitro P-glycoprotein depresses cisplatin sensitivity in L1210 cells by inhibiting cisplatin-induced caspase-3 activation. *Toxicology in Vitro*, *26*, 435–444. https://doi.org/10.1016/j.tiv.2012.01.014

Gildea, J. J., Shah, I., Weiss, R., Casscells, N. D., McGrath, H. E., Zhang, J., & Felder, R. A. (2010). The HK-2 human renal proximal tubule cell as a model for GRK4-mediated dopamine-1 receptor uncoupling. *Hypertension*, *56*(3), 505–511. https://doi.org/10.1161/HYPERTENSIONAHA.110.152256.The

Gillies, M. A., Kakar, V., Parker, R. J., Honoré, P. M., & Ostermann, M. (2015). Fenoldopam to prevent acute kidney injury after major surgery — a systematic review and meta-analysis. *Critical Care*, *19*, 449. https://doi.org/10.1186/s13054-015-1166-4

Gingrich, J. A., & Caron, M. G. (1993). Recent Advances in the Molecular Biology of Dopamine Receptors. *Annual Review of Neuroscience*, *16*(1), 299–321. https://doi.org/10.1146/annurev.ne.16.030193.001503

Giorgi, C., Baldassari, F., Bononi, A., Bonora, M., Marchi, E. De, Marchi, S., … Pinton, P. (2012). Cell Calcium Mitochondrial Ca2+ and apoptosis. *Cell Calcium*, *52*(1), 36–43. https://doi.org/10.1016/j.ceca.2012.02.008

Gittelman, J. X., Perkel, D. J., & Portfors, C. V. (2013). Dopamine modulates auditory responses in the inferior colliculus in a heterogeneous manner. *JARO - Journal of the Association for Research in Otolaryngology*, *14*(5), 719–729. https://doi.org/10.1007/s10162-013-0405-0

Go, R. S., & Adjei, A. A. (1999). Review of the comparative pharmacology and clinical activity of cisplatin and carboplatin. *Journal of Clinical Oncology*, *17*(1), 409–422.

Goldberg, R. M., Sargent, D. J., Morton, R. F., Fuchs, C. S., Ramanathan, R. K., Williamson, S. K., … Alberts, S. R. (2004). A Randomized Controlled Trial of Fluorouracil Plus Leucovorin, Irinotecan, and Oxaliplatin Combinations in Patients With Previously Untreated Metastatic Colorectal Cancer. *Journal of Clinical Oncology*, *22*(1), 23–30. https://doi.org/10.1200/JCO.2004.09.046

Gompel, N., Cubedo, N., Thisse, C., Thisse, B., & Dambly-Chaudie, C. (2001). Pattern formation in the lateral line of zebrafish. *Mechanisms of Development*, *105*, 69–77.

Goncalve, M. S., Silveira, A. F., Teixeira, A. R., & Hyppolito, M. A. (2013). Mechanisms of cisplatin ototoxicity: theoretical review. *The Journal of Laryngology & Otology*, *127*, 536–541. https://doi.org/10.1017/S0022215113000947

Gonzales-Vitale, J., Hayes, D., Cvitkovic, E., & Sternberg, S. (1977). The renal pathology in clinical trials of cis-platinum(II)diamminedichloride. *Cancer*, *39*, 1362–1371.

Green, J. L., Reynolds, K. M., & Albert, D. (2013). Oral and Intravenous Acetylcysteine for Treatment of Acetaminophen Toxicity: A Systematic Review and Meta-analysis. *Western Journal of Emergency Medicine*, *14*(3), 218–226. https://doi.org/10.5811/westjem.2012.4.6885

Gstraunthaler, G., Pfaller, W., & Kotanko, P. (1985). Biochemical characterization of renal epithelial cell cultures (LLC-PK1 and MDCK). *American Journal of Physiology-Renal Physiology*, *248*(4), F536–F544. https://doi.org/10.1152/ajprenal.1985.248.4.F536

Gullo, J. J., Litterst, C. L., Maguire, P. J., Sikic, B. I., Hoth, D. F., & Woolley, P. V. (1980). Pharmacokinetics and protein binding of cis-dichlorodiammine platinum (II) administered as a one hour or as a twenty hour infusion. *Cancer Chemotherapy and Pharmacology*, *5*, 21–26.

Guo, Q., Lan, F. E. I., Yan, X. U., Xiao, Z. H. U., Wu, Y., & Zhang, Q. I. N. (2018). Hypoxia exposure induced cisplatin resistance partially via activating p53 and hypoxia inducible factor-1 α in non-small cell lung cancer A549 cells. *Oncology Letters*, *16*, 801–808. https://doi.org/10.3892/ol.2018.8767

Haddad, F., Sawalha, M., Khawaja, Y., Najjar, A., & Karaman, R. (2018). Dopamine and Levodopa Prodrugs for the Treatment of Parkinson's Disease. *Molecules*, *23*, 40. https://doi.org/10.3390/molecules23010040

Haddon, C., & Lewis, J. (1996). Early Ear Development in the Embryo of the Zebrafish, Danio rerio. *The Journal of Comparative Neurology*, *125*, 113–125.

Hagleitner, M. M., Coenen, M. J. H., Patino-Garcia, A., De Bont, E. S. J. M., Gonzalez-Neira, A., Vos, H. I., … Te Loo, M. W. M. (2014). Influence of genetic variants in TPMT and COMT associated with cisplatin induced hearing loss in patients with cancer: Two new cohorts and a meta-analysis reveal significant heterogeneity between cohorts. *PLoS ONE*, *9*(12), 1–13. https://doi.org/10.1371/journal.pone.0115869

Haldi, M., Ton, C., Seng, W. L., & McGrath, P. (2006). Human melanoma cells transplanted into zebrafish proliferate, migrate, produce melanin, form masses and stimulate angiogenesis in zebrafish. *Angiogenesis*, *9*(3), 139–151. https://doi.org/10.1007/s10456-006-9040-2

Hammond, K. L., & Whitfield, T. T. (2006). The developing lamprey ear closely resembles the zebrafish otic vesicle: otx1 expression can account for all major patterning differences. *Development*, *133*, 1347–1357. https://doi.org/10.1242/dev.02306

Hans, B., Hans, S. S., Mittal, V. K., Khan, T. A., Patel, N., & Dahn, M. S. (1990). Renal functional response to dopamine during and after arteriography in patients with chronic renal insufficiency. *Radiology*, *176*(3), 651–654. https://doi.org/10.1148/radiology.176.3.2202010

Harned, T. M., Kalous, O., Neuwelt, A., Loera, J., Ji, L., Iovine, P., … Reynolds, C. P. (2008). Sodium Thiosulfate Administered Six Hours after Cisplatin Does Not Compromise Antineuroblastoma Activity. *Clinical Cancer Research*, *14*(2), 533–541. https://doi.org/10.1158/1078-0432.CCR-06-2289

Harris, J. A., Cheng, A. G., Cunningham, L. L., MacDonald, G., Raible, D. W., & Rubel, E. W. (2003). Neomycin-Induced Hair Cell Death and Rapid Regeneration in the Lateral Line of Zebrafish (Danio rerio). *Journal of the Association for Research in Otolaryngology*, *234*, 219–234. https://doi.org/10.1007/s10162-002-3022-x

Harris, R. C., & Zhang, M. (2012). Dopamine, the Kidney, and Hypertension. *Curr Hypertens Rep*, *14*, 138–143. https://doi.org/10.1007/s11906-012-0253-z

Hashiguch, H., & Takahashi, H. (1976). Inhibition of Two Copper-Containing Enzymes, Tyrosinase and Dopamine Beta-hyrdoxylase by L-Mimosine. *Molecular Pharmacology*, *13*, 362–367.

Hassan, S. M., Khalaf, M. M., Sadek, S. A., & Abo-youssef, A. M. (2017). Protective effects of apigenin and myricetin against cisplatin-induced nephrotoxicity in mice. *Pharmaceutical Biology*, *55*(1), 766–774. https://doi.org/10.1080/13880209.2016.1275704

Haura, E. B., Ricart, A. D., Larson, T. G., Stella, P. J., Bazhenova, L., Miller, V. A., … Gadgeel, S. M. (2010). A Phase II Study of PD-0325901 , an Oral MEK Inhibitor, in Previously Treated Patients with Advanced Non–Small Cell Lung Cancer. *Clinical Cancer Research*, *16*(8), 2450–2458. https://doi.org/10.1158/1078-0432.CCR-09-1920

Hentschel, D. M., Park, K. M., Cilenti, L., Zervos, A. S., Drummond, I., Bonventre, J. V, … Antonis, S. (2005). Acute renal failure in zebrafish: a novel system to study a complex disease. *Am J Physiol Renal Physiol*, *288*, 923–929. https://doi.org/10.1152/ajprenal.00386.2004.

Herman, F., Kozelka, J., Stoven, V., Guittet, E., Girault, J., Huynh-dinh, T., … Chottard, J. (1990). A d(GpG)-platinated decanucleotide duplex is kinked An extended NMR and molecular mechanics study. *Eur J Biochem*, *194*, 119–133.

Higby, J., & Wallace, H. J. (1974). Diaminodichloroplatinum: a phase I study showing responses in testicular and other tumors. *Cancer*, *33*(May), 1219–1225.

Higgs, D. M., Rollo, A. K., Souza, M. J., & Popper, A. N. (2003). Development of form and function in peripheral auditory structures of the zebrafish (Danio rerio). *The Journal of the Acoustical Society of America*, *113*(2), 1145–1154. https://doi.org/10.1121/1.1536185

Hilder, T. A., & Hill, J. M. (2007). Modelling the encapsulation of the anticancer drug cisplatin into carbon nanotubes. *Nanotechnology*, *18*(27), 275704. https://doi.org/10.1088/0957-4484/18/27/275704

Hill, P., Shukla, D., Tran, M. G. B., Aragones, J., Cook, H. T., Carmeliet, P., & Maxwell, P. H. (2008). Inhibition of Hypoxia Inducible Factor Hydroxylases Protects Against Renal Ischemia-Reperfusion Injury. *J Am Soc Nephrol*, *19*, 39–46. https://doi.org/10.1681/ASN.2006090998

Hirama, M., Isonishi, S., Yasuda, M., & Ishikawa, H. (2006). Characterization of mitochondria in cisplatin- resistant human ovarian carcinoma cells. *Oncology Reports*, *16*, 997–1002.

Holzer, A. K., Samimi, G., Katano, K., Naerdemann, W., Lin, X., Safaei, R., & Howell, S. B. (2004). The Copper Influx Transporter Human Copper Transport Protein 1 Regulates the Uptake of Cisplatin in Human Ovarian Carcinoma Cells. *Molecular Pharmacology*, *66*(4), 817 LP – 823. https://doi.org/10.1124/mol.104.001198

Ishida, S., Lee, J., Thiele, D. J., & Herskowitz, I. (2002). Uptake of the anticancer drug cisplatin mediated by the copper transporter Ctr1 in yeast and mammals. *PNAS*, *99*(22).

Ivy, K. D., & Kaplan, J. H. (2013). A Re-Evaluation of the Role of hCTR1 , the Human High-Affinity Copper Transporter , in Platinum-Drug Entry into Human Cells. *Molecular Pharmacology*, *83*(June), 1237–1246.

Jan, M., Reddy, A., Miller, T. O. M., Hendricks, J. D., & Bailey, G. S. (2000). Neoplasia in Zebrafish (Danio rerio) Treated with N-methyl-N-nitrosoguanidine by Three Exposure Routes at ifferent Developmental Stages. *Toxicologic Pathology*, *28*(5), 716–725.

Jat, P. S., Noble, M. D., Ataliotis, P., Tanakat, Y., Yannoutsost, N., Larsent, L., & Kioussist, D. (1991). Direct derivation of conditionally immortal cell lines from an H-2Kb-tsA58 transgenic mouse. *Proc Natl Acad Sci*, *88*(June), 5096–5100.

Jeong, M., Reilly, M. O., Kirkwood, N. K., Al-aama, J., Lako, M., & Armstrong, L. (2018). Generating inner ear organoids containing putative cochlear hair cells from human pluripotent stem cells. *Cell Death and Disease*, *9*, 922. https://doi.org/10.1038/s41419-018-0967-1

Jones, C. A., McQuillan, G. M., Kusek, J. W., Eberhardt, M. S., Herman, W. H., Coresh, J., … Agodoa, L. Y. (1998). Serum creatinine levels in the US population: third National Health and Nutrition Examination Survey. *American Journal of Kidney Diseases : The Official Journal of the National Kidney Foundation*, *32*(6), 992–999. https://doi.org/10.1016/s0272-6386(98)70074-5

Jonge, M. J. A. De, & Verweij, J. (2006). Renal Toxicities of Chemotherapy. *Seminars in Oncology*, *33*, 68–73. https://doi.org/10.1053/j.seminoncol.2005.11.011

Jose, A., Carey, M., Raymond, R., Bates, D., & Felder, A. (1992). The renal dopamine receptors. *J Am Soc Nephrol*, *2*, 1265–1278.

Ju, S. M., Kang, J. G., Bae, J. S., Pae, H. O., Lyu, Y. S., & Jeon, B. H. (2015). The Flavonoid Apigenin Ameliorates Cisplatin-Induced Nephrotoxicity through Reduction of p53 Activation and Promotion of PI3K / Akt Pathway in Human Renal Proximal Tubular Epithelial Cells. *Evidence-Based Complimentary and Alternative Medicine*, (186436).

Kadikoylu, G., Bolaman, Z., Demir, S., Balkaya, M., Akalin, N., & Enli, Y. (2004). The Effects of Desferrioxamine on Cisplatin-Induced Lipid Peroxidation and the Activities of Antioxidant Enzymes in Rat Kidneys. *Human and Experimental Toxicology*, *23*(1), 29–34. https://doi.org/10.1191/0960327104ht413oa

Kalayda, G. V, Wagner, C. H., Buß, I., Reedijk, J., & Jaehde, U. (2008). Altered localisation of the copper efflux transporters ATP7A and ATP7B associated with cisplatin resistance in human ovarian carcinoma cells. *BMC Cancer*, 175. https://doi.org/10.1186/1471-2407-8-175

Kalinec, G. M., Webster, P., Lim, D. J., & Kalinec, F. (2003). A cochlear cell line as an in vitro system for drug ototoxicity screening. *Audiology and Neuro-Otology*, *8*(4), 177–189. https://doi.org/10.1159/000071059

Kardasz, S. (2012). The function of the nephron and the formation of urine. *Anaesthesia and Intensive Care Medicine*, *13*(7), 309–314. https://doi.org/10.1016/j.mpaic.2012.04.008

Katzenstein, H., Change, K., Krailo, M., Finegold, M., Rowland, J., Reyonolds, M., … Group, C. O. (2009). Amifostine does not prevent platinum-induced hearing loss associated with the treatment of children with hepatoblastoma. A report of the Intergroup Hepatoblastoma Study P9645 as a part of the Children's Oncology Group. *Cancer*, *155*(24), 5828–5835. https://doi.org/10.1002/cncr.24667.Amifostine

Kauffman, G. B. (2010). Michele Peyrone (1813 – 1883), Discoverer of Cisplatin. *Platinum Metals Rev*, *54*(4), 250–256. https://doi.org/10.1595/147106710X534326

Kelland, L. (2007). The resurgence of platinum-based cancer chemotherapy. *Nature Reviews Cancer*, *7*(8), 573–584. https://doi.org/10.1038/nrc2167

Kellum, J. A. (1997). Systematic review: The use of diuretics and dopamine in acute renal failure: a systematic review of the evidence. *Critical Care*, *1*, 53.

Khorevin, V. I. (2008). The Lagena (the Third Otolith Endorgan in Vertebrates). *Neurophysiology*, *40*(2), 142–159.

Kimmel, C. B., Ballard, W. W., Kimmel, S. R., Ullmann, B., & Schilling, T. F. (1995). Stages of Embryonic Development of the Zebrafish. *Developmental Dynamics*, *203*, 253–310.

Kischkel, F. C., Hellbardt, S., Behrmann, I., Germer, M., Pawlita, M., Krammer, P. H., & Peter, M. E. (1995). Cytotoxicity-dependent APO-1 (Fas/CD95)- associated proteins form a death-inducing signaling complex (DISC) with the receptor. *The EMBO Journal*, *14*(22), 5579–5588.

Kitcher, S. R., Kirkwood, N. K., Camci, E. D., Wu, P., Gibson, R. M., Redila, V. A., … Kros, C. J. (2019). ORC-13661 protects sensory hair cells from aminoglycoside and cisplatin ototoxicity. *JCI Insight*, *4*(15), 1–19.

Knight, K. R., Kraemer, D. P., Winter, C., & Neuwelt, E. A. (2007). Early changes in auditory function as a result of platinum chemotherapy: Use of extended high-frequency audiometry and evoked distortion product otoacoustic emissions. *Journal of Clinical Oncology*, *25*(10), 1190–1195. https://doi.org/10.1200/JCO.2006.07.9723

Knight, Kraemer, D. F., & Neuwelt, E. A. (2005). Ototoxicity in children receiving platinum chemotherapy: Underestimating a commonly occurring toxicity that may influence academic and social development. *J. Clin. Oncol.*, *23*, 8588–8596.

Knox, R. J., Friedlos, F., Lydall, D. A., & Roberts, J. J. (1986). Mechanism of Cytotoxicity of Anticancer Platinum Drugs: Evidence that cis-Diamminedichloroplatinum(II) and cis-Diammine-(1,1-cyclobutanedicarboxylato)platinum(II) Differ Only in the Kinetics of Their Interaction with DNA. *Cancer Research*, *46*, 1972–1979.

Kociba, R. J., & Sleight, S. D. (1971). Acute toxicologic and pathologic effects of cis-diamminedichloroplatinum (NSC-119875) in the male rat. *Cancer Chemotherapy Reports*, *55*(1), 1–8.

Koehler, K. R., Nie, J., Longworth-mills, E., Liu, X., Lee, J., Holt, J. R., & Hashino, E. (2017). Generation of inner ear organoids containing functional hair cells from human pluripotent stem cells. *Nature Biotechnology*, *35*(6). https://doi.org/10.1038/nbt.3840

Kolinsky, D. C., Hayashi, S. S., Karzon, R., Mao, J., & Hayashi, R. J. (2010). Late onset hearing loss: A Significant complication of cancer survivors treated with cisplatin containing chemotherapy regimens. *Journal of Pediatric Hematology/Oncology*, *32*(2), 119–123. https://doi.org/10.1097/MPH.0b013e3181cb8593

Komatsu, M., Sumizawa, T., Mutoh, M., Chen, Z., Terada, K., Furukawa, T., … Akiyama, S. (2000). Copper-transporting P-Type Adenosine Triphosphatase (ATP7B) Is Associated with Cisplatin Resistance. *Cancer Research*, *60*, 1312–1316.

Kopelman, J., Budnick, A. S., Sessions, R. B., Kramer, M. B., & Wong, G. Y. (1988). Ototoxicity of high-dose cisplatin by bolus administration in patients with advanced cancers and normal hearing. *Laryngoscope*, *98*, 858–864.

Kopke, R., Liu, W., Gabaizadeh, R., Jacono, A., Feghali, J., Spray, D., … Van De Walter, T. (1997). Use of organotropic cultures of Corti's Organ to study the protective effects of antioxidant molecules on cisplatin-induced damage of auditory hair cells. *The American Journal of Otology*, *18*, 559–571.

Kouvaris, J., Kouloulias, V., & Vlahos, L. (2007). Amifostine: the first selective-target and broad-spectrum radioprotector. *The Oncologist*, *12*, 738–747. https://doi.org/10.1634/theoncologist.12-6-738

Kramer-Zucker, A. G., Olale, F., Haycraft, C. J., Yoder, B. K., Schier, A. F., & Drummond, I. A. (2005). Cilia-driven fluid flow in the zebrafish pronephros, brain and Kupffer's vesicle is required for normal organogenesis. *Development*, *132*(8), 1907–1921. https://doi.org/10.1242/dev.01772

Kramer-Zucker, A., Wiessner, S., Jensen, A., & Drummond, I. (2005). Organization of the pronephric filtration apparatus in zebrafish requires Nephrin, Podocin and the FERM domain protein Moasic eyes. *Developmental Biology*, *285*(2), 316–329. https://doi.org/10.1016/j.ydbio.2005.06.038.Organization

Krefeld, B., Dinnesen, A. G., Deuster, D., Seifert, E., Jaehde, U., Pieck, A. C., & Boos, J. (2006). Continuous or Repeated Prolonged Cisplatin Infusions in Children: A Prospective Study on Ototoxicity , Platinum Concentrations , and Standard Serum Parameters. *Pediatr Blood Cancer*, *47*(March 2005), 183–193. https://doi.org/10.1002/pbc

Krejci, L., Altmannova, V., Spirek, M., & Zhao, X. (2012). Homologous recombination and its regulation. *Nucleic Acids Research*, *40*(13), 5795–5818. https://doi.org/10.1093/nar/gks270

Kroning, R., Lichtenstein, A., & Nagami, G. (2000). Sulfur-containing amino acids decrease cisplatin cytotoxicity and uptake in renal tubule epithelial cell lines. *Cancer Chemotherapy and Pharmacology*, *45*, 43–49.

Kuhlmann, M. K., Burkhardt, G., & Ko, H. (1997). Insights into potential cellular mechanisms of cisplatin nephrotoxicity and their clinical application. *Nephrology Dialysis Transplantation*, *12*, 2478–2480.

Kulp, K. S., & Vulliet, P. R. (1996). Mimosine Blocks Cell Cycle Progression by Chelating Iron in Asynchronous Human Breast Cancer Cells. *Toxicology and Applied Pharmacology*, *364*, 356–364.

Laat, W. L. De, Jaspers, N. G. J., & Hoeijmakers, J. H. J. (1999). Molecular mechanism of nucleotide excision repair. *Genes & Development*, *13*, 768–785.

Lai, Y., Lin, S., Wu, Y., Chen, H., & Chen, J. J. W. (2017). AC-93253 iodide a novel Src inhibitor, suppresses NSCLC progression by modulating multiple Src-related signaling pathways. *Journal of Hematology & Oncology*, *10*, 172. https://doi.org/10.1186/s13045-017-0539-3

Landier, W. (2016). Ototoxicity and cancer therapy. *Cancer*, *122*(11), 1647–1658. https://doi.org/10.1002/cncr.29779

Lange, S. S., Takata, K., & Wood, R. D. (2011). DNA polymerases and cancer. *Nature Reviews Cancer*, *11*(2), 96–110. https://doi.org/10.1038/nrc2998.DNA

Langenau, D. M., Traver, D., Ferrando, A. A., Kutok, J. L., Aster, J. C., Kanki, J. P., … Look, A. T. (2003). Myc-induced T cell leukemia in transgenic zebrafish. *Science*, *299*(5608), 887–890. https://doi.org/10.1126/science.1080280

Langer, T., Zehnhoff-dinnesen, A., Radtke, S., Meitert, J., & Zolk, O. (2013). Understanding platinum-induced ototoxicity. *Trends in Pharmacological Sciences*, *34*(8), 458–469. https://doi.org/10.1016/j.tips.2013.05.006

Latcha, S., Jaimes, E. A., Patil, S., Glezerman, I. G., Mehta, S., & Flombaum, C. D. (2016). Long–Term Renal Outcomes after Cisplatin Treatment. *Clinical Journal of the American Society of Nephrology*, *11*, 1173–1179. https://doi.org/10.2215/CJN.08070715

Lautermann, J., Song, B., Mclaren, J., & Schacht, J. (1995). Diet is a risk factor in cisplatin ototoxicity. *Hearing Research*, *88*, 47–53.

Lee, L. M. J., Seftor, E. a, Bonde, G., Cornell, R. a, & Hendrix, M. J. C. (2005). The fate of human malignant melanoma cells transplanted into zebrafish embryos: assessment of migration and cell division in the absence of tumor formation. *Developmental Dynamics : An Official Publication of the American Association of Anatomists*, *233*(4), 1560–1570. https://doi.org/10.1002/dvdy.20471

Lendvai, B., Halmos, G. B., Polony, G., Kapocsi, J., Horváth, T., Aller, M., … Zelles, T. (2011). Chemical neuroprotection in the cochlea: The modulation of dopamine release from lateral olivocochlear efferents. *Neurochemistry International*, *59*, 150–158. https://doi.org/10.1016/j.neuint.2011.05.015

Lewis, M. J., DuBois, S. G., Fligor, B., Li, X., Goorin, A., & Grier, H. E. (2009). Ototoxicity in Children Treated for Osteosarcoma. *Pediatric Blood & Cancer*, *52*, 387–391. https://doi.org/10.1002/pbc

Li, P., Shah, S., Huang, L., Carr, A. L., Gao, Y., Thisse, C., … Li, L. (2007). Cloning and Spatial and Temporal Expression of the Zebrafish Dopamine D1 Receptor. *Developmental Dynamics*, *236*, 1339–1346. https://doi.org/10.1002/dvdy.21130

Li, Y., Womer, R. B., & Silber, J. H. (2004). Predicting cisplatin ototoxicity in children: The influence of age and the cumulative dose. *European Journal of Cancer*, *40*(16), 2445–2451. https://doi.org/10.1016/j.ejca.2003.08.009

Lieschke, G. J., & Currie, P. D. (2007). Animal models of human disease: zebrafish swim into view. *Nature Reviews. Genetics*, *8*(5), 353–367. https://doi.org/10.1038/nrg2091

Lim, T. K. (2012). Leucaena leucocephala BT - Edible Medicinal And Non-Medicinal Plants: Volume 2, Fruits. In T. K. Lim (Ed.) (pp. 754–762). Dordrecht: Springer Netherlands. https://doi.org/10.1007/978-94-007-1764-0_86

Lim, T. K. (2014). Mimosa pudica BT - Edible Medicinal And Non-Medicinal Plants: Volume 7, Flowers. In T. K. Lim (Ed.) (pp. 821–835). Dordrecht: Springer Netherlands. https://doi.org/10.1007/978-94-007-7395-0_66

Lipinski, C A. (1995). *Computational alerts for potential absorption problems: profiles of clinically tested drugs. Part Two. Predicting HUman Absorption. Tools for Oral Absorption.* Miami.

Lipinski, Christopher A, Lombardo, F., Dominy, B. W., & Feeney, P. J. (2012). Experimental and computational approaches to estimate solubility and permeability in drug discovery and development settings i. *Advanced Drug Delivery Reviews*, *64*, 4–17. https://doi.org/10.1016/j.addr.2012.09.019

Liu, Y., Asnani, A., Zou, L., Bentley, V. L., Yu, M., Wang, Y., … Peterson, R. T. (2014). Visnagin protects against doxorubicin-induced cardiomyopathy through modulation of mitochondrial malate dehydrogenase. *Sci Transl Med*, *6*(266), 68–75. https://doi.org/10.1002/aur.1474.Replication

Lokich, J. (2001). What Is the “Best” Platinum: Cisplatin, Carboplatin, or Oxaliplatin? *Cancer Investigation*, *19*(7), 756–760. https://doi.org/10.1081/CNV-100106152

Lorito, G., Hatzopoulos, S., Laurell, G. G., Campbell, K. C. M., Petruccelli, J., Giordano, P., … Skarzynski, H. (2011). Dose-dependent protection on cisplatin-induced ototoxicity - an electrophysiological study on the effect of three antioxidants in the Sprague-Dawley rat animal model. *Medical Science Monitor*, *17*(8), BR179-R186. https://doi.org/881894 [pii]

Lorusso, D., Ferrandina, G., Greggi, S., Gadducci, A., Pignata, S., Tateo, S., … Scambia, G. (2003). Phase III multicenter randomized trial of amifostine as cytoprotectant in first-line chemotherapy in ovarian cancer patients. *Annals of Oncology*, *14*, 1086–1093. https://doi.org/10.1093/annonc/mdg301

Lou, X., Nakagawa, T., Ohnishi, H., Nishimura, K., & Ito, J. (2013). Otospheres derived from neonatal mouse cochleae retain the progenitor cell phenotype after ex vivo expansions. *Neuroscience Letters*, *534*, 18–23. https://doi.org/10.1016/j.neulet.2012.12.001

Ludwig, T., Riethmuller, C., Geckle, M., Schwerdt, G., & Oberleithner, H. (2004). Nephrotoxicity of platinum complexes is related to basolateral organic cation transport. *Kidney International*, *66*, 196–202. https://doi.org/10.1111/j.1523-1755.2004.00720.x

Lugassy, G., & Shapira, A. (1996). A prospective cohort study of the effect of vincristine on audition.pdf.

Maison, F., Liu, X., Eatock, R. A., Sibley, D. R., Grandy, D. K., & Liberman, M. C. (2012). Dopaminergic Signaling in the Cochlea: Receptor Expression Patterns and Deletion Phenotypes. *The Journal of Neuroscience*, *32*(1), 344–355. https://doi.org/10.1523/JNEUROSCI.4720-11.2012

Majumder, P., Duchen, M. R., & Gale, J. E. (2015). Cellular glutathione content in the organ of Corti and its role during ototoxicity. *Frontiers in Cellular Neuroscience*, *9*(April), 1–8. https://doi.org/10.3389/fncel.2015.00143

Mann, S. C., Andrews, P. A., & Howell, S. B. (1990). Short-term cis-diamminedichloroplatinum(II) accumulation in sensitive and resistant human ovarian carcinoma cells *. *Cancer Chemotherapy and Pharmacology*, *25*, 236–240.

Mann, Z. F., & Kelley, M. W. (2011). Development of tonotopy in the auditory periphery. *Hearing Research*, *276*(1–2), 2–15. https://doi.org/10.1016/j.heares.2011.01.011

Manohar, S., & Leung, N. (2018). Cisplatin nephrotoxicity: a review of the literature. *Journal of Nephrology*, *31*, 15–25. https://doi.org/10.1007/s40620-017-0392-z

Marteijn, J. A., Lans, H., Vermeulen, W., & Hoeijmakers, J. H. J. (2014). Understanding nucleotide excision repair and its roles in cancer and ageing. *Nature Reviews Molecular Cell Biology*, *15*(7), 465–481. https://doi.org/10.1038/nrm3822

Masuda, S., Terada, T., Yonezawa, A., Tanihara, Y., Kishimoto, K., Katsura, T., … Inui, K. (2006). Identification and Functional Characterization of a New Human Kidney-Specific H+/Organic Cation Antiporter, Kidney-Specific Multidrug and Toxin Extrusion 2. *J Am Soc Nephrol*, *17*, 2127–2135. https://doi.org/10.1681/ASN.2006030205

Matsui, J. I., Gale, J. E., & Warchol, M. E. (2004). Critical Signaling Events during the Aminoglycoside-Induced Death of Sensory Hair Cells In Vitro. *Journal of Neurobiology*, *1364*(July), 250–266. https://doi.org/10.1002/neu.20054

Mccaffrey, T. A., Pomerantz, K. B., Sanbom, T. A., Spokojny, A. M., Du, B., Park, M., … Hanauske-Abel, H. M. (1995). Specific Inhibition of elF-5A and Collagen Hydroxylation by a Single Agent. *J Clin Invest*, *95*, 446–455.

McCampbell, K. K., Springer, K. N., & Wingert, R. A. (2015). Atlas of Cellular Dynamics during Zebrafish Adult Kidney Regeneration. *Stem Cells International*.

Mcdermott, B. M., Asai, Y., Baucom, J. M., Jani, S. D., Castellanos, Y., Gomez, G., … Hudspeth, A. J. (2010). Gene Expression Patterns Transgenic labeling of hair cells in the zebrafish acousticolateralis system. *Gene Expression Patterns*, *10*(2–3), 113–118. https://doi.org/10.1016/j.gep.2010.01.001

McMahon, A. P. (2016). Development of the Mammalian Kidney. *Current Topics in Developmental Biology*, *117*, 31–64. https://doi.org/10.1016/bs.ctdb.2015.10.010.Development

Miki, Y., Swensen, J., Shattuck-Eidens, D., & Futreal, A. (1994). A strong candidate for the breast and ovarian cancer susceptibility gene BRCA1. *Science*, *266*(5182), 66–71.

Milan, D. J., Peterson, T. A., Ruskin, J. N., Peterson, R. T., & Macrae, C. A. (2003). Drugs That Induce Repolarization Abnormalities Cause Bradycardia in Zebrafish. *Circulation*, *107*, 1355–1358. https://doi.org/10.1161/01.CIR.0000061912.88753.87

Miller, R. P., Tadagavadi, R. K., Ramesh, G., & Reeves, W. B. (2010). Mechanisms of Cisplatin Nephrotoxicity. *Toxins*, *2*, 2490–2518. https://doi.org/10.3390/toxins2112490

Mills, C. C., Kolb, E. A., & Sampson, V. B. (2018). Development of Chemotherapy with Cell-Cycle Inhibitors for Adult and Pediatric Cancer Therapy. *Cancer Research*, *78*. https://doi.org/10.1158/0008-5472.CAN-17-2782

Missale, C., Nash, S. R., Robinson, S. W., Jaber, M., Caron, M. G., Nash, S. R., … Dopamine, M. G. C. (1998). Dopamine Receptors: From Structure to Function. *Physiological Reviews*, *78*(1), 189–225.

Mizuta, K., Saito, A., Watanabe, T., Nagura, M., Arakawa, M., Shimizu, F., & Hoshino, T. (1999). Ultrastructural localization of megalin in the rat cochlear duct. *Hearing Research*, *129*(1), 83–91. https://doi.org/https://doi.org/10.1016/S0378-5955(98)00221-4

Montgomery, J. C., Baker, C. F., & Carton, A. G. (1997). The lateral line can mediate rheotaxis in fish. *Nature*, *389*, 960–964.

Morgenstern, D. a, Baruchel, S., & Irwin, M. S. (2013). Current and future strategies for relapsed neuroblastoma: challenges on the road to precision therapy. *Journal of Pediatric Hematology/Oncology*, *35*(5), 337–347. https://doi.org/10.1097/MPH.0b013e318299d637

Mostad, A., Romming, C., & Rosenqvist, E. (1973). The structure of L-mimosine, an L-DOPA analogue. *Acta Chemica Scandinavica*, *27*(1), 164–176.

Moynahan, M. E., Chiu, J. W., Koller, B. H., Jasin, M., Hill, C., & Carolina, N. (1999). Brca1 Controls Homology-Directed DNA Repair. *Molecular Cell*, *4*, 511–518.

Moynahan, M. E., Pierce, A. J., & Jasin, M. (2001). BRCA2 Is Required for Homology-Directed Repair of Chromosomal Breaks. *Molecular Cell*, *7*, 263–272.

Mukherjea, D, & Rybak, L. (2011). Pharmacogenomics of cisplatin-induced ototoxicity. *Pharmacogenomics*, *12*(7), 1039–1050. https://doi.org/10.2217/pgs.11.48.Pharmacogenomics

Mukherjea, D, Whitworth, C. A., & Nandish, S. (2006). Expression of the kidney injury molecule 1 in the rat cochlea and induction by cisplatin. *Neuroscience*, *139*, 733–740. https://doi.org/10.1016/j.neuroscience.2005.12.044

Mukherjea, Debashree, Jajoo, S., Kaur, T., Sheehan, K., Ramkumar, V., & Rybak, L. P. (2010). Transtympanic Administration of Short Interfering (si) RNA for the NOX3 Isoform of NADPH Oxidase Protects Against Cisplatin-Induced Hearing Loss in the Rat. *Antioxidants & Redox Signaling*, *13*(5), 589–598. https://doi.org/10.1089/ars.2010.3110

Muldoon, L. L., Pagel, M. A., Kroll, R. A., Brummett, R. E., Doolittle, N. D., Zuhowski, E. G., … Neuwelt, E. A. (2000). Delayed administration of sodium thiosulfate in animal models reduces platinum ototoxicity without reduction of antitumor activity. *Clinical Cancer Research*, *6*(1), 309–315.

Muldoon, L., Wu, J., Pagel, M., & Neuwelt, E. (2015). N-acetylcysteine chemoprotection without decreased cisplatin antitumor efficacy in pediatric tumor models. *J Neurooncol*, *121*(3), 433–440. https://doi.org/10.1007/s11060-014-1657-1.N-acetylcysteine

Muller, H.-D., Cvikl, B., Janji, K., Moritz, A., Gruber, R., Sylvia, N., & Agis, H. (2015). Effects of Prolyl Hydroxylase Inhibitor L-mimosine on Dental Pulp in the Presence of Advanced Glycation End Products. *Journal of Endodontics*, *41*(11). https://doi.org/10.1016/j.joen.2015.08.002

Muñoz, K., Olson, W. A., Twohig, M. P., Preston, E., Blaiser, K., & White, K. R. (2015). Pediatric Hearing Aid Use: Parent-Reported Challenges. *Ear & Hearing*, *36*, 279–287.

Nakamura, T., Yonezawa, A., Hashimoto, S., Katsura, T., & Inui, K. (2010). Disruption of multidrug and toxin extrusion MATE1 potentiates cisplatin-induced nephrotoxicity. *Biochemical Pharmacology*, *80*(11), 1762–1767. https://doi.org/10.1016/j.bcp.2010.08.019

Neuwelt, E. a, Pagel, M. a, Kraemer, D. F., Peterson, D. R., & Muldoon, L. L. (2004). Bone marrow chemoprotection without compromise of chemotherapy efficacy in a rat brain tumor model. *The Journal of Pharmacology and Experimental Therapeutics*, *309*(2), 594–599. https://doi.org/10.1124/jpet.103.063347

Nho, J., Jung, H., Lee, M., Jang, J., Sim, M., Jeong, D., … Kim, J. (2018). Beneficial Effects of Cynaroside on Cisplatin-Induced Kidney Injury In Vitro and In Vivo. *Toxicological Research*, *34*(2), 133–141.

Noonan, H. R., Metelo, A. M., Kamei, C. N., Peterson, R. T., Drummond, I. A., & Iliopoulos, O. (2016). Loss of *vhl* in the zebrafish pronephros recapitulates early stages of human clear cell renal cell carcinoma. *Disease Models & Mechanisms*, *9*(8), 873–884. https://doi.org/10.1242/dmm.024380

Nouvian, Â., Gervais, C., Pujol, Â., Eybalin, M., & Puel, J. (2001). Dopamine inhibition of auditory nerve activity in the adult mammalian cochlea. *European Journal of Neuroscience*, *14*, 977–986.

Nunez, G., Benedict, M. A., Hu, Y., & Inohara, N. (1998). Caspases: the proteases of the apoptotic pathway. *Oncogene*, *17*, 3237–3245.

O'Brien, V., & Brown, R. (2006). Signalling cell cycle arrest and cell death through the MMR System. *Carcinogenesis*, *27*(4), 682–692. https://doi.org/10.1093/carcin/bgi298

O'Dwyer, P. J., Stevenson, J. P., & Johnson, S. W. (2000). Clinical Pharmacokinetics and Administration of Established Platinum Drugs. *Drugs*, *59*(4), 19–27. https://doi.org/10.2165/00003495-200059004-00003

Obholzer, N., Wolfson, S., Trapani, J. G., Mo, W., Nechiporuk, A., Busch-nentwich, E., … Nicolson, T. (2008). Vesicular Glutamate Transporter 3 Is Required for Synaptic Transmission in Zebrafish Hair Cells. *The Journal of Neuroscience*, *28*(9), 2110–2118. https://doi.org/10.1523/JNEUROSCI.5230-07.2008

Oestreicher, E., Arnold, W., Ehrenberger, K., & Felix, D. (1997). Dopamine regulates the glutamatergic inner hair cell activity in guinea pigs. *Hearing Research*, *107*(1), 46–52. https://doi.org/https://doi.org/10.1016/S0378-5955(97)00023-3

Ohinata, Y., Yamasoba, T., Schacht, J., & Miller, J. M. (2000). Glutathione limits noise-induced hearing loss. *Hearing Research*, *146*, 28–34.

Olive, P. L., & Banath, J. P. (2009). Kinetics of H2AX Phosphorylation After Exposure to Cisplatin. *Clinical Cytometry*, *76B*, 79–90. https://doi.org/10.1002/cyto.b.20450

Olivero, O. A., Chang, P. K., Lopez-Larraza, D. M., Cristina Semino-Mora, M., & Poirier, M. C. (1997). Preferential formation and decreased removal of cisplatin–DNA adducts in Chinese hamster ovary cell mitochondrial DNA as compared to nuclear DNA. *Mutation Research/Genetic Toxicology and Environmental Mutagenesis*, *391*(1), 79–86. https://doi.org/https://doi.org/10.1016/S0165-1218(97)00037-2

Olivero, O. A., Semino, C., Kassim, A., Lopez-Larraza, D. M., & Poirier, M. C. (1995). Preferential binding of cisplatin to mitochondrial DNA of Chinese hamster ovary cells. *Mutation Research Letters*, *346*(4), 221–230. https://doi.org/https://doi.org/10.1016/0165-7992(95)90039-X

Oltval, Z. N., Milliman, C. L., & Korsmeyer, S. J. (1993). Bcl-2 heterodimerizes in vivo with a conserved homolog, Bax, that accelerates programed cell death. *Cell*, *74*(4), 609–619. https://doi.org/10.1016/0092-8674(93)90509-O

Ortiz de Montellano, P. R. (2018). 1-Aminobenzotriazole: A mechanism-based cytochrome P450 inhibitor and probe of cytochrome P450 biology. *Med Chem (Los Angeles)*, *8*(3). https://doi.org/10.4172/2161-0444.1000495.1-Aminobenzotriazole

Ototoxicity, C., Wimmer, C., Mees, K., Stumpf, P., Welsch, U., Reichel, O., & Suckfu, M. (2004). Round Window Application of D-Methionine , Sodium Thiosulfate, Brain-Derived Neurotrophic Factor, and Fibroblast Growth Factor-2 in CIsplatin-Induced Ototoxicity. *Otology and Neurotology*, (12), 33–40.

Otsuka, M., Matsumoto, T., Morimoto, R., Arioka, S., Omote, H., & Moriyama, Y. (2005). A human transporter protein that mediates the final excretion step for toxic cations. *PNAS*, *102*(50).

Ou, H. C., Cunningham, L. L., Francis, S. P., Brandon, C. S., Simon, J. A., Raible, D. W., & Rubel, E. W. (2009). Identification of FDA-Approved Drugs and Bioactives that Protect Hair Cells in the Zebrafish (Danio rerio) Lateral Line and Mouse (Mus musculus) Utricle. *Journal of the Association for Research in Otolaryngology*, *10*, 191–203. https://doi.org/10.1007/s10162-009-0158-y

Ou, H. C., Santos, F., Raible, D. W., Simon, J. A., & Edwin, W. (2010). Drug screening for hearing loss: using the zebrafish lateral line to screen for drugs that prevent and cause hearing loss. *Drug Discovery Today*, *15*(7–8), 265–271. https://doi.org/10.1016/j.drudis.2010.01.001.Drug

Ou, H., Raible, D., & Rubel, E. (2007). Cisplatin-induced hair cell loss in zebrafish (Danio rerio) lateral line. *Hearing Research*, *233*(206), 46–53. https://doi.org/10.1016/j.bbi.2008.05.010

Ouchi, A., Asano, M., Aono, K., Watanabe, T., & Kato, T. (2014). Comparison of Short and Continuous Hydration Regimen in Chemotherapy Containing Intermediate-to High-Dose Cisplatin. *Journal of Oncology*, 767652. https://doi.org/10.1155/2014/767652

Owens, K. N., Santos, F., Roberts, B., Linbo, T., Coffin, A. B., Knisely, A. J., … Raible, D. W. (2008). Identification of Genetic and Chemical Modulators of Zebrafish Mechanosensory Hair Cell Death. *PLoS Genetics*, *4*(2). https://doi.org/10.1371/journal.pgen.1000020

Paken, J., Govender, C. D., Pillay, M., & Sewram, V. (2016). Cisplatin-Associated Ototoxicity: A Review for the Health Professional. *Journal of Toxicology*, *2016*, 1809394.

Palmieri, G., Morabito, A., Lauria, R., Montesarchio, V., Matano, E., Rea, A., … Libetta, C. (1993). Low-dose dopamine induces early recovery of recombinant interleukin-2-impaired renal function. *European Journal of Cancer*, *29*(8), 1119–1122. https://doi.org/10.1016/S0959-8049(05)80300-4

Papsin, B. C., & Gordon, K. A. (2007). Cochlear Implants for Children with Severe-to-Profound Hearing Loss. *The New England Journal of Medicine*, *357*, 2380–2388.

Pasetto, L. M., D'Andrea, M. R., Brandes, A. A., Rossi, E., & Monfardini, S. (2006). The development of platinum compounds and their possible combination. *Critical Reviews in Oncology/Hematology*, *60*(1), 59–75. https://doi.org/10.1016/j.critrevonc.2006.02.003

Perco, P., Ju, W., Kerschbaum, J., Leierer, J., Menon, R., Zhu, C., … Syndrome, N. (2019). Identification of dicarbonyl and L-xylulose reductase as a therapeutic target in human chronic kidney disease. *JCI Insight*, *4*(12), e128120.

Peters, Hebeisen, A., Hahn, M., Seifert, E., Lanvers, C., Heinecke, A., … Ju, H. (2000). Glutathione S-transferase genetic polymorphisms and individual sensitivity to the ototoxic effect of cisplatin. *Anti-Cancer Drugs*, *11*, 639–643.

Philip, R. C., Rodriguez, J. J., Niihori, M., Francis, R. H., Mudery, J. A., Caskey, J. S., … Jacob, A. (2018). Automated High-Throughput Damage Scoring of Zebrafish Lateral Line Hair Cells After Ototoxin Exposure. *Zebrafish*, *00*(00), zeb.2017.1451. https://doi.org/10.1089/zeb.2017.1451

Pierson, M., & Moller, A. (1981). Prophylaxis of kanamycin-induced ototoxicity by a radioprotectant. *Hearing Research*, *4*, 79–87.

Pirklbauer, X. M., Schupart, R., Fuchs, L., Staudinger, P., Corazza, U., Sallaberger, S., … Unraveling, S. H. (2019). Unraveling reno-protective effects of SGLT2 inhibition in human proximal tubular cells. *Am J Physiol Renal Physiol*, *316*, F449–F462. https://doi.org/10.1152/ajprenal.00431.2018

Pisani, V., Sisto, R., Moleti, A., Di, R., Pisani, A., Brusa, L., … Di, S. (2015). An investigation of hearing impairment in de-novo Parkinson's disease patients: A preliminary study. *Parkinsonism and Related Disorders*, *21*(8), 987–991. https://doi.org/10.1016/j.parkreldis.2015.06.007

Pliss, G. B., Zabezhinski, M. A., Petrov, A. S., & Khudoley, V. V. (1982). Peculiarities of N-nitramines carcinogenic action. *Archiv Fur Geschwulstforschung*, *52*(8), 629—634. Retrieved from http://europepmc.org/abstract/MED/6984817

Pokkunuri, I. D., Chugh, G., & Asghar, M. (2013). Human kidney-2 cells harbor functional dopamine D1 receptors that require Gialpha for Gq/11 alpha signaling. *American Journal of Physiology - Renal Physiology*, *305*, F560–F567. https://doi.org/10.1152/ajprenal.00644.2012

Prestayko, A. W., Crooke, S. T., & Carter, S. K. (1980). *Cisplatin: Current Status and New Developments*. (A. W. Prestayko, S. T. Crooke, & S. K. Carter, Eds.). New York: Academic Press.

Pringle, E., Wertman, J., Melong, N., Coombs, A., Young, A., O'Leary, D., … Berman, J. (2019). The zebrafish xenograft platform - A novel tool for modeling KSHV-associated diseases. *Preprints*, *2019110081*. https://doi.org/1020944/preprints201911.0081.v1

Prykhozhij, S., Caceres, L., & Berman, J. (2017). New Developments in CRISPR/Cas-based Functional Genomics and their Implications for Research using Zebrafish. *Current Gene Therapy*, *17*.

Qian, W., Nishikawa, M., Haque, A., Hirose, M., Mashimo, M., Sato, E., … Inoue, M. (2005). Mitochondrial density determines the cellular sensitivity to cisplatin-induced cell death. *Am J Physiol Cell Physiol*, 1466–1475. https://doi.org/10.1152/ajpcell.00265.2005.

Qin, H., Zhao, L., Sun, J., Ren, L., Guo, W., & Liu, H. (2011). The differentiation of mesenchymal stem cells into inner ear hair cell-like cells in vitro. *Acta Oto-Laryngologica*, *131*(11), 1136–1141. https://doi.org/10.3109/00016489.2011.603135

Racusen, L. C., Monteil, C., Sgrignoli, A., Lucskay, M., Marouillat, S., Rhim, J. G. S., & Morin, J. (1996). Cell lines with extended in vitro growth potential from human renal proximal tubule :Characterization, response to inducers, and comparison with established cell lines. *J Lab Clin Med*, *129*, 318–329.

Ramesh, G., Reeves, W. B., Ramesh, G., & Reeves, W. B. (2002). TNF-a mediates chemokine and cytokine expression and renal injury in cisplatin nephrotoxicity. *JCI*, *110*(6), 835–842. https://doi.org/10.1172/JCI200215606.Introduction

Ratain, M. J., Cox, N. J., & Henderson, T. O. (2013). Challenges in interpreting the evidence for genetic predictors of ototoxicity. *Clinical Pharmacology and Therapeutics*, *94*(6), 631–635. https://doi.org/10.1038/clpt.2013.178

Raymond, E., Faivre, S., Chaney, S., Woynarowski, J., & Cvitkovic, E. (2002). Cellular and Molecular Pharmacology of Oxaliplatin. *Molecular Cancer Therapeutics*, *1*, 227–235.

Reddel, R., Kefford, R., Grant, J., Coates, A., Fox, R., & Tattersall, M. (1982). Ototoxicity in patients receiving cisplatin: importance of dose and method of drug administration. *Cancer Treatment Reports*, *66*(1), 19–23.

Rider, S. A., Tucker, C. S., Rose, K. N., Macrae, C. A., Bailey, M. A., & Mullins, J. J. (2012). Techniques for the in vivo assessment of cardio-renal function in zebrafish (Danio rerio) larvae. *Journal of Physiology*, *8*, 1803–1809. https://doi.org/10.1113/jphysiol.2011.224352

Riedemann, L., Lanvers, C., Deuster, D., Peters, U., & Boos, J. (2008). Megalin genetic polymorphisms and individual sensitivity to the ototoxic effect of cisplatin. *The Pharmacogenomics Journal*, *8*, 23–28. https://doi.org/10.1038/sj.tpj.6500455

Riga, M., Psarommatis, I., Korres, S., Lyra, C., & Papadeas, E. (2006). The effect of treatment with vincristine on transient evoked and distortion product otoacoustic emissions. *International Journal of Pediatric Otorhinolaryngology*, *70*, 1003–1008. https://doi.org/10.1016/j.ijporl.2005.10.011

Riley, B. B., & Moorman, S. J. (2000). Development of Utricular Otoliths, but not Saccular Otoliths, Is Necessary for Vestibular Function and Survival in Zebrafish. *Journal of Neurobiology*, *43*, 329–337.

Ritz, C., Baty, F., Streibig, J. C., & Gerhard, D. (2015). Dose-Response Analysis Using R, 1–13. https://doi.org/10.1371/journal.pone.0146021

Rivolta, M. N., & Holley, M. C. (2002). Cell Lines in Inner Ear Research, (May), 306–318. https://doi.org/10.1002/neu.10111

Rogakou, E. P., Boon, C., Redon, C., & Bonner, W. M. (1999). Megabase Chromatin Domains Involved in DNA Double-Strand Breaks In Vivo. *The Journdal of Cell Biology*, *146*(5), 905–915.

Rogakou, E. P., Pilch, D. R., Orr, A. H., Ivanova, V. S., & Bonner, W. M. (1998). DNA Double-stranded Breaks Induce Histone H2AX Phosphorylation on Serine 139. *The Journal of Biological Chemistry*, *273*(10), 5858–5868.

Ronco, P., Antoine, M., Baudouin, B., Geniteau-legendre, M., Lelongt, B., Chatelet, F., … Vandewalle, A. (1990). Polarized membrane expression of brush-border hydrolases in primary cultures of kidney proximal tubular cells depends on cell differentiation and is induced by dexamethasone. *Journal of Cellular Physiology*, *145*(2), 222–237. https://doi.org/10.1002/jcp.1041450206

Rosenberg, B., VanCamp, L., & Krigas, T. (1965). Inhibition of cell division in Escherichia coli by electrolysis products from a platinum electrode. *Nature*, *205*, 698–699.

Rosenberg, Barnett, & VanCamp, L. (1969). Platinum compounds: a new class of potent antitumor agents. *Nature*, *222*, 385–386.

Ross, C. J. D., Katzov-Eckert, H., Dubé, M. P., Brooks, B., Rassekh, S. R., Barhdadi, A., … Hayden, M. R. (2009). Genetic variants in TPMT and COMT are associated with hearing loss in children receiving cisplatin chemotherapy. *Nature Genetics*, *41*(12), 1345–1349. https://doi.org/10.1038/ng.478

Rothenberg, M. L., Oza, A. M., Bigelow, R. H., Berlin, J. D., Marshall, J. L., Ramanathan, R. K., … Haller, D. G. (2003). Superiority of Oxaliplatin and Fluorouracil-Leucovorin Compared With Either Therapy Alone in Patients With Progressive Colorectal Cancer After Irinotecan and Fluorouracil-Leucovorin: Interim Results of a Phase III Trial. *Journal of Clinical Oncology*, *21*(11), 2059–2069. https://doi.org/10.1200/JCO.2003.11.126

Rueden, C. T., Schindelin, J., Hiner, M. C., Dezonia, B. E., Walter, A. E., Arena, E. T., & Eliceiri, K. W. (2017). ImageJ2: ImageJ for the next generation of scientific image data. *BMC Bioinformatics*, *18*(529), 1–26. https://doi.org/10.1186/s12859-017-1934-z

Ruzicka, L., Howe, D. G., Ramachandran, S., Toro, S., Van Slyke, C. E., Bradford, Y. M., … Westerfield, M. (2018). The Zebrafish Information Network: new support for non-coding genes, richer Gene Ontology annotations and the Alliance of Genome Resources. *Nucleic Acids Research*, *47*(D1), D867–D873. https://doi.org/10.1093/nar/gky1090

Ryan, M. J., Johnson, G., Kiiu, J., Fuerstenberg, S. M., Zager, R. A., & Torok-storb, B. (1994). HK-2: An immortalized proximal tubule epithelial cell line from normal adult human kidney. *Kidney International*, *45*, 48–57. https://doi.org/10.1038/ki.1994.6

Rybak, L P, & Ramkumar, V. (2007). Ototoxicity. *Kidney International*, *72*, 931–935. https://doi.org/10.1038/sj.ki.5002434

Rybak, Leonard P., Whitworth, C. A., Mukherjea, D., & Ramkumar, V. (2007). Mechanisms of cisplatin-induced ototoxicity and prevention. *Hearing Research*, *226*(1–2), 157–167. https://doi.org/10.1016/j.heares.2006.09.015

Rybak, Leonard P, Husain, K., Whitworth, C., & Somani, S. M. (1999). Dose Dependent Protection by Lipoic Acid against Cisplatin-Induced Ototoxicity in Rats : Antioxidant Defense System. *Toxicological Studies*, *47*, 195–202.

Rybak, Leonard P, Mukherjea, D., Jajoo, S., Kaur, T., & Ramkumar, V. (2017). siRNA-mediated knock-down of NOX3: therapy for hearing loss? *Cell Mol Life Sci*, *69*(14), 2429–2434. https://doi.org/10.1007/s00018-012-1016-3.siRNA-mediated

Rybak, P., & Whitworth, C. (1999). Application of Antioxidants and Other Agents to Prevent Cisplatin Ototoxicity. *The Laryngoscope*, *109*, 1740–1744.

Safaei, R. (2006). Role of copper transporters in the uptake and efflux of platinum containing drugs. *Cancer Letters*, *234*, 34–39. https://doi.org/10.1016/j.canlet.2005.07.046

Safirstein, R., Miller, P., & Guttenplan, J. B. (1984). Uptake and metabolism of cisplatin by rat kidney. *Kidney International*, *25*(5), 753–758. https://doi.org/10.1038/ki.1984.86

Sakai, W., Swisher, E. M., Jacquemont, C., Venkatapoorna, K., Couch, F. J., Langdon, S. P., … Taniguchi, T. (2009). Functional restoration of BRCA2 protein by secondary BRCA2 mutations in BRCA2-mutated ovarian carcinoma. *Cancer Research*, *69*(16), 6381–6386. https://doi.org/10.1158/0008-5472.CAN-09-1178.Functional

Salat, D., & Tolosa, E. (2013). Levodopa in the treatment of Parkinson's disease: Current status and new developments. *Journal of Parkinson's Disease*, *3*(3), 255–269. https://doi.org/10.3233/JPD-130186

Samimi, G., Katano, K., Holzer, A. K., Safaei, R., & Howell, S. B. (2004). Modulation of the Cellular Pharmacology of Cisplatin and Its Analogs by the Copper Exporters ATP7A and ATP7B. *Molecular Pharmacology*, *66*(1), 25–32.

Schell, M. J., McHaney, V. A., Green, A. A., Kun, L. E., Hayes, F. A., Horowitz, M., & Meyer, W. H. (1989). Hearing loss in children and young adults receiving cisplatin with or without prior cranial irradiation. *Journal of Clinical Oncology*, *7*(6), 754–760. https://doi.org/10.1200/JCO.1989.7.6.754

Schilsky, R., & Anderson, T. (1979). Hypomagnesemia and Renal Magnesium Wasting in Patients Receiving Cisplatin. *Annals of Internal Medicine*, *90*(6), 929–931. https://doi.org/10.7326/0003-4819-90-6-929

Schindelin, J., Arganda-carreras, I., Frise, E., Kaynig, V., Longair, M., Pietzsch, T., … Cardona, A. (2012). Fiji: an open-source platform for biological-image analysis. *Nature Methods*, *9*(7), 676–682. https://doi.org/10.1038/nmeth.2019

Schumaker, L. M., Egorin, M. J., Zuhowski, E. G., Guo, Z., & Cullen, K. J. (2006). Cisplatin Preferentially Binds Mitochondrial DNA and Voltage- Dependent Anion Channel Protein in the Mitochondrial Membrane of Head and Neck Squamous Cell Carcinoma: Possible Role in Apoptosis. *Cancer Therapy: Preclinical*, *12*(19), 5817–5826. https://doi.org/10.1158/1078-0432.CCR-06-1037

Scott, R. P., & Quaggin, S. E. (2015). The cell biology of renal filtration. *Journal of Cell Biology*, *209*(2), 199–210. https://doi.org/10.1083/jcb.201410017

Sener, G., Satiroglu, H., Kabasakal, L., Arbak, S., Oner, S., Ercan, F., & Keyer-Uysa, M. (2000). The protective effect of melatonin on cisplatin nephrotoxicity. *Fundamental & Clinical Pharmacology*, *14*(6), 553–560. https://doi.org/S0767398100010872 [pii]

Sethi, K. (2010). The Impact of Levodopa on Quality of Life in Patients With Parkinson Disease. *The Neurologist*, *16*, 76–83. https://doi.org/10.1097/NRL.0b013e3181be6d15

Shaikh, F., Nathan, P. C., Hale, J., Uleryk, E., & Fraizer, L. (2013). Is there a role for carboplatin in the treatment of malignant germ cell tumors? A systematic review of adult and pediatric trials. *Pediatr Blood Cancer*, *60*, 587–592. https://doi.org/10.1002/pbc

Simon, B. R., Wilson, M. J., & Wickliffe, J. K. (2014). The RPTEC/TERT1 cell line models key renal cell responses to the environmental toxicants, benzo[a]pyrene and cadmium. *Toxicology Reports*, *1*, 231–242. https://doi.org/10.1016/j.toxrep.2014.05.010

Skinner, R, Pearson, a D., English, M. W., Price, L., Wyllie, R. a, Coulthard, M. G., & Craft, a W. (1998). Cisplatin dose rate as a risk factor for nephrotoxicity in children. *British Journal of Cancer*, *77*(10), 1677–1682. https://doi.org/10.1038/bjc.1998.276

Skinner, Roderick, Parry, A., Price, L., Cole, M., Craft, A. W., & Pearson, A. D. J. (2009). Persistent nephrotoxicity during 10-year follow-up after cisplatin or carboplatin treatment in childhood: Relevance of age and dose as risk factors 5. *European Journal of Cancer*, *45*(18), 3213–3219. https://doi.org/10.1016/j.ejca.2009.06.032

Smits, C., Swen, S. J., Goverts, S. T., Moll, A. C., Imhof, S. M., & Meeteren, A. Y. N. S. (2006). Assessment of hearing in very young children receiving carboplatin for retinoblastoma. *European Journal of Cancer*, *42*, 492–500. https://doi.org/10.1016/j.ejca.2005.11.004

Somlo, G., Doroshow, J. H., Lev-ran, A., Ahn, D. C., Hwang, L., Raschko, J. W., … Menard, P. (1995). Effect of Low-Dose Prophylactic Dopamine on High-Dose Cisplatin-Induced Electrolyte Wasting, Ototoxicity, and Epidermal Growth Factor Excretion: A Randomized, Placebo-Controlled, Double-Blind Trial. *Journal of Clinical Oncology*, *13*(5), 1231–1237.

Sooriyaarachchi, M., Narendran, A., & Gailer, J. (2012). The effect of sodium thiosulfate on the metabolism of cisplatin in human plasma in vitro. *Metallomics*, *4*, 960–967. https://doi.org/10.1039/c3mt00012e

Sorbe, B. (1988). Betamethasone-Dixyrazine Versus Metoclopramide as Antiemetic Treatment in Cancer Chemotherapy. *Acta Oncologica*, *27*(4), 357–360. https://doi.org/10.3109/02841868809093554

Sörös, P. (2012). On variability and genes: inter-individual differences in auditory brain function. *Frontiers in Human Neuroscience*, *6*(June), 1–3. https://doi.org/10.3389/fnhum.2012.00150

Souders, E. C. S. C. L., & Schmidt, I. I. J. T. (2018). Domperidone upregulates dopamine receptor expression and stimulates locomotor activity in larval zebrafish (Danio rerio). *Genes, Brain and Behavior*, (December 2017), 1–10. https://doi.org/10.1111/gbb.12460

Spitsbergen, J., & Kent, M. (2003). The State of the Art of the Zebrafish Model for Toxicology and Toxicologic Pathology Research - Advantages and Current Limitations. *Toxicologic Pathology*, *31*(1), 62–87. https://doi.org/10.1080/01926230390174959

Spitsbergen, J., Tsai, H.-W., Reddy, A., Miller, T. O. M., Arbogast, D. A. N., Hendricks, J. D., & Bailey, G. S. (2000). Neoplasia in zebrafish (Danio rerio) treated with 7,12-Dimethylbenz[a]anthracene by two exposure routes at different developmental stages. *Toxicologic Pathology*, *28*(5), 705–715.

Sprowl, J. A., Doorn, L. Van, Hu, S., Gerven, L. Van, Bruijn, P. De, Li, L., … Sparreboom, A. (2013). Conjunctive Therapy of Cisplatin With the OCT2 Inhibitor Cimetidine: Influence on Antitumor Efficacy and Systemic Clearance. *Clinical Pharmacology and Therapeutics*, *94*(5), 585–592. https://doi.org/10.1038/clpt.2013.145

Sprowl, J., Ness, R., & Sparreboom, A. (2013). Polymoprhic transporters and platinum pharmacodynamics. *Drug Metab Pharmacokinet*, *28*(1), 19–27.

Stach, B. (1998). *Clinical Audiology: An Introduction* (Second). San Diego: Singular.

Stawicki, T. M., Owens, K. N., Linbo, T., Reinhart, K. E., Rubel, E. W., & Raible, D. W. (2014). The zebrafish merovingian mutant reveals a role for pH regulation in hair cell toxicity and function. *Disease Models & Mechanisms*, *7*(7), 847–856. https://doi.org/10.1242/dmm.016576

Stawicki, Tamara M, Esterberg, R., Hailey, D. W., Raible, D. W., & Rubel, E. W. (2015). Using the zebrafish lateral line to uncover novel mechanisms of action and prevention in drug-induced hair cell death. *Frontiers in Cellular Neuroscience*, *9*(February), 1–7. https://doi.org/10.3389/fncel.2015.00046

Steinhausen, M., Weis, S., Fleming, J., & Dussel, R. (1986). Responses of in vivo renal microvessels to dopamine. *Kidney International*, *30*(3), 361–370. https://doi.org/10.1038/ki.1986.193

Stelmachowicz, P. G., Pittman, A. L., Hoover, B. M., Lewis, D. E., & Moeller, M. P. (2004). The Importance of High-Frequency Audibility in the Speech and Language Development of Children With Hearing Loss. *Arch Otolaryngol Head Neck Surg*, *130*, 556–562.

Stevens, L., Coresh, J., Greene, T., & Levey, A. (2006). Assessing Kidney Function — Measured and Estimated Glomerular Filtration Rate. *The New England Journal of Medicine*, *354*(23), 2473–2484.

Stewart, D. J., Mikhael, N. Z., & Deidre, M. (1997). Association of cisplatin nephrotoxicity with patient characteristics and cisplatin administration methods. *Cancer Chemotherapy and Pharmacology*, *40*, 293–308.

Stohr, W., Paulides, M., Bielacj, S., Jurgens, H., Koscielniak, E., Rossi, R., … Beck, J. D. (2007). Nephrotoxicity of cisplatin and carboplatin in sarcoma patients: A report from the late effects surveillance system. *Pediatr Blood Cancer*, *48*, 140–147. https://doi.org/10.1002/pbc

Strategies, A., Sato, S., Murata, A., Shirakawa, T., & Uesugi, M. (2010). Biochemical Target Isolation for Novices: Affinity-Based Strategies. *Chemistry & Biology*, *17*(6), 616–623. https://doi.org/10.1016/j.chembiol.2010.05.015

Subramanya, A. R., & Ellison, D. H. (2014). Distal convoluted tubule. *Clinical Journal of the American Society of Nephrology*, *9*, 2147–2163. https://doi.org/10.2215/CJN.05920613

Suh, J. H., & Miner, J. H. (2014). The glomerular basement membrane as a barrier to Albumin. *Nature Review Nephrology*, *9*(8), 1–13. https://doi.org/10.1038/nrneph.2013.109.The

Suli, A., Watson, G. M., Rubel, E. W., & Raible, D. W. (2012). Rheotaxis in Larval Zebrafish Is Mediated by Lateral Line Mechanosensory Hair Cells. *PLOS One*, *7*(2), 1–6. https://doi.org/10.1371/journal.pone.0029727

Swinney, D C. (2013). Phenotypic vs. Target-Based Drug Discovery for First-in-Class Medicines. *Clinical Pharmacology and Therapeutics*, *93*(4), 299–301. https://doi.org/10.1038/clpt.2012.236

Swinney, David C, & Anthony, J. (2011). How were new medicines discovered? *Drug Discovery*, *10*, 507–519. https://doi.org/10.1038/nrd3480

Takano, M., Inui, K.-I., Okano, T., Saito, H., & Hori, R. (1984). Carrier-mediated transport systems of tetraethylammonium in rat renal brush-border and basolateral membrane vesicles. *Biochimica et Biophysica Acta (BBA) - Biomembranes*, *773*(1), 113–124. https://doi.org/https://doi.org/10.1016/0005-2736(84)90556-X

Tebbi, C. K., London, W. B., Friedman, D., Villaluna, D., De Alarcon, P. A., Constine, L. S., … Schwartz, C. L. (2007). Dexrazoxane-associated risk for acute myeloid leukemia/myelodysplastic syndrome and other secondary malignancies in pediatric Hodgkin's disease. *Journal of Clinical Oncology*, *25*(5), 493–500. https://doi.org/10.1200/JCO.2005.02.3879

Teitz, T., Fang, J., Goktug, A. N., Bonga, J. D., Diao, S., Hazlitt, R. A., … Zuo, J. (2018). CDK2 inhibitors as candidate therapeutics for cisplatin- and noise-induced hearing loss. *The Journal of Experimental Medicine*, jem.20172246. https://doi.org/10.1084/jem.20172246

Tekce, B. K., Uyeturk, U., Tekce, H., Uyeturk, U., & Aktas, G. (2015). Does the kidney injury molecule-1 predict cisplatin-induced kidney injury in early stage ? *Annals of Clinical Biochemistry*, *52*(1), 88–94. https://doi.org/10.1177/0004563214528312

Tepel, M., Van Der Giet, M., Schwarzfeld, C., Laufer, U., Liermann, D., & Zidek, W. (2000). Prevention of radiographic-contrast-agent-induced reductions in renal function by acetylcysteine. *The New England Journal of Medicine*, *343*(180–184).

Theunissen, E. A. R., Dreschler, W. A., Latenstein, M. N., Rasch, C. R. N., Baan, S. Van Der, Boer, J. P. De, … Zuur, C. L. (2014). A New Grading System for Ototoxicity in Adults. *Annals of Otology, Rhinology & Laryngology*, *123*(10), 711–718. https://doi.org/10.1177/0003489414534010

Thiebaut, F., Tsuruot, T., Hamadat, H., Gottesman, M. M., & Pastan, I. R. A. (1987). Cellular localization of the multidrug-resistance gene product P-glycoprotein in normal human tissues. *PNAS*, *84*(November), 7735–7738.

Thomas, A. J., Hailey, D. W., Stawicki, T. M., Wu, P., Coffin, A. B., Rubel, E. W., … Ou, H. C. (2013). Functional Mechanotransduction Is Required for Cisplatin-Induced Hair Cell Death in the Zebrafish Lateral Line. *Journal of Neuroscience*, *33*(10), 4405–4414. https://doi.org/10.1523/JNEUROSCI.3940-12.2013

Thomas, Andrew J., Wu, P., Raible, D. W., Rubel, E. W., Simon, J. A., & Ou, H. C. (2015). Identification of small molecule inhibitors of cisplatin-induced hair cell death: Results of a 10,000 compound screen in the zebrafish lateral line. *Otology and Neurotology*, *36*(3), 519–525. https://doi.org/10.1097/MAO.0000000000000487

Tiseo, M., Martelli, O., Mancuso, A., Sormani, M. P., Bruzzi, P., Di Salvia, R., … Ardizzoni, A. (2007). Short Hydration Regimen and Nephrotoxicity of Intermediate to High-Dose Cisplatin-Based Chemotherapy for Outpatient Treatment in Lung Cancer and Mesothelioma. *Tumori Journal*, *93*(2), 138–144. https://doi.org/10.1177/030089160709300205

Toro, C., Trapani, J. G., Pacentine, I., Maeda, R., Sheets, L., Mo, W., & Nicolson, T. (2015). Dopamine Modulates the Activity of Sensory Hair Cells. *Journal of Neuroscience*, *35*(50), 16494–16503. https://doi.org/10.1523/JNEUROSCI.1691-15.2015

Townsend, D., Deng, M., Zhang, L., Lapus, M., & Hanigan, M. (2003). Metabolism of cisplatin to a nephrotoxin in proximal tubule cells. *J Am Soc Nephrol*, *14*(1), 1–10.

Townsend, D. M., & Hanigan, M. H. (2002). Inhibition of gamma-glutamyl transpeptidase or cysteine S-conjugate beta-lyase activity blocks the nephrotoxicity of cisplatin in mice. *J Pharmacol Exp Ther*, *300*(1), 142–148.

Tsai, W.-C., & Ling, K.-H. (1971). Toxic action of mimosine—I. Inhibition of mitosis and DNA synthesis of H.Ep-2 cell by mimosine and 3,4-dihydroxypyridine. *Toxicon*, *9*(3), 241–247. https://doi.org/https://doi.org/10.1016/0041-0101(71)90076-6

Tumlin, J. A., Finkel, K. W., Murray, P. T., Samuels, J., Cotsonis, G., & Shaw, A. D. (2005). Fenoldopam Mesylate in early acute tubular necrosis : A randomied, double-blind, placebo-controlled clinical trial. *Am J of Kidney Diseases*, *46*(1), 26–34. https://doi.org/10.1053/j.ajkd.2005.04.002

Tutt, A., Bertwistle, D., Valentine, J., Gabriel, A., Swift, S., Ross, G., … Ashworth, A. (2001). Mutation in Brca2 stimulates error-prone homology-directed repair of DNA double-strand breaks occurring between repeated sequences. *EMBO*, *20*(17), 4704–4716.

Udilova, N., Kozlov, A. V, & Bieberschulte, W. (2003). The antioxidant activity of caroverine. *Biochemical Pharmacology*, *65*, 59–65.

Uribe, P. M., Mueller, M. a, Gleichman, J. S., Kramer, M. D., Wang, Q., Sibrian-Vazquez, M., … Matsui, J. I. (2013). Dimethyl sulfoxide (DMSO) exacerbates cisplatin-induced sensory hair cell death in zebrafish (Danio rerio). *PloS One*, *8*(2), e55359. https://doi.org/10.1371/journal.pone.0055359

Urien, S., & Lokiec, F. (2004). Population pharmacokinetics of total and unbound plasma cisplatin in adult patients. *British Journal of Clinical Pharmacology*, *57*(6), 756–776. https://doi.org/10.1111/j.1365-2125.2004.02082.x

van Dalen, E., Caron, H., Dickinson, H., & Kremer, L. (2008). Cardioprotective interventions for cancer patients receiving anthracyclines (Review). *Cochrane Database of Systematic Reviews*, (2), CD003917. https://doi.org/10.1002/14651858.CD003917.pub3.www.cochranelibrary.com

Vermeulen, K., Bockstaele, D. R. Van, & Berneman, Z. N. (2003). The cell cycle: a review of regulation, deregulation and therapeutic targets in cancer. *Cell Prolif*, *36*, 131–149.

Vitale, C., Marcelli, V., Allocca, R., Santangelo, G., Riccardi, P., Erro, R., … Barone, P. (2012). Hearing impairment in Parkinson's disease: Expanding the nonmotor phenotype. *Movement Disorders*, *27*(12), 1530–1535. https://doi.org/10.1002/mds.25149

Vlasits, A., Simon, J., Raible, D., Rubel, E., & Owens, K. (2012). Screen of FDA-approved drug library reveals compounds that protect hair cells from aminoglycosides and cisplatin. *Hear Res*, *294*, 153–165. https://doi.org/10.1016/j.heares.2012.08.002.Screen

Vrooman, L. M., Neuberg, D. S., Stevenson, K. E., Asselin, B. L., Athale, U. H., Clavell, L., … Sallan, S. E. (2011). The low incidence of secondary acute myelogenous leukaemia in children and adolescents treated with dexrazoxane for acute lymphoblastic leukaemia: A report from the Dana-Farber Cancer Institute ALL Consortium. *European Journal of Cancer*, *47*(9), 1373–1379. https://doi.org/https://doi.org/10.1016/j.ejca.2011.03.022

Waguespack, J., & Ricci, A. (2005). Aminoglycoside ototoxicity: permeant drugs cause permanent hair cell loss. *J Physiol*, *2*, 359–360. https://doi.org/10.1113/jphysiol.2005.094474

Wake, M., Hughes, E. K., Hons, B., Collins, C. M., & Poulakis, Z. (2004). Parent-Reported Health-Related Quality of Life in Children With Congenital Hearing Loss: A Population Study. *Ambulatory Pediatrics*, *4*, 411–417.

Wang, D., & Lippard, S. J. (2005). Cellular processing of platinum anticancer drugs. *Nature Reviews Drug Discovery*, *4*(April), 307–320. https://doi.org/10.1038/nrd1691

Warda, K. A., & Harrij, R. L. N. (1976). Inhibition of Wool Follicle DNA Synthesis by Mimosine and Related 4 (lH) -Pyridones. *Aust J Biol Sci*, *29*, 189–196.

Warnecke, C., Griethe, W., Weidemann, A., Jurgensen, J., Willam, C., Bachmann, S., … Eckardt, K. (2003). Activation of the hypoxia-inducible factor pathway and stimulation of angiogenesis by application of prolyl hydroxylase inhibitors. *The FASEB Journal*, *17*(9), 1186–1188. https://doi.org/10.1096/fj.02-1062fje

Watanabe, K., Hess, A., Bloch, W., & Michel, O. (2000). Nitric oxide synthase inhibitor suppresses the ototoxic side effect of cisplatin in guinea pigs. *Anti-Cancer Drugs*, *11*, 401–406.

Weijl, N. I., Elsendoorn, T. J., Lentjes, E. G. W. M., Hopman, G. D., Wipkink-Bakker, A., Zwinderman, A. H., … Osanto, S. (2004). Supplementation with antioxidant micronutrients and chemotherapy-induced toxicity in cancer patients treated with cisplatin-based chemotherapy: A randomised, double-blind, placebo-controlled study. *European Journal of Cancer*, *40*(11), 1713–1723. https://doi.org/10.1016/j.ejca.2004.02.029

Welsh, C., Day, R., McGurk, C., Masters, J., Wood, R. D., & Koberle, B. (2004). Reduced levels of XPA, ERCC1 and XPF DNA repair proteins in testis tumor cell lines. *International Journal of Cancer*, *110*, 352–361. https://doi.org/10.1002/ijc.20134

Wen, J., Zeng, M., Shu, Y., & Guo, D. (2015). Aging increases the susceptibility of cisplatin-induced nephrotoxicity. *Age*, *37*, 112. https://doi.org/10.1007/s11357-015-9844-3

Wertman, Veinotte, C. J., Dellaire, G., & Berman, J. N. (2016). *The zebrafish xenograft platform: Evolution of a novel cancer model and preclinical screening tool*. *Advances in Experimental Medicine and Biology* (Vol. 916). https://doi.org/10.1007/978-3-319-30654-4_13

Westerfield, M. (1995). *The Zebrafish Book*. Eugene, OR: University of Oregon Press.

White, R. M., Sessa, A., Burke, C., Bowman, T., Leblanc, J., Ceol, C., … Zon, L. I. (2008). Transparent Adult Zebrafish as a Tool for In Vivo Transplantation Analysis. *Cell Stem Cell*, *2*, 183–189. https://doi.org/10.1016/j.stem.2007.11.002

Whitfield, T. T., Granato, M., Eeden, F. J. M. Van, Schach, U., & Brand, M. (1997). Mutations affecting development of the zebrafish inner ear and lateral line. *Development*, *123*, 241–254.

Williams, J. A., & Holder, N. (2000). Cell turnover in neuromasts of zebrafish larvae. *Hearing Research*, *143*, 171–181.

Wilmer, M. J., Ng, C. P., Lanz, H. L., Vulto, P., Suter-dick, L., & Masereeuw, R. (2016). Kidney-on-a-Chip Technology for Drug-Induced Nephrotoxicity Screening. *Trends in Biotechnology*, *34*(2), 156–170. https://doi.org/10.1016/j.tibtech.2015.11.001

Wingert, & Davidson, A. J. (2008). The zebrafish pronephros: A model to study nephron segmentation. *Kidney International*, *73*(10), 1120–1127. https://doi.org/10.1038/ki.2008.37

Wingert, R. A., Selleck, R., Yu, J., Song, H., Chen, Z., Song, A., … Davidson, A. J. (2007). The cdx Genes and Retinoic Acid Control the Positioning and Segmentation of the Zebrafish Pronephros. *PLOS Genetics*, *3*(10), e189. https://doi.org/10.1371/journal.pgen.0030189

Wisnovsky, S., Jean, S. R., & Kelley, S. O. (2016). Mitochondrial DNA repair and replication proteins revealed by targeted chemical probes. *Nature Chemical Biology*, *12*(7), 567–573. https://doi.org/10.1038/nchembio.2102

Wooster, R., Bignell, G., Lancastert, J., Swiftt, S., Seal, S., Mangion, J., … Stratton, M. R. (1995). Identification of the breast cancer susceptibility gene BRCA2. *Nature*, *378*, 789–792.

World Health Organization Model List of Essential Medicines, 21st List. (2019). Geneva: World Health Organization.

Xiao, T., Roeser, T., Staub, W., & Baier, H. (2005). A GFP-based genetic screen reveals mutations that disrupt the architecture of the zebrafish retinotectal projection. *Development*, *132*(13), 2955–2967. https://doi.org/10.1242/dev.01861

Yan, C., Brunson, D. C., Tang, Q., Haber, D. A., Rawls, J. F., Langenau, D. M., … Sgroi, D. C. (2019). Visualizing Engrafted Human Cancer and Therapy Responses in Immunodeficient Zebrafish Resource. *Cell*, *177*(7), 1903-1914.e14. https://doi.org/10.1016/j.cell.2019.04.004

Yan, X., Qi, M., Li, P., Zhan, Y., & Shao, H. (2017). Apigenin in cancer therapy: anti-cancer effects and mechanisms of action. *Cell & Bioscience*, *7*(50). https://doi.org/10.1186/s13578-017-0179-x

Yancey, A., Harris, M. S., Egbelakin, A., Gilbert, J., Pisoni, D. B., & Renbarger, J. (2012). Risk Factors for Cisplatin-Associated Ototoxicity in Pediatric Oncology Patients. *Pediatric Blood & Cancer*, *59*, 144–148. https://doi.org/10.1002/pbc

Yang, J. J., Lim, J. Y., Huang, J., Bass, J., Wu, J., Evans, W. E., … Onar-thomas, A. (2013). The role of inherited TMPT and COMT genetic variation in cisplatin-induced ototoxicity in children with cancer. *Clin Pharmacol Ther*, *94*(2), 1–16. https://doi.org/10.1038/clpt.2013.121.The

Yao, X., Panichpisal, K., Kurtzman, N., & Nugent, K. (2007). Cisplatin nephrotoxicity: A review. *The American Journal of the Medical Sciences*, *334*(2), 115–124. https://doi.org/10.1007/BF00694330

Yatsu, T., Arai, Y., Takizawa, K., Kasai-nakagawa, C., Takanashi, M., Uchida, W., … Takenaka, T. (1998). Effect of YM435, a Dopamine DA1 Receptor Agonist, in a Canine Model of Ischemic Acute Renal Failure. *Gen. Pharmac*, *31*(5), 803–807.

Yonezawa, A., & Inui, K. (2011). Organic cation transporter OCT/SLC22A and H +/organic cation antiporter MATE/SLC47A are key molecules for nephrotoxicity of platinum agents. *Biochemical Pharmacology*, *81*(5), 563–568. https://doi.org/10.1016/j.bcp.2010.11.016

Yonezawa, A., Masuda, S., Nishihara, K., Yano, I., Katsura, T., & Inui, K. (2005). Association between tubular toxicity of cisplatin and expression of organic cation transporter rOCT2 (Slc22a2) in the rat. *Biochemical Pharmacology*, *70*(12), 1823–1831. https://doi.org/https://doi.org/10.1016/j.bcp.2005.09.020

Yonezawa, A., Masuda, S., Yokoo, S., Katsura, T., & Inui, K. (2006). Cisplatin and Oxaliplatin, but Not Carboplatin and Nedaplatin, Are Substrates for Human Organic Cation Transporters (SLC22A1–3 and Multidrug and Toxin Extrusion Family). *The Journal of Pharmacology and Experimental Therapeutics*, *319*(2), 879–886. https://doi.org/10.1124/jpet.106.110346.lato

Yu, X., Fang, Y. I., Ding, X., Liu, H., Zhu, J., Zou, J., … Zhong, Y. (2012). Transient hypoxia-inducible factor activation in rat renal ablation and reduced fibrosis with L-mimosine. *Nephrology*, *17*, 58–67. https://doi.org/10.1111/j.1440-1797.2011.01498.x

Yuhas, J. M., Jackson, T., & Harbor, B. (1969). Differential Chemoproteetion of Normal and Malignant Tissues. *J Nat Cancer Inst*, *42*, 331–335.

Zalatnai, A. (2005). P-glycoprotein Expression is Induced in Human Pancreatic Cancer Xenografts During Treatment with a Cell Cycle Regulator, Mimosine. *Pathology Oncology Research*, *11*(3), 164–169.

Zazuli, Z., Vijverberg, S., Slob, E., Liu, G., Carleton, B., Veltman, J., … Masereeuw, R. (2018). Genetic Variations and Cisplatin Nephrotoxicity: A Systematic Review. *Frontiers in Pharmacology*, *9*(1111). https://doi.org/10.3389/fphar.2018.01111

Zeddies, D. G., & Fay, R. R. (2005). Development of the acoustically evoked behavioral response in zebrafish to pure tones. *The Journal of Experimental Biology*, *208*, 1363–1372. https://doi.org/10.1242/jeb.01534

Zhang, M., Yao, B., Fang, X., Wang, S., Smith, J. P., & Raymond, C. (2009). Intrarenal dopaminergic system regulates renin expression. *Hypertension*, *53*(3), 564–570. https://doi.org/10.1161/HYPERTENSIONAHA.108.127035.Intrarenal

Zhang, Y. R., & Yuan, Z. Y. (2010). Dopamine-mediated inhibition of renal Na+/K+-ATPase in HK-2 cells is reduced by ouabain. *Clinical and Experimental Pharmacology and Physiology*, *37*(5–6), 613–618. https://doi.org/10.1111/j.1440-1681.2010.05364.x

Zhao, T., Zhu, Y., Morinibu, A., Kobayashi, M., Shinomiya, K., Itasaka, S., … Harada, H. (2014). HIF-1-mediated metabolic reprogramming reduces ROS levels and facilitates the metastatic colonization of cancers in lungs. *Scientific Reports*, *4*, 3793. https://doi.org/10.1038/srep03793

Zhou, S. (2008). Structure, function and regulation of P- glycoprotein and its clinical relevance in drug disposition. *Xenobiotica*, *38*(7–8), 802–832. https://doi.org/10.1080/00498250701867889

Zhou, W., Boucher, R. C., Bollig, F., Englert, C., & Hildebrandt, F. (2010). Characterization of mesonephric development and regeneration using transgenic zebrafish. *American Journal of Physiology - Renal Physiology*, *299*, 1040–1047. https://doi.org/10.1152/ajprenal.00394.2010.

Zhu, S., Lee, J.-S., Guo, F., Shin, J., Perez-Atayde, A. R., Kutok, J. A., … Look, T. A. (2012). Activated ALK Collaborates with MYCN in Neuroblastoma Pathogenesis. *Cancer Cell*, *21*(3), 362–373. https://doi.org/10.1038/nature11130.Reduced

Ziegler, S., Pries, V., Hedberg, C., & Waldmann, H. (2013). Target Identification for Small Bioactive Molecules: Finding the Needle in the Haystack. *Angewandte Reviews*, *52*, 2744–2792. https://doi.org/10.1002/anie.201208749

Zlotnik, Y., Patya, M., Vanichkin, A., & Novogrodsky, A. (2005). Tyrphostins reduce chemotherapy-induced intestinal injury in mice: assessment by a biochemical assay. *British Journal of Cancer*, *92*, 294–297. https://doi.org/10.1038/sj.bjc.6602324

Zon, L. I., & Peterson, R. T. (2005). In vivo drug discovery in the zebrafish. *Nature Reviews. Drug Discovery*, *4*(1), 35–44. https://doi.org/10.1038/nrd1606

Appendix A Audiological Grading Systems

Name and Year	Criteria	Target Population	Benefits	Disadvantages
Brock, 1991 (Brock, Bellman, Yeomans, Pinkerton, & Pritchard, 1991)	Grades 0-5: 0 = <40dB loss at all frequencies; 1= >40dB loss at 8kHz; 2 = >40dB loss at ≥4kHz; 3 = >40 dB HL at ≥kHz; 4 = >40 dB loss at ≥kHz	Pediatric	Used widely, no baseline required, designed to test hearing loss at high frequencies	Only captures significant hearing loss (≥40dB), intended for pediatric use
ASHA, 1994 (*Audiologic management of individuals receiving cochleotoxic drug therapy*, 1994)	20dB decline at 1 frequency, 10dB decline at 2 adjacent frequencies, or complete lack of response at maximum dB for ≥3 adjacent frequencies, compared to baseline	Adult and pediatric	Easy to understand, suitable for all age groups	Baseline required, does not have a scale (binary system)
Chang, 2010 (K. W. Chang & Chinosornvatana, 2010)	Grades 0-4, with subgrades for 1 and 2: 0 = ≤20dB loss at 1, 2 and 4kHz; 1a = ≥40dB loss at any 1 frequency from 6-12kHz; 1b = 20-40dB loss at 4kHz; 2a = ≥40dB at 4kHz and up; 2b = 20-40dB loss <40kHz; 3 = ≥40dB loss at 2 or 3 kHz and up; 4 = ≥40dB loss at 1kHz and up	Pediatric	No baseline required, more comprehensive than Brock	Complex, intended for pediatric use
SIOP Boston, 2012 (Brock et al., 2012)	Grades 0-4: 0 = ≤20dB loss at all frequencies; 1 = >20dB loss at frequencies >4kHz; 2 = >20dB loss at frequencies 4kHz and up; 3 = >20dB loss at 2 or 3kHz and up; 4 = >dB loss at 2kHz and up	Pediatric	No baseline required, developed by international working group	Limited use to date, intended for pediatric use
TUNE system, 2014 (Theunissen et al., 2014)	Grades 0-4, with subgrades for 1 and 2: 0 = No loss; 1a* = ≥10dB at 8-12.5kHz, or subjective complaints; 1b* = ≥10dB at 1-4kHz; 2a* = ≥20dB at 8-12.5kHz; 2b* = ≥20dB at 1-4kHz; 3 = ≥35dB at 1-4kHzt; 4 = ≥70dB at 1-4kHzt, all based on air conduction thresholds * = in comparison with pretreatment assessment	Adults	Includes subjective symptoms, designed to reflect real-world situations	Time consuming, limited use to date, intended for adult use, baseline required
NCI CTCAE, version 5.0, 2017 ("Common termniology criteria for adverse events (CTCAE)," 2017)	Adults: Grades 0-4: 0 = no hearing loss; 1 = 15-25dB average loss at 2 adjacent frequencies in 1 or both ears, or subjective complaints; 2 = >25dB loss averaged at 2 adjacent frequencies in 1 or both ears; 3 = >25dB loss averaged 3 adjacent frequencies in 1 or both ears; 4 = profound bilateral hearing loss, >80dB at 2kHz and up	Adult and pediatric	Familiar system, suitable for all age groups	Baseline required, not geared towards detection of broad range of hearing frequencies often altered by cochleotoxic drugs

Appendix B Flow Cytometry Gating Details

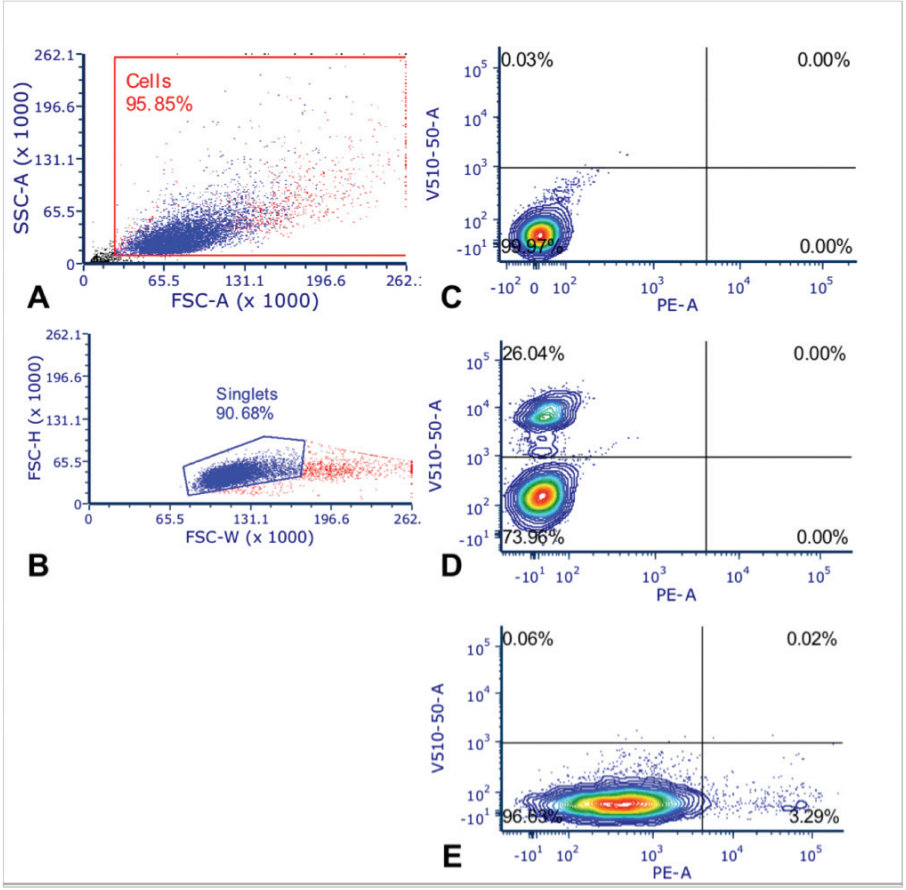

Appendix B Flow cytometry gating strategies for the detection of late-stage apoptosis and cell death in SK-N-AS neuroblastoma (NBL) cells. A) General gating strategy to identify living and dead cells in sample and to eliminate cell debris. B) Doublet discrimination gating strategy. C) Unstained control cells. D) Gating strategy to identify SYTOX+ dead cells. Representative plots from heat-killed SYTOX+ control cells. E) Gating strategy to identify Annexin+ cells. Representative plot from cells treated with Camptothecin to induce apoptosis.